

Pyridazinediones and amino acid receptors: theoretical studies, design, synthesis, and evaluation of novel analogues

[Jeremy R Greenwood](#)

A thesis submitted for the degree of Doctor of Philosophy

The Department of Pharmacology, The University of Sydney, March 1999

Contents

Contents	2
Opening remarks	13
Declaration	14
Acknowledgements	15

Text

1. Introduction	18
1.1 Preamble	18
1.2 Guide to chapters	19
1.3 Key references	21
2. Tautomerism of hydroxy-pyridazines: the N-oxides	24
2.1 Introduction	25
2.2 Methods and results	27
2.3 Discussion	32
2.4 Conclusion	36
2.5 Calculation details	37
2.6 Acknowledgments	37
2.7 References	37
3. The tautomerism of pyridazinediones	50
3.1 Introduction	51
3.2 Methods and results	53
3.2.1 Generation of tautomers and conformers	
3.2.2 Discrimination of preferred conformers and low energy tautomers	
3.2.3 Calculation of gas phase geometries	
3.2.4 Calculation of gas phase energies	
3.2.5 Calculation of aqueous phase properties	

<u>3.3 Key to Tables, Charts, Figures and geometries</u>	57
<u>3.4 Discussion</u>	58
<u>3.4.1 Conformation</u>	
<u>3.4.2 Structure determination</u>	
<u>3.4.3 Gas phase tautomerism predictions</u>	
<u>3.4.4 Solvation effects according to different models</u>	
<u>3.4.5 Aqueous phase tautomerism</u>	
<u>3.4.6 <i>Ab initio</i> prediction of relative pK_a</u>	
<u>3.5 Conclusion</u>	66
<u>3.6 Calculation details</u>	67
<u>3.7 References</u>	67
<u>4. Pyridazinediones as candidates for neuroactive amino acid analogues</u>	
	89
<u>4.1. Brief introduction to GABA receptors</u>	90
<u>4.2. Brief introduction to Excitatory Amino Acid (EAA) receptors</u>	93
<u>4.3. Pyridazinediones as amino acid analogues</u>	97
<u>4.3.1. The resemblance of pyridazinediones to 3-isoxazolols</u>	
<u>4.3.2. Choosing to investigate maleic hydrazide derivatives</u>	
<u>4.3.3. The role of tautomerism</u>	
<u>4.3.4. The target series</u>	
<u>4.4. References</u>	105
<u>5. Synthesis of pyridazinedione amino acid analogues</u>	116
<u>5.1 Analogues of muscimol (5-aminomethyl-3-isoxazolol)</u>	118
<u>5.1.1 4-Aminomethylpyridazine-3,6(1,2<i>H</i>)-dione</u>	
<u>5.1.2 2-Methyl-4-aminomethyl-6-hydroxypyridazin-3(2<i>H</i>)-one</u>	
<u>5.1.3 2-Methyl-5-aminomethyl-6-hydroxypyridazin-3(2<i>H</i>)-one</u>	

<u>5.2 Analogues of THIP (4,5,6,7-tetrahydroisoxazolo[5,4-c]pyridine-3-ol)</u>	128
<u>5.2.1 5,6,7,8-Tetrahydropyrido[3,4-d]pyridazine-1,4(2,3<i>H</i>)-dione</u>	
<u>5.2.2 1-Hydroxy-3-methyl-5,6,7,8-tetrahydropyrido[3,4-d]pyridazin-4(3<i>H</i>)-one</u>	
<u>5.2.3 2-Methyl-4-hydroxy-5,6,7,8-tetrahydropyrido[3,4-d]pyridazin-1(2<i>H</i>)-one</u>	
<u>5.3 AMPA / HIBO analogues</u>	132
<u>5.3.1 2-Amino-3-(pyridazine-3,6(1,2<i>H</i>)-dion-4-yl)propanoic acid</u>	
<u>5.3.2 2-Amino-3-(2-methyl-6-hydroxypyridazin-3(2<i>H</i>)-on-4-yl)propanoic acid</u>	
<u>5.3.3 2-Amino-3-(2-methyl-6-hydroxypyridazin-3(2<i>H</i>)-on-5-yl)propanoic acid</u>	
<u>5.3.4 2-Amino-3-(6-hydroxypyridazin-3(2<i>H</i>)-on-2-yl)propanoic acid</u>	
<u>5.4 AMAA / ibotenic acid analogues</u>	139
<u>5.4.1 Pyridazine glycines via ring nucleophilic substitution</u>	
<u>5.4.2 Glycino pyridazinones via pyridazine aldehydes</u>	
<u>5.4.3 Glycino pyridazinones via ethyl 2-(pyridazinyl)acetates</u>	
<u>5.5 Conclusion</u>	146
<u>5.6 Experimental</u>	147
<u>5.7 Acknowledgments</u>	170
<u>5.8 References</u>	170
<u>6. Theoretical studies on the free-radical bromination of methyl-pyridazines</u>	172
<u>6.1 Introduction</u>	173
<u>6.2 Method</u>	174
<u>6.3 Results</u>	175
<u>6.4 Discussion</u>	176
<u>6.5 Experimental</u>	178
<u>6.6 Calculation Details</u>	179
<u>6.7 Conclusion</u>	180

<u>6.8 Acknowledgments</u>	180
<u>6.9 References</u>	181
<u>7. Pharmacological screening <i>in vitro</i></u>	191
<u>7.1 GABA_A activity: Guinea-pig isolated ileum preparation</u>	192
<u>7.1.1 Results</u>	
<u>7.1.2 Discussion</u>	
<u>7.1.3 Experimental</u>	
<u>7.2 EAA activity: Cortical wedge preparation</u>	195
<u>7.2.1 Results</u>	
<u>7.2.2 Discussion</u>	
<u>7.2.3 Experimental</u>	
<u>7.3 GABA_C activity</u>	198
<u>7.4 Conclusion</u>	199
<u>7.5 Acknowledgments</u>	199
<u>7.6 References</u>	199
<u>8. Heterocycles as bioisosteres for the α-carboxylate moiety of glutamate in AMPA receptor agonists: A review and theoretical study</u>	209
<u>8.1 Introduction</u>	211
<u>8.1.1 Carboxylate bioisosterism and drug design</u>	
<u>8.1.2 EAA and AMPA receptors</u>	
<u>8.1.3 Alanino heterocycles active at AMPA receptors</u>	
<u>8.1.4 The theoretical study of heterocycles related to AMPA receptors</u>	
<u>8.2 Methods and results</u>	214
<u>8.2.1 Choice of model compounds</u>	
<u>8.2.2 Structure determination</u>	

8.2.3 Gas phase thermochemistry and tautomerism	
8.2.4 Point charges and dipoles	
8.2.5 Aqueous phase modelling and tautomerism	
8.2.6 pK_a estimation	
8.3 Key to tables, graphs, charts and figures	219
8.4 Discussion	222
8.4.1 Tautomerism	
8.4.2 pK_a behaviour	
8.4.3 Observations on the requirements for carboxylate bioisosterism at the AMPA receptor	
8.5 Conclusion	234
8.6 Calculation details	235
8.7 Acknowledgments	235
8.8 References	236

Tables

[Chapter 2.](#)

Table 2.1 Hydroxy conformers	40
Table 2.2 All tautomers at HF/6-31G(d)	40
Table 2.3 Compound energies and free energies at 298.15K	41
Table 2.4 Higher level calculations on 4-hydroxy-pyridazine 1-oxide	42
Table 2.5 Free energies of solvation	43
Table 2.6 Tautomer ratios in solution	44
Table 2.7 Relative acidities	44
Table 2.8 Literature pK _a values	45

[Chapter 3.](#)

Table 3.1 Unfavourable conformers	70
Table 3.2 Gas phase tautomer energies	72

Table 3.3 Effect of large basis set optimisation on 3	74
Table 3.4 Comparison of 2h with X-ray structure	75
Table 3.5 Comparison of 3b with X-ray structures	75
Table 3.6 Free energies of solvation	76
Table 3.7 Estimated tautomer ratios	78
Table 3.8 Equilibrium free energies and pK _a	79
Table 3.9 Experimental pK _a s	80
Chapter 4.	
Table 4.1 Target series	103
Chapter 6.	
Table 6.1 Experimental products	182
Table 6.2 Relative and absolute energies	185
Table 6.3 Heats of reaction	186
Chapter 8.	
Table 8.1 Summary of AMPA analogue activities	241
Table 8.2 Energies and tautomerism of model heterocycles	245
Table 8.3 Solvation energies, pK _a predictions and literature values	248
Figures and traces	
Chapter 2.	
Figure 2.1 pyridazine 1,2-dioxide	45
Figure 2.2 3-hydroxypyridazine 1-oxide	46
Figure 2.3 4-hydroxypyridazine 1-oxide	46
Figure 2.4 5-hydroxypyridazine 1-oxide	47
Figure 2.5 6-hydroxypyridazine 1-oxide	47
Chapter 3.	
Figure 3.1 Summary of tautomeric behaviour	57

[Figure 3.2](#) Formal structures of [3c](#), [3f](#), and [3f](#) 60

[Figure 3.3](#) Resonance of [2-b](#) 66

[Chapter 4.](#)

[Figure 4.1](#) maleic hydrazide 99

[Figure 4.2](#) 3-hydroxy pyridazine 1-oxide 99

[Figure 4.3](#) 4,5-dimethyl-3-isoxazolol 99

[Figure 4.4](#) Overlay: 3, 17a 107

[Figure 4.5](#) Overlay: 4, 17b 108

[Figure 4.6](#) Overlay: 5, 18a 109

[Figure 4.7](#) Overlay: 6, 18b 110

[Figure 4.8](#) Overlay: 13, 19a 111

[Figure 4.9](#) Overlay: 14, 19b 112

[Figure 4.10](#) Overlay: 15, 20a 113

[Figure 4.11](#) Overlay: 11, 20b 114

[Chapter 6.](#)

[Figure 6.1](#) Image and PM3 energies of 9(2), 9(4), 10(2), 10(5) 187

[Figure 6.2](#) Wavefunction map of HOMO of 9(2), 9(4), 10(2), 10(5) 188

[Chapter 7.](#)

[Trace 7.1](#) 1 followed by GABA 201

[Trace 7.2](#) 2 followed by GABA 201

[Trace 7.3](#) 3 followed by GABA 201

[Trace 7.4](#) 5 followed by GABA 201

[Trace 7.5](#) 6 followed by GABA 202

[Trace 7.6](#) 7 followed by GABA 202

[Trace 7.7](#) GABA followed by TACA 202

[Trace 7.8](#) 9 203

[Trace 7.9](#) CPP plus 9 203

[Trace 7.10](#) CNQX plus 9 203

Trace 7.11 10	204
Trace 7.12 CPP plus 10	204
Trace 7.13 CNQX plus 10	205

Chapter 8.

Figures 8.1.26 to 8.1.38 Conjugate base anions of model acidic heterocycles, CPK rendering, point charge distributions	250
Figures 8.2.26 to 8.2.38 Conjugate base anions of model acidic heterocycles, Van der Waals surfaces, electrostatic potentials	252
Figure 8.3 Conjugate base anions 26- to 33- overlaid	254
Figure 8.4 1-methyl uracil anion, methyl guanidinium cation, and methanol complex	254
Figure 8.5 4,5-dimethyl-3-isoxazolol anion, methyl-guanidinium cation, water, and methanol complex	254

Charts and Schemes

Chapter 1.

Scheme 1.1 maleic hydrazide	18
Scheme 1.2 important amino acids	19

Chapter 2.

Chart 2.1 structures referred to in text	48
--	----

Chapter 3.

Chart 3.1 3,4-substituted structures, 1	82
Chart 3.2 3,5-substituted structures, 2	83
Chart 3.3 3,6-substituted structures, 3	84
Chart 3.4 4,5-substituted structures, 4	85
Chart 3.5 related structures	86

Chapter 4.

Scheme 4.1 Some compounds acting at the GABA receptor	90
Scheme 4.2 3-isoxazolols with varying activity at GABA receptors	92
Scheme 4.3 Two endogenous excitatory amino acids	93
Scheme 4.4 Agonists which have been used to characterise ionotropic EAA receptor subtypes	95
Scheme 4.5 isoxazole α -amino acids with varying activity at EAA receptors, and the amino acid willardiine	97

Chapter 5.

Scheme 5.1 Synthesis of 4-aminomethylpyridazine-3,6(1,2 <i>H</i>)-dione 7	118
Scheme 5.2 Synthesis of 2-methyl-4-aminomethyl-6-hydroxypyridazin-3(2 <i>H</i>)-one 15	121
Scheme 5.3 Synthesis of 2-methyl-5-aminomethyl-6-hydroxypyridazin-3(2 <i>H</i>)-one 20	124
Scheme 5.4 Synthesis of 5,6,7,8-Tetrahydropyrido[3,4- <i>d</i>]pyridazine-1,4(2,3 <i>H</i>)-dione 25	128
Scheme 5.5 Synthesis of 1-hydroxy-3-methyl-5,6,7,8-tetrahydropyrido[3,4- <i>d</i>]pyridazin-4(3 <i>H</i>)-one 30	130
Scheme 5.6 Synthesis of 2-Amino-3-(pyridazine-3,6(1,2 <i>H</i>)-dion-4-yl)propanoic acid 33	132
Scheme 5.7 Synthesis of 2-amino-3-(2-methyl-6-hydroxypyridazin-3(2 <i>H</i>)-on-4-yl)propanoic acid 35	134
Scheme 5.8 Synthesis of 2-amino-3-(2-methyl-6-hydroxypyridazin-3(2 <i>H</i>)-on-5-yl)propanoic acid 37	135
Scheme 5.9 Synthesis of 2-amino-3-(6-hydroxypyridazin-3(2 <i>H</i>)-on-2-yl)propanoic acid 43	136
Scheme 5.10 Chloropyridazines synthesised as starting materials for ring nucleophilic substitution	140
Scheme 5.11 Failure of Modified Sørensen Reaction on ring halogen	141
Scheme 5.12 Synthesis of a pyridazinyl aldehyde 49 but failure of α -amino acid	

syntheses	142
Scheme 5.13 Synthesis of an ethyl 2-(dimethoxypyridazinyl)acetate 53 , and its oxime and bromide, but failure of synthesis of the glycino pyridazinone 58	144
Chapter 6.	
Scheme 6.1 Mechanism of the Wohl-Zeigler reaction	173
Chapter 7.	
Chart 7.1 muscimol, THIP, and GABA analogues tested	206
Chart 7.2 AMPA, AMAA, and glutamate analogues tested	207
Chart 7.3 other analogues referred to	208
Chapter 8.	
Chart 8.1 Structures with moderate to high potency	255
Chart 8.2 Structures with reduced or abolished potency	256
Chart 8.3 Model des-glycino heterocyclic conjugate base anions	257
Chart 8.4 Tautomerism of model heterocycles	258
Chart 8.5 Tridentate binding models at AMPA receptors	259
Chart 8.6 Tridentate binding to two putative residues, with and without water mediation	260
Graphs	
Chapter 7.	
Graph 7.1 log[Dose] - response curves for 9 and 10 , compared with AMPA and NMDA	196
Chapter 8.	
Graph 8.1 Experimental pK _a s vs. <i>ab initio</i> predictions	261
Graph 8.2 Experimental pK _a s vs. empirical predictions	261
Graph 8.3 pK _a s: <i>ab initio</i> vs. empirical predictions	262

Molecules

Indices of optimised geometries (.pdb format)

Chapter 2	49
Chapter 3	86
Chapter 4	115
Chapter 6	189
Chapter 8	216

Opening remarks

NOTE: The hard copy you are reading is for archival purposes only, and does not contain all of the information in the thesis. It has been printed from the hypertext to meet faculty requirements. Please use the hypertext version.

In 1998, the University of Sydney Academic Board (AB 11.3.98) made provision for the electronic submission of PhD theses. This thesis is presented in hypertext format, primarily because of the advantage of being able to include various resources, such as interactive three dimensional molecular data and multiple colour images, impossible within traditional media. Other advantages include rapid and cheap dissemination and the preservation of numerical data in a readily useable form. Effort has been made to make the work as general and standard for long-term accessibility as possible. The interface is designed to be simple and self-explanatory. The thesis is world readable via the web server

<http://gabacus.pharmacol.usyd.edu.au/thesis> and will be cut onto CD-ROM plus hard copy of the text for storage by the university. While it is possible to print the text, the work is intended to be read electronically.

[Chapters 2, 3, 6](#) and [8](#) have previously been published through electronic conferences, and also via the print journal J. Molecular Structure (Theochem), or the electronic [Internet Journal of Chemistry](#). Most of the other material has been presented through conference posters and talks.

Links to all required software for browsing on various platforms are included in the [software directory](#) to assist archival. The text is presented in Hypertext Markup Language (.htm) and is designed to be browsed using any standard web browser on any platform, [Netscape 2.x](#) or higher, [Internet Explorer 3.x](#) or higher. Images are in standard formats (.jpg, .gif). Molecules are presented mostly as Cambridge Protein Data Bank (.pdb) format, some are offered in an alternative X-Mol cartesian coordinates (.xyz) format. In order to view molecular structures, a viewer such as [Rasmol](#) or preferably the browser plugin [MDL's Chemscape Chime](#) should be installed (see the [software directory](#) for a copy). In some instances, use has been

made of the Chime format <embed> tag to call molecular data within the text or tables.

The [search](#) facility included with the thesis is a PERL script which requires that it be served from an appropriately configured web server; this feature may not operate from an archival copy on an isolated machine. The MIME types associated with interactive molecules may also require client and server configuration in order for them to be recognised by a molecular browser should the thesis be mounted on a new site, however the numerical data will still remain readable. While these features of the thesis may become more difficult to access from an archival copy, they are over and above those available in hard copy.

Declaration

The work presented in this thesis is the original work of the author, except where acknowledgment has been made to results supplied by co-workers or previously published. The work was carried out at the Adrien Albert Laboratory of Medicinal Chemistry and Biomolecular Computer Graphics Facility, Department of Pharmacology, University of Sydney, and has not been previously submitted for a degree at any institution.

[Jeremy R Greenwood](#)

Acknowledgments

This *magnum opus* would never have been possible without the generous and long-term support of so many people.

First and foremost, I'd like to thank my supervisors: [Robin Allan](#), [Hugh Capper](#), and [Graham Johnston](#). They provided for my every need: financial, material, and intellectual support - I could not have asked for more. Special thanks over and above and beyond goes to Hugh Capper, companion and friend through long shared hours of coding. And to [Malcolm Gillies](#) for helping to bring me to this point and to whom I owe much of what I know and who installed systems which were vital to the production of this thesis. To my Adrien Albert laboratory co-workers: [Ken Mewett](#), the finest organic chemist I have worked with, an unsung hero, a virtuoso, to whom I am greatly indebted for so much support and advice with chemistry. To [Hue Tran](#), a careful and scrupulous scientist, companion through long hours of synthesis and of much assistance with chemistry and pharmacology. And [Rujee Duke](#), a fine chemist with whom I have enjoyed many a collaboration and conversation. To [Graziano Vaccarella](#): collaborator, co-author, assistant - congratulations on finishing!

And also to the man I have not known, but often cited, the late [Adrien Albert](#) who gave his name to [our lab](#) and devoted his life to the science of heterocycles which I have pursued.

To my mentors at ANU: [Leo Radom](#) and [Ming Wah Wong \(Richard\)](#). With the passing of the years I realise how fortunate I was to have learnt so much in such a short time, and from their inspiration develop a passion for applied quantum chemistry.

To the team at the Royal Danish School of Pharmacy, especially [Povl Krosgaard-Larsen](#) and [Tommy Liljefors](#), whose research has also been an inspiration and whom I'll soon join.

To the men and women who sorted every logistical detail and difficulty, especially [Virginia Fascioli](#) who could always be relied on to pull the rabbit out of the hat just when it was needed. To [Keith Rippon](#) and [Norm Oetsch](#) - magicians with machines of all kinds.

To the computer support teams: [Ben Simons](#), [Geoff Horne](#), and the others who've been at the [NSWCPC](#) to make this project possible. To [Doug Scoullar](#) and [Andy Winter](#) from Architecture for their many rescues and advices. To [Hristo Nikolov](#) and [John Dodson](#) for running a tight ship, prompt support, and an excellent network.

To [Mary Collins](#), collaborator and delicious falafel maker, and her husband [Brad](#) and his collection of the finest Belgian beers - my sanity is due in part to you. Also helping me to stay sane, especially after hours at the Grandstand, friends and colleagues [Jim Delikatny](#), [Harry Wilson](#), [Ian Spence](#), [Slade Mathews](#), [Hilary Lloyd](#), [Peter Burden](#), [Jane Hanrahan](#), [Macdonald Christie](#), [Rachael Jones](#), and [Pat Groenstein](#), among others. And for reminding me of my insanity: [Suzanne Habjan](#) - we worked hard, had fun and enjoyed many wonderful dinners. To the people I've taught with, particularly [Izabela Brzuszcak](#), it was highly rewarding. To [Ann Mitrovic](#), for her unending patience with everyone, especially my brief stint with rat brain slices, and without whom I could not have tested my compounds. To [Jill Maddison](#) and the [Australian Veterinary Association](#) for providing me with both an income and the .htm experience to produce this thesis.

To the [coke](#) machine down the hall for providing my two most crucial synthetic starting materials: caffeine and sucrose.

To my family and the special women and men who have supported me financially, physically, and emotionally: My mother [Janet Paterson](#) who has been through it all and understands, and moreover has provided me a roof to sleep under for much of the duration. My grandmother **Jean Paterson** who also understands, and has provided for me generously. My father [Tony](#). My brother [Philip](#) for many a midnight swim and much good company. And to my special friends: [Camille](#) and

Anna Shanahan, [Tim Booth](#), Jo Lobb, Kevin Brigden, [David Chisholm](#), [Manuela Crank](#), [Margaret Mayhew](#), [Jeremy Lawrence](#), [Margaret Nicholson](#), Jolyon Campbell *requiescat in pace*, [Angela Dean](#), and above all, to [Justine Arnot](#). "Justine, here's a kiss... I'm saving you to end this list".

To all of these people and the many I've neglected to mention, I am grateful and owe a great debt. We've had fun and we've done some science.

[Jeremy R Greenwood](#)

1. Introduction

[1.1 Preamble](#)

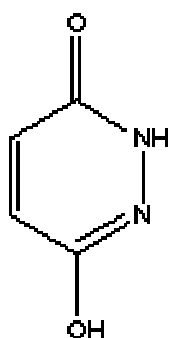
[1.2 Guide to chapters](#)

[1.3 Key references](#)

1.1 Preamble

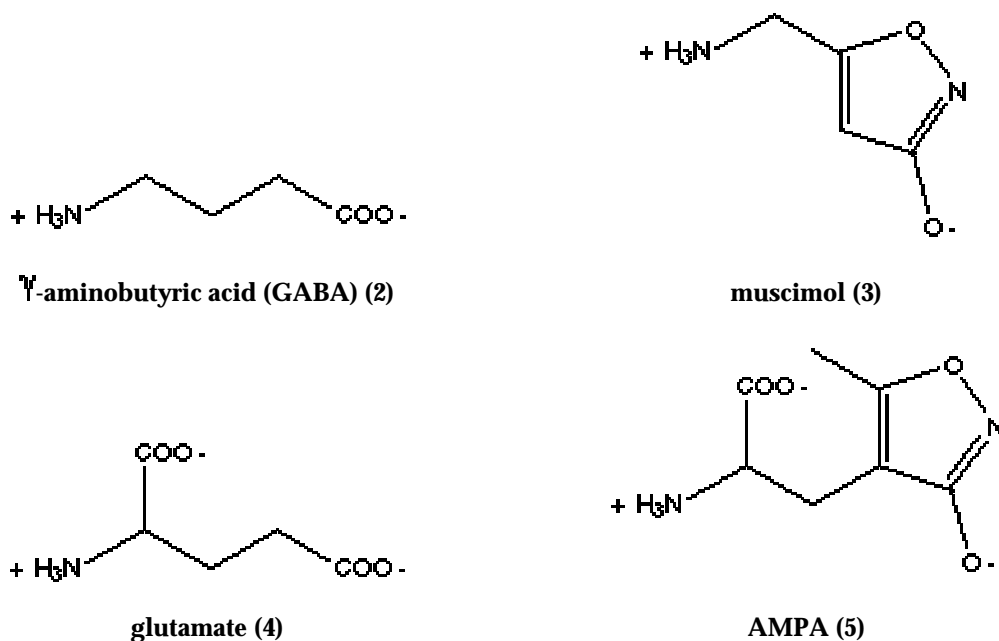
This thesis is primarily concerned with a class of chemical compounds known as pyridazinediones, being 6-membered aromatic rings containing two adjacent nitrogen atoms (pyridazine), doubly substituted with oxygen. In particular, the work focuses on pyridazine-3,6-diones, derivatives of maleic hydrazide (1).

Understanding of the chemistry of these compounds is extended, using theoretical and synthetic techniques.



Scheme 1.1 maleic hydrazide (1)

This thesis is also concerned with two very important classes of receptors which bind amino acids in the brain: firstly, the inhibitory GABA receptor, which binds γ -aminobutyric acid (GABA) (2) *in vivo*, and for which muscimol (3) is an agonist of the GABA_A subclass; secondly, Excitatory Amino Acid (EAA) receptors, which bind glutamate (4) *in vivo*, and in particular the AMPA subclass, for which (S)-2-amino-3-(3-hydroxy-5-methylisoxazol-4-yl)propionic acid (AMPA) (5) is an agonist.



Scheme 1.2 important amino acids

The connection between pyridazinediones and amino acid receptors is the design, synthesis, and evaluation of structures based on pyridazinediones as potential GABA and EAA receptor ligands. Techniques of theoretical chemistry, molecular modelling, synthetic chemistry, and *in vitro* pharmacology are used to explore pyridazine-3,6-dione derivatives as ligands.

1.2 Guide to chapters

[Chapter 1](#) (this chapter) describes the way in which the other stand-alone chapters are linked, and provides some background.

[Chapter 2](#) is concerned with an exhaustive theoretical investigation into the tautomerism of the four isomeric pyridazinone *N*-oxides, and pyridazine 1,2-dioxide, positional isomers of maleic hydrazide ([1](#)). It also describes aspects of the structure and pK_a behaviour of these isomers, and their conjugate bases. Whereas the tautomerism of ([1](#)) and other diazine diones is well studied, the structure and tautomerism of these compounds has been previously considered only briefly. High level quantum computational techniques are used, and compared with experiment

where possible. Tautomerism is an important chemical study in its own right, has long been a challenge to computational and experimental techniques. It is also important for understanding the way that heterocycles behave biologically, as a prelude to medicinal chemistry.

[Chapter 3](#) extends the study in [Chapter 2](#) to the four isomeric pyridazinediones, including maleic hydrazide (**1**), capable of very highly complex tautomerism. Previous theoretical studies on (**1**) are improved upon, and the tautomerism and properties of the conjugate bases of these isomers is examined for the first time. Since pyridazinediones are acidic in solution, and predominantly ionised at physiological pH, the study of their anionic forms is of particular interest as background to the medicinal chemistry of their derivatives.

[Chapter 4](#) introduces the GABA and EAA receptors with a brief discussion of their history and therapeutic importance. The role that 3-isoxazolols such as muscimol (**3**) and AMPA (**5**) *et al.* have had in defining these receptors is described. The rationale for examining pyridazinedione derivatives as ligands for these receptors is discussed, with the aid of molecular modelling. A set of twelve target compounds to be evaluated is presented.

[Chapter 5](#) describes synthetic efforts to produce the twelve compounds described in [Chapter 4](#): glycino-, alanino-, aminomethyl-, and tetrahydropyrido- derivatives of (**1**), and their *N*-methyl substituted counterparts. Several stumbling blocks were encountered, leading to the abandonment of the synthesis of the glycino-pyridazinediones. An unexpected synthetic result yielded another test compound.

[Chapter 6](#) concerns one aspect of the synthesis of pyridazinone amino acid analogues: free-radical bromination by *N*-bromosuccinimide (NBS) as described in [Chapter 5](#). A crucial step in the synthesis, this reaction is difficult to control, and often produces mixtures or unexpected products. In this chapter, several NBS reactions on methyl pyridazinones are investigated using techniques from theoretical chemistry. A rapid method of predicting the results of the reaction is developed, increasing understanding of the reaction.

[Chapter 7](#) describes the pharmacological experiments performed to evaluate the ten analogues synthesised in [Chapter 5](#) for activity. The guinea-pig ilium is used to test muscimol and THIP analogues for GABA_A activity, and xenopus oocytes are used to test for GABA_C activity. The rat cortical wedge preparation is used to test the AMPA analogues for EAA (NMDA and AMPA receptor) activity.

[Chapter 8](#) concerns the AMPA receptor, and in particular, the types of oxygen-substituted heterocycles which may act as bioisosteres for the ω -carboxylate group of glutamate at this receptor. A range of heterocycles producing AMPA analogues of varying activity are submitted to theoretical investigation, including the study of their tautomerism and pK_a behaviour. The tested pyridazinones are evaluated and compared with other bioisosteres, and predictions are made about the nature of AMPA receptor binding and the future direction of medicinal chemistry in this area.

1.3 Key references and background

Familiarity with chemical nomenclature is assumed throughout. Reasonable familiarity with organic chemistry, molecular modelling, applied *ab initio* and semi-empirical quantum theory are assumed for Chapters [2](#), [3](#), [4](#), [6](#), and [8](#). A basic understanding of synthetic heterocyclic chemistry is assumed in Chapters [5](#) and [6](#). Chapters [4](#), [7](#), and [8](#) assume a basic understanding of drug design and pharmacology.

The following key references provide much of the necessary background for the material presented

Molecular modelling and applied *ab initio* quantum theory:

- JB Foresman, A Frisch, *Exploring Chemistry with Electronic Structure Methods*, 2nd Ed., Gaussian Inc., (1995-6).
- WJ Hehre, *Practical Strategies for Electronic Structure Calculations*, Wavefunction Inc., (1995)

Heterocyclic tautomerism:

- J Elguero, C Marzin, AR Katritzky, P Linda, The Tautomerism of Heterocycles, *Advances in Heterocyclic Chemistry, Supplement 1* (1976)

Pyridazine synthetic chemistry:

- RN Castle, Pyridazines, *The Chemistry of Heterocyclic Compounds*, Wiley Interscience, **28**, (1973)

Pyridazine medicinal chemistry:

- G Heinisch, H Frank, *Progress in Medicinal Chemistry*, **27**, 1 (1990)
- G Heinisch, H Frank, *Progress in Medicinal Chemistry*, **29**, 141 (1992)

Bioisosterism in drug design:

- T Fujita, Similarities in bioanalogous structural transformation patterns among various bioactive compound series, *Biosci. Biotech. Biochem.*, **60**(4), 557-566 (1996)
- GA Patani, EJ LaVoie, Bioisosterism: A rational approach in drug design, *Chem. Rev.*, **96**, 3147-3176 (1996).
- CA Lipinski, Bioisosterism in drug design, Ch 27, *Annual reports in Medicinal Chemistry*, **21**, (1986)

GABA receptor medicinal chemistry and pharmacology:

- SJ Enna, NG Bowery, *The GABA Receptors*, Humana Press (Totowa, NJ), 2nd ed. (1997)
- P Krosgaard-Larsen, B Frølund, FS Jørgensen and A Schousboe. GABA_A receptor agonists, partial agonists, and antagonists. Design and therapeutic prospects, *Journal of Medicinal Chemistry* **37**(16), 2489-2505 (1994)

- DIB Kerr and J Ong, GABA agonists and antagonists, *Medicinal Research Reviews*, **12**(6) 593-636 (1992).
- GAR Johnston, GABA_A agonists as targets for drug development, *Clinical and Experimental Pharmacology and Physiology*, **19**, 73-78 (1992)

Excitatory Amino Acid receptor medicinal chemistry and pharmacology:

- G Vaccarella, *Synthesis and activity of Pyridazine analogues of glutamic acid*, PhD thesis, Department of Pharmacology, University of Sydney (1998)
- DT Monaghan, R Wenthold, *The Ionotropic Glutamate Receptors*, Humana Press (Totowa, NJ), 2nd ed. (1997)
- P Krogsgaard-Larsen, B Ebert, TM Lund, H Bräuner-Osborne, FA Sløk, TN Johansen, L Brehm, U Madsen, Design of excitatory amino acid receptor agonists, partial agonists and antagonists: ibotenic acid as a key lead structure, *European Journal of Medicinal Chemistry* **31**, 515-537 (1996)
- JJ Hansen, P Krogsgaard-Larsen, Structural, Conformational, and Stereochemical Requirements of Central Excitatory Amino Acid Receptors, *Medicinal Research Reviews*, **10**(1), 55-94 (1990)

Medical applications:

- P Krogsgaard-Larsen, Amino acid neurotransmitters in Alzheimer's disease: focus on AMPA and GABA_A receptors, *European Journal of Pharmaceutical Sciences*, **2**, 59-61 (1994)

2. Tautomerism of hydroxy pyridazines: the *N*-oxides.

Abstract

A comprehensive theoretical study of the structure and tautomerism of the four isomeric hydroxy pyridazine *N*-oxides, as well as pyridazine-1,2-dioxide is presented. Gas phase properties are modelled with high-level *ab initio* calculations employing large basis sets (6-311++G(3df,3pd)) and quadratic configuration interaction treatment of electron correlation (QCISD(T)). Since these acidic heterocycles are of interest as novel carboxylate bio-isosteres, their anionic conjugate bases are also examined. Aqueous solution-phase properties are investigated using the isodensity polarised continuum model (IPCM), and the semi-empirical AM1-SM2 and PM3-SM3 models, and relative acidities compared. The calculated properties are generally in good agreement with existing experimental data, indicating that the 1-hydroxy tautomer predominates both in the gas phase and in solution in the case of the 6- substituted system, and that hydroxy 1-oxide tautomers predominate in the 3- and 5- substituted systems. The behaviour of the 4-substituted isomer is less clear, with non-planar 1-hydroxy and planar 4-hydroxy tautomers being similar in stability.

"Tautomerism of hydroxy pyridazines: the *N*-oxides" JR Greenwood, HR Capper, RD Allan, GAR Johnston. *Journal of Molecular Structure (Theochem)* 419, 97-111 (1997)

Index

[2.1 Introduction](#)

[2.2 Methods and results](#)

[Table 2.1](#) hydroxy conformers

[Table 2.2](#) all tautomers at HF/6-31G(d)

[Table 2.3](#) compound energies and free energies at 298.15K

[Table 2.4](#) higher level calculations on 4-hydroxypyridazine 1-oxide

[Table 2.5](#) free energies of solvation

[Table 2.6](#) tautomer ratios in solution

[Table 2.7](#) relative acidities

[Table 2.8](#) literature pK_a values

[Figure 2.1](#) pyridazine 1,2-dioxide

[Figure 2.2](#) 3-hydroxypyridazine 1-oxide

[Figure 2.3](#) 4-hydroxypyridazine 1-oxide

[Figure 2.4](#) 5-hydroxypyridazine 1-oxide

[Figure 2.5](#) 6-hydroxypyridazine 1-oxide

[Chart 2.1](#) structures referred to in text

[Index of optimised geometries](#)

[2.3 Discussion](#)

[2.4 Conclusion](#)

[2.5 Calculation details](#)

[2.6 Acknowledgments](#)

[2.7 References](#)

2.1 Introduction

As a class, the pyridazines are the least studied and understood of the six-membered diazine heterocycles, both experimentally, and theoretically [1]. With the resurgence of interest in pyridazine derivatives as novel bio-active molecules [2,3,4] and with the close structural similarity of some hydroxy pyridazines to better known systems such as uracil, these compounds are expected to be the subject of further synthetic and medicinal study. In particular, being relatively strong acids and having comparatively large dipoles, these heterocycles show promise as novel carboxylate bio-isosteres.

Pyridazine-1,2-dioxide 1, and 3-, 4-, and 5-hydroxy pyridazine 1-oxides 2, 3, 4, are known synthetically [5,6,7,8]. Various ring-substituted derivatives of 6-hydroxypyridazine 1-oxide 5 are also known [9], although the parent compound appears to have eluded synthesis, despite the fact that its immediate precursors 6-chloro and 6-methoxy pyridazine 1-oxide are known [10].

Experimental studies on the tautomerism of these compounds are few, and apparently the subject has been neglected since the 1960s. Itai [11] suggests that 2c

is favoured over [2b](#), [3a](#) over [3d](#), [4d](#) over [4b](#), and [5a](#) over [5d](#), i.e. that hydroxy *N*-oxides are preferred for [2](#) and [4](#), and *N*-hydroxy ketones for [3](#) and [5](#), citing [[6,8,9,12,13](#)] as evidence. Igeta [[6,14](#)] has made a thorough study of [2](#), and based on NMR and UV spectroscopic data has concluded the preference for the lactim form [2c](#), and found a pK_a value of 4.1 for this system. [4](#) is also well studied by UV spectroscopy by Okusa and Kamiya [[8](#)] who concluded that the phenolic [4d](#) is preferred. By contrast, [3](#) and [5](#) are poorly studied. Aspects of the chemistry of derivatives of [5](#), such as facile demethylation of 6-methoxy pyridazine 1-oxides or methyl migration to form 1-methoxy pyridazin-6(1*H*)-ones [[15](#)], along with comparisons with other better-studied *N*-hydroxy alpha-oxo heterocycles (e.g. [9](#), [[37](#)]), may be taken to support the hypothesis of the predominance of 1-hydroxy tautomers in the absence of direct studies. The tautomerism of [3](#) and its derivatives is even less well studied; certainly alkylation and acylation yield 1-OR derivatives [[7](#)] suggesting [3a](#), but this is not conclusive, as kinetics or thermodynamics may render alkylation favourable or unfavourable regardless of tautomer prevalence. The conclusions of Itai [[11](#)] would seem valid in the case of the solution-phase behaviour of [2](#) and [4](#), and open to further investigation in the case of [5](#) and particularly [3](#).

The hydroxy-pyridazine 1-oxides are apparently previously unstudied theoretically. Pyridazine 1,2-dioxide [1](#) has received limited attention as the subject of semi-empirical MINDO/2, CNDO/2 and other calculations [[16,17](#)]. The closely related 3- and 4-hydroxy-pyridazines [12](#), [13](#) are better studied. Fabian [[18,19](#)] reports a semi-empirical (AM1, PM3, MNDO, MINDO/3) and *ab initio* (HF/3-21G) study of these compounds, in conjunction with 3,6-pyridazinedione [15](#) (maleic hydrazide) and 3,5-pyridazinedione [14](#), concluding *inter alia* that PM3 handles these systems better than other low-cost methods. La Manna *et al.* [[20,21](#)] report calculations to HF/6-31G(d)//3-21G, finding 3(2*H*)-pyridazinone and 4(1*H*)-pyridazinone to be favoured tautomers. Lapinski *et al.* [[22,23](#)] studied the 3-hydroxy pyridazine [12](#) system at HF/3-21G and SCF-MBPT(2)/DZ(d,p) theories, in conjunction with IR experiments, and predicted 3(2*H*)-pyridazinone to be heavily favoured, in agreement with experiment. Maleic hydrazide [15](#), being perhaps the

best known pyridazine derivative and a commercial plant-growth inhibitor, and having been determined as preferring the somewhat unusual lactam-lactim structure in numerous experiments [24], has been more thoroughly studied, and attempts made to include solvation effects. In addition to the work of Fabian [18,19], Hofmann *et al.* [25] studied maleic hydrazide tautomerism up to HF/6-31G(d), and calculated the free-energy of solvation of the favoured lactam-lactim tautomer to be -12.2 Kcal, via Tomasi's polarisable continuum model (PCM) [26]. A more extensive treatment was performed by Burton *et al.* [27], who conducted gas-phase calculations to MP4/6-31G(d,p)//6-31G(d,p), made comparisons with experiments based on the pK_as of known methyl-derivative model compounds, and estimated solvent effects by three methods: molecular dynamics simulation (free-energy perturbation, FEP), self-consistent reaction field (SCRF) in an ellipsoidal cavity, and the PCM model.

The aim of this study of hydroxy pyridazine 1-oxides [2](#), [3](#), [4](#), [5](#) is to describe the complex tautomerism of these molecules by applying and building on the theoretical methods previously applied to similar systems. Additionally, the same methods are applied to their anionic conjugate bases, likely to be present at physiological pH. In order to lay theoretical ground for medicinal chemistry studies, aqueous solution-phase modelling is performed, including semi-empirical methods not previously applied to pyridazines, but described in detail for the tautomerism of 5-isoxazolols by Cramer and Truhlar [28]. For completeness and comparison, the non-acidic non-tautomeric pyridazine-1,2-dioxide [1](#) is also included in this study.

2.2 Methods and Results

Following the description of heterocyclic tautomerism given by Elguero *et al.* [24], a set of all possible tautomers and their conjugate bases were generated. Firstly, non-substituted ring carbons were assumed to be at least singly protonated. This defines the four anions [2-](#), [3-](#), [4-](#), [5-](#). To each of these, the addition of a proton to the unsubstituted nitrogen, either of the two oxygens, or to a carbon α - to an oxygen substituent (forming a methylene), defines a complete set of structures; five neutral

tautomers for **2**, six for **3**, five for **4**, and four for **5**. No tautomerism is possible, nor may an anion be formed of **1** under this system. [Chart 2.1](#) provides a key to these structures.

Initially, all structures were built with planar geometry. Rotation of 180° about the carbon-oxygen bond generates two distinct conformers in the case of hydroxy tautomers. Optimisations of both conformers of each hydroxy tautomer were performed at HF / 6-31G(d), and the results summarised in [Table 2.1](#). The higher energy conformer of each hydroxy tautomer was discarded from the study set.

Optimisation and frequency calculations were performed at HF / 6-31G(d) on all tautomers, including the recommended scaling factor of 0.8929 for frequencies and thermochemistry calculated at 298.15K. Structures **3a**, **3f**, and **5c** were found to have imaginary frequencies at this level, and were re-optimised in C₁ symmetry. A high energy minimum for structure **5c** was found in C₁ symmetry at HF / 3-21G, but optimisation failed to find a minimum at HF / 6-31G(d). In addition, methylene-containing tautomers **2d**, **2e**, **3c** and **4c** were found to have particularly small lowest vibrational frequencies, e.g. 34 cm⁻¹ for **2d**, indicating very soft bending of the methylene out of the ring plane at this level of theory and basis set. Minima and energies are presented in [Table 2.2](#).

Tautomers whose energies were greater than 25 Kcal above that of the lowest energy tautomer at HF / 6-31G(d), i.e. **3b**, **3e**, **3f**, **5b** and **5c**, were then discarded from the set as being very unlikely to contribute significantly to tautomerism (cf [\[25\]](#)). A second form of **3a**, the planar structure **3a'**, found to be a transition structure at this level, was added to the set for further study on account of the very small difference between the energies of the C_s and C₁ structures. The remaining set of structures was optimised at MP2 / 6-31G(d,p), and this geometry was used in all subsequent *ab initio* calculations.

Ideally, high accuracy gas-phase energies would be obtained from a compound method such as G2 theory, or alternately a complete basis set method such as CBS-Q, but such calculations were too expensive to apply to each system. Instead, single

point energies were calculated at MP2 theory with the large basis set 6-311++G(3df,3pd). The extra diffuse functions and high angular momentum functions are employed to treat as far as possible on equal footing anions and neutral species, and atoms of differing hybridisation, known to present problems for calculations of heterocyclic tautomerism [28]. Higher order correlation effects were considered by performing single point energy calculations at QCISD(T) / 6-31G(d,p). Compound energies were then calculated by correcting the MP2 / 6-31g(d,p) energy as follows, and are presented in [Table 2.3](#).

$$E_0 = \text{ZPE}\{\text{HF}/6\text{-}31\text{G}(\text{d})\} * 0.8929 + E\{\text{MP2}/6\text{-}311\text{++G}(3\text{df},3\text{pd})\} + E\{\text{QCISD}(\text{T})/6\text{-}31\text{G}(\text{d},\text{p})\} - E\{\text{MP2}/6\text{-}31\text{G}(\text{d},\text{p})\}$$

The basis set for the base energy of this method is intermediate in size between the G2(MP2,SVP) theory of Smith and Radom, and Curtiss *et al.* [29,30] i.e. 6-31G(d), and G2(MP2) theory [31] i.e. /6-311G(d,p). Both these methods include an empirical ΔE^{HLC} term in the calculation of E_0 , to correct for residual basis set deficiencies. Since this term is a linear combination of the number of alpha and beta electrons, which are identical for all of the isomeric structures considered, this term cancels for relative energies, and has not been included. Relative energies calculated by the above means are expected to be more accurate than G2(MP2,SVP) theory, but probably not better than the more expensive G2(MP2) theory, despite the larger basis set correction term employed. In particular, poor or inconsistent treatment by MP2 at the base level of calculation is a possible source of error.

From the scaled thermochemical properties calculated at HF / 6-31G(d), gas phase relative free energies of tautomerism and of proton loss at 298.15K were calculated, and these values are included in [Table 2.3](#).

Since the compound E_0 values and free energies calculated for [3a](#), [3a'](#), and [3d](#) were found to be very similar, a series of higher level calculations were performed on these three structures, summarised in [Table 2.4](#). Modified and extended G2 and G2(MP2) energies were calculated, and relative free energies at 298.15K calculated from the compound energy derived from the highest level calculations available.

The high cost of the MP4/6-311G(2df,p) calculation has prevented the direct calculation of G2 energies for the C₁ symmetry structure [3a](#). For comparison, this energy is approximated as follows: the unknown effect of higher level (MP4 vs MP2) correlation on [3a](#) at 6-311G(2df,p) is estimated as the known effect on the C_s symmetry conformer [3a'](#), corrected by the known difference between these two effects calculated with the smaller basis set 6-311G(d,p).

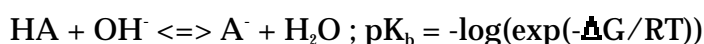
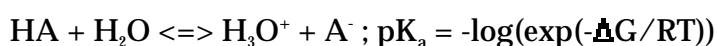
Free energies of aqueous solvation were estimated by three different theories, and the results presented in [Table 2.5](#). Firstly, the isodensity polarised continuum model (IPCM) [\[32\]](#), an extension to the PCM model used previously for solvation of pyridazinones [\[25,27\]](#), was used to calculate single point energies at MP2 / 6-31G(d,p), using a solvent dielectric constant of 78.4 and the recommended isodensity value of 0.001, from which were subtracted the gas-phase energies at this level. Secondly, both single point energies at the MP2 / 6-31G(d,p) geometries and optimisations were performed using the semi-empirical AM1, and AM1-SM2 aqueous solvation model of Truhlar and Cramer [\[33\]](#), and free energies of solvation determined as the difference between the two. Single point energies may be more reliable than optimised calculations, due to poor semi-empirical geometries, however both types of calculation are presented for comparison. For several optimisations, maximum gradients remained large, a known tendency of aromatic systems in this model [\[40\]](#). Thirdly, the same calculations were performed using the PM3-SM3 model [\[34\]](#). The PM3-based semi-empirical calculations are of interest in light of the known superior treatment of pyridazinediones by PM3 vs. AM1 [\[19,35\]](#). The alternative AM1-SM1a model which requires explicit declaration of atom type, suggested by Cramer and Truhlar for the calculation of heterocyclic tautomerism [\[28\]](#), was not used because of the ambiguous hybridisation of certain atoms in the set, particularly with respect to anions.

Addition of the free-energies of solvation to the gas-phase free energies gives an estimate of the relative free energies of tautomers in aqueous solution at 298.15K. For two tautomers in equilibrium, if the free energies in solution are known to a sufficient degree of accuracy, the tautomeric ratio may be calculated:



From the relative free energies, normalised tautomer ratios (neglecting tautomers of very low concentration) have been calculated by this method, and are presented in [Table 2.6](#).

In principle, assuming one acid produces one base in solution, pK_a or pK_b can be calculated *ab initio* by modelling the following reactions in the gas phase, and correcting with free energy of solvation for each species



The latter reaction has the attraction of equal numbers of charged species on both sides, thus minimising systematic error. Unfortunately, the difficulty of treating different anions equally in the gas phase, and in particular the difficulty of modelling the hydroxide ion, and the difficulty of obtaining sufficiently precise and consistent treatment of ΔG of aqueous solvation across all species preclude the accurate *ab initio* calculation of pK_a by this approach at present.

By making the assumption that systematic errors are consistent across similar systems, we may write the following:

$$\text{pK}_a = k - \log(\exp((G_{\text{HA}} - G_{\text{A}^-})/RT))$$

where k is assumed to be constant across a series of closely related acid-base pairs, and is the sum of systematic errors and free energy terms of neglected species.

Given the tautomeric proportions a_i calculated as above, if a single base gives rise to multiple acid tautomers, this may be extended:

$$\text{pK}_a = k - a_1 \cdot \log(\exp((G_{\text{HA}1} - G_{\text{A}^-})/RT)) - a_2 \cdot \log(\exp((G_{\text{HA}2} - G_{\text{A}^-})/RT)) - \dots$$

Estimations of relative pK_a s by this method are given in [Table 2.7](#).

Some literature pK_a values of closely related systems are given in [Table 2.8](#) for comparison.

Figures

The anions and low energy tautomers optimised at MP2/6-31G(d,p) for each system are presented as spheres of the van der Waals radii. Gas phase free energies of tautomers relative to the anion are indicated in pink, calculated at 298.15K from compound energies ([Table 2.3](#)) Electrostatic potential-derived charges from the Merz-Kollman-Singh scheme are overlaid on atoms in yellow. Dipoles are indicated by overlaid vectors, with units of 1 debye corresponding to distances of 1 angstrom.

[Figure 2.1](#) pyridazine-1,2-dioxide

[Figure 2.2](#) 3-hydroxypyridazine 1-oxide

[Figure 2.3](#) 4-hydroxypyridazine 1-oxide

[Figure 2.4](#) 5-hydroxypyridazine 1-oxide

[Figure 2.5](#) 6-hydroxypyridazine 1-oxide

A key to structures referred to in the text is given in [Chart 2.1](#), and the optimised geometries [indexed](#) as .pdb files.

2.3 Discussion

In order to evaluate these results, discussion of the major sources of error is in order. Smith and Radom [29], and Curtiss *et al.* [30] compare gas phase energies calculated by G2(MP2) and G2(MP2,SVP) with experiment for a large test suite of small acyclic species, including dissociation and ionisation energies, and electron and proton affinities. The relative gas phase energies calculated by the compound method described here should be intermediate in accuracy between G2(MP2) and G2(MP2,SVP). While we are actually considering proton affinities in this work, the test suite only concerned cations in this regard. Hence, electron affinities, incorporating inherently less reliable calculations on anions, are probably a better indication of accuracy. The results obtained were mean absolute deviations (MAD) from experiment of 0.6 Kcal and 0.7 Kcal for the two methods respectively for

proton affinities, and 1.9 and 2.1 Kcal respectively for electron affinities. This gives an indication of the magnitudes of error in comparing the gas-phase acidities of different systems. The accuracy of the relative gas phase free energies of tautomerism, being between neutral tautomeric species within a single system, is likely to be handled somewhat better than this.

Energy calculations on these heterocycles are slow to converge with increasing basis set and correlation method; a glance at [Table 2.4](#) shows variation in qualitative predictions to the highest levels trialed. Very high levels of theory may be necessary to evaluate relative energies to the degree required for accurate prediction of tautomer proportions; a difference of only 1.36 Kcal corresponds to a ten-fold difference in tautomeric ratio. None the less, other than for [3](#), we are confident that the required level of accuracy has been attained for qualitative prediction of gas phase tautomerism.

The highest level calculations performed have been unable to resolve the issue of which tautomer of [3](#) is preferred in the gas phase. Both the *N*-hydroxy [3a](#) and 4-hydroxy [3d](#) structures are low in energy. The qualitative predictions vary with basis set, correlation treatment, and compound method employed. The issue of whether the planar [3a'](#) or non-planar [3a](#) is preferred is also unresolved; larger basis sets seem to favour planar geometry, while better treatment of electron correlation favours non-planar. Optimisation with a larger basis set, i.e. at 6-311+G(d,p) seems to make a small difference, but between structures so close in energy, perhaps a significant one. The inference from these results is that any difference in energy between [3a](#) and [3d](#) is sufficiently small to indicate the likely presence of both structures in the gas phase. Entropy and thermal terms appear to favour [3a](#) over [3d](#) slightly. Concerning the structure of [3a](#): if the planar [3a'](#) actually represents a local maximum (saddle point), as indicated by the HF/6-31G(d) frequency calculation, then the energy barrier of inversion of conformation is exceedingly small. Conversely, if [3a'](#) is lower in energy than [3a](#) as suggested by compound theories, and is a truly a local minimum, then either the hydroxyl rotation out of the plane

and ring puckering is an exceedingly soft vibrational mode, or the compound will display significant populations in both non-planar and planar minima.

By contrast, the energies of tautomers of **2**, **4**, and **5** are sufficiently separated to allow confident prediction of tautomerism. The 3-substituted system **2** shows a clear preference of 3.3 Kcal in the gas phase for the 3-hydroxy tautomer **2c** over the NH oxo-oxo tautomer **2b**, in accordance with the predictions of Itai [11], with all other tautomers being substantially less significant. Also predicted was the preference of **4** for the 5-hydroxy 1-oxide tautomer **4d** over the NH oxo-oxo tautomer **4b**, and this is indeed found to be the case by 6.5 Kcal at 0K. However, it is the *N*-hydroxy-oxo tautomer **4a** which is found to be next lowest in energy, being 4.3 Kcal relative to **4d**. The comparative stability of **4a** was not suggested in Okusa's experimental study [8], and stands in contrast to the much less favoured analogous *N*-hydroxy-oxo tautomer **2a**. 3.3 Kcal separates the *N*-hydroxy-oxo tautomer **5a** from the 6-hydroxy 1-oxide **5d**, in accordance with literature predictions, with no other significant contributing tautomers. Strong intramolecular hydrogen bonding is observed for this species, affecting the conformation, and reversing the normal preference for the HONN dihedral to be 0°. This bonding would also be likely to have implications for physical properties, e.g. solid state where hydrogen bonded dimers are recorded for similar systems, and acidity.

It is also noteworthy that while none of the methylene-containing tautomers appear to contribute significantly to tautomerism - Elguero [24] suggests these are more important in five-membered heterocyclic rings than six - none the less, some methylene tautomers are less unfavourable than expected. For example, 4(3*H*)-pyridazinone 1-oxide **3c** is more stable than the NH isomer, 4(2*H*)-pyridazinone 1-oxide **3b**.

The accurate prediction of solution-phase properties is a much more challenging task than the prediction of gas phase properties, particularly for an aqueous system such as this one, for which hydrogen bonding interactions in the first solvation sheath are likely to be crucial. Of the commonly used methods, molecular dynamics (FEP) treatments generally ignore the effects of solute polarisation, and to a large

extent, solvent polarisation [28], while giving fair treatment of first solvation sheath effects. Conversely, continuum model (SCRF) treatments neglect first solvation sheath effects, but potentially consider polarisation effects accurately. The improvement of continuum models to include a cavity defined by an isodensity surface (IPCM) is recent in origin, and little data exists to indicate how well it handles these kinds of systems. Concern also exists about the suitability of IPCM for calculations on anions due to "charge leakage" which occurs with truncation of wavefunctions as the isodensity cavity is contracted. The semi-empirical SMx models hold the attraction of consideration of both polarisation terms, and through empirical atomic parametrisation, first solvation sheath effects, and are therefore the methods of choice for this problem.

Across the different solvation methods trialed, the estimates of ΔG are generally in fair agreement, with some anomalies (Table 2.5). As expected, the IPCM method shows greater variability, while the semi-empirical models are more concordant. Certain qualitative trends are reversed for IPCM, e.g. the comparison of 3a and 3a', which alters the predicted preferred structure in solution; IPCM predicts the non-planar structure, while SMx more credibly predicts the stabilisation of the planar structure. The solvation energies of the anions also appear to be under-estimated by IPCM compared with semi-empirical methods, as is the solvation of 1, and non-hydroxy tautomers in general. Despite the variability of these figures, the qualitative predictions of tautomer distribution (Table 2.6) remain substantially similar across all methods, with the exception of 3. The quoted [40] RMS errors for neutral species and ions using AM1-SM2 and PM3-SM3, are 0.9 and 4.0, and 1.2 and 5.6 respectively. The indication is that qualitative comparisons from these treatments between tautomers in the aqueous phase are probably valid, except where tautomers lie very close in energy (3). Quantitative estimates, taking into account both gas phase and solution phase errors, may easily be in error by an order of magnitude or more. Comparisons of aqueous acidities between systems, requiring consistent treatment of different anions vs. neutrals, are unlikely to be accurate within 5 Kcal/mol at best. Given that a difference of only 5 Kcal translates to a pK_a difference of 3.7, the quantities in Table 2.7 should be viewed with a great

deal of scepticism; current models are simply unable to make quantitative predictions by this means. The literature only contains a single pK_a value for a hydroxy pyridazine *N*-oxide with which to judge these results - that of **2**, which has been determined to be 4.1 [6]. This would imply pK_a values of well below zero for **3** and **4**, according to the semi-empirical solvation methods, which seems unlikely to be correct. On the other hand, all methods trialed gave the same qualitative predictions of the order of acidity, i.e. pK_a **4** > **3** > **5** > **2**. This prediction can be compared with experimental pK_a values of closely related hydroxy heterocycles (Table 2.8.) Comparing **12** with **13**, and **14** with **15** indicates increased acidity of a hydroxyl in the 4- vs. the 3- position of pyridazine, which is consistent with the prediction of **3** and **4** to be more acidic than **2** and **5**. *N*-oxidation of hydroxy-pyridines causes a substantial drop in pK_a , of between 2.3 and 5.7 units, and *N*-oxidation of **12** to **2** causes a drop of 5.8 units, thus the *N*-oxides of **13**, i.e. **3** and **4**, are expected to be strongly acidic, in accordance with these qualitative predictions. The pK_a of **10**, having a hydroxyl meta- to an *N*-oxide, is 0.5 units higher than that of the ortho- and para- isomers **9** and **11**. This is in accordance with the prediction that **4** is more acidic than **3**, and **5** is more acidic than **2**. Note also, that the predicted relative acidity of **5** increases from the gas phase to solution, compared with other tautomers. This is to be expected if the extra stability of strong intramolecular hydrogen bonding of the neutral species in the gas-phase is diminished in aqueous solution, allowing easier dissociation.

2.4 Conclusion

The literature experimentally-based predictions of the tautomerism of 3-, 5-, and 6-hydroxy-pyridazine 1-oxides **2**, **4**, **5** are confirmed by theory. The hydroxy *N*-oxide tautomers are predicted to be substantially favoured in the case of **2** and **4**, both in solution and in the gas phase. The *N*-hydroxy-oxo tautomer of **5** is predicted to be substantially favoured in both phases, a result suggested by experiments on similar structures. No firm conclusion has been reached regarding 4-hydroxy-pyridazine 1-oxide **3**, nor has sufficient experimental data been found with which to make comparisons. However, it seems likely that in solution both planar *N*-hydroxy and

4-hydroxy tautomers are present in significant quantities. Likewise, in the gas phase, both *N*-hydroxy and 4-hydroxy tautomers are likely to be significant, although the preferred structure of the *N*-hydroxy compound remains unresolved.

2.5 Calculation details

MP4 and QCISD(T) energies were calculated using Molpro 96 [39]. AM1-SM2 and PM3-SM3 were performed using AMSOL 5.4 [40]. All other calculations were performed using Gaussian 94 [41]. Platforms used were SGI R10000 Power Challenge and IBM RS6000.

2.6 Acknowledgments

I acknowledge the NSW Centre for Parallel Computing and the Australian National University Supercomputer Facility for support and donation of computing resources, and Malcolm Gillies for technical support.

2.7 References

1. AG Lenhert, RN Castle, Physical Properties of Pyridazines, *The Chemistry of Heterocyclic Compounds*, Interscience, **28**(1), 2 (1973)
2. C-G Wermuth. *et al.* *J. Med. Chem.*, **30**, 239-249 (1987)
3. T Boulanger *et al.*, *J. Crystallographic and Spectroscopic Research*, **19**(2), (1989)
4. M Brennan, *Chemical and Engineering News*, May 13, **41**, (1996)
5. Yu N Sheinker *et al.*, *J. Chim Phys.*, **55**, 217 (1958); *Chem. Abstr.*, **52**, 16873 (1958)
6. H Igeta, *Chem. Pharm. Bull. (Tokyo)*, **7**, 938 (1959)
7. T Itai, S Natsume, *Chem. Pharm. Bull. (Tokyo)*, **11**, 83 (1963)
8. G Okusa, S Kamiya, *Chem. Pharm. Bull. (Tokyo)*, **16**, 142 (1968)
9. T Nakagome, *Yakugaku Zasshi*, **82**, 244-252 (1962)
10. S Sako, *Chem. Pharm. Bull. (Tokyo)*, **11**, 261 (1963)
11. T Itai, Pyridazine N-oxides, *The Chemistry of Heterocyclic Compounds*, Interscience, **28**(8), 721 (1973)
12. S Sako, *Chem. Pharm. Bull. (Tokyo)*, **11**, 337, (1963); S. Sako, *Yakugaku Zasshi*, **82**, 1208 (1962)
13. T Itai, S Kamiya, *Chem. Pharm. Bull. (Tokyo)*, **11**, 1060, 1063 (1963)

14. H Igeta et al., *Chem. Pharm. Bull. (Tokyo)*, **17**(4), 763-769 (1969)
15. T Itai, S Kamiya, *Chem. Pharm. Bull. (Tokyo)*, **11**, 1073-1077 (1963)
16. JP Maier et al., *Helv. Chim. Acta*, **58**, 1634-1640 (1975)
17. GV Kulkarni et al., *Proc. Indian Acad. Sci.*, **86A**(3), 273-281 (1977)
18. WMF Fabian, *J. Molec. Struct. (Theochem)*, **208**, 295-307 (1990)
19. WMF Fabian, *J. Computational Chem.*, **12**, 17-35 (1991)
20. G La Manna, M Cignitti, *Gazzetta Chimica Italiana*, **102**, 325-329 (1972)
21. G La Manna, F Biondi, *J. Molec. Struct. (Theochem)*, **208**, 57-61 (1990)
22. L Lapinski, J Fulara, R Czaerninski, MJ Nowak, *Spectrochimica Acta*, **46A**(7), 1087-1096 (1990)
23. L Lapinski, *J. Phys. Chem.*, **96**, 6250-6254 (1992)
24. J Elguero, C Marzin, AR Katritzky, P Linda, *The Tautomerism of Heterocycles, Advances in Heterocyclic Chemistry, Supplement 1*, Academic Press (1976)
25. H-J Hofmann, R Cimiraaglia, J Tomasi, R Bonaccorsi, *J. Molec Struct. (Theochem)*, **227** 321-326 (1991)
26. S Miertus et al., *Chem. Phys.*, **55**, 117 (1981)
27. NA Burton, DVS Green, IH Hillier, PJ Taylor, MA Vincent, S Woodcock, *J. Chem. Soc. Perkin Trans. 2*, 331-335 (1993)
28. CJ Cramer, DG Truhlar, *J. Am. Chem. Soc.*, **115**, 8810-8817, (1993)
29. BJ Smith, L Radom, *J. Phys. Chem.*, **99**, 6468-6471 (1995)
30. LA Curtiss et al., *J. Chem. Phys.*, **104**, 13, (1996)
31. LA Curtiss et al., *J. Chem. Phys.*, **98**, 1293 (1993)
32. JB Foresman, TA Keith, KB Wiberg, J Snoonian, MJ Frisch, *J. Phys. Chem.*, **100**(40), 16098-16104 (1996)
33. CJ Cramer, DG Truhlar, *Science*, **256**, 213-217 (1992)
34. CJ Cramer, DG Truhlar, *J. Computational Chem.*, **13**, 1089-1097 (1992)
35. JR Greenwood, G Vaccarella, HR Capper, KN Mewett, RD Allan, GAR Johnston, *J. Molec. Struct. (Theochem)* **368**, 235-243 (1996) Second Electronic Computational Chemistry Conference Proceedings (1996) <http://www.elsevier.nl/locate/eccc2>
36. A Albert, J.N. Phillips, *J. Chem. Soc.*, 1294 (1956)
37. E Shaw, *J. Am. Chem. Soc.*, **71**, 67 (1949)
38. U Wagner, C Kratky, T Kappe, *Monatschfte fur Chemie*, **120**, 329-342 (1989)

39. H-J Verner, PJ Knowles *et al.*, MOLPRO 96.1,
<http://www.tc.bham.ac.uk/molpro/>, *Chem. Phys. Lett.*, **190**, 1 (1992)
40. GD Hawkins *et al.*, AMSOL v-5.4, QCPE Program 606 (1995), based on D.A. Liotard *et al.* AMPAC v-2.1. QCPE Program 506 (1989)
41. MJ Frisch *et al.*, *Gaussian 94*, Rev D.3, Gaussian Inc. Carnegie Office Park, Building 6. Pittsburg, PA 15106 USA.

Table 2.1. Discrimination of favourable conformers at RHF/6-31G(d)

Name	Energy (a.u.)	Name	Energy
2a	-412.29334	4a	-412.29453
2a'	-412.27514	4a'	-412.28151
2c	-412.30854	4d	-412.29677
2c'	-412.29831	4d'	-412.29640
3a (C ₁)	-412.30633	5a	-412.32359
3a' (C _s)	-412.30307	5a'	-412.31483
3d	-412.28906	5d	-412.30545
3d'	-412.28834	5d'	-412.28316

N.B. All structures are minima in C_s symmetry, apart from 3a/3a'; see [text](#) for further details.

Table 2.2. Relative (absolute) energies of all possible tautomers at RHF / 6-31G(d) in Kcal (a.u.)

Name	Symmetry	Energy	Name	Symmetry	Energy
1	C _{2v}	(-412.20302)	3e	C _s	-323.91
2-	C _s	(-411.75091)	3f	C ₁	-280.94
2a	C _s	-340.38	4-	C _s	(-411.75740)
2b	C _s	-350.01	4a	C _s	-337.05
2c	C _s	-349.92	4b	C _s	-335.17
2d	C _s	-335.60	4c	C _s	-326.34
2e	C _s	-337.44	4d	C _s	-338.46
3-	C _s	(-411.74632)	4e	C _s	-331.45
3a	C ₁	-351.41	5-	C _s	(-411.73895)
3a'	<u>C_s</u>	-349.37	5a	C _s	-366.87
3b	C _s	-318.57	5b	C _s	-324.99
3c	C _s	-330.02	5c	C ₁	Not optimised
3d	C _s	-340.57	5d	C _s	-355.48

3a': One imaginary frequency at RHF / 6-31G(d); see text

5c: High energy minimum found at RHF / 3-21G in C₁ symmetry, but not at RHF / 6-31G(d)

Table 2.3. Structures¹, relative (absolute) compound energies², and relative (absolute) free energies³ of low energy tautomers

Name	E0	G	Name	E0	G
1	(-413.88799)	(-413.91716)	3d	-327.79	-328.26
2-	(-413.43647)	(-413.45429)	4-	(-413.43990)	(-413.46982)
2a	-323.47	-331.33	4a	-320.75	-321.03
2b	-330.51	-338.34	4b	-318.50	-319.01
2c	-333.83	-341.46	4c	-315.95	-311.22
2d	-315.83	-324.52	4d	-325.04	-325.16
2e	-317.13	-325.41	4e	-313.10	-313.81
3-	(-413.43020)	(-413.46017)	5-	(-413.43415)	(-413.46412)
3a	-327.47	-328.03	5a	-339.88	-340.12
3a'	-327.74	-328.09	5d	-336.59	-336.49
3c	-311.77	-312.72			

Notes

1. All structures optimised at MP2 / 6-31G(d,p)

2. Compound energies: $E_0 = E\{\text{MP2} / 6-311++G(3df,3pd)\} + E\{\text{QCISD}(T) / 6-31G(d,p)\} - E\{\text{MP2} / 6-31G(d,p)\} + 0.8929 * \text{ZPE}\{\text{HF} / 6-31G(d)\}$

Relative energies in Kcal with respect to conjugate base anion.

Absolute energies in Hartree in parentheses.

Lowest energies shown in bold

3. Gibbs free energies calculated at 298.15K by correcting E0 with thermochemical data calculated at HF / 6-31G(d) scaled by 0.8929.

Table 2.4: High level gas-phase calculations of 4-hydroxy-pyridazine 1-oxide tautomers. Absolute energies (a.u.)¹

Name	MP2 / 6-31G (d,p)	MP2 / 6-311G (d,p)	MP2 / 6-311+G (d,p)	opt MP2 / 6-311+G (d,p) ¹	MP2 / 6-311G (2df,p)	MP2 / 6-311+G (3df,2p)	MP2 / 6-311++G (3df,3pd)
3a(C1)	-413.52188	-413.68659	-413.70682	-413.70710	-413.90550	-413.94931	-413.95751
3a'(Cs)	-413.52180	-413.68609	-413.70589	-413.70610	-413.90587	-413.94962	-413.95781
3d	-413.52619	-413.68815	-413.70965	-413.70983	-413.91033	-413.95566	-413.96405

Name	MP4 / 6-311G(d,p)	MP4 / 6-311+G(d,p)	MP4 / 6-311G(2df,p)	QCISD(T)/ 6-31G(d,p)	QCISD(T)/ 6-311G(d,p)
3a(C1)	-413.77684	-413.79797	-414.00456 ⁵	-413.59872	-413.76735
3a'(Cs)	-413.77589	-413.79657	-414.00449	-413.59795	-413.76622
3d	-413.77544	-413.79785	-414.00621	-413.59720	-413.76318

Name	E0 compound ²	G2(MP2,**) ³	G2(MP2,++) ⁴	G2(**) ³	G2(++) ⁴	Best free energies ⁶
3a(C1)	-413.95206	-414.05278	-413.95598	-414.03891	-413.94211	0 Kcal
3a'(Cs)	-413.95248	-414.05327	-413.95646	-414.03902	-413.94221	0.13 Kcal
3d	-413.95256	-414.05320	-413.95659	-414.03885	-413.94224	0.00 Kcal

Notes

- All calculations performed using MP2/6-31G(d,p) geometry except MP2/6-311+G(d,p) optimisation. Lowest energies (Hartree) indicated in bold.
- E0 compound: Modified G2(MP2,SVP) theory neglecting ΔE^{HLC} . As used for all other structures. See [Table 2.3](#) for definition
- ** Modified G2 and G2(MP2) theories: Geometries at MP2/6-31G(d,p) substituted for MP2(full)/6-31g(d) throughout. $\Delta E^{\text{HLC}} = -0.105$ for all structures
- ++ Extended G2 and G2(MP2) theories: Geometries at MP2/6-31G(d,p). E{MP2/6-311++G(3df,3pd)} substituted for E{MP2/6-311+G(2df,p)}. ΔE^{HLC} is neglected.
- Calculation of energy of 3a at MP4/6-311G(2df,p) prohibitively expensive. Approximation used:

$$E\{3a,MP4/6-311G(2df,p)\} \sim E\{3a,MP4/6-311G(d,p)\} + E\{3a,MP2/6-311G(2df,p)\} - E\{3a,MP2/6-311G(d,p)\} - E\{3a',MP2/6-311G(2df,p)\} + E\{3a',MP2/6-311G(d,p)\} + E\{3a',MP4/6-311G(2df,p)\} - E\{3a',MP4/6-311G(d,p)\}$$
- Relative gas phase free energies at 298.15K in Kcal, from HF/6-31G(d) thermochemistry and G2(++) theory

Table 2.5. Free energies of solvation (Kcal/mol)

Name	IPCM ¹	AM1-SM2// MP2/6- 31G(d,p) ²	AM1-SM2 ³	PM3-SM3// MP2/6- 31G(d,p) ⁴	PM3-SM3 ⁵
1	-6.66	-14.52	-16.28	-14.63	-16.10
2-	-63.56	-68.92	-68.27	-65.65	-65.23
2a	-13.73	-15.80	(-17.18) ⁶	-14.44	-15.00
2b	-8.68	-9.30	(-9.53) ⁶	-11.73	-12.25
2c	-11.54	-13.72	(-13.09) ⁶	-13.63	-13.89
2d	-9.93	-11.60	-11.89	-15.92	-16.57
2e	-10.34	-10.51	-11.13	-13.29	(-14.76) ⁶
3-	-60.08	-68.52	-68.70	-66.99	(-68.14) ⁶
3a	-16.79	-14.06	-12.47	-15.20	-12.90
3a'	-10.96	-14.20	-14.33	-15.03	-14.61
3c	-7.18	-10.99	-11.41	-14.51	-16.07
3d	-16.18	-14.95	-14.78	-15.74	-16.28
4-	-58.53	-66.32	-66.48	-65.74	-66.06
4a	-9.31	-13.48	(-14.25) ⁶	-14.37	(-14.22) ⁶
4b	-12.77	-14.03	(-14.88) ⁶	-18.07	-17.11
4c	-8.06	-12.03	-12.64	-17.61	-17.51
4d	-14.59	-14.49	-14.02	-15.34	-15.75
4e	-7.20	-8.48	-8.74	-11.51	-13.04
5-	-61.15	-74.44	-74.59	-71.95	-72.66
5a	-8.62	-11.18	(-14.75) ⁶	-11.60	-14.08
5d	-7.45	-14.21	-14.90	-13.54	-16.66

Notes:

1. Isodensity polarised continuum model: Dielectric constant = 78.4. Isodensity value = 0.001.

$\Delta G = E\{\text{MP2/6-31G(d,p)}, \text{IPCM} // \text{MP2/6-31G(d,p)}\} - E\{\text{MP2/6-31G(d,p)}\}$

2. AM1-SM2 model: $\Delta G = H_r(\text{AM1-SM2}) - H_r(\text{AM1})$, single point energies at MP2/6-31G(d,p) geometries

3. AM1-SM2 model: $\Delta G = H_r(\text{AM1-SM2}) - H_r(\text{AM1})$, full electronic and geometry relaxation.

4. PM3-SM3 model: $\Delta G = H_r(\text{PM3-SM3}) - H_r(\text{AM1})$, single point energies at MP2/6-31G(d,p) geometries

5. PM3-SM3 model: $\Delta G = H_r(\text{PM3-SM3}) - H_r(\text{AM1})$, full electronic and geometry relaxation.

6. AM1-SM2 or PM3-SM3 geometry optimisation failure. Energies stable, but maximum gradients remain above cutoff. Probably not significant.

Table 2.6. Estimated normalised tautomer ratios¹ in gas phase and aqueous solution.

Name	Gas phase	IPCM	AM1-SM2//MP2/6-31G(d,p)	AM1-SM2	PM3-SM3//MP2/6-31G(d,p)	PM3-SM3
<u>1</u>	1.	1.	1.	1.	1.	1.
<u>2a</u>	3.7E-08	1.5E-6	1.3E-06	3.8E-5	1.47E-07	2.5E-7
<u>2b</u>	0.0052	4.1E-5	3.0E-06	1.3E-5	2.1E-4	3.3E-4
<u>2c</u>	0.9948	0.99996	1.	0.99995	0.99979	0.9997
<u>2d</u>	3.8E-13	2.5E-14	1.1E-14	5.0E-14	1.8E-11	3.5E-11
<u>2e</u>	1.7E-12	2.2E-13	7.6E-15	6.3E-14	9.5E-13	7.5E-12
<u>3a</u> ²	0.59	0.65	0.27	0.27	0.34	0.046
<u>3c</u>	1.7E-12	3.6E-19	3.7E-15	1.0E-14	3.4E-13	2.8E-12
<u>3d</u>	0.41	0.35	0.73	0.73	0.66	0.954
<u>4a</u>	9.4E-4	1.3E-7	1.7E-04	1.4E-3	1.8E-4	7.1E-5
<u>4b</u>	3.1E-05	1.4E-6	1.5E-05	1.3E-4	0.0031	3.1E-4
<u>4c</u>	6.1E-11	9.9E-16	9.6E-13	5.9E-12	2.8E-09	1.2E-9
<u>4d</u>	0.9990	1.	0.99981	0.9985	0.9967	0.9996
<u>4e</u>	4.8E-09	1.8E-14	1.9E-13	6.5E-13	7.5E-12	4.9E-11
<u>5a</u>	0.9978	0.9996	0.74	0.997	0.946	0.86
<u>5d</u>	0.0022	3.0E-4	0.26	2.8E-3	0.054	0.14

Notes:

1. $[HA_2]/[HA_1] = \exp((G_1 - G_2)/RT)$; $G = G_{298.15, gas} + \Delta G_{solv}$

2. The planar conformer of 1-hydroxy-3(1H)-pyridazinone 3a' is predicted to be favoured in solution by AM1-SM2 and PM3-SM3, and the non-planar conformer 3a by IPCM. The figures given are the sum of the predicted proportions of both conformers.

Table 2.7. Estimated relative¹ pK_as of isomers.

Isomer	gas phase	IPCM	AM1-SM2//MP2/6-31G(d,p)	AM1-SM2	PM3-SM3//MP2/6-31G(d,p)	PM3-SM3
2	0.	0.	0.	0.	0.	0.
3	-9.8	-3.6	-8.7	-8.9	-9.3	-10.1
4	-11.9	-6.0	-9.5	-10.0	-10.8	-11.2
5	-1.0	-1.4	-7.0	-4.4	-7.2	-6.4

Notes:

1. Calculated relative to isomer 2; $\Delta pK_a = \Delta[-0.4343 \cdot \sum_i \{a_i \cdot (G_{HA_i} - G_A)/RT\}]$

Table 2.8. Literature pK_as of related structures

Name	Structure	pK _a	Reference
2-hydroxy pyridine	6	11.6	[36]
3-hydroxy pyridine	7	8.7	[36]
4-hydroxy pyridine	8	11.1	[36]
2-hydroxy pyridine 1-oxide	9	5.9	[37]
3-hydroxy pyridine 1-oxide	10	6.4	[37]
4-hydroxy pyridine 1-oxide	11	5.9	[37]
3-hydroxy pyridazine	12	10.5	[36]
4-hydroxy pyridazine	13	8.7	[36]
3,5-dihydroxy pyridazine	14	4.8	[38]
3,6-dihydroxy pyridazine	15	5.7	[36]
3-hydroxy pyridazine 1-oxide	2	4.1	[6]

Figure 2.1 pyridazine 1,2-dioxide

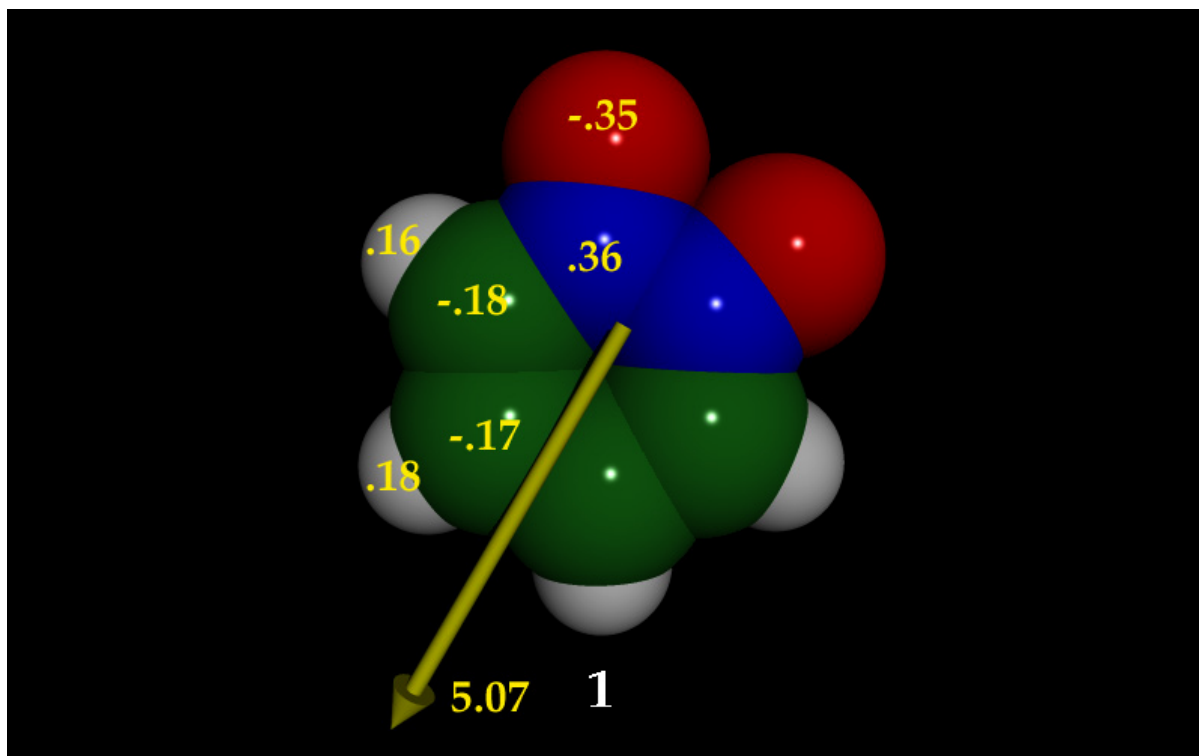


Figure 2.2 3-hydroxypyridazine 1-oxide

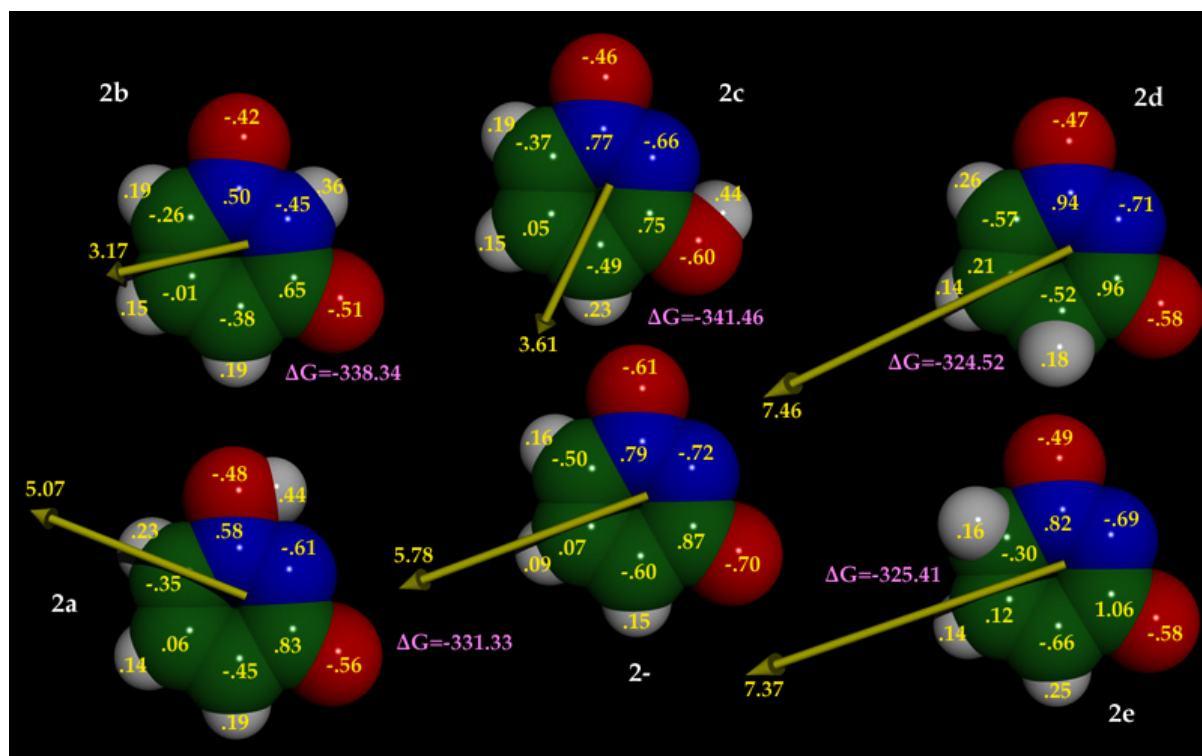


Figure 2.3 4-hydroxypyridazine 1-oxide

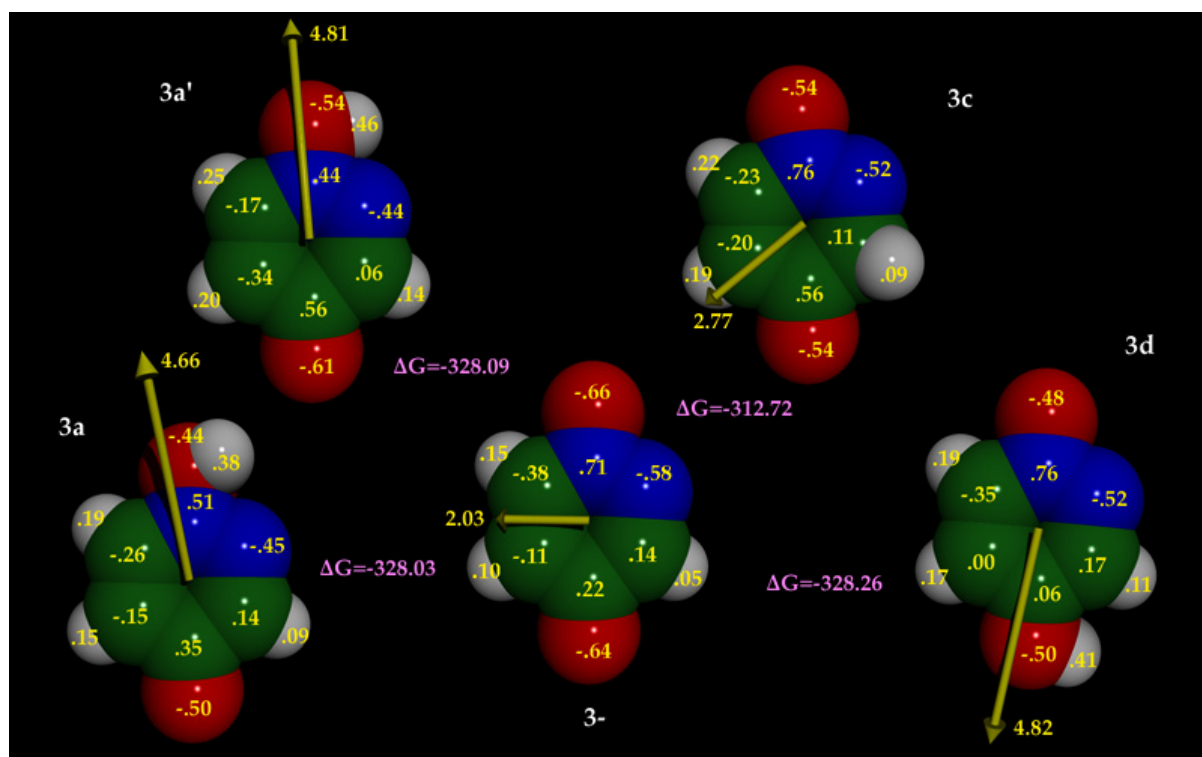


Figure 2.4 5-hydroxypyridazine 1-oxide

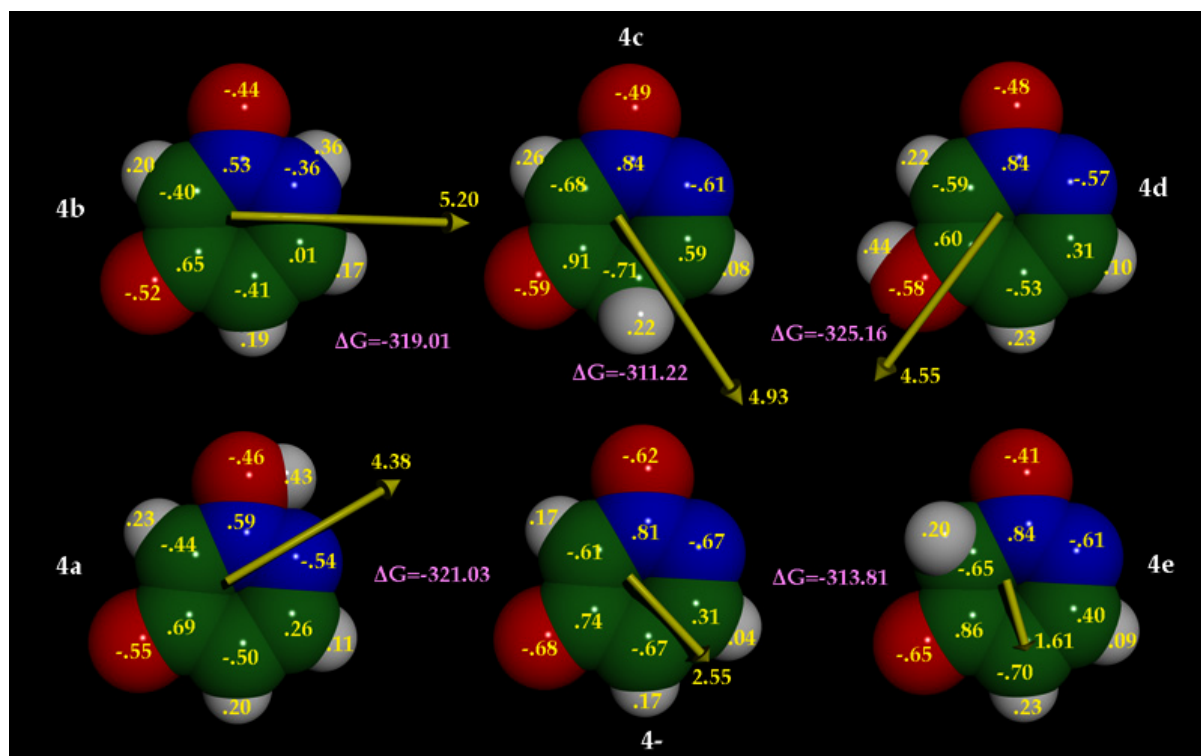


Figure 2.5 6-hydroxypyridazine 1-oxide

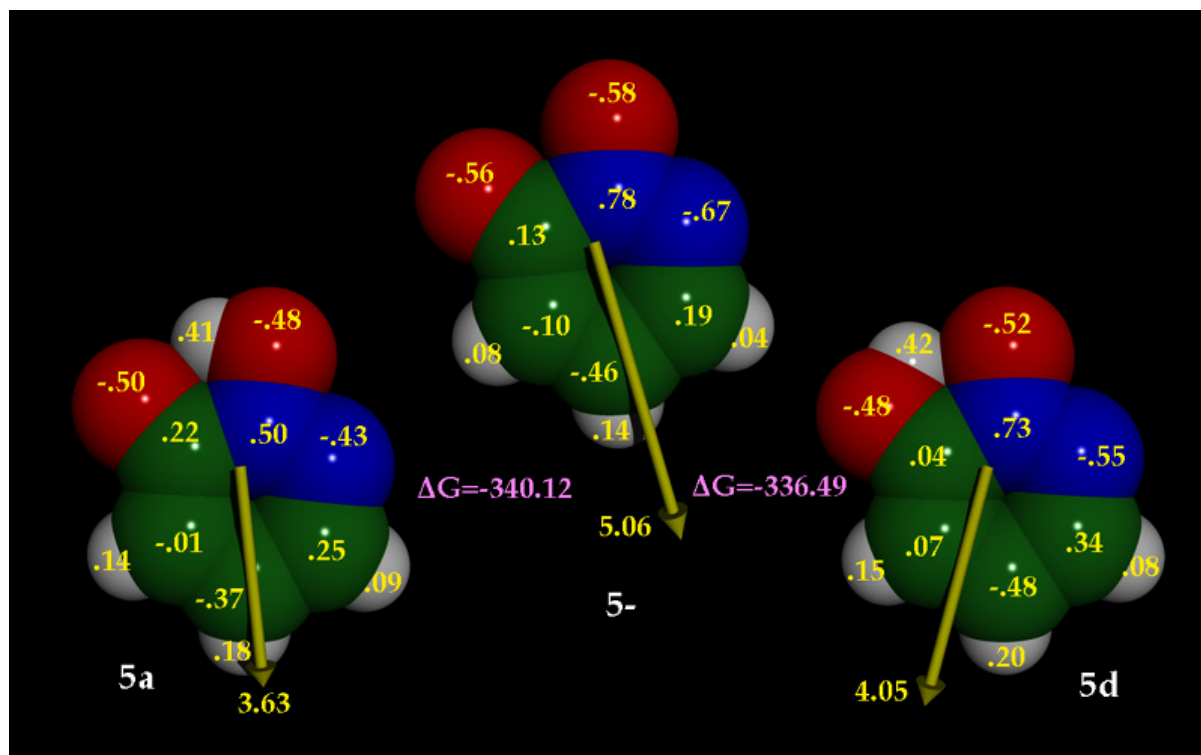
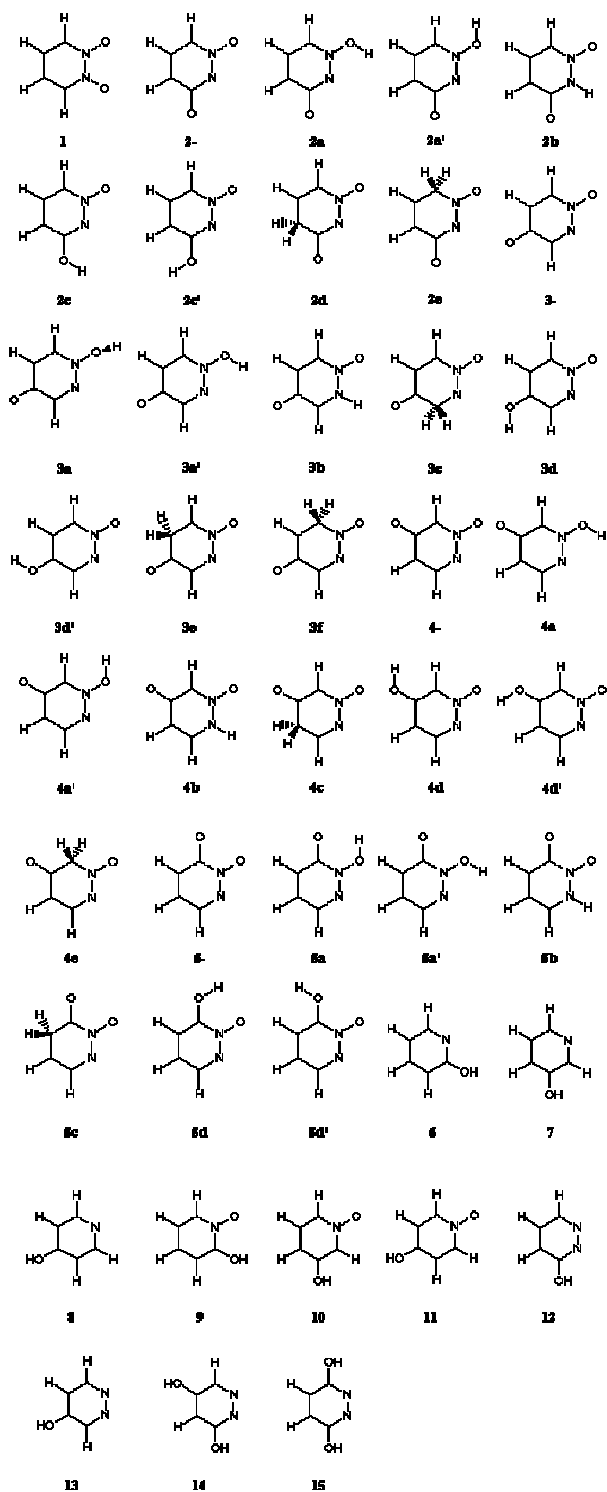


Chart 2.1: All structures referred to in Chapter 2

Optimised geometries at HF / 6-31G(d) and MP2 / 6-31G(d,p) linked.



Index of optimised geometries from chapter 2.

[1 HF/6-31G\(d\) \(12-34566.pdb\)](#)
[1 MP2 / 6-31G\(d,p\) \(12-3456m.pdb\)](#)
[2a HF/6-31G\(d\) \(13-14566.pdb\)](#)
[2a MP2 / 6-31G\(d,p\) \(13-1456m.pdb\)](#)
[2a' HF/6-31G\(d\) \(13-1456a.pdb\)](#)
[2b HF/6-31G\(d\) \(13-24566.pdb\)](#)
[2b MP2 / 6-31G\(d,p\) \(13-2456m.pdb\)](#)
[2c HF/6-31G\(d\) \(13-34566.pdb\)](#)
[2c MP2 / 6-31G\(d,p\) \(13-3456m.pdb\)](#)
[2c' HF/6-31G\(d\) \(13-3456a.pdb\)](#)
[2d HF/6-31G\(d\) \(13-44566.pdb\)](#)
[2d MP2 / 6-31G\(d,p\) \(13-4456m.pdb\)](#)
[2- HF/6-31G\(d\) \(13-456-6.pdb\)](#)
[2- MP2 / 6-31G\(d,p\) \(13-456-m.pdb\)](#)
[2e HF/6-31G\(d\) \(13-45666.pdb\)](#)
[2e MP2 / 6-31G\(d,p\) \(13-4566m.pdb\)](#)
[3a HF/6-31G\(d\) \(14-13561.pdb\)](#)
[3a' HF/6-31G\(d\) \(14-1356s.pdb\)](#)
[3a MP2 / 6-31G\(d,p\) \(14-135m1.pdb\)](#)
[3a' MP2 / 6-31G\(d,p\) \(14-135ms.pdb\)](#)
[3b HF/6-31G\(d\) \(14-23566.pdb\)](#)
[3c HF/6-31G\(d\) \(14-33566.pdb\)](#)
[3c MP2 / 6-31G\(d,p\) \(14-3356m.pdb\)](#)
[3d HF/6-31G\(d\) \(14-34566.pdb\)](#)
[3d MP2 / 6-31G\(d,p\) \(14-3456m.pdb\)](#)
[3d' HF/6-31G\(d\) \(14-3456a.pdb\)](#)
[3e HF/6-31G\(d\) \(14-35566.pdb\)](#)
[3- HF/6-31G\(d\) \(14-356-6.pdb\)](#)
[3- MP2 / 6-31G\(d,p\) \(14-356-m.pdb\)](#)
[3f HF/6-31G\(d\) \(14-35666.pdb\)](#)
[4a HF/6-31G\(d\) \(15-13466.pdb\)](#)
[4a MP2 / 6-31G\(d,p\) \(15-1346m.pdb\)](#)
[4a' HF/6-31G\(d\) \(15-1346a.pdb\)](#)
[4b HF/6-31G\(d\) \(15-23466.pdb\)](#)
[4b MP2 / 6-31G\(d,p\) \(15-2346m.pdb\)](#)
[4c HF/6-31G\(d\) \(15-34466.pdb\)](#)
[4c MP2 / 6-31G\(d,p\) \(15-3446m.pdb\)](#)
[4d HF/6-31G\(d\) \(15-34566.pdb\)](#)
[4d MP2 / 6-31G\(d,p\) \(15-3456m.pdb\)](#)
[4d' HF/6-31G\(d\) \(15-3456a.pdb\)](#)
[4- HF/6-31G\(d\) \(15-346-6.pdb\)](#)
[4- MP2 / 6-31G\(d,p\) \(15-346-m.pdb\)](#)
[4e HF/6-31G\(d\) \(15-34666.pdb\)](#)
[4e MP2 / 6-31G\(d,p\) \(15-3466m.pdb\)](#)
[5a HF/6-31G\(d\) \(16-13456.pdb\)](#)
[5a MP2 / 6-31G\(d,p\) \(16-1345m.pdb\)](#)
[5a' HF/6-31G\(d\) \(16-1345a.pdb\)](#)
[5b HF/6-31G\(d\) \(16-23456.pdb\)](#)
[5- HF/6-31G\(d\) \(16-345-6.pdb\)](#)
[5- MP2 / 6-31G\(d,p\) \(16-345-m.pdb\)](#)
[5d HF/6-31G\(d\) \(16-34566.pdb\)](#)
[5d MP2 / 6-31G\(d,p\) \(16-3456m.pdb\)](#)
[5d' HF/6-31G\(d\) \(16-3456a.pdb\)](#)

3. The tautomerism of pyridazinediones

Abstract

Pyridazine-3,6-dione, maleic hydrazide (**3**), is one of the best known pyridazine derivatives, and has been the subject of several theoretical investigations. Its three positional isomers, pyridazine-3,4-dione (**1**), pyridazine-3,5-dione (**2**), and pyridazine-4,5-dione (**4**), while apparently known synthetically, have received comparatively little attention. These isomers, being relatively strong acids, are potential heteroaromatic carboxylate bioisosteres, and of interest in the design of novel bioactive agents. Both the isomers and their conjugate base anions may potentially exist in a large number of tautomeric forms: ten acid and five basic forms of **1**, fifteen and six of **2**, nine and three of **3**, and nine and three of **4**, respectively, many of which are potentially conformationally flexible. This chapter presents a thorough theoretical investigation of the four systems, employing extended basis set G2(MP2,SVP) theory *ab initio* calculations to model gas phase behaviour, and Isodensity Polarised Continuum Model and semi-empirical AM1-SM2 and PM3-SM3 calculations to model aqueous and pK_a behaviour. Existing solid-phase data are compared with theoretical predictions, and found to be in good agreement. The well-documented lactam-lactim form of **3** predominates, and the lactam-hydroxy tautomer of **2** is prominent, the hydroxyl proton being most acidic in both cases. However, in the gas phase, a non-aromatic diketo 4,4 diprotonated tautomer of **2** is found to be relatively stable, and in aqueous phase, AM1-SM2 theory predicts the stability of a 1-hydro, lactim-keto zwitterionic tautomer of **2**. Hydroxy-keto tautomers are found to predominate in both gas phase and aqueous phase for **4**, with a zwitterionic 1-hydro, 4-hydroxy form preferentially stabilised in aqueous phase. Strong intramolecular hydrogen bonding is observed, with preferential loss of the labile ring proton to form the base of **4**. The tautomerism of **1** is found to be particularly complex, although again, hydroxy-keto acid forms are favoured in both gas and aqueous phases, zwitterions being preferentially stabilised in water. Hydroxyl proton loss from **1** is favoured in both phases, although intramolecular hydrogen bonding stabilises a hydroxy-keto anion in the gas phase. **2** is predicted to be the strongest acid of the series, but no confident prediction of the relative acidities of **1**, **3** and **4** can be made, other than that they are of similar pK_a. Comparisons with the known pK_a behaviour of series of closely related pyridazinones and pyridones are made.

"The tautomerism of pyridazinediones" JR Greenwood, HR Capper, RD Allan and GAR Johnston. [Internet Journal of Chemistry](#) 1, 21 (1998)

Index

[3.1. Introduction](#)

[3.2. Methods and results](#)

[3.2.1. Generation of tautomers and conformers](#)

[3.2.2. Discrimination of preferred conformers and low energy tautomers](#)

[3.2.3. Calculation of gas phase geometries](#)

[3.2.4. Calculation of gas phase energies](#)

[3.2.5. Calculation of aqueous phase properties](#)

[3.3. Key to Tables, Charts, Figures and geometries](#)

[3.4. Discussion](#)

[3.4.1. Conformation](#)

[3.4.2. Structure determination](#)

[3.4.3. Gas phase tautomerism predictions](#)

[3.4.4. Solvation effects according to different models](#)

[3.4.5. Aqueous phase tautomerism](#)

[3.4.6. *Ab initio* prediction of relative \$pK_a\$](#)

[3.5. Conclusion](#)

[3.6. Calculation details](#)

[3.7. References](#)

3.1. Introduction

As a class, the pyridazines are the least well studied and understood of the six-membered diazines [1]. One of the best known pyridazine derivatives is maleic hydrazide, or 6-hydroxy-3(2*H*)-pyridazinone **3**, due to its ease of synthesis and commercial use as a plant-growth inhibitor [1,2]. Its unusual lactam-lactim

tautomeric behaviour has been the subject of several experimental studies and reviews [1,3-10] and has long been a favoured test case for theoretical methods [11-15].

By comparison, the three positional isomers of **3**, those pyridazines having two potential hydroxy groups in positions 3,4 (**1**), 3,5 (**2**) and 4,5 (**4**), have received little attention. The synthesis of **2**, its pK_a , and X-ray crystal structure, have been extensively studied by Wagner *et al.* [16], but only low level *ab initio* (HF / 3-21G) and semi-empirical gas phase theoretical studies have been conducted on this system [12,13]. Less well known still are **1** and **4**, which are previously unstudied theoretically, other than a cursory treatment of **4** by Gastmans *et al.* [11]. Both the synthesis [17] and biosynthesis [18] of **4** as a metabolite of pyridazine have been described, but its structure and tautomerism have remained unexplored. While the synthesis of **1** has been claimed in a patent [19], the lack of physical data, and of other references to **1** in the literature, cast doubt on this claim. Near derivatives of **1** such as its 2-methyl derivative [20] and the immediate precursor, 4-chloro-3(2*H*)-pyridazinone [21,22] are known.

The pyridazinones are of increasing interest as frameworks for novel bioactive molecules [23,24]. Isosterism for biochemical bases, phenyl groups, and acids have led to applications as wide ranging as antibiotics [25], insecticides [26], plant-growth regulators [2], herbicides [27] and neuroactive agents [28-30] to name a few. The interest in these structures here stems from observations [31], [Chapters 7, 8], that several derivatives of 3(2*H*)-pyridazinone show activity at subtypes of Excitatory Amino Acid (glutamate) neuroreceptors, the pyridazinone base anion forming a carboxylate bioisostere.

The tautomerism of oxygen-substituted azines is a long studied field in its own right, as well as being of importance to the understanding of the many bioactive materials which fall into this class [3]. The tautomeric behaviour of the pyridazinediones is particularly rich and complex on account of the many potential structures which **1** to **4** may adopt (Charts 3.1, 3.2, 3.3 and 3.4).

This study employs methods pioneered by Cramer *et al.* [32] for treatment of heterocyclic tautomerism of this kind, with emphasis on the need for high level *ab initio* calculations to consistently treat atoms of varying hybridisation, and the relative success of semi-empirical solvation models for probing the aqueous behaviour of tautomers.

The existing *ab initio* calculations on maleic hydrazide **3** [12-15] are extended to higher levels of theory and larger basis sets, and these methods are applied to the positional isomers **1**, **2** and **4**. Semi-empirical and isodensity polarised continuum models (I-PCM) of aqueous solvation are used, where previous work has modelled solvation using an ellipsoidal Onsage cavity model, free energy perturbation (molecular dynamics simulation), and polarised continuum models [14,15]. No theoretical work appears to have previously examined the anionic conjugate bases of these structures, **1-** to **4-**, themselves capable of tautomerism. These are considered here, on account of their likely prevalence at physiological pH, and hence biological importance.

[Chapter 2](#) reported high-level *ab initio* gas phase and semi-empirical aqueous phase modelling of the four closely related potential hydroxy pyridazine 1-oxides **15**, **16**, **17**, **18**, their conjugate base anions, and pyridazine 1,2-dioxide **19** [33], discussing the methods used here and their limitations in some detail. This treatment of **1** to **4** completes the series of theoretical studies on the nine doubly oxygen-substituted pyridazines.

3.2. Methods and Results

Ab initio Hartree-Fock theory, and electron correlated methods, second order Møller-Plesset perturbation theory (MP2), and Quadratic Configuration Interaction theory (QCISD(T)) [34] were used to probe the gas-phase structure and tautomerism of **1** to **4** and their conjugate bases. Aqueous phase behaviour was studied by both *ab initio* (Isodensity Polarised Continuum Model (I-PCM) [35] and semi-empirical (AM1-SM2 and PM3-SM3) [36] solvation models.

3.2.1 Generation of neutral and conjugate base anion tautomers and conformers

Following the description of heterocyclic tautomerism given by Elguero *et al.* [3], a complete set of tautomers of **1** to **4** and their conjugate bases were generated. All structures were initially built with planar geometry. Firstly, each pair of non-substituted pyridazine ring carbons were assumed to be at least singly protonated. Addition of a single proton to either ring nitrogen, either oxygen substituent, or any carbon located α - to an oxygen substituent (forming a methylene), neglecting repetition through symmetry, generates all possible anionic tautomers: **1-a** to **1-e**, **2-a** to **2-f**, **3-a** to **3-c**, **4-a** to **4-c** (see [Charts 3.1](#), [3.2](#), [3.3](#), [3.4](#)). Addition of a second proton to remaining unsubstituted nitrogens, oxygens, or α - ring carbons of each of these anions, and neglecting repetition through symmetry, generates all possible neutral tautomers **1a** to **1j**, **2a** to **2o**, **3a** to **3i**, **4a** to **4i** (see [Charts 3.1](#) to [3.4](#)). Structures containing one or two hydroxyls are capable of conformational flexibility. Two to four initial structures with hydroxyls rotated 180° were generated respectively in these cases (indicated as ', ', "' in [Charts 3.1](#) to [3.4](#)) for a complete set of planar conformers.

3.2.2 Discrimination of preferred conformers and low energy tautomers

Optimisations of all conformers and tautomers were attempted at the HF / 6-31G(d) level, initially with planar geometry, with frequency calculations to determine minima. Those structures not at a minimum (having at least one imaginary frequency) were re-optimised with reduced symmetry, with optimisation failures occurring for six structures: **1h'**, **3-b'**, **3c**, **3f**, **3f** and **4i'**. The results are summarised in [Table 3.1](#) and [Table 3.2](#). In the case of **3c**, no stable ring closed form could be found, the system optimising to an open ketene in both planar and unrestricted geometries, under both Berny and Fletcher-Powell optimisation schemes. In the cases of **3f** and **3f**, no stable pyridazine structure could be found, ring contraction to a bicyclic system occurring in both planar and unrestricted geometries under optimisation. The other optimisation failures were the result of the conformation specified being a maximum, and optimising to a lower energy conformation in unrestricted symmetry.

All conformers with energies above the minimum energy conformer for each tautomer at this level of theory and basis set were discarded from the set of structures under investigation. Likewise, those anionic or neutral tautomers with energies greater than 25 Kcal/mol above the lowest energy anion or neutral tautomer respectively were also discarded as being unlikely to play a significant role in tautomerism, [14,33].

3.2.3 Calculation of gas phase geometries

The remaining tautomers were optimised at MP2 / 6-31G(d,p). Inclusion of electron correlation causes substantial differences in the preferred structures of certain tautomers. In order to test for geometry convergence with respect to basis set, [3-a](#), [3a](#), [3b](#) and [3h](#) were optimised at MP2 / 6-311+G(2d,p), and compared with MP2 / 6-31G(d) optimised structures in [Table 3.3](#). The differences were found to be very small for [3-a](#), [3b](#) and [3h](#), and somewhat larger in the case of [3a](#) (RMS change = 0.015 Å). All calculated geometries are accessible via [Charts 3.1](#), [3.2](#), [3.3](#) and [3.4](#), and the [index of geometries](#).

[Tables 3.4](#) and [3.5](#) show a comparison of the calculated and experimental (X-ray crystal) geometries of tautomers [2h](#) [16] and [3b](#) [37, 38]. The positions of heavy atoms are in good agreement (RMS = 0.030 Å for [2h](#), and RMS = 0.028 Å and 0.029 Å for the polymorphs MH2 and MH1 of [3b](#) described).

3.2.4 Calculation of high level gas phase energies

[Table 3.2](#) includes the base level energies of optimised structures at MP2 / 6-31G(d,p). Those anionic and neutral tautomers found to be in excess of 20 Kcal/mol higher in energy relative to minimum energy anionic or neutral tautomers respectively were again discarded from the set as being unlikely to contribute significantly to tautomerism. The remaining structures were subjected to single point energy calculations, both with a large basis set employing both high angular momentum and diffuse functions on all atoms (MP2 / 6-311++G(3df,3pd)) and with a higher level treatment of electron correlation (QCISD(T) / 6-31G(d,p)). The combination of these two corrections to the base energy, with the addition of the

scaled zero point energy calculated at HF / 6-31G(d) gives a compound gas phase energy E_0 . This method is comparable [33] to G2(MP2) [39] and G2(MP2,SVP) [40] theories, although neglecting the higher level correlation energy, ΔE^{HLC} , a term which cancels for relative energies calculated for the structures under investigation. Thermochemistry calculated at HF / 6-31G(d,p) was then used to calculate free energies at 298.15K. These results are shown in [Table 3.2](#), and summarised in [Figure 3.1](#).

In addition, the same high level gas phase calculations were conducted on [3-a](#), [3a](#), [3b](#) and [3h](#), optimised at MP2 / 6-311+G(2d,p), to test for the effect of increased basis set optimisation on single point energies. This was found to be insignificant (0.19 Kcal/mol maximum change in relative energies). These results are shown in [Table 3.3](#).

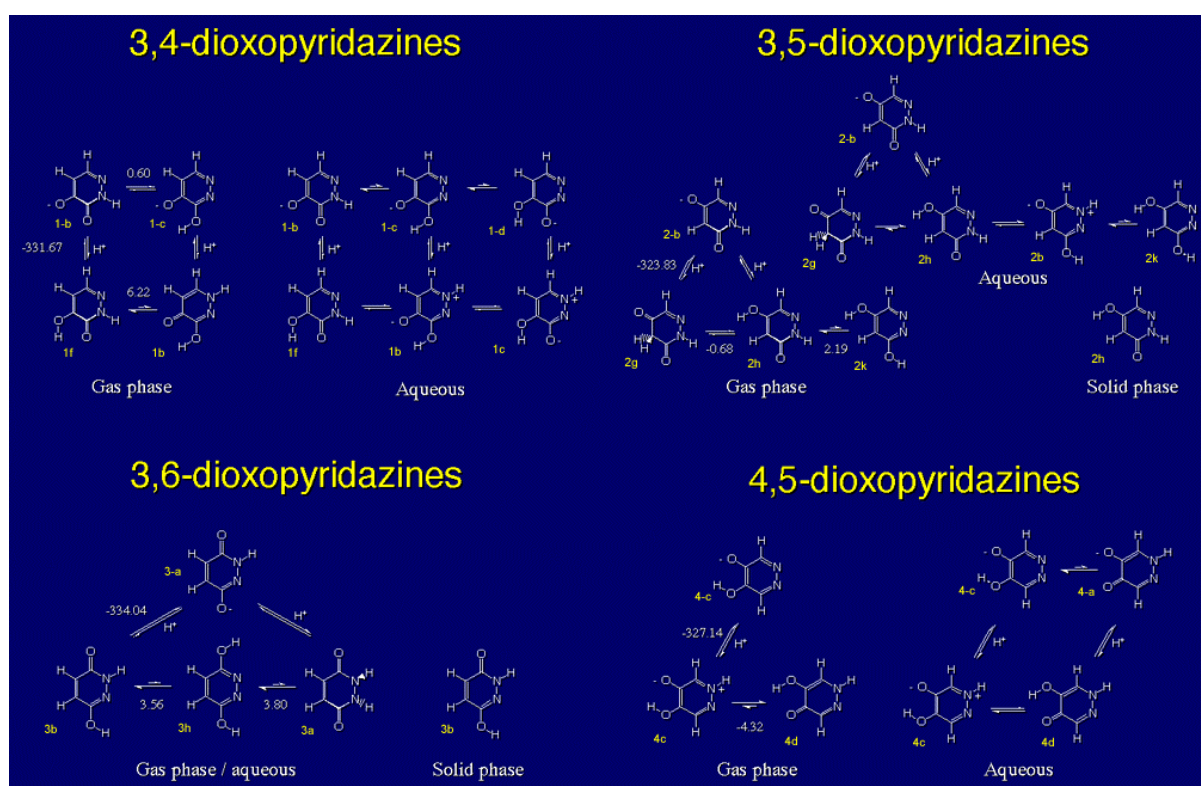
3.2.5 Calculation of free energies of aqueous solvation, and solution phase properties

Free energies of aqueous solvation ([Table 3.6](#)) were calculated by five methods: Single point energies using the I-PCM model [35] with an isodensity cutoff of 0.001 and a dielectric constant of 78.4, and the semi-empirical solvation methods AM1-SM2 and PM3-SM3 [36], with and without geometry optimisation. Addition of free energies of solvation to gas phase free energies at 298.15K gives free energies in solution, from which were estimated tautomer ratios by normalising equilibrium constants separately for both neutral and basic tautomers ([Table 3.7](#)). Aqueous tautomerism is summarised in [Figure 3.1](#). Combining tautomer ratios with free energies gives overall free energy differences between neutral acidic tautomer systems and their anionic conjugate bases, from which may be estimated relative pK_a values ([Table 3.8](#)).

3.3. Key to charts, tables and figures, and geometries

Chart 3.1	3,4-substituted structures, 1
Chart 3.2	3,5-substituted structures, 2
Chart 3.3	3,6-substituted structures, 3
Chart 3.4	4,5-substituted structures, 4
Chart 3.5	related structures
Table 3.1	Unfavourable conformers
Table 3.2	Gas phase tautomer energies
Table 3.3	Effect of large basis set optimisation on 3
Table 3.4	Comparison of 2h with X-ray structure
Table 3.5	Comparison of 3b with X-ray structures
Table 3.6	Free energies of solvation
Table 3.7	Estimated tautomer ratios
Table 3.8	Equilibrium free energies and pK _a
Table 3.9	Experimental pK _a s
Figure 3.1	Summary of tautomeric behaviour
Figure 3.2	Formal structures of 3c , 3f , and 3f
Figure 3.3	Resonance of 2-b
Index of geometries	Brookhaven .pdb format

Figure 3.1 Tautomerism of dioxopyridazines



3.4. Discussion

3.4.1 Conformation

Considering first conformational preferences of hydroxy tautomers calculated at HF / 6-31G(d) ([Table 3.1](#) vs [3.2](#)) we note the following:

Steric hindrance causes certain conformations to fail to converge as minima, i.e. [4i'](#), [3-b'](#) and [1h''](#).

Where opportunity exists for an intramolecular hydrogen bond, i.e. hydroxy tautomers of [1](#) and [4](#), deviation from this conformation involves a large energy cost (e.g. [4c'](#) = 10 Kcal/mol, [1f](#) = 8 Kcal/mol).

A hydroxyl α^- to an unsubstituted nitrogen (tautomers of [1](#), [2](#), and [3](#)) generally prefers an HOCN dihedral of 0° , there being an increased energy in the 180° position due to extra steric interaction between hydrogens and lone pair repulsion between the oxygen and the nitrogen, as opposed to the energy lowering effect of proton interaction with the nitrogen lone pair. In the case of [3h](#), this effect is around 8 Kcal/mol in magnitude per rotation. For [1-c'](#) and [1b'](#), this offsets the energy lowering effect of the intramolecular hydrogen bond, and in the case of [1i](#), where the hydrogen bond acceptor strength of the 4-oxygen is weakened by 5,5 diprotonation, exceeds it. Conversely, a hydroxyl α^- to a protonated nitrogen generally prefers the 180° position, presumably because of a weak intramolecular hydrogen bond formed between the oxygen and the N- proton, although the effect is not as great (e.g. [3e'](#) = 2 Kcal/mol).

In the absence of the above effects, in the case of [2d](#), [2h](#), [2k](#), 5-hydroxy substituents prefer to align such that the 5-oxygen lone pairs lie away from the 3-oxygen substituent. The effect may be a result of intramolecular dipole effects, and is particularly subtle in the case of [2k''](#) (= 0.5 Kcal/mol) which does not contain a carbonyl group.

3.4.2 Structure determination

It is apparent that optimisation at HF / 6-31G(d) is inadequate for determination of gas phase geometries for these systems. Comparing geometries optimised at HF / 6-31G(d) with geometries optimised at MP2 / 6-31G(d,p), differences are noted for several structures, including changes in symmetry. A number of methylene-bridge containing tautomers in particular, seem to be handled differently post-SCF, with slightly puckered to very puckered ring systems predominating, vs. more planar structures at HF / 6-31G(d), for example [1g](#), [1i](#), [2-d](#), [2g](#) and [2j](#).

Of particular note is the way in which certain optimisations involving methylene tautomers have failed to produce pyridazines ([Table 3.2](#)). After considerable searching, it may be confidently asserted that either local minima which are pyridazines do not exist for these structures, or if they do, they are very high in energy. Firstly, [3f](#) and [3f](#) undergo a ring contraction to a high-energy pyrazole. What makes this interesting is the known tendency of certain pyridazine-3(2*H*)-ones to undergo ring contraction to pyrazole products when heated with aqueous base [[1](#)]. Further study of this phenomenon may shed light on the mechanism of these reactions. The fact that this tautomer undergoes a change in ring structure may be understood by considering that no neutral or favourable zwitterionic formal structure (i.e. one having a negative charge on an oxygen and a positive charge on a tetravalent nitrogen) may be drawn for the structure, whereas bridging N1 - C5 creates a neutral structure.

Secondly, [3c](#) undergoes ring opening to a high energy ketene, rather than optimise as a pyridazine. Ring opening reactions of pyridazinones are apparently rare, except under reducing conditions. Again, the ring opening may be understood in terms of there being no neutral structure or sensible zwitterionic formal structure able to be drawn, except by a bond order of zero between N1 and C6.

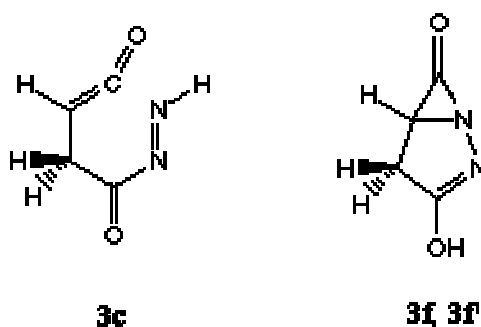


Figure 3.2 Formal structures of [3c](#), [3f](#), and [3f'](#)

Since substantial geometry changes are noted on proceeding from optimisation at HF/6-31G(d) to MP2/6-31G(d,p), particularly in the case of non-aromatic tautomers, this begs the questions: is the geometry converged at this level, and if not, how will larger basis set optimisation affect single point energies and hence tautomerism predictions? In particular, it is known that a satisfactory treatment of the geometry around amide bonds using MP2 theory may require large triple- ζ basis sets, and this is an ongoing area of investigation [52]. Insufficient basis sets tend to over-estimate the degree to which an amide nitrogen is pyramidal. The limited set of optimisations and subsequent single point energies performed at 6-311+G(2d,p), as reported in [Table 3.3](#), were chosen to investigate these questions. The set is comprised of the lactim-lactim [3h](#), lactim-lactam [3b](#), and lactam-lactam [3a](#) tautomers of the well-studied maleic hydrazide [3](#), vs. the preferred conjugate base [3-a](#). These structures are aromatic, semiaromatic and non-aromatic, and contain zero, one and two amide linkages respectively, and thus should highlight differences in the treatment of amidic and non-amidic nitrogens.

A number of conclusions may be drawn: Firstly, and most importantly, in no case does the change in relative energy for a calculation exceed 0.19 Kcal/mol, and is generally small. This means that errors caused by the deficiencies of optimisation with the smaller basis set are unlikely to affect our predictions of tautomerism, and are expected to be smaller than the deficiencies of the compound energy methods used throughout; the G2(MP2) and G2(MP2,SVP) methods having a mean absolute deviation of 1.58 Kcal/mol and 1.63 Kcal/mol respectively for the 125 systems in

the G2 test suite [40]. Secondly, the alteration in geometry of the lactam-lactam tautomer **3a**, having pyramidal nitrogens in C_2 symmetry, is substantially greater than that of the other tautomers (RMS 0.015 Å vs 0.004-6 Å). The sum of the bond angles around the nitrogen of the MP2/6-311+G(2d,p) optimised structure is 348.3°, vs. 345.7° for MP2/6-31G(d), i.e. the previously noted flattening of amide pyramidal quality with increased basis set size.

It may be concluded that while the use of the less expensive basis set optimisation in the present work provides a satisfactory description, future workers with greater computing resources employing more accurate methods should consider higher level geometry optimisation, particularly if the precise geometry of the amide linkage is of interest.

3.4.3 Gas phase tautomerism predictions

It has long been suggested that adjacent heteroatoms prefer to adopt different hybridisations [3,15,41]. In the case of dihydroxy pyridazine tautomers, there would clearly be an energy cost associated with repulsion of co-planar lone pairs of the sp² hybridised nitrogens.

However, there is an energy cost associated with losing full aromatic character of the pyridazine ring by proton substitution of a nitrogen to form a planar semi-aromatic system. Furthermore, there is an energy cost associated with loss of conjugation through ring puckering. On the other hand, constraint of a substituted hydrazine to a planar conformation rather than its preferred twisted structure involves an energy cost.

The interplay of these factors, lone pair repulsion vs. resonance energy, assists in the interpretation of the calculated tautomer energies and distributions (Tables 3.2 and 3.7). The current results suggest, with the possible exception of **2k** in the gas phase, that fully aromatic dihydroxy tautomers do not appear to play a major role. Likewise, 1,2-dihydro tautomers are conspicuously absent. The preferred structures are a balance between lone pair repulsion, and resonance energy gain. Thus, keto-hydroxy tautomers predominate. With respect to which oxygen takes which form,

oxygens α - to a nitrogen generally prefer a keto form in the gas phase, whereas the β - substituent adopts the hydroxy form. This may be compared with the behaviour of 2-pyridone and 3-hydroxy-pyridine [3], and is in accordance with the analysis of hydroxy-pyridazine 1-oxide tautomerism [33] (Chapter 2). Zwitterionic structures are generally unfavourable in the gas phase, **4c** being one of the more stable at 4.2 Kcal/mol above **4d** at 298.15K. In summary, **1f**, **2h**, **3b**, and **4d** are predicted to be the most favoured tautomers in the gas phase, in accordance with solution and solid phase experiments in the cases of **2** and **3**.

Particularly interesting is the low energy of the 4,4-diprotonated tautomer, **2g**. While it exceeds **2h** in energy by 1.8 Kcal/mol at 0 K, inclusion of thermochemistry at 298 K gives a free energy difference of only 0.6 Kcal/mol, sufficient for substantial gas phase contribution. With the dihydroxy tautomer **2k** also predicted to be only 2.19 Kcal/mol above **2h** and hence a possible contributor, **2** is worthy of closer experimental study. Methylene containing azine tautomers are exceedingly rare, compared with their 5-membered counterparts, the disruption to aromaticity caused by carbon protonation incurring a large energy cost. It may be speculated that the comparative stability of 5-membered methylene tautomers is a driving force for the ring contraction behaviour noted above. However, meta- dioxo substitution is one of the few known cases where six-membered nitrogen heterocycles are known to adopt this kind of structure [3,42]. This underscores the importance of not neglecting such tautomers when analysing hydroxy-azine tautomerism. The only other theoretical examinations of this system, those of Fabian [12, 13], while correctly predicting the stability of **2h** over **2f**, **2f'**, **2h'**, **2k**, and **2k''** at HF /3-21G, failed to consider **2g** *et al.* Semi-empirical calculations failed to reproduce *ab initio* or experimental qualitative results.

The previous best gas phase calculations reported on maleic hydrazide **3** [15] were a combination of the unscaled zero point energies calculated at HF / 3-21G and the single point energies at MP4/6-31G(d,p)//6-31G(d,p). They found **3b** favoured over **3a** by 3.3 Kcal/mol, and over **3h** by 5.5 Kcal/mol. The results here at 0K show a greater difference between these tautomers: 4.2 and 7.2 Kcal/mol respectively.

This indicates that geometry optimisation with correlated treatments, large basis sets, and high level treatment of electron correlation are required to approach convergence for these systems even for neutral tautomers. Particularly where tautomers lie close in energy, less expensive approaches may not give correct qualitative results.

3.4.4 Solvation effects according to different models

An examination of [Table 3.6](#) shows that free energies of solvation calculated by the I-PCM method differ markedly from those calculated by either single point or optimised semi-empirical calculations, which are fairly concordant. Generally, they are lower, particularly for the anions, where the solvation energies are around 10 Kcal/mol smaller than for semi-empirical methods. The I-PCM method was used here for comparison with semi-empirical methods, and because previous work [\[14,15\]](#) has attempted to describe pyridazinone aqueous solvation using solvent continuum models. Recently, Cramer described in detail the shortcomings of the I-PCM method for determining the solvation of anions [\[43\]](#). Firstly, diffuse electron density associated with anions will tend to increase isodensity cavity size, causing a decrease in solvation energy. Secondly, the so-called charge penetration problem, whereby for an anion, a substantial proportion of the charge may lie outside the cavity, and solvation energy is again underestimated.

With respect to neutral tautomers, it is worth noting differences in the order in which I-PCM and semi-empirical methods rank the solvation energy of different kinds of tautomers. All methods agree that the solvation of methylene tautomers is generally less favourable than other kinds of tautomers. The semi-empirical methods strongly favour the solvation of zwitterionic tautomers. Hydroxy-keto tautomers which are not zwitterionic are less strongly solvated, as are hydrazide dioxo tautomers, and dihydroxy tautomers are poorly solvated, in accordance with chemical expectation. The I-PCM method on the other hand seems less consistent, and in the best studied case, [3](#), actually reverses the order of preferential solvation, i.e. ΔG oxo-oxo ([3a](#)) > hydroxy-oxo ([3b](#)) > dihydroxy ([3h](#)).

The choice of whether to use single point or optimised semi-empirical calculations is unclear. Whereas single point calculations are more likely to be accurate for neutral species due to poor semi-empirical geometries, they may be less accurate for anions, because anionic geometry may alter significantly in the aqueous phase. The aqueous modelling of anions remains a challenge.

3.4.5 Aqueous phase tautomerism

[Table 3.7](#) and [Figure 3.1](#) summarise the findings of the aqueous phase equilibrium of the title compounds.

The effect of solvation on anionic ortho-substituted systems [1-](#) and [4-](#) is to reduce the stability of intramolecular hydrogen bonded bases with respect to their *N*-protonated counterparts, such that [4-a](#) may play a greater role, and [1-c](#) a lesser role in the equilibrium. With respect to the neutral tautomers of these structures, there is disagreement between AM1-SM2 and PM3-SM3, the proximity of the energies of various tautomers being finer than the expected error range of the methods. However it is clear that there is preferential solvation of the zwitterionic oxo-hydroxy forms, and there may well be a mixture of tautomers in aqueous solution.

For system [2](#), the favourable gas phase tautomer [2g](#) is poorly solvated, whereas the zwitterionic [2b](#) is well solvated, such that the former probably plays no role but the latter may in the aqueous equilibrium. [2h](#), the structure found in the solid phase, remains highly favoured. Once again, small differences between treatment by AM1-SM2 and PM3-SM3 cause large differences in the estimated equilibrium.

The qualitative aqueous phase findings for maleic hydrazide [3](#) are the same as in the gas phase, i.e. [3b](#) > [3h](#) > [3a](#), despite better solvation of [3a](#) tautomer according to semi-empirical theories. Burton *et al.* [[15](#)] found that both free energy perturbation calculations and an elliptical Onsage cavity model gave solvation energies in the expected order [3a](#) > [3b](#) > [3h](#), in reasonable agreement with our calculations. However, when combined with their gas phase energies, they considered [3a](#) to be close in energy to [3b](#) in solution, a conclusion at odds with the findings here, and unsupported by experimental data as far as is known. They also found the PCM

method gave less credible results than the other methods trialed, and preferred molecular dynamics to continuum models.

Semi-empirical methods hold the promise of superiority over both continuum models and molecular dynamics for the treatment of aqueous solvation of tautomeric systems, overcoming the neglect of electronic and polarisation effects by the former, and first hydration shell hydrogen bonding effects by the latter [32]. Alternately, mixed quantum mechanical and molecular dynamics approaches may become the method of choice for this kind of problem as they become further developed.

3.4.6 *Ab initio* prediction of relative pK_a

Turning now to the estimation of relative pK_a presented in [Table 3.8](#), compared with the available data, it is immediately apparent that the methods used are not providing consistent quantitative results. No method trialed gives good agreement with the known experimental pK_a difference between [2](#) and [3](#). While I-PCM comes closest to a reasonable prediction in this regard, it is otherwise discordant with the semi-empirical methods, and its relative treatment of anions is dubious. On the other hand, all methods make the qualitatively correct prediction that [2](#) is more acidic than [3](#). Moreover, all semi-empirical methods predict that [1](#), [3](#) and [4](#) are close in acidity. Examining [Table 3.9](#), the following trend may be discerned: for both pyridines and pyridazines, structures with an oxygen meta- to a ring nitrogen ([6](#), [14](#)) are more acidic than structures with an oxygen ortho- to a ring nitrogen ([5](#), [13](#)). Also, ortho- dioxo-substituted structures ([8](#), [12](#), [18](#)) tend to be generally less acidic than their positional isomers, possibly because of the intramolecular hydrogen bond which stabilises the acid form. Most pertinently, structures [8](#), [9](#), [10](#), and [12](#), are pyridine analogues of [1](#), [2](#), [3](#), and [4](#) respectively. Here, [8](#), [10](#) and [12](#) are all close in acidity, and higher in pK_a than [9](#), in good qualitative agreement with the relative pK_a s of [1](#), [3](#) and [4](#) vs [2](#) in [Table 3.8](#).

It remains to explain the large predicted pK_a difference between [2](#) and the other isomers. The anion, [2-b](#), is predicted to be particularly low in energy in the gas

phase, compared with its isomers, hence proton removal is favoured from the neutral tautomers. This may be understood as being a result of the fact that this meta- substituted anion has accessible to it two fully conjugated canonical resonance forms, where its isomers do not:

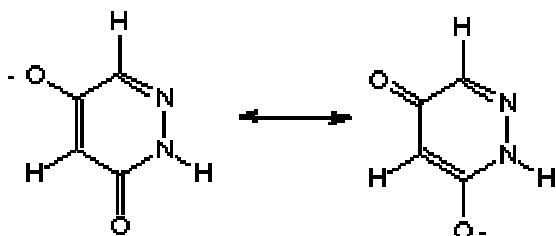


Figure 3.3. Two conjugated resonance forms of [2-b](#)

The likely errors in the aqueous phase calculations far outweigh those of the gas phase, particularly for anions, so it is a fair assumption that the solvation models are overestimating the differential solvation of [2-](#) compared with its isomers.

3.5. Conclusion

In summary, fully aromatic dihydroxy tautomers of dioxopyridazines are unfavourable in gas and moreso in aqueous phase, due to nitrogen lone-pair repulsion. Hydrazine tautomers, constrained from their preferred conformation, are similarly unfavourable, due to loss of aromaticity and conjugation. The most stable structures in the gas phase are those having a conjugated neutral hydroxy-oxo structure, and are rivalled in solution by those hydroxy-oxo structures which exist as aromatic zwitterions. Ketones are favoured α^- to a ring nitrogen and hydroxyls favoured β^- . Intramolecular hydrogen bonding is an important factor in the gas phase, and less so in solution, both for neutral species and their conjugate bases. Methylene tautomers should not be discounted when considering gas phase tautomerism of oxo-azines, but are unlikely to contribute to aqueous equilibrium. Gas phase calculations are approaching the required degree of accuracy to make quantitative judgements on tautomer equilibria, while aqueous solvation models remain qualitative. The *ab initio* prediction of relative pK_a of aromatic heterocycles is

qualitative at best. The results from methods used throughout have been in close agreement with available experimental data.

3.6. Calculation details

QCISD(T) energies were calculated using Molpro 96 [44]. All other *ab initio* calculations were performed using Gaussian 94, revision D.3 [45]. AM1-SM2 calculations were performed using AMSOL 5.4 [46]. Platforms used were SGI R10000 Power Challenge (IRIX 6.2) and IBM RS6000 (AIX 3.2).

3.7. References

1. RN Castle, Pyridazines, *The Chemistry of Heterocyclic Compounds*, Wiley Interscience, **28**, (1973)
2. US Rubber Co., *A literature Summary of Maleic Hydrazide, 1949-1957 and 1957-1963* (1964)
3. J Elguero, C Marzin, AR Katritzky, P Linda, *The Tautomerism of Heterocycles, Advances in Heterocyclic Chemistry, Supplement 1* (1976)
4. F Arndt, *Rev. Fac. Sci. Univ. Istanbul*, **9a**, 19 (1944); *Chem. Abstr.*, **40**, 1787 (1946)
5. Y Sheinker, Y Pomerantzev, *Zh. Fiz. Khim.*, **30**, 79 (1956)
6. Y Sheinker, T Gortinskaya, T Sycheva, *Zh. Fiz. Khim.*, **31**, 599 (1957)
7. Y Sheinker, T Gortinskaya, T Sycheva, *J. Chem Phys.*, **55**, 217 (1958)
8. W Overend, L Turton, L Wiggins, *J. Chem. Soc.*, 3500, (1950)
9. Ohashi, M Mashima, M Kubo, *Can. J. Chem.*, **42**, 970 (1964)
10. A Katritzky, A Waring, *J. Chem. Soc.*, 1523 (1964)
11. JP Gastmans, DF Gastmans, MHM Ferraz, *Eclectica Quimica*, **4**, 71-7 (1979).
12. WMF Fabian, *J. Molec. Struct. (Theochem)*, **208**, 295-307 (1990)
13. WMF Fabian, *J. Computational Chem.*, **12**, 17-35 (1991)
14. H-J. Hofmann, R Cimiraglia, J Tomasi, R Bonaccorsi, *J. Molec Struct. (Theochem)*, **227**, 321-326 (1991)
15. NA Burton, DVS Green, IH Hillier, PJ Taylor, MA Vincent, S Woodcock, *J. Chem. Soc. Perkin Trans. 2*, 331-335 (1993)
16. U Wagner, C Kratky, T Kappe, *Monatshefte für Chemie*, **120**, 329-342 (1989)
17. D Wise, R. Castle, *J. Heterocyclic Chem.*, **11**(6), 1001-9 (1974)

18. H Borchert, S Pfeifer, B Helbig, P Franke, G Heinsch, *Pharmazie*, **44**, 625-630 (1989)
19. GE Gymer, K Richardson, Pfizer Ltd., *UK Patent Application* GV 2 025 416 A (1979)
20. F Farina, MV Martin, A Tito, *Anales de Quimica*, **77**, 188 (1981)
21. R Schoenbeck, E Kloimstein, *Monatshefte für Chemie*, **99**,15 (1968)
22. M Yanai et al., *Yakugaku Zasshi*, **85**, 334 (1965)
23. G Heinisch, H Frank, *Progress in Medicinal Chemistry*, **27**, 1 (1990)
24. G Heinisch, H Frank, *Progress in Medicinal Chemistry*, **29**, 141 (1992)
25. K Imae, S Limura, T Hasegawa, T Okita, M Hirano, H Kamachi, H Kamei, *J. Antibiot.*, **46**(5), 840-9 (1993)
26. V Konecny, S Kovac, S Varkonda, *Chem. Zvesti*, **36**(2), 259-66 (1982)
27. B Schober, G Megyeri, T Kappe, *J. Heterocyclic Chem.*, **26**, 169 (1989)
28. *Abstracts of Papers of the American Chemical Society, Division of Medicinal Chemistry*, **211**, pp 038-043, 105 (1996)
29. M Brennan. *Chemical and Engineering News*, May 13, **41**, (1996)
30. J-M Autin, D Bigg, J Patoiseau, *Eur. Pat. Appl.* EP 515257 A1 921125; CA **118**:254945
31. JR Greenwood, G Vaccarella, HR Capper, RD Allan, GAR Johnston, *Proceedings, Second Molecular Graphics and Modelling Electronic Conference (1997)*, *Internet Journal of Chemistry*, **1**, 38 (1998)
32. CJ Cramer, DG Truhlar, *J. Am. Chem. Soc.*, **115**, 8810-8817 (1993)
33. JR Greenwood, HR Capper, RD Allan, and GAR Johnston. *Proceedings, Third Electronic Computational Chemistry Conference. (1996)* *J. Molec. Struct. (Theochem)* **419**, 97-111 (1997)
34. WJ Hehre, L Radom, PvR Schleyer, JA Pople. *Ab Initio Molecular Orbital Theory*, Wiley, New York (1986)
35. JB Foresman, TA Keith, KB Wiberg, J Snoonian, MJ Frisch, *J. Phys. Chem.*, **100**(40) 16098-16104 (1996)
36. CJ Cramer, DG Truhlar, *Journal of Computer-Aided Molecular Design*, **6**, 629-666 (1992)
37. P Cradwick, *J. Chem. Soc. Perkin Trans. 2*, 1386-1389 (1976)
38. A Katrusiak, *Acta Cryst.*, **C49**, 36-39 (1993)
39. LA Curtiss, K Raghavachari, JA Pople, *J. Chem. Phys.*, **98**, 1293 (1993)

40. LA Curtiss, PC Redfern, BJ Smith, L Radom, *J. Chem. Phys.*, **104**(13), 5148-5152 (1996)
41. RW Taft, F Anvia, M Taagepera, J Catalan, J Elguero, *J. Am. Chem. Soc.*, **108**, 3237 (1986)
42. G Pangon, G Thuillier, P Rumpf., *Bull. Soc. Chim. Fr.*, **1991** (1970)
43. C Cramer. Listserv Communication, *Computational Chemistry List*, Tue, 4 Aug 1997 10:04:51 <http://ccl.osc.edu/chemistry.html>
44. H-J Verner, PJ Knowles, *MOLPRO 96.1*, <http://www.tc.bham.ac.uk/molpro/>, *Chem. Phys. Lett.* **190**, 1 (1992)
45. *Gaussian 94*, Revision D.3, MJ Frisch, GW Trucks, HB Schlegel, PMW Gill, BG Johnson, MA Robb, JR Cheeseman, T Keith, GA Petersson, JA Montgomery, K Raghavachari, MA Al-Laham, VG Zakrzewski, JV Ortiz, JB Foresman, J Cioslowski, BB Stefanov, A Nanayakkara, M Challacombe, CY Peng, PY Ayala, W Chen, MW Wong, JL Andres, ES Replogle, R Gomperts, RL Martin, DJ Fox, JS Binkley, DJ Defrees, J Baker, JP Stewart, M Head-Gordon, C Gonzalez, and JA Pople, Gaussian, Inc., Pittsburgh PA, (1995)
46. GD Hawkins, GC Lynch, DJ Giesen, I Rossi, JW Storer, DA Liotard, CJ Cramer, and DG Truhlar, *AMSOL v-5.4*, QCPE Program 606 (1995); based on DA Liotard, EF Healy, JM Ruiz, and MJS Dewar, *AMPAC*, version 2.1, QCPE Program 506 (1989)
47. A Albert, JN Phillips, *J. Chem. Soc.*, 1294 (1956)
48. A Albert, *J. Chem. Soc.*, 1020 (1960)
49. H Stunzi, RLN Harris, DD Perrin, T Teitei, *Aust. J. Chem.*, **33**, 2207 (1980)
50. E Spinner, JCB White, *J. Chem. Soc., B*, 991 (1966)
51. H Igeta, *Chem. Pharm. Bull. (Tokyo)*, **7**, 938 (1959)
52. H-G Mack, H Oberhammer, *J. Am. Chem. Soc.*, **119**, 3567-3570 (1997)

Table 3.1. Relative energies of less favoured conformers.

Conformer	Symmetry	Bond rotated	Relative energy ^a	Conformer	Symmetry	Bond rotated	Relative energy ^a
<u>1-c'</u>	C _s	3-OH	6.35	<u>3-b'</u>	C _s ^c	3-OH	(7.71)
<u>1-d'</u>	C _s	4-OH	15.34	<u>3b'</u>	C _s	3-OH	6.90
<u>1b'</u>	C _s	3-OH	4.56	<u>3e'</u>	C _s	6-OH	2.14
<u>1c'</u>	C _s	4-OH	13.82	<u>3f'</u>	C ₁ ^d	3-OH	7.21
<u>1e'</u>	C _s	3-OH	16.07	<u>3g'</u>	C ₁	3-OH	3.85
<u>1f'</u>	C _s	4-OH	7.99	<u>3h'</u>	C _s	3-OH	7.66
						or 6-OH	
<u>1h'</u>	C _s	4-OH	4.26	<u>3h''</u>	C _{2v}	3-OH and 6-OH	15.53
<u>1h''</u>	C _s ^b	3-OH	(15.32)				
<u>1h'''</u>	C _s	3-OH and 4-OH	7.41	<u>4-c'</u>	C _s	4-OH	11.23
<u>1i'</u>	C _s	3-OH	0.92	<u>4c'</u>	C _s	4-OH	10.05
<u>1j'</u>	C ₁	4-OH	20.88	<u>4d'</u>	C _s	5-OH	8.94
				<u>4f'</u>	C ₁	4-OH	17.52
<u>2-c'</u>	C _s	3-OH	5.61	<u>4g'</u>	C _s	5-OH	5.49
<u>2-e'</u>	C _s	5-OH	1.24	<u>4i'</u>	C _{2v} ^e	5-OH ^f	(6.98)
<u>2b'</u>	C _s	3-OH	3.09	<u>4i''</u>	C _{2v}	4-OH ^f	3.60
<u>2d'</u>	C _s	5-OH	4.00				
<u>2f'</u>	C ₁	3-OH	5.30				
<u>2h'</u>	C _s	5-OH	2.56				
<u>2j'</u>	C _s	3-OH	9.08				
<u>2k'</u>	C _s	3-OH	8.04				
<u>2k''</u>	C _s	5-OH	0.51				
<u>2k'''</u>	C _s	3-OH and 5-OH	7.55				
<u>2l'</u>	C _s	3-OH	3.40				
<u>2m'</u>	C ₁	5-OH	2.69				
<u>2o'</u>	C _s	5-OH	3.60				

Notes:

^a Energies relative to minimum energy conformer in Kcal/mol, at RHF/6-31G(d) optimised geometries. See [Table 3.2](#) for relative and absolute energies of minimum energy conformers.

^b **1h''**: Not a minimum. Two imaginary frequencies in C_s symmetry. Relaxing symmetry constraints optimises structure to **1h**.

^c **3-b'**: Not a minimum. Two imaginary frequencies in C_s symmetry. Relaxing symmetry constraints optimises structure to **3-b**.

^d **3f'**: Not a pyridazine: optimised structure shows ring contraction via bonding between N1 and C5, to form a bicyclic system.

^e **4i'**: Not a minimum. One imaginary frequency in C_{2v} symmetry. Relaxing symmetry constraints optimises structure to **4i**.

^f **4i'**: hydroxyl protons near. **4i''**: hydroxyl protons far.

Table 3.2. Energies^a of all tautomers at RHF/6-31G(d) and selected tautomers post-SCF.

Structure	Symmetry	E {HF/6-31G(d)}	E {MP2/6-31G(d,p)}	E ₀ (best)	G ₂₉₈ (gas)
1-a	C _s	20.51	20.26		
1-b	C _s	(-411.83038)	1.11	(-413.50124)	(-413.53167)
1-c	C _s	3.98	(-413.04628)	0.27	0.60
1-d	C _s	9.84	4.18	4.21	4.55
1-e	C ₁	24.02	28.57		
1a	C ₁	-338.12	-331.83		
1b	C _s	-347.11	-348.17	-331.78	-331.67
1c	C _s	-334.65	-342.94	-325.07	-324.83
1d	C ₁	-312.45			
1e	C _s	-338.32	-344.21	-325.49	-325.27
1f	C _s	-355.33	-356.30	-338.03	-337.89
1g	C ₁	-345.46	-339.80	-320.22	-321.45
1h	C _s	-342.71	-345.65	-328.12	-328.00
1i	C ₁ ^{b,c}	-327.92	-323.22		
1j	C _s	-287.37			
2-a	C _s	34.37			
2-b	C _s	(-411.84220)	(-413.04904)	(-413.50826)	(-413.53911)
2-c	C _s	10.99	6.46	7.73	8.20
2-d	C ₁ ^{b,c}	16.42	17.24	18.00	17.34
2-e	C _s	25.10			
2-f	C _s	22.39	24.32		
2a	C ₁	-303.93			
2b	C _s	-323.43	-334.74	-314.53	-314.18
2c	C _s ^b	-312.69			
2d	C _s	-313.97			
2e	C _s	-287.91			
2f	C _s	-336.90	-338.63	-316.76	-316.60
2g	C ₁ ^{b,c}	-346.37	-343.67	-322.95	-323.83
2h	C _s	-344.97	-348.20	-324.78	-324.51
2i	C _s	-300.73			
2j	C ₁ ^{b,c}	-326.84	-325.82		
2k	C _s	-335.83	-342.20	-322.69	-322.32

2l	C _s ^b	-316.18			
2m	C ₁	-310.67			
2n	C ₁	-320.56			
2o	C _s	-314.92			
3-a	C _s	(-411.82891)	(-413.03899)	(-413.49775)	(-413.52771)
3-b	C _s	15.51	8.00	9.43	9.28
3-c	C _s	36.77			
3a	C ₂	-354.48	-348.64	-330.10	-330.23
3b	C _s	-356.44	-357.20	-337.30	-337.60
3c	C ₁ ^d	-313.96			
3d	C _s ^b	-280.98			
3e	C _s	-322.28			
3f	C ₁ ^e	-304.10			
3g	C ₁	-317.56			
3h	C _{2v}	-349.34	-354.75	-334.30	-334.04
3i	C ₂	-275.20			
4-a	C _s	20.30	17.67	15.21	14.92
4-b	C ₁	20.35	27.31		
4-c	C _s	(-411.81382)	(-413.04001)	(-413.49312)	(-413.52311)
4a	C _{2v}	-288.45			
4b	C ₁	-311.12			
4c	C _s	-339.09	-345.99	-327.05	-327.14
4d	C _s	-349.77	-347.32	-331.21	-331.46
4e	C ₁	-338.41	-325.83		
4f	C _s	-293.75			
4g	C _s	-328.62			
4h	C _s ^f	-327.21	-313.82		
4i	C _s	-343.38	-340.48	-324.97	-325.35

Notes:

^a Absolute energies of lowest energy anionic tautomer of each system are indicated in parentheses, given in Hartree. Energies of lowest energy conformations of other tautomers relative to these structures (**1-b** or **1-c**, **2-b**, **3-a**, **4-c**) are given in Kcal/mol. Lowest energy neutral tautomers are displayed in **bold**.

$$E_{0(\text{best})} = E_{\text{elec}} + 0.8929 * \text{ZPE}\{\text{HF}/6-31\text{G}(\text{d})\}$$

$$E_{\text{elec}} = E\{\text{MP2}/6-311++\text{G}(3\text{df},3\text{pd})\} + E\{\text{QCISD}(\text{T})/6-31\text{G}(\text{d},\text{p})\} - E\{\text{MP2}/6-31\text{G}(\text{d},\text{p})\}$$

$$G_{298(\text{gas})} = E_{\text{elec}} + E_{\text{thermal},298} + RT - TS$$

^b Minimum found in C_s symmetry at HF / 6-31G(d). One small real frequency, indicating soft ring puckering vibrational mode and likely breaking of symmetry at higher level of theory and larger basis set.

^c Minimum found in C_1 symmetry with substantial deviation from planarity at MP2 / 6-31G(d,p).

^d **3c**: Not a pyridazine: optimised structure in C_s symmetry has two imaginary frequencies, and shows lengthening of C6-N1 bond. C_1 symmetry optimised structure is a ring-opened ketene.

^e **3f**: Not a pyridazine: optimised structure shows ring contraction via bonding between N1 and C5, to form a bicyclic system.

^f **4h**: Minimum is a puckered ring with a vertical plane of symmetry.

Table 3.3. Effect of large basis set optimisation on favoured tautomers of **3**

Optimisation level	//MP2/ 6-31G(d)	//MP2/ 6-311+G (2d,p)	//MP2 / 6- 31G(d)	//MP2/ 6-311+G (2d,p)	//MP2/ 6-31G(d)	//MP2/ 6-311+G (2d,p)	//MP2/ 6-31G(d)	//MP2/ 6-311+G (2d,p)	
Structures	3-a	3-a	3a	3a	3b	3b	3h	3h	
Energies ^a	MP2/ 6-311++G (3df,3pd)	-413.49747	-413.49772	-333.22	-333.43	-343.02	-343.06	-341.06	-341.02
	QCISD(T)/ 6-31G(d)	-413.11014	-413.10985	-353.55	-353.39	-359.52	-359.68	-355.55	-355.60
	E_0	-413.49775	-413.49786	-330.10	-330.28	-337.30	-337.49	-334.30	-334.30
RMS geometry change	0.005 Å		0.015 Å		0.004 Å		0.006 Å		

Notes:

^a Energies relative to **3-a** in Kcal/mol (absolute energies of **3-a** in *italics* in Hartree). See [Table 3.2](#) for definition of E_0 .

Table 3.4. Comparison of [2h](#) geometry with X-ray crystal structure.

lengths ^a	X-ray structure ^b	MP2 / 6-31G(d,p)	angles ^a	X-ray structure ^b	MP2 / 6-31G(d,p)
N(1)-N(2)	1.344	1.343	N(1)-N(2)-C(3)	125.7	129.1
H(2)-N(2)	0.881	1.012	H(2)-N(2)-C(3)	119.4	116.0
C(3)-N(2)	1.361	1.403	N(2)-C(3)-C(4)	116.7	112.5
O(7)-C(3)	1.268	1.233	O(7)-C(3)-C(4)	125.2	127.1
C(4)-C(3)	1.407	1.447	C(3)-C(4)-C(5)	119.1	120.2
H(4)-C(4)	0.958	1.083	H(4)-C(4)-C(5)	123.5	122.6
C(5)-C(4)	1.354	1.367	C(4)-C(5)-C(6)	118.7	119.8
O(8)-C(5)	1.325	1.360	O(8)-C(5)-C(6)	115.6	114.8
H(8)-O(8)	0.828	0.967	H(8)-O(8)-C(5)	113.3	108.9
C(6)-C(5)	1.428	1.429	C(5)-C(6)-N(1)	122.9	122.6
H(6)-C(6)	0.964	1.080	H(6)-C(6)-N(1)	115.3	116.6
N(1)-C(6)	1.297	1.316	C(6)-N(1)-N(2)	115.9	115.9

Notes:

^a Bond lengths in Å, bond angles in degrees.

^b Crystal structure of hydrogen-bonded coplanar dimers described by Wagner et al. [[16](#)]

Table 3.5. Comparison of [3b](#) geometry with X-ray crystal structures.

lengths ^a	MH2 ^b	MH1 ^b	MP2 / 6-31G(d,p)	angles ^a	MH2 ^b	MH1 ^b	MP2 / 6-31G(d,p)
				N(2)-N(1)-C(6)	128.1	127.9	129.1
				N(1)-N(2)-C(3)	115.0	115.0	115.3
N(1)-N(2)	1.363	1.364	1.354	N(2)-C(3)-O(3)	118.5	118.9	118.4
N(1)-C(6)	1.334	1.329	1.394	N(2)-C(3)-C(4)	123.6	124.0	124.6
N(2)-C(3)	1.298	1.304	1.313	O(3)-C(3)-C(4)	117.9	117.1	117.6
C(3)-O(3)	1.338	1.337	1.358	C(3)-C(4)-C(5)	119.0	117.7	118.5
C(3)-C(4)	1.415	1.422	1.426	C(4)-C(5)-C(6)	119.4	120.9	121.2
C(4)-C(5)	1.346	1.336	1.362	N(1)-C(6)-C(5)	114.9	114.5	112.1
C(5)-C(6)	1.435	1.437	1.456	N(1)-C(6)-O(6)	120.8	120.4	121.2
C(6)-O(6)	1.260	1.257	1.235	C(5)-C(6)-O(6)	124.3	125.1	126.7
N(1)-H(1)	0.82	0.90	1.011	N(2)-N(1)-H(1)	114	121	114.7
O(3)-H(3)	1.00	0.89	0.910	C(3)-O(3)-H(3)	109	116	106.5

Notes:

^a Bond lengths in Å, bond angles in degrees.

^b Two crystalline polymorphs of maleic hydrazide are described; triclinic MH1 from P Cradwick [[37](#)] and monoclinic MH2 from A Katrusiak [[38](#)]

Table 3.6. Free energies of aqueous solvation ^a

Structure	Solvation method				
	IPCM-MP2 / 6-31G(d,p) 1SCF ^{b,c}	AM1-SM2 1SCF ^e	AM1-SM2 opt ^d	PM3-SM3 1SCF ^e	PM3-SM3 opt ^d
1-b	-63.61	-70.42	-72.86	-72.42	-73.41
1-c	-58.44	-68.78	-69.81	-68.66	-69.95 ^e
1-d	-60.60	-72.33	-71.98	-71.84	-71.93
1b	-13.95	-20.21	-20.63 ^e	-21.34	-20.66
1c	-15.59	-26.79	-28.68 ^e	-25.71	-25.51
1e	-13.83	-19.24	-21.25 ^e	-21.99	-22.84
1f	-9.81	-13.58	-14.68 ^e	-17.11	-17.68
1g	-10.22	-12.03	-13.14	-16.79	-16.69
1h	-11.16	-13.20	-13.18	-13.75	-13.57
2-b	-59.42	-68.96	-70.37 ^e	-72.54	-73.29
2-c	-59.30	-70.42	-70.54	-70.70	-70.90
2-d	-58.60	-64.17	-63.67 ^e	-64.91	-64.61
2b	-13.99	-25.44	-26.73 ^e	-25.65	-25.38 ^e
2f	-15.68	-17.62	-18.77 ^e	-21.40	-21.20
2g	-8.68	-10.45	-11.43	-15.07	-15.16
2h	-14.34	-14.43	-15.51 ^e	-18.44	-18.95
2k	-13.80	-14.60	-14.23	-15.36	-14.69
3-a	-62.56	-71.68	-73.94	-72.63	-73.89
3-b	-65.36	-73.54	-72.48 ^e	-73.95	-72.93
3a	-9.55	-15.28	-15.83	-18.16	-17.08
3b	-9.87	-14.49	-15.24 ^e	-17.80	-18.22
3h	-11.70	-14.22	-14.39	-14.80	-14.94
4-a	-68.96	-78.25	-80.30 ^e	-80.14	-81.14 ^e
4-c	-57.28	-69.61	-70.27	-69.38	-70.41 ^e
4c	-13.34	-22.68	-25.07	-23.65	-24.35
4d	-13.78	-20.01	-20.40 ^e	-21.98	-21.11
4i	-14.51	-13.78	-13.81	-14.60	-14.38

Notes:

^a $\Delta G_{\text{solv}} = E_{\text{aq}} - E_{\text{gas}}$

^b Isodensity polarised continuum model single point calculations at MP2 / 6-31G(d,p) geometries, using an isodensity value of 0.001 and a dielectric constant of 78.4.

^c 1SCF: Single point energies using MP2 / 6-31G(d,p) optimised geometries.

^d Opt: All energies obtained from structures optimised using AM1 and PM3, with and without SM2 and SM3 solvation models respectively.

^e Failure to fully optimise structure in aqueous phase: largest component of gradient remains greater than 0.45, but energy stationary. Probably not significant.

Table 3.7. Estimated tautomer ratios in gas phase and in aqueous solution^a

Structure	Solvation method					
	None (Gas phase)	IPCM-MP2/ 6-31G(d,p) 1SCF	AM1-SM2 1SCF	AM1-SM2 opt	PM3-SM3 1SCF	PM3-SM3 opt
1-b	73.44%	99.99%	96.69%	99.78%	99.92%	99.89%
1-c	26.52%	0.01%	2.19%	0.21%	0.06%	0.10%
1-d	0.03%	3E-06	1.11%	0.01%	0.02%	4E-05
1b	3E-05	2.89%	46.26%	9.73%	3.37%	0.42%
1c	3E-10	5E-06	30.25%	74.99%	0.05%	0.01%
1e	6E-10	5E-07	2E-06	6E-06	2E-06	3E-06
1f	100.00%	97.11%	23.49%	15.27%	96.57%	99.57%
1g	9E-13	2E-12	2E-14	1E-14	5E-13	2E-13
1h	6E-08	5E-07	7E-09	7E-10	2E-10	5E-11
2-b	100.00%	100.00%	100.00%	100.00%	100.00%	100.00%
2-c	1E-06	8E-07	1E-05	1E-06	4E-08	2E-08
2-d	2E-13	5E-14	6E-17	2E-18	5E-19	9E-20
2b	2E-08	1E-08	75.31%	81.67%	0.51%	0.14%
2f	1E-06	2E-05	0.01%	0.01%	0.02%	0.01%
2g	23.71%	2E-05	0.01%	0.01%	0.11%	0.05%
2h	74.46%	99.01%	23.90%	18.26%	99.34%	99.80%
2k	1.84%	0.99%	0.78%	0.05%	0.01%	2E-05
3-a	100.00%	100.00%	100.00%	100.00%	100.00%	100.00%
3-b	2E-07	2E-05	4E-06	1E-08	1E-06	3E-08
3a	4E-06	2E-06	2E-05	1E-05	7E-06	6E-07
3b	99.75%	94.87%	99.84%	99.94%	100.00%	100.00%
3h	0.24%	5.13%	0.15%	0.06%	2E-05	1E-05
4-a	1E-11	0.42%	3E-05	0.03%	0.09%	0.09%
4-c	100.00%	99.58%	100.00%	99.97%	99.91%	99.91%
4c	0.07%	0.03%	5.85%	64.39%	1.13%	13.98%
4d	99.93%	99.96%	94.15%	35.61%	98.87%	86.02%
4i	3E-05	0.01%	9E-10	2E-10	1E-10	3E-10

Notes:

^a Calculated at 298.15 K, based on ΔG_{298} in gas phase and solution.

$HA_i \rightleftharpoons HA_j$; $K_{j,i} = [HA_j]/[HA_i] = \exp((G_i - G_j)/RT)$; $\sum [HA] = 1$

Anions and neutral tautomers calculated and normalised separately.

Predominant tautomers shown in **bold**.

See [Table 3.6](#) for explanation of solvation methods.

Table 3.8. Equilibrium free energies^a and relative pK_a estimates^b in gas phase and in solution at 298.15K

Quantity, system	Solvation method					
	None (gas phase)	IPCM-MP2/6-31G(d,p)1SCF	AM1-SM21SCF	AM1-SM2opt	PM3-SM31SCF	PM3-SM3opt
	<i>3,4-dioxo-pyridazine</i>					
G ₂₉₈ (1-)	-413.53141	-413.63304	-413.64377	-413.64777	-413.64706	-413.64865
G ₂₉₈ (1)	-414.07013	-414.08567	-414.09214	-414.09461	-414.09728	-414.09829
pK _a rel (1)	14.88	8.20	12.79	12.15	13.70	13.60
	<i>3,5-dioxo-pyridazine</i>					
G ₂₉₈ (2-)	-413.53911	-413.53911	-413.63380	-413.64901	-413.65124	-413.65470
G ₂₉₈ (2)	-414.05593	-414.07905	-414.08004	-414.08212	-414.08560	-414.08643
pK _a rel (2) (lit. 4.81)	4.81	4.81	4.81	4.81	4.81	4.81
	<i>3,6-dioxo-pyridazine</i>					
G ₂₉₈ (3-)	-413.52771	-413.62740	-413.64193	-413.64554	-413.64345	-413.64545
G ₂₉₈ (3)	-414.06569	-414.08879	-414.08128	-414.08879	-414.08999	-414.09407
pK _a rel (3) (lit. 5.67)	14.55	8.78	12.09	11.05	13.88	13.43
	<i>4,5-dioxo-pyridazine</i>					
G ₂₉₈ (4-)	-413.52311	-413.61437	-413.63403	-413.63508	-413.63366	-413.63531
G ₂₉₈ (4)	-414.05132	-414.08305	-414.07328	-414.08420	-414.08631	-414.08472
pK _a rel (4)	10.05	11.09	13.08	13.20	14.81	13.50
pK _a order	1 ~ 3 > 4 > 2	4 > 3 ~ 1 > 2	4 ~ 1 > 3 > 2	4 > 1 > 3 > 2	4 > 3 ~ 1 > 2	1 ~ 4 ~ 3 > 2

Notes:

^a Weighted free energies over all anion and neutral tautomers respectively, based on estimated tautomer ratios and G₂₉₈ of individual components, in Hartree.

^b $\Delta pK_a = \Delta(-\log_{10}(\exp(-\Delta G_{298}/RT)))$. Relative to system **2** = 4.81.

Table 3.9. Literature pK_as of related structures

Name	Structure	pK _a	Reference
2-hydroxy pyridine	5	11.6	[47]
3-hydroxy pyridine	6	8.7	[47]
4-hydroxy pyridine	7	11.1	[47]
2,3-dihydroxy pyridine	8	8.7	[49]
2,4-dihydroxy pyridine	9	6.5	[47]
2,5-dihydroxy pyridine	10	8.5	[48]
2,6-dihydroxy pyridine	11	4.5	[50]
3,4-dihydroxy pyridine	12	8.9	[49]
3-hydroxy pyridazine	13	10.5	[47]
4-hydroxy pyridazine	14	8.7	[47]
3-hydroxy pyridazine 1-oxide	15	4.1	[51]
4-hydroxy pyridazine 1-oxide	16	< 18	[33]
5-hydroxy pyridazine 1-oxide	17	< 16	[33]
6-hydroxy pyridazine 1-oxide	18	< 15	[33]
3,5-dihydroxy pyridazine	2	4.8	[16]
3,6-dihydroxy pyridazine	3	5.7	[47]

Chart 3.1. 3,4-dioxo pyridazines

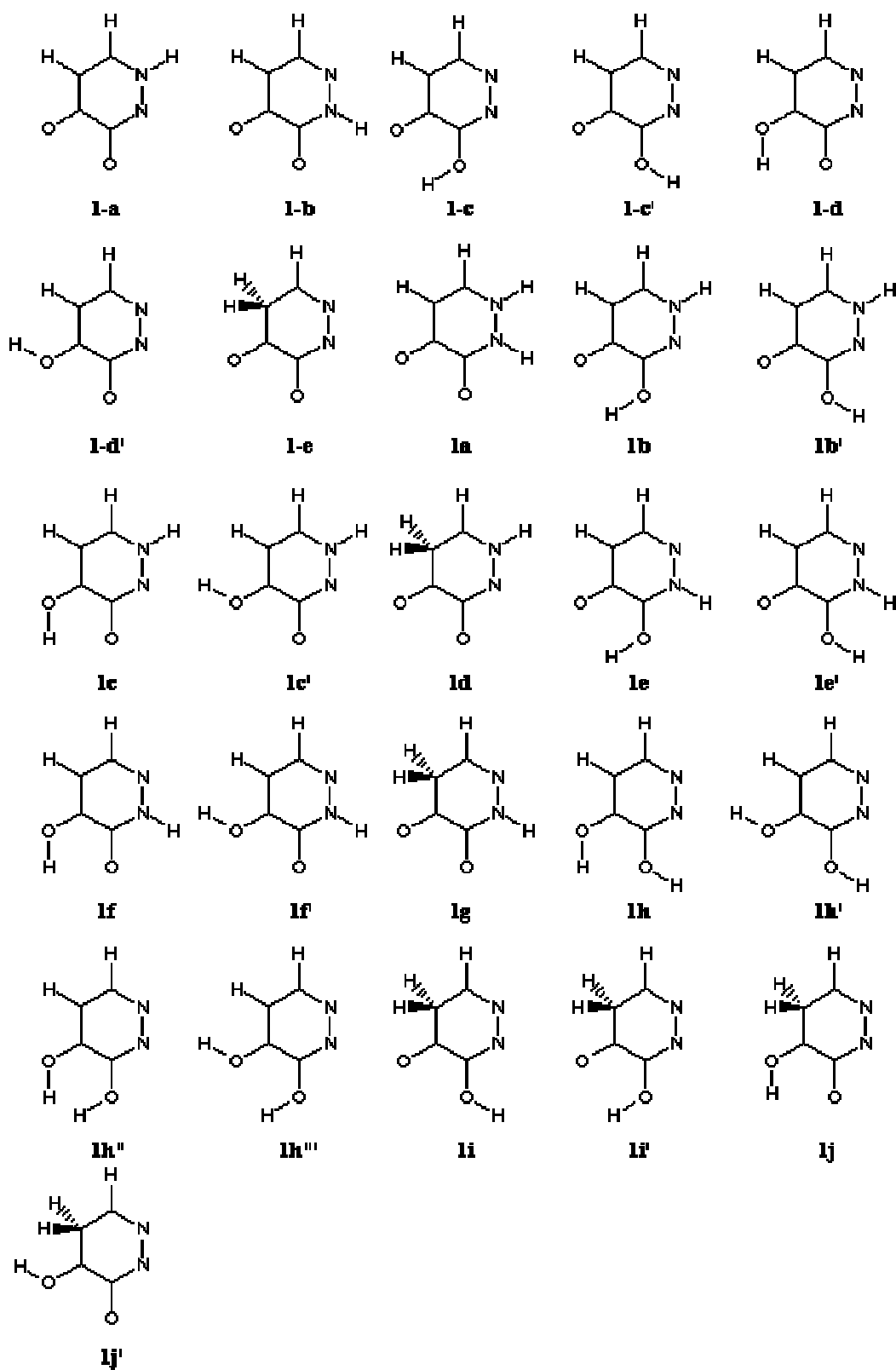


Chart 3.2. 3,5-dioxo-pyridazines

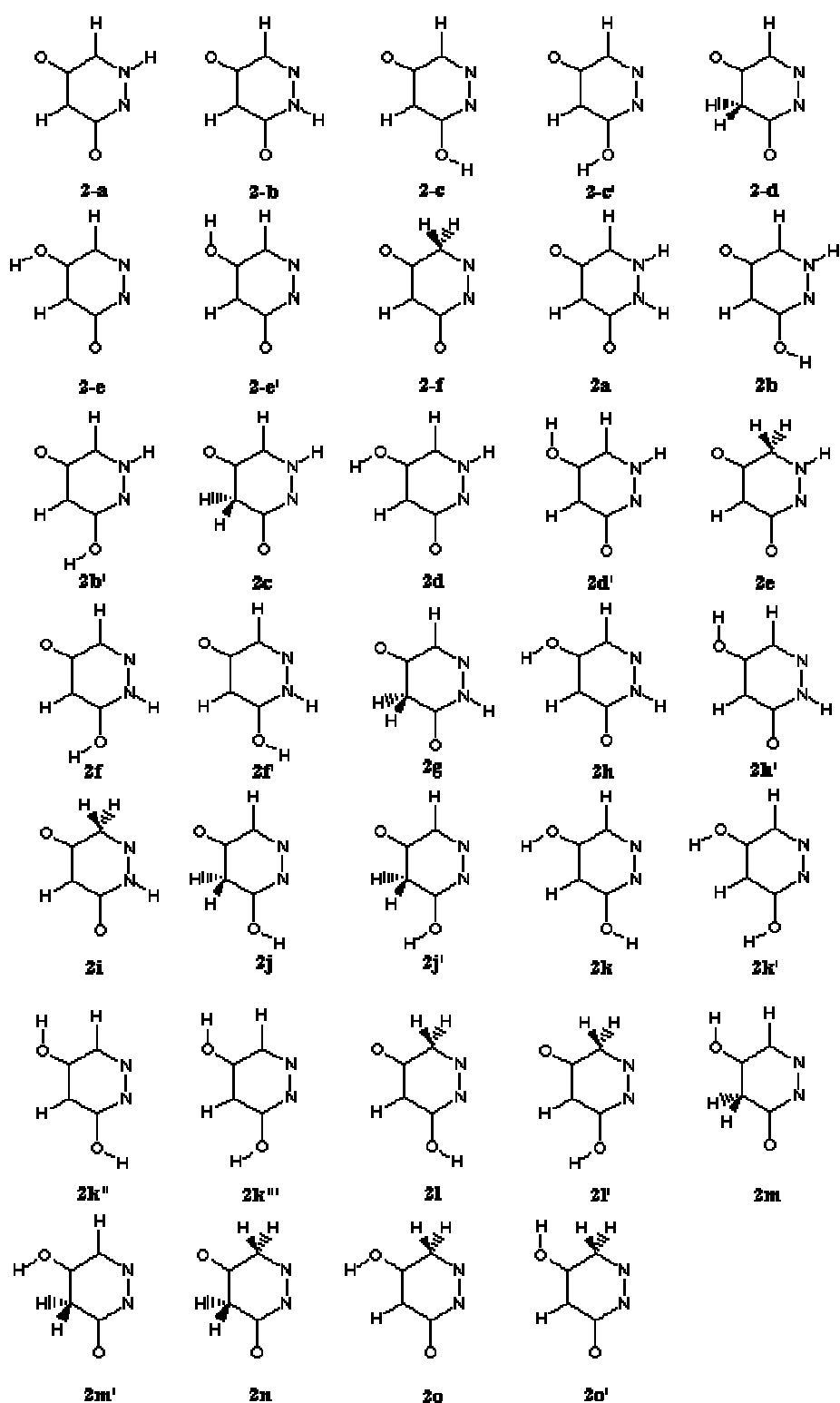
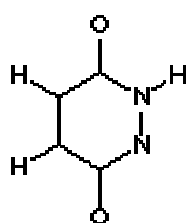
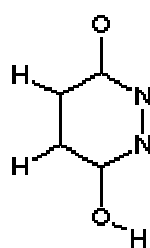


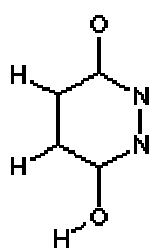
Chart 3.3. 3,6-dioxo-pyridazines



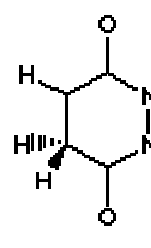
3-a



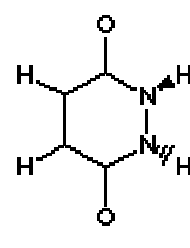
3-b



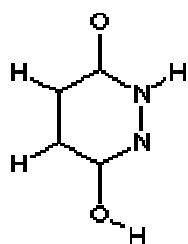
3-b'



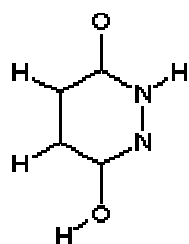
3-c



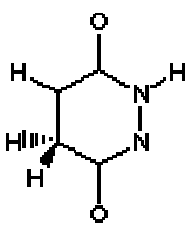
3a



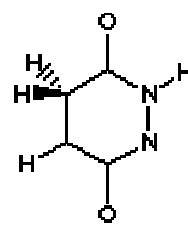
3b



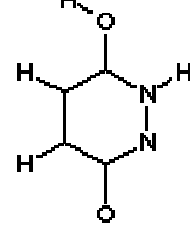
3b'



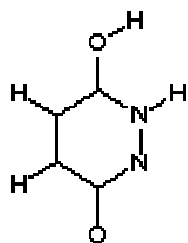
3c



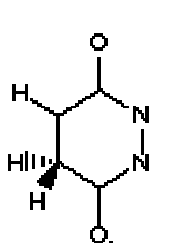
3d



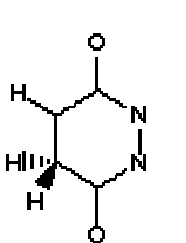
3e



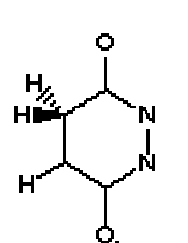
3e'



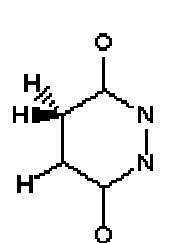
3f



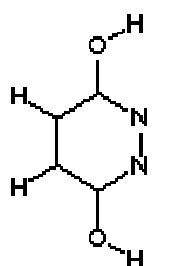
3f'



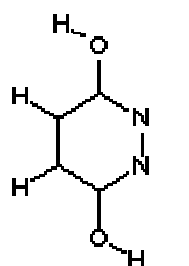
3g



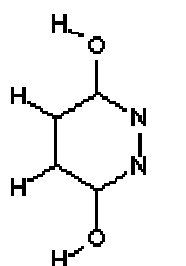
3g'



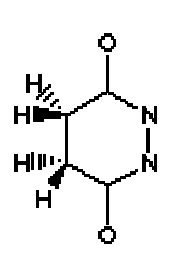
3h



3h'

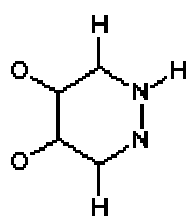


3h''

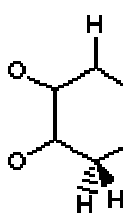


3i

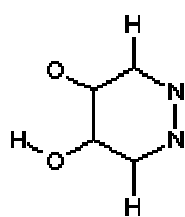
Chart 3.4. 4,5-dioxo-pyridazines



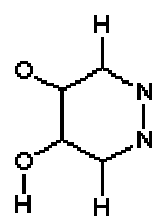
4-a



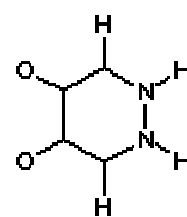
4-b



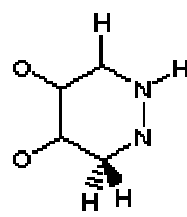
4-c



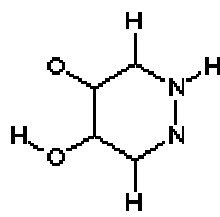
4-c'



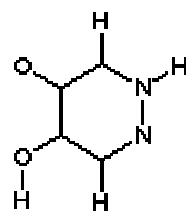
4a



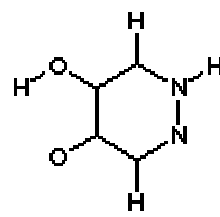
4b



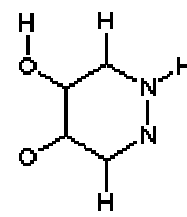
4c



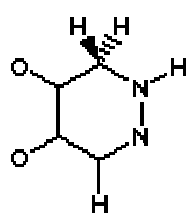
4c'



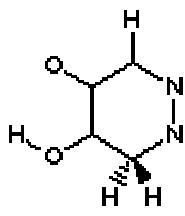
4d



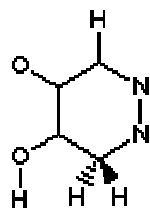
4d'



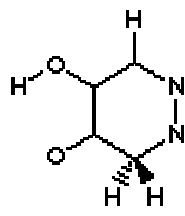
4e



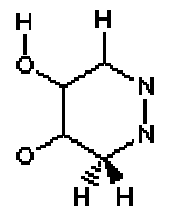
4f



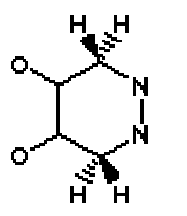
4f'



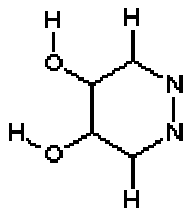
4g



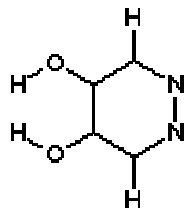
4g'



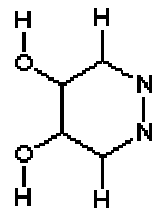
4h



4i

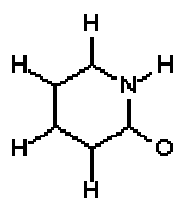


4i'

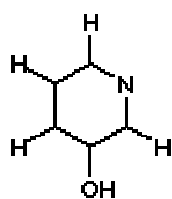


4i''

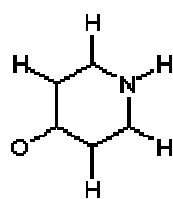
Chart 3.5. Other structures referred to in Chapter 3



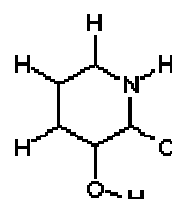
5



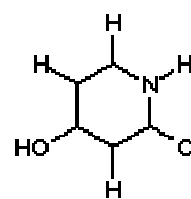
6



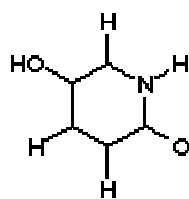
7



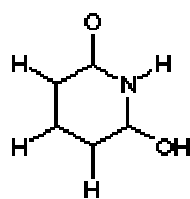
8



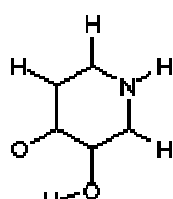
9



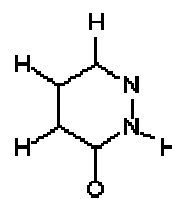
10



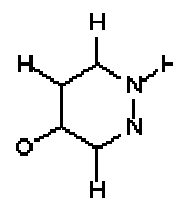
11



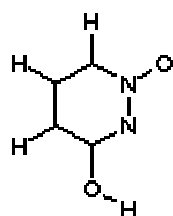
12



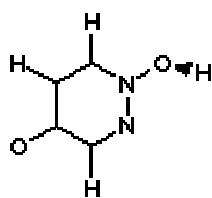
13



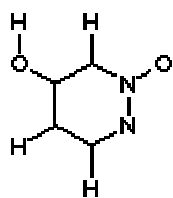
14



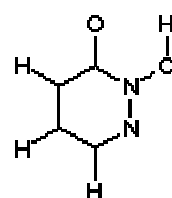
15



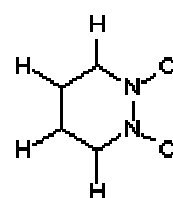
16



17



18



19

Chapter 3. Index of /pdb/

[1a HF/6-31G\(d\) \(34-12566.pdb\)](#)
[1a MP2/6-31G\(d,p\) \(34-1256m.pdb\)](#)
[1b HF/6-31G\(d\) \(34-13566.pdb\)](#)
[1b MP2/6-31G\(d,p\) \(34-1356m.pdb\)](#)
[1b' HF/6-31G\(d\) \(34-1356a.pdb\)](#)
[1c HF/6-31G\(d\) \(34-14566.pdb\)](#)
[1c MP2/6-31G\(d,p\) \(34-1456m.pdb\)](#)
[1c' HF/6-31G\(d\) \(34-1456a.pdb\)](#)
[1d HF/6-31G\(d\) \(34-15566.pdb\)](#)
[1-a HF/6-31G\(d\) \(34-156-6.pdb\)](#)
[1-a MP2/6-31G\(d,p\) \(34-156-m.pdb\)](#)
[1e HF/6-31G\(d\) \(34-23566.pdb\)](#)
[1e MP2/6-31G\(d,p\) \(34-2356m.pdb\)](#)
[1e' HF/6-31G\(d\) \(34-2356a.pdb\)](#)
[1f HF/6-31G\(d\) \(34-24566.pdb\)](#)
[1f MP2/6-31G\(d,p\) \(34-2456m.pdb\)](#)
[1f' HF/6-31G\(d\) \(34-2456a.pdb\)](#)
[1g HF/6-31G\(d\) \(34-25566.pdb\)](#)
[1g MP2/6-31G\(d,p\) \(34-2556m.pdb\)](#)
[1-b HF/6-31G\(d\) \(34-256-6.pdb\)](#)
[1-b MP2/6-31G\(d,p\) \(34-256-m.pdb\)](#)
[1h HF/6-31G\(d\) \(34-34566.pdb\)](#)
[1h MP2/6-31G\(d,p\) \(34-3456m.pdb\)](#)
[1h' HF/6-31G\(d\) \(34-3456a.pdb\)](#)
[1h''' HF/6-31G\(d\) \(34-3456c.pdb\)](#)
[1i HF/6-31G\(d\) \(34-35566.pdb\)](#)
[1i MP2/6-31G\(d,p\) \(34-3556m.pdb\)](#)
[1i' HF/6-31G\(d\) \(34-3556a.pdb\)](#)
[1-c HF/6-31G\(d\) \(34-356-6.pdb\)](#)
[1-c MP2/6-31G\(d,p\) \(34-356-m.pdb\)](#)
[1-c' HF/6-31G\(d\) \(34-356-a.pdb\)](#)
[1j HF/6-31G\(d\) \(34-45566.pdb\)](#)
[1j' HF/6-31G\(d\) \(34-4556a.pdb\)](#)
[1-d HF/6-31G\(d\) \(34-456-6.pdb\)](#)
[1-d MP2/6-31G\(d,p\) \(34-456-m.pdb\)](#)
[1-d' HF/6-31G\(d\) \(34-456-a.pdb\)](#)
[1-e HF/6-31G\(d\) \(34-556-6.pdb\)](#)
[1-e MP2/6-31G\(d,p\) \(34-556-m.pdb\)](#)
[2a HF/6-31G\(d\) \(35-12466.pdb\)](#)
[2b HF/6-31G\(d\) \(35-13466.pdb\)](#)
[2b MP2/6-31G\(d,p\) \(35-1346m.pdb\)](#)
[2b' HF/6-31G\(d\) \(35-1346a.pdb\)](#)
[2c HF/6-31G\(d\) \(35-14466.pdb\)](#)
[2d HF/6-31G\(d\) \(35-14566.pdb\)](#)
[2d' HF/6-31G\(d\) \(35-1456a.pdb\)](#)
[2-a HF/6-31G\(d\) \(35-146-6.pdb\)](#)
[2e HF/6-31G\(d\) \(35-14666.pdb\)](#)
[2f HF/6-31G\(d\) \(35-23466.pdb\)](#)
[2f MP2/6-31G\(d,p\) \(35-2346m.pdb\)](#)
[2f' HF/6-31G\(d\) \(35-2346a.pdb\)](#)

[2g HF/6-31G\(d\) \(35-24466.pdb\)](#)
[2g MP2/6-31G\(d,p\) \(35-2446m.pdb\)](#)
[2h HF/6-31G\(d\) \(35-24566.pdb\)](#)
[2h MP2/6-31G\(d,p\) \(35-2456m.pdb\)](#)
[2h' HF/6-31G\(d\) \(35-2456a.pdb\)](#)
[2-b HF/6-31G\(d\) \(35-246-6.pdb\)](#)
[2-b MP2/6-31G\(d,p\) \(35-246-m.pdb\)](#)
[2i HF/6-31G\(d\) \(35-24666.pdb\)](#)
[2j HF/6-31G\(d\) \(35-34466.pdb\)](#)
[2j MP2/6-31G\(d,p\) \(35-3446m.pdb\)](#)
[2j' HF/6-31G\(d\) \(35-3446a.pdb\)](#)
[2k HF/6-31G\(d\) \(35-34566.pdb\)](#)
[2k MP2/6-31G\(d,p\) \(35-3456m.pdb\)](#)
[2k' HF/6-31G\(d\) \(35-3456a.pdb\)](#)
[2k'' HF/6-31G\(d\) \(35-3456b.pdb\)](#)
[2k''' HF/6-31G\(d\) \(35-3456c.pdb\)](#)
[2-c HF/6-31G\(d\) \(35-346-6.pdb\)](#)
[2-c MP2/6-31G\(d,p\) \(35-346-m.pdb\)](#)
[2-c' HF/6-31G\(d\) \(35-346-a.pdb\)](#)
[2l HF/6-31G\(d\) \(35-34666.pdb\)](#)
[2l' HF/6-31G\(d\) \(35-3466a.pdb\)](#)
[2m HF/6-31G\(d\) \(35-44566.pdb\)](#)
[2m' HF/6-31G\(d\) \(35-4456a.pdb\)](#)
[2-d HF/6-31G\(d\) \(35-446-6.pdb\)](#)
[2-d MP2/6-31G\(d,p\) \(35-446-m.pdb\)](#)
[2n HF/6-31G\(d\) \(35-44666.pdb\)](#)
[2-e HF/6-31G\(d\) \(35-456-6.pdb\)](#)
[2-e' HF/6-31G\(d\) \(35-456-a.pdb\)](#)
[2o HF/6-31G\(d\) \(35-45666.pdb\)](#)
[2o' HF/6-31G\(d\) \(35-4566a.pdb\)](#)
[2-f HF/6-31G\(d\) \(35-466-6.pdb\)](#)
[2-f MP2/6-31G\(d,p\) \(35-466-m.pdb\)](#)
[3a HF/6-31G\(d\) \(36-12456.pdb\)](#)
[3a MP2/6-31G\(d,p\) \(36-1245m.pdb\)](#)
[3a MP2/6-311+G\(2d,p\) \(36-1245m.pdb\)](#)
[3b HF/6-31G\(d\) \(36-13456.pdb\)](#)
[3b MP2/6-31G\(d,p\) \(36-1345m.pdb\)](#)
[3b MP2/6-311+G\(2d,p\) \(36-1345o.pdb\)](#)
[3b' HF/6-31G\(d\) \(36-1345a.pdb\)](#)
[3-a HF/6-31G\(d\) \(36-145-6.pdb\)](#)
[3-a MP2/6-31G\(d,p\) \(36-145-m.pdb\)](#)
[3-a MP2/6-311+G\(2d,p\) \(36-145-o.pdb\)](#)
[3c HF/6-31G\(d\) \(36-14456.pdb\)](#)
[3d HF/6-31G\(d\) \(36-14556.pdb\)](#)
[3e HF/6-31G\(d\) \(36-14566.pdb\)](#)
[3e' HF/6-31G\(d\) \(36-1456a.pdb\)](#)
[3f HF/6-31G\(d\) \(36-34456.pdb\)](#)
[3f' HF/6-31G\(d\) \(36-3445a.pdb\)](#)
[3-b HF/6-31G\(d\) \(36-345-6.pdb\)](#)
[3-b MP2/6-31G\(d,p\) \(36-345-m.pdb\)](#)
[3g HF/6-31G\(d\) \(36-34556.pdb\)](#)
[3g' HF/6-31G\(d\) \(36-3455a.pdb\)](#)

[3h HF/6-31G\(d\) \(36-34566.pdb\)](#)
[3h MP2/6-31G\(d,p\) \(36-3456m.pdb\)](#)
[3h MP2/6-311+G\(2d,p\) \(36-3456o.pdb\)](#)
[3h' HF/6-31G\(d\) \(36-3456a.pdb\)](#)
[3h'' HF/6-31G\(d\) \(36-3456b.pdb\)](#)
[3-c HF/6-31G\(d\) \(36-445-6.pdb\)](#)
[3i HF/6-31G\(d\) \(36-44556.pdb\)](#)
[4a HF/6-31G\(d\) \(45-12366.pdb\)](#)
[4b HF/6-31G\(d\) \(45-13366.pdb\)](#)
[4c HF/6-31G\(d\) \(45-13466.pdb\)](#)
[4c MP2/6-31G\(d,p\) \(45-1346m.pdb\)](#)
[4c' HF/6-31G\(d\) \(45-1346a.pdb\)](#)
[4d HF/6-31G\(d\) \(45-13566.pdb\)](#)
[4d MP2/6-31G\(d,p\) \(45-1356m.pdb\)](#)
[4d' HF/6-31G\(d\) \(45-1356a.pdb\)](#)
[4-a HF/6-31G\(d\) \(45-136-6.pdb\)](#)
[4-a MP2/6-31G\(d,p\) \(45-136-m.pdb\)](#)
[4e HF/6-31G\(d\) \(45-13666.pdb\)](#)
[4e MP2/6-31G\(d,p\) \(45-1366m.pdb\)](#)
[4f HF/6-31G\(d\) \(45-33466.pdb\)](#)
[4f' HF/6-31G\(d\) \(45-3346a.pdb\)](#)
[4g HF/6-31G\(d\) \(45-33566.pdb\)](#)
[4g' HF/6-31G\(d\) \(45-3356a.pdb\)](#)
[4-b HF/6-31G\(d\) \(45-336-6.pdb\)](#)
[4-b MP2/6-31G\(d,p\) \(45-336-m.pdb\)](#)
[4h HF/6-31G\(d\) \(45-33666.pdb\)](#)
[4h MP2/6-31G\(d,p\) \(45-3366m.pdb\)](#)
[4i HF/6-31G\(d\) \(45-34566.pdb\)](#)
[4i'' HF/6-31G\(d\) \(45-3456b.pdb\)](#)
[4i MP2/6-31G\(d,p\) \(45-3456m.pdb\)](#)
[4-c HF/6-31G\(d\) \(45-346-6.pdb\)](#)
[4-c MP2/6-31G\(d,p\) \(45-346-m.pdb\)](#)
[4-c' HF/6-31G\(d\) \(45-346-a.pdb\)](#)

4. Pyridazinediones as candidates for neuroactive amino acid analogues

Abstract

The primary inhibitory amino acid neurotransmitter GABA and the primary excitatory amino acid neurotransmitter glutamate are introduced, with emphasis on GABA_A and AMPA receptors respectively. Medicinal chemistry, pharmacology, therapeutics, and molecular biology are discussed briefly. The role 3-isoxazolols have played historically in developing our understanding of these receptors is emphasised. A rationale for investigating the replacement of the ring oxygen of 3-isoxazolols by an amide to form a pyridazinediones is offered, and illustrated with molecular modelling. The significance of pyridazinedione tautomerism and the rationale for investigating non-tautomeric *N*-methyl derivatives is discussed. Analogues of some of the more significant 3-isoxazolol GABA and EAA analogues are earmarked for synthesis, a total of 12 target compounds being selected.

Index

[4.1. Brief introduction to GABA receptors](#)

[4.2. Brief introduction to Excitatory Amino Acid \(EAA\) receptors](#)

[4.3. Pyridazinediones as amino acid analogues](#)

[4.3.1. The resemblance of pyridazinediones to 3-isoxazolols](#)

[4.3.2. Choosing to investigate maleic hydrazide derivatives](#)

[4.3.3. The role of tautomerism](#)

[4.3.4. The target series](#)

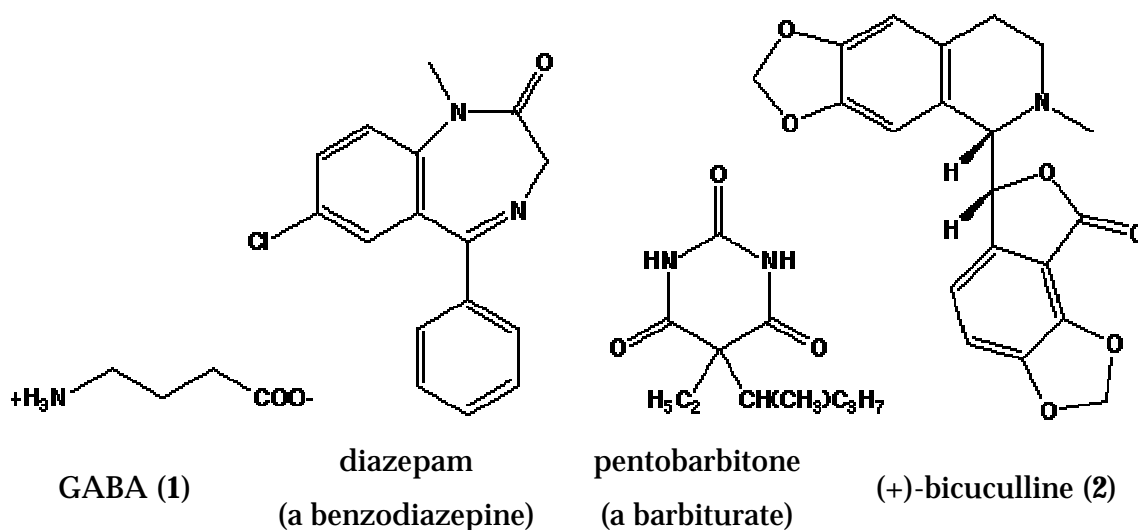
[4.4. References](#)

A number of excellent and recent reviews of GABA and EAA receptor pharmacology and medicinal chemistry are available [1,2]. It is not within the scope of this chapter to cover these subjects in any detail, rather to provide an overview of

the context in which the theoretical and synthetic studies described in the other chapters took place.

4.1. Brief introduction to GABA receptors

The ubiquitous amino acid γ -aminobutyric acid (GABA, **1**) has long been regarded as the most important and prevalent inhibitory neurotransmitter in the mammalian brain (Central Nervous System, CNS) [3,4]. To indicate its therapeutic importance, one need only consider the range of therapeutically useful compounds which owe at least some of their activity to the GABA system: sedatives such as barbiturates and benzodiazepines (see [scheme 4.1](#)), and steroid anaesthetics modulate the activation of various populations of GABA receptors, and the action of volatile anaesthetics and alcohol is also believed to be mediated at least in part by the GABA system [5]. GABA receptors are implicated in a wide range of neurological phenomena such as anxiety, analgesia, convulsions, coma, dementia, epilepsy, hypertension and schizophrenia [6].



Scheme 4.1 Some compounds acting at the GABA receptor

As a very simple, flexible amino acid, it comes as no surprise that it has been found to activate a highly heterogeneous population of receptors. On the basis of medicinal chemistry, i.e. the synthesis or extraction from natural sources of GABA analogues, and the testing of these on various preparations, and to a lesser extent on the basis of molecular genetics, GABA receptors have been classified into three classes: GABA_A, GABA_B, and GABA_C [1].

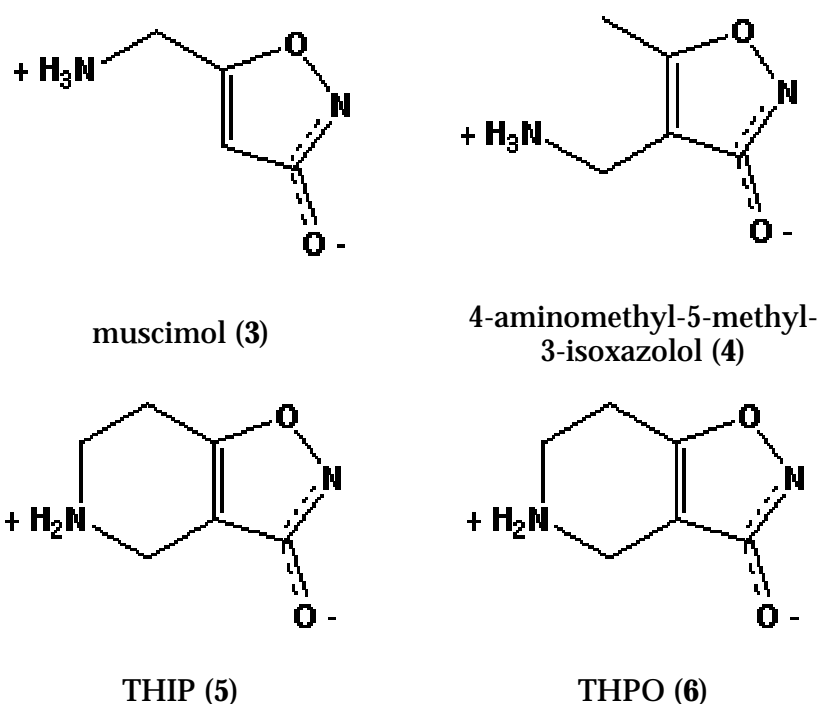
GABA_A receptors, the longest classified and best understood, as well as the most prevalent, and with which this study is primarily concerned, are ligand-gated chloride ion channels. They are blocked by the potent competitive antagonist (+)-bicuculline (2), a phthalideisoquinoline alkaloid isolated from *Dicentra cucullaria* [7].

A major leap forward in the study of GABA receptors was made when it was found that a muscimol (5-aminomethyl-3-isoxazolol, 3) is a potent agonist of GABA receptors, whose action is mostly blocked by bicuculline (2) [8]. Thus it is a potent GABA_A agonist, but more recent work shows that it has some affinity for GABA_B receptors, and is now known to be a partial agonist at GABA_C [1,4]. Muscimol is the main psychoactive component of *Amanita muscaria* (the red-and-white toadstool of fairytale fame) known since antiquity to cause sedation and a kind of toxic delirium when ingested [9].

A large number of muscimol (3) analogues were synthesised in the effort to gain further insight into the nature of the GABA_A receptor [10]. Mostly, activity was poorer, although dihydromuscimol and homomuscimol (5-aminoethyl-3-isoxazolol) are worthy of some note. The methylated positional isomer of muscimol, 4-aminomethyl-5-methyl-3-isoxazolol (4), a compound of minor significance in this study, was found to be without activity [10].

The discovery that a cyclised form of muscimol, THIP (5), also activated the GABA_A receptors, although with somewhat less efficacy than muscimol, was another leap forward [11]. It was noted that the action of THIP, for example with respect to benzodiazepine binding, showed differences from GABA and muscimol [12]. Later, it was found that unlike muscimol which is a GABA_C agonist, THIP is a GABA_C

antagonist [1]. The differences in action of compounds such as THIP and muscimol were instrumental in indicating the heterogeneity of the GABA_A receptor, now confirmed from molecular biology by the "mix-and-match" of various cloned subunits which can be assembled in a multitude of ways to form the pentameric receptor [1]. THIP is also noteworthy for its potent analgesic effects, and for having proceeded to clinical trials in this regard. The isomer of THIP, 4,5,6,7-tetrahydroisoxazole[4,5-c]pyridin-3-ol (THPO, 6) was found to be not an agonist, but a GABA uptake inhibitor [13,14], whose minor significance to this study will also become apparent.



Scheme 4.2 3-isoxazolols with varying activity at GABA receptors

The search for new kinds of substances active at GABA_A receptors goes on, both because of the therapeutic potential of potent and specific compounds, and because the more the (currently small) catalogue of compounds known to be active is expanded, the better understanding we gain of this vital neurochemical system.

As was alluded to in the previous chapters, much of this thesis is concerned with carboxylate bioisosteres. Very few classes of structures containing a replacement for carboxylate are currently known to produce agonists at GABA_A. By far the best

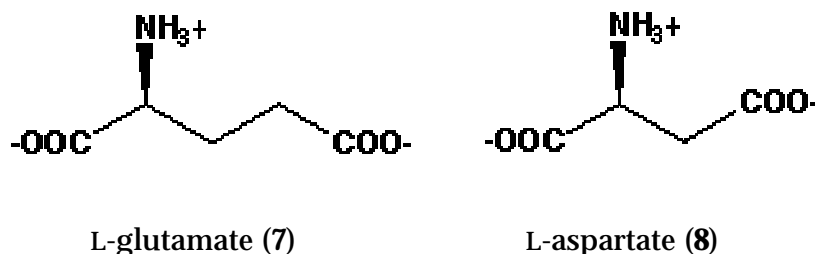
studied are the 3-isoxazolols. Subsequently, their sulfur analogues, the 3-isothiazolols have been shown to be active [15]. However, 5-isoxazolols and 3-diazolols have been shown to be inactive, underscoring strict requirements for activity [1]. Sketchy reports indicate possible activity for two additional classes, quisqualamine - an oxadiazolodione derivative, and kojic amine, a 3-hydroxypyran-4-one. See [section 7.1.2](#) for a discussion of these two compounds. Other structures known to produce analogues with agonist or partial agonist properties contain a naked carboxylate, or in a very few instances, sulfonate moiety [1].

This begs the question: are there other as yet untested acidic hydroxy heterocycles which can act as carboxylate bioisosteres at the GABA_A receptor?

One of the main reasons to examine heterocyclic carboxylate bioisosteres rather than analogues featuring a naked carboxylate, is because incorporation of the acidic function within a ring greatly increases the lipophilicity of the compound, and thus its ability to permeate the blood brain barrier (BBB), vital to the development of systemically administerable therapeutics.

4.2. Brief introduction to Excitatory Amino Acid (EAA) receptors

It has long been known that the CNS contains high concentrations of glutamate (7), and that glutamate and aspartate (8) cause near universal neuronal excitation. Glutamate is now accepted as the major excitatory neurotransmitter in the CNS, while the role of aspartate is less well defined [5]. The receptors for such substances are known as Excitatory Amino Acid (EAA) receptors [16].



Scheme 4.3 Two endogenous excitatory amino acids

As might be expected from their ubiquitous occurrence, EAA receptors are suggested to play a role in a wide variety of brain functions and abnormalities. To name a few, EAA receptors are implicated in such disorders as epilepsy [16], Huntington's chorea [17], Alzheimer dementias [18], AIDS-related dementia, schizophrenia and Parkinsonism [19]. One of the most significant potential applications of EAA-related compounds concerns neuroprotection under conditions of ischaemia such as stroke. It is known that high levels of glutamate are excitotoxic to neurones, and are released under ischaemic conditions. It is reasoned therefore that glutamate blockers (particularly of the AMPA subclass) are potentially able to protect the brain from damage immediately following a stroke. Drugs based on this principle have been trialled clinically, and new agents are greatly sought after [20].

Glutamate receptors, implicated in learning and memory, are important in mediating the phenomenon of Long Term Potentiation (LTP) which has been the subject of intense discussion and research since the 1980s, as a postulated cellular mechanism of memory [21,22].

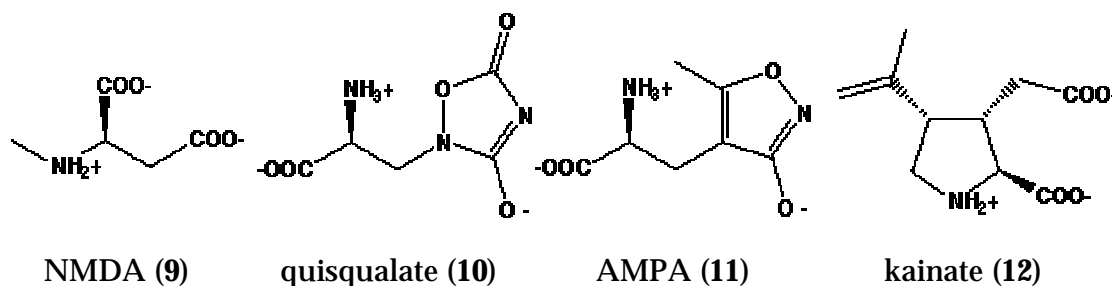
The very importance of EAA receptors is actually an impediment to furthering their understanding: the development of therapeutic agents acting at various EAA receptors is hampered by the very widespread distribution and function of the receptors. This serves as an impetus for research into more specific and localised targets.

In recent years, molecular biology and extensive medicinal chemistry have seen the classification of EAA receptors into a number of classes [5]. The primary division is between the metabotropic and ionotropic classes of receptors. On the basis of sequence homology and agonist/antagonist pharmacology, three classes of metabotropic (G-protein-coupled) receptors are now recognised [23]. Better understood are the ionotropic receptors (permeable to Na⁺ and in some cases to Ca²⁺) with which this thesis is chiefly concerned.

The ionotropic receptors are also currently divided into three classes, on the basis of medicinal chemistry and molecular biology [2]. A number of different subunits

which comprise these receptors have been cloned, and homo- and hetero-oligomers exist for all three classes. The first class to be identified was the NMDA receptor, after the potent and specific agonist *N*-methyl-D-aspartate (9), and it remains the best understood [24]. As with the other classes of EAA receptors, specific antagonists have been found to aid characterisation.

Non-NMDA ionotropic EAA receptors, originally named quisqualate (QUIS) receptors, after the potent naturally occurring excitotoxin quisqualic acid (10), (*S*)- α -amino-3,5-dioxo-1,2,4-oxadiazolidine-2-propanoic acid (from *Quisqualis* sp.), have been shown to belong to two classes named AMPA receptors and kainate (KAIN) receptors, after the potent and selective agonist AMPA (2-amino-3-(3-hydroxy-5-methylisoxazol-4-yl)propanoic acid, 11) and the potent, but somewhat less selective agonist kainic acid (12) [16].



Scheme 4.4 Agonists which have been used to characterise ionotropic EAA receptor subtypes

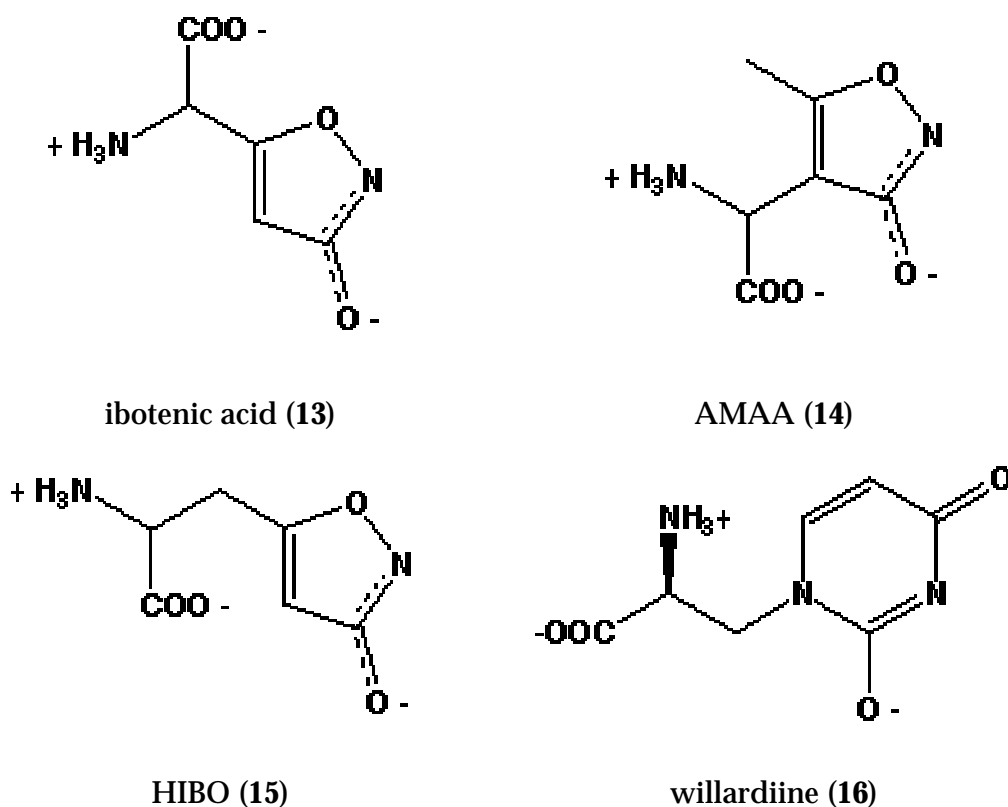
Just as the identification of muscimol as a GABA agonist was a watershed, likewise, another component of *Amanita muscaria*, the α -carboxylate derivative of muscimol, known as ibotenic acid (13), proved to be a crucial lead in the development of understanding of ionotropic glutamate receptors. The similarity {muscimol is to GABA, as ibotenic acid is to glutamate} is immediately apparent. However, no such general homology exists across the range of known active compounds at amino acid receptors. Ibotenic acid proved to be a non-specific agonist, activating both NMDA and non-NMDA ionotropic receptors, and also possessing metabotropic activity [25].

Its positional methylated isomer AMAA (*R,S*)-2-amino-2-(3-hydroxy-5-methylisoxazol-4-yl)acetic acid (14) was found to be a potent specific agonist of

NMDA receptors [26]. 3-Isoxazolols unsubstituted at position 5-, though not unknown, appear to be particularly difficult to synthesise. Interestingly, whereas the (*S*) isomer of ibotenic acid and also of most AMPA-specific agonists is the more potent, the (*R*) isomer of AMAA has recently been found to be the more potent [27]. This thesis considers for the most part racemic mixtures, being much easier to produce and screen initially.

Homologisation of ibotenic acid by adding an extra methylene to the α -amino acid moiety, substantially increased the specificity with respect to non-NMDA receptors. It was found that homoibotenic acid (HIBO, 15) is a specific AMPA agonist, and that while fairly weak, certain 4-substituted derivatives are potent agonists [28] (see [chapter 8](#), [table 8.1](#) for a full list).

The methylated positional isomer of HIBO (15), which is also the homologue of AMAA (14), is 2-amino-3-(3-hydroxy-5-methylisoxazol-4-yl)propanoic acid (AMPA, 11) [29]. The discovery of AMPA was of great importance in differentiating non-NMDA receptors, which were subsequently known as AMPA and Kainate after their respective potent agonists.



Scheme 4.5 isoxazole α -amino acids with varying activity at EAA receptors, and the amino acid willardiine

The extensive range of hydroxy heterocycles which are now known to be capable of incorporation as α -carboxylate bioisosteres in potent AMPA analogues is reviewed in detail in [chapter 8](#), but when the current investigation was commenced, only a small handful were known, the six-membered uracil derivative willardiine (16) [30] being the most important example, other than the 3-isoxazolols. The question was asked: are there other as yet untested acidic hydroxy heterocycles which can act as carboxylate bioisosteres at the AMPA receptor?

4.3. Pyridazinediones as amino acid analogues

Having introduced the two most important types of amino acid neuroreceptors, we now turn our attention to the pyridazinediones, and the ways in which they might be used to advance our understanding of these receptors.

Firstly, a note regarding nomenclature: tautomerism of maleic hydrazides makes precise naming difficult. In the case of the non- *N*-methylated compounds, a mixture of two tautomers is expected for all structures, or at any rate, the precise structure cannot be determined. The literature has called such compounds both 3,6-dihydroxypyridazines, 3,6-pyridazinediols, and more often, 3,6-pyridazinediones, pyridazine-3,6-diones, and so on. In general, the convention of calling maleic hydrazide derivatives pyridazine-3,6(1,2*H*)-diones has been used in this text, even though we know that the actual structures are a mixture of tautomeric hydroxypyridazinones. In the case of the *N*-methyl derivatives, naming has followed the correct structure, e.g. 2-methyl-6-hydroxypyridazin-3(2*H*)-one, even though this might be referred to as a pyridazinedione in the literature. "Dioxypyridazines" and "pyridazinediones" have also been used as colloquialisms for the whole class of structures.

4.3.1 The resemblance of pyridazinediones to 3-isoxazolols

The heterocycle which has proved the most fertile source of GABA_A and AMPA analogues is 3-isoxazolol. The conjugate base of this acidic heterocycle contains an O-C-N portion which closely resembles the O-C-O of carboxylate; 3-isoxazolol is considered to be a carboxylate bioisostere. However, there is a greater degree of charge delocalisation associated with the heteroaromatic ring than is the case for carboxylate, and depending on the receptor environment, this may promote binding.

When considering which pyridazinediones might be employed as novel amino acid analogues, a first step was to examine the similarities and differences between various pyridazinediones and 3-isoxazolol.

[Chapters 2](#) and [3](#) examined in some detail the structures, charge distributions, and tautomeric preferences of all dioxo substituted pyridazines. All four of the acidic hydroxy pyridazine 1-oxides and four pyridazinediones might be considered as potential carboxylate bioisosteres. However, examining the structures and tautomeric preferences of the conjugate bases, it is apparent that 4,5-

dioxypyridazine is not capable of forming an O-X-N anionic structure, and that 3,4-dioxypyridazine and 3,5-dioxypyridazine do not show a tautomeric preference for an O-X-N anionic system such as is found in the base of 3-isoxazolol. Furthermore, of the remaining structures, only two possess the negatively charged structure O-C-N which most closely resembles the base of 3-isoxazolol. Examining the point charges calculated from electrostatic potentials, these same two structures, namely pyridazine-3,6-dione (maleic hydrazide) and 3-hydroxy pyridazine 1-oxide, also show the largest negative charge distributions on the O-X-N structure. Thus, these two were the acidic pyridazinones considered most worthy of investigation as novel ring structures around which to design amino acid analogues.

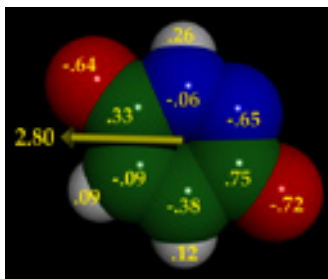


Figure 4.1 base of maleic hydrazide (linked to full size image)

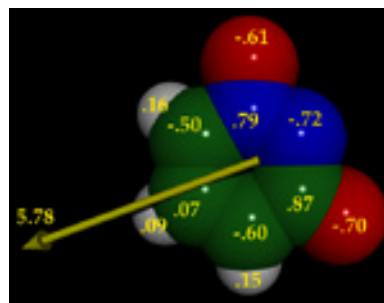


Figure 4.2 base of 3-hydroxypyridazine 1-oxide (linked to full size image)

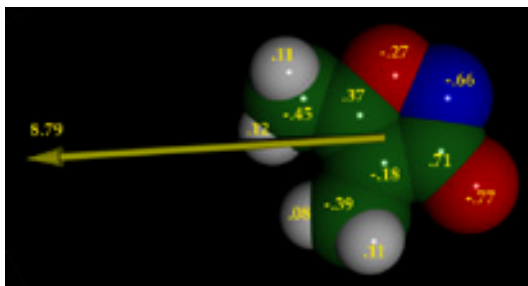


Figure 4.3 base of 4,5-dimethyl-3-isoxazolol (linked to full size image)

[Figures 4.1](#), [4.2](#), and [4.3](#) depict anionic base structures optimised at the MP2 / 6-31G(d,p) level of *ab initio* theory. Point charges and dipoles were calculated using the Merz-Kollman-Singh method [34] and are depicted in yellow. All three structures show similar geometry and charge distribution in the O-C-N region. The pyridazines however have a second region of negative charge associated with the second oxygen substituent.

4.3.2 Choosing to investigate maleic hydrazide derivatives

Of all the pyridazinones, the most accessible in terms of ease of synthesis and large synthetic knowledge base, is maleic hydrazide and its derivatives. In fact, maleic hydrazide itself is employed commercially as a plant growth inhibitor under trade names such as Fazor, Malazide and Regulox [35]. Though less well understood, 3-hydroxypyridazine 1-oxide chemistry is also fairly well documented by comparison with other pyridazinediones [31].

Pyridazine-3,6-diones are attractive as potential carboxylate bioisosteres for a number of reasons. As discussed in [chapter 3](#), though slightly less acidic, they are of comparable acidity to carboxylic acids, within a couple of pH units of the ω -carboxylate of glutamate for example. Both are almost entirely deprotonated at physiological pH

The pyridazine ring, having two adjacent nitrogen atoms, possesses a large dipole; larger than other diazoles or pyridine [31]. It is hypothesised that the local binding region of the AMPA receptor in particular is strongly polarised, and that employing a highly polar heteroaromatic group could increase activity. Pyridazines have been highly favoured in certain areas of medicinal chemistry as aromatic bioisosteres on account of their large dipoles [32,33]

The structural difference between pyridazine-3,6-dione and 3-isoxazolol, lies in the replacement of the ring oxygen of isoxazole with an amide linkage. Whether amino acid analogues based on pyridazine-3,6-dione are active or not should depend heavily on whether this larger more negatively charged amide region can be accommodated by the various receptors.

A potential advantage of pyridazinediones over 3-isoxazolols, whose behaviour as GABA and EAA analogues has now been explored fairly exhaustively, is that being six-membered rather than five-membered rings, should a potent lead compound be found, there is a greater opportunity for a more diverse range of derivatives with specifically located substituents. In particular, having the extra position for substitution was considered an advantage for the potential for design of

antagonists. In the early 1990s when pyridazinediones were first postulated as potential amino acid neurotransmitter analogues, only one active compound containing a six-membered ring had achieved prominence: the naturally occurring (Family *Leguminosae*) amino acid willardiine (16), a uracil-derived AMPA analogue [30]. In chapter 8, the larger range of AMPA analogues based on six-membered heterocyclic carboxylate bioisosteres now known is reviewed. Willardiines and other six-membered heterocycles remain a fertile area of amino acid neurotransmitter analogue research.

While 3-isoxazolols possess only one ring oxygen substituent, quisqualate (10) and willardiine (16), like pyridazindiones, have two. While both 4- and 5- alanino substituted isoxazolols, e.g. AMPA (11) and HIBO (15), and 4- and 5- glycino substituted isoxazolols, e.g. AMAA (13) and ibotenic acid (14) were known to produce analogues active at EAA receptors of varying potency, little had been determined about the dependence of activity on the relative positions of oxygen substituents, particularly when the heterocycle is six-membered and contains more than one potential acidic group. Even less was known about the possibilities of six-membered heterocycles as scaffolds for GABA analogues. Studying a variety of substituted pyridazinediones was therefore an attractive means for probing the relationship between oxygen substitution and amino acid analogue activity.

4.3.3 The role of tautomerism

As discussed in chapter 3, maleic hydrazide strongly prefers a lactam-lactim structure. The structure of the preferred anion of maleic hydrazide is *N*-protonated. But in the case of derivatisation at position 4 to produce an amino acid analogue, symmetry is broken and the two *N*-protonated tautomers are no longer identical. Very little energy separates the structures bearing the two possible sites of *N*-protonation, and the solution structure is likely to be a dynamic equilibrium mixture of both. That means that the maleic hydrazide derivatives may be present as analogues of either, or more likely both, of the isomeric 4- and 5- substituted 3-isoxazolols.

Therefore, maleic hydrazides are uniquely placed to serve simultaneously as analogues of both 4- and 5- substituted 3-isoxazolols. However, should maleic hydrazide be *N*-substituted with a group other than a labile proton, the tautomeric ambiguity is at once removed. The simplest such substituent to introduce would be a methyl group. Whereas a proton is labile in aqueous solution, an *N*-methyl group is not.

Thus in addition to attempting the synthesis of ambiguous maleic hydrazides derivatised at the 4-position, it was also considered desirable to attempt to make the derivatives which had the carboxylate-like region "locked" in either form. So, 4-substituted and 5-substituted 2-methyl-6-hydroxypyridazin-3(2*H*)-ones would putatively be able to provide information about the dependence of activity on the relative position of the side chain and the negatively charged ring oxygen. It was hoped that the *N*-methylated versions would assist in differentiating how any activity found in the unmethylated maleic hydrazide derivatives was dependent on tautomeric structure.

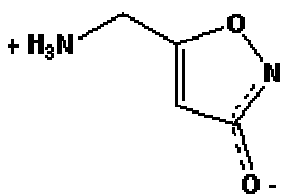
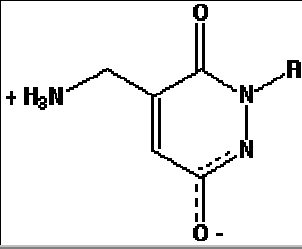
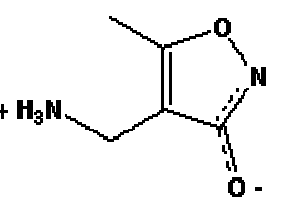
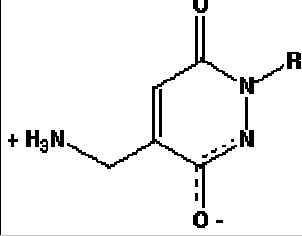
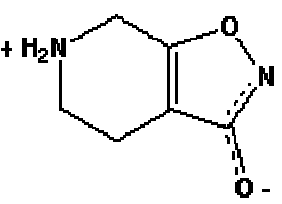
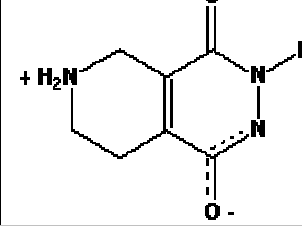
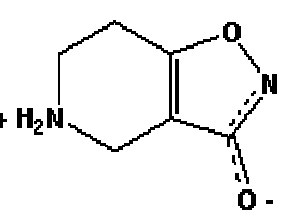
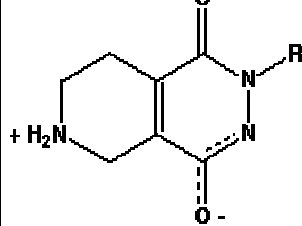
4.3.4 The target series

The central question to be determined is posed thus: can the ring oxygen of an archetypal isoxazolol which is active at EAA or GABA_A receptors be replaced by an amide linkage, to form a pyridazinedione, and retain activity? And since this creates a mixture of tautomers, each of which may be considered analogues of two isoxazolols, what is the result of fixing the relative positions of the side-chain and acidic bioisostere by *N*-methylation?

To answer these questions, a set of test compounds to be synthesised and evaluated for activity was proposed, based on analogy with the most significant 3-isoxazolols known to possess GABA and EAA agonist activity, discussed above. Four basic kinds of derivatisation were found to account broadly for the range of 3-isoxazolols with agonist activity: substitution by an aminomethyl group or fusion with a tetrahydropyridine ring to produce GABA_A agonists, and substitution by a glycine group or alanine group to produce EAA agonists.

This suggested the following target series: maleic hydrazide analogues of muscimol (3) and its inactive analogue 4-aminomethyl-5-methyl-3-isoxazolol (4); analogues of THIP (5) and THPO (6); analogues of ibotenic acid (13) and AMAA (14); and analogues of HIBO (15) and AMPA (11). The inclusion of the two *N*-methyl derivatives of each of these four paired systems, removing tautomeric ambiguity, gives a total target series of twelve compounds by which to thoroughly investigate the potential of pyridazine-3,6-diones as amino acid analogues. These structures (17 to 28) are presented in table 4.1.

Table 4.1 Target series: structures of known amino acid analogues and their pyridazinedione counterparts

name	3-isoxazolol		pyridazinedione (R=H, CH ₃)		figures (overlays)
	structure (linked to .pdb geometry)	activity	numbers	structure (linked to .pdb geometry)	
muscimol (3)		potent non-specific GABA agonist	17a (R=H) 21 (R=CH ₃)		Figure 4.4
4-aminomethyl-5-methyl-3-isoxazolol (4)		no GABA binding inhibition no <i>in vivo</i> activity at spinal neurones	17b (R=H) 22 (R=CH ₃)		Figure 4.5
THIP (5)		potent GABA _A partial agonist, GABA _C antagonist	18a (R=H) 23 (R=CH ₃)		Figure 4.6
THPO (6)		potent GABA reuptake inhibitor	18b (R=H) 24 (R=CH ₃)		Figure 4.7

ibotenic acid (13)		potent non-specific NMDA/AMPA agonist	19a (R=H) 25 (R=CH ₃)		Figure 4.8
AMAA (14)		specific NMDA agonist	19b (R=H) 26 (R=CH ₃)		Figure 4.9
homoibotenic acid (15)		weak specific AMPA agonist	20a (R=H) 27 (R=CH ₃)		Figure 4.10
AMPA (11)		potent specific AMPA agonist	20b (R=H) 28 (R=CH ₃)		Figure 4.11

The [structures in table 4.1](#) were optimised using AM1-SM2 aqueous semi-empirical theory in low energy conformations. Electrostatic isopotentials in the plane of the aromatic ring were determined from the wavefunction using Spartan 5.0 [36]. Compounds were overlaid with matching ionic groups and carbon backbone, and are depicted in figures 4.3 to 4.10

The [next chapters](#) describe the pursuit of the pyridazine-3,6-diones proposed here as neuroactive amino acid analogues. As suggested above, 3-hydroxy pyridazine 1-oxides were also considered worthwhile candidates for synthesis and testing. While these compounds do not possess the kind of interesting tautomeric properties of the pyridazine-3,6-diones, and were thought to be somewhat more challenging to produce synthetically, they do have a larger dipole, and more closely resemble the known AMPA agonist willardiine (16). Co-workers [37] were therefore investigating the 3-hydroxypyridazine 1-oxides, among other structures, at the

same time as this work on pyridazine-3,6-diones was undertaken. As it turned out, it was the 3-hydroxypyridazine 1-oxides which proved the richer source of active AMPA analogues, and these results are described in the review of heterocycles active at AMPA receptors in [chapter 8](#). To date, their synthesis and activity as GABA analogues remains unexplored.

4.4 References

1. SJ Enna, NG Bowery, *The GABA Receptors*, 2nd ed., Humana Press, Totowa, New Jersey (1997)
2. DT Monaghan, R Wenthold, *The Ionotropic Glutamate Receptors*, Humana Press, Totowa, New Jersey (1997)
3. M Otsuka, *Pharmacology and the Future of Man: Proceedings of the Fifth International Congress on Pharmacology*, **4**, 186-201 (1973)
4. DIB Kerr, J Ong, *Medicinal Research Reviews*, **12(6)**, 593-636 (1992)
5. JG Hardman, LE Limbird, PB Molinoff, RW Ruddon, A Goodman Gilman, *The Pharmacological Basis of Therapeutics*, 9th ed., McGraw-Hill, 280-282 (1996)
6. GAR Johnston, *Clinical and Experimental Pharmacology and Physiology*, **19**, 73-78 (1992)
7. DR Curtis, AW Duggan, D Felix, GAR Johnston, *Nature*, **266**, 1222-1224 (1970)
8. DR Curtis, AW Duggan, D Felix, GAR Johnston, *Brain Res.*, **32**, 69-96 (1971)
9. J Mann, *Murder Magic and Medicine*, Oxford University Press (1992)
10. P Krogsgaard-Larsen, GAR Johnston, *J. Neurochem.*, **30**, 1377-1382 (1978)
11. P Krogsgaard-Larsen, GAR Johnston, D Lodge, DR Curtis, *Nature*, **268**, 53 (1977)
12. JH Skerritt, GAR Johnston. *Neurosci. Lett.*, **38**, 315-329 (1983)
13. P Krogsgaard-Larsen, GAR Johnston. *J. Neurochem.*, **25**, 797-802 (1975)
14. P Krogsgaard-Larsen, L Brehm, K Schaumburg, *Acta Chem. Scand. Ser. B*, **35**, 311 (1981)
15. P Krogsgaard-Larsen, H Hjeds, DR Curtis, D Lodge, GAR Johnston, *J. Neurochem.*, **32**, 1717 (1979)
16. JJ Hansen, P Krogsgaard-Larsen, *Medicinal Research Reviews*, **10(1)**, 55-94 (1990)
17. AJ Gross, P Slater, GP Reynolds, *Neurosci. Lett.*, **67**, 198 (1986)
18. WF Maragos, JT Greenamyre, JB Penney, AB Young, *Trends Neurosci.*, **10**, 65 (1987)

19. SA Lipton, PA Rosenburg, *The New England Journal of Medicine*, **330**, 613-622 (1994)
20. R Gill, D Lodge, *International Review of Neurobiology*, **40**, 197-232 (1997)
21. TVP Bliss, GL Collingridge, *Nature*, **361**, 31-39 (1993)
22. JT Wroblewski, W Danysz, *Annual Review of Pharmacology and Toxicology*, **29**, 441-474 (1989)
23. JP Pin, R Duvoisin, *Neuropharmacology*, **34**, 1-26 (1995)
24. GL Collingridge, JC Watkins, *The NMDA receptor*, 2nd ed., Oxford, New York, Oxford University Press (1994)
25. DD Schoepp, BG Johnson. *J. Neurochem.*, **50**, 1605-1613 (1988)
26. U Madsen, JW Ferkany, BE Jones, B Ebert, TN Johansen, T Holm, P Krogsgaard-Larsen, *Eur. J. Pharmacol., Mol. Pharmacol. Sect.* **189**, 381-391 (1990)
27. U Madsen, K Frydenvang, B Ebert, TN Johansen, L Brehm, P Krogsgaard-Larsen, *J. Med. Chem.*, **39**, 183-190 (1996)
28. P Krogsgaard-Larsen, T Honore, JJ Hansen, *Nature*, **284**, 64-66 (1980)
29. JJ Hansen, P Krogsgaard-Larsen, *J. Chem. Soc., Perkin Tr. I*, 1826 (1980)
30. RH Evans, AW Jones, JC Watkins, *J. Physiol. Lond.*, **308**, 72P (1980)
31. RN Castle, Pyridazines, *The Chemistry of Heterocyclic Compounds*, Wiley Interscience, **28**, (1973)
32. G Heinisch, H Frank, *Progress in Medicinal Chemistry*, **27**, 1 (1990)
33. G Heinisch, H Frank, *Progress in Medicinal Chemistry*, **29**, 141 (1992)
34. BH Besler, KM Merz, Jr., PA Kollman, *J. Comp. Chem.*, **11**, 431 (1990)
35. *The Merck Index*, 12th ed., Merck & Co., Whitehouse Station, NJ, 5745 (1996)
36. WJ Hehre. *Spartan 5.0*. Wavefunction Inc., 18401 Von Karman, Suite 370, Irvine, California 92715 (1998)
37. G Vaccarella, *Synthesis and Activity of Pyridazine Analogues of Glutamic Acid*, PhD thesis, Department of Pharmacology, University of Sydney (1998)

Figure 4.4 Overlay: 3, 17a

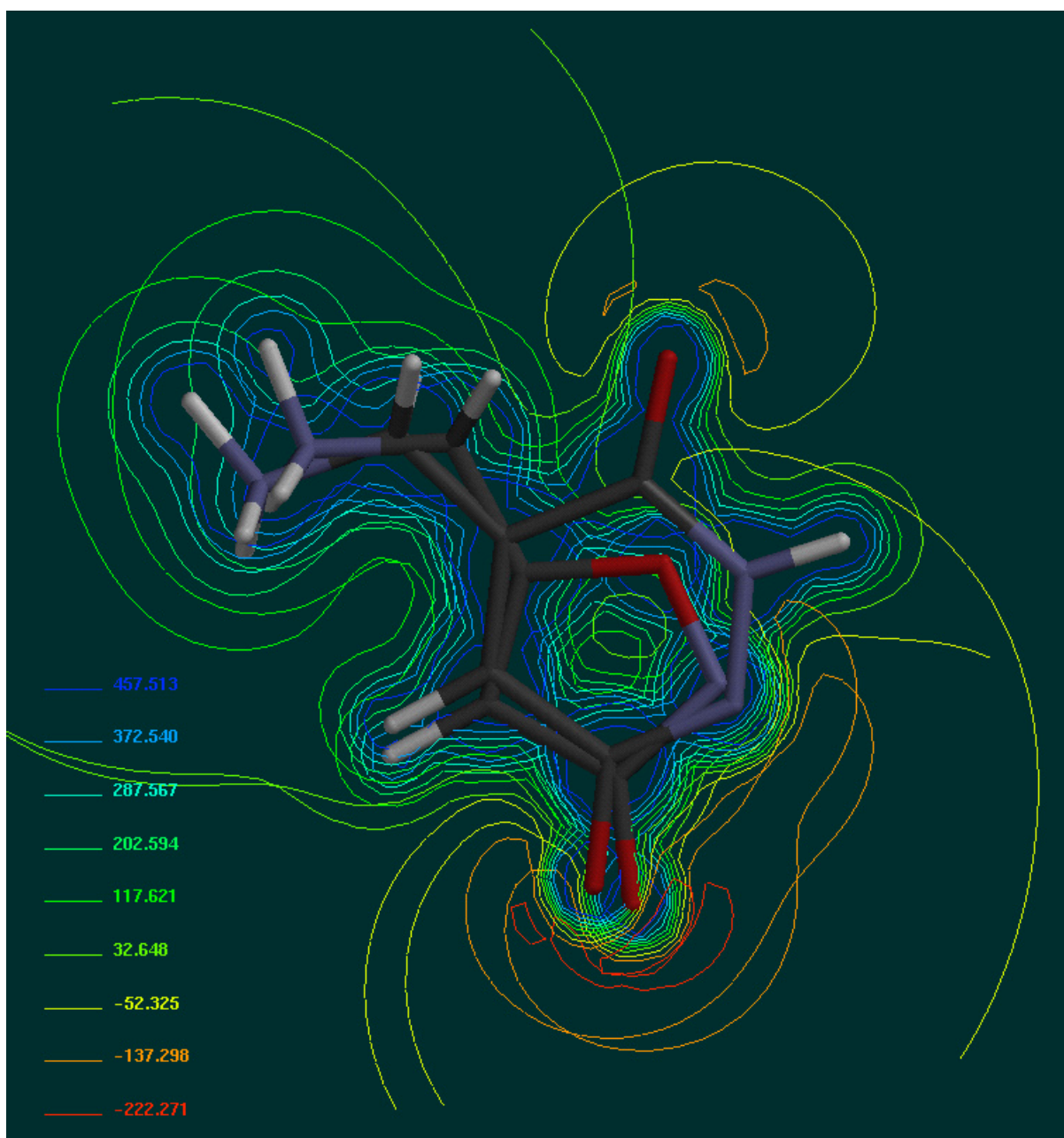


Figure 4.5 Overlay: 4, 17b

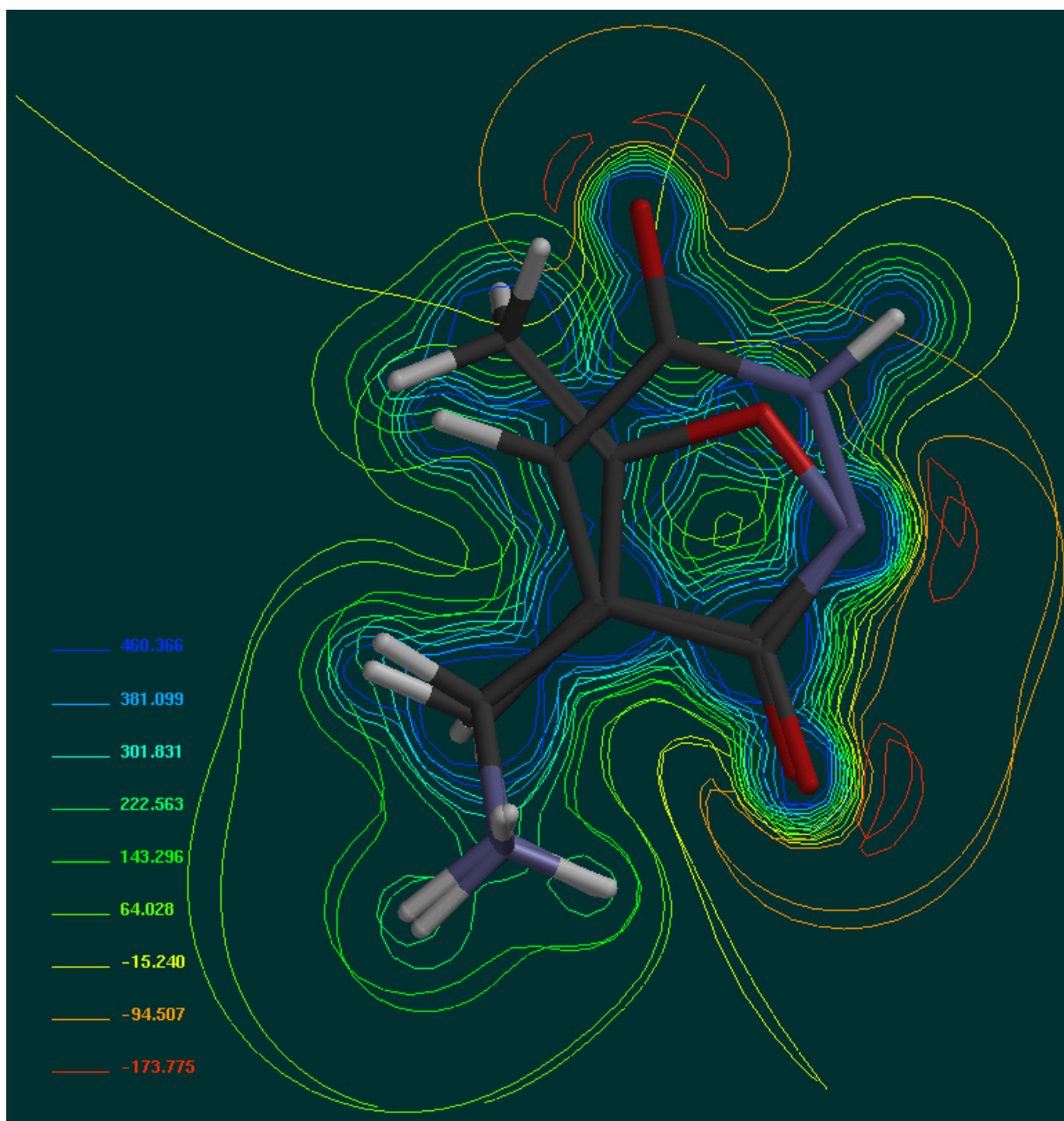


Figure 4.6 Overlay: 5, 18a

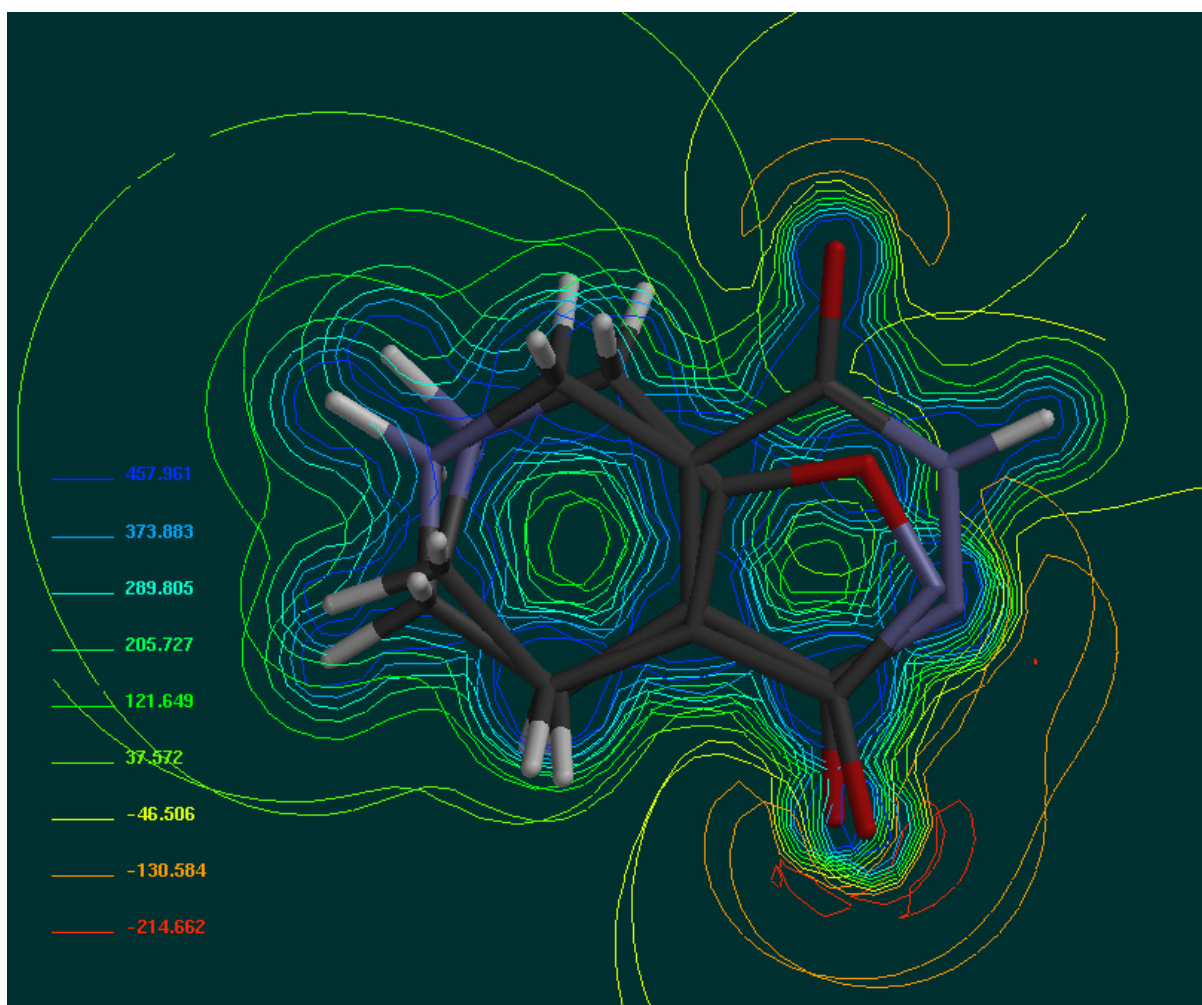


Figure 4.7 Overlay: 6, 18b

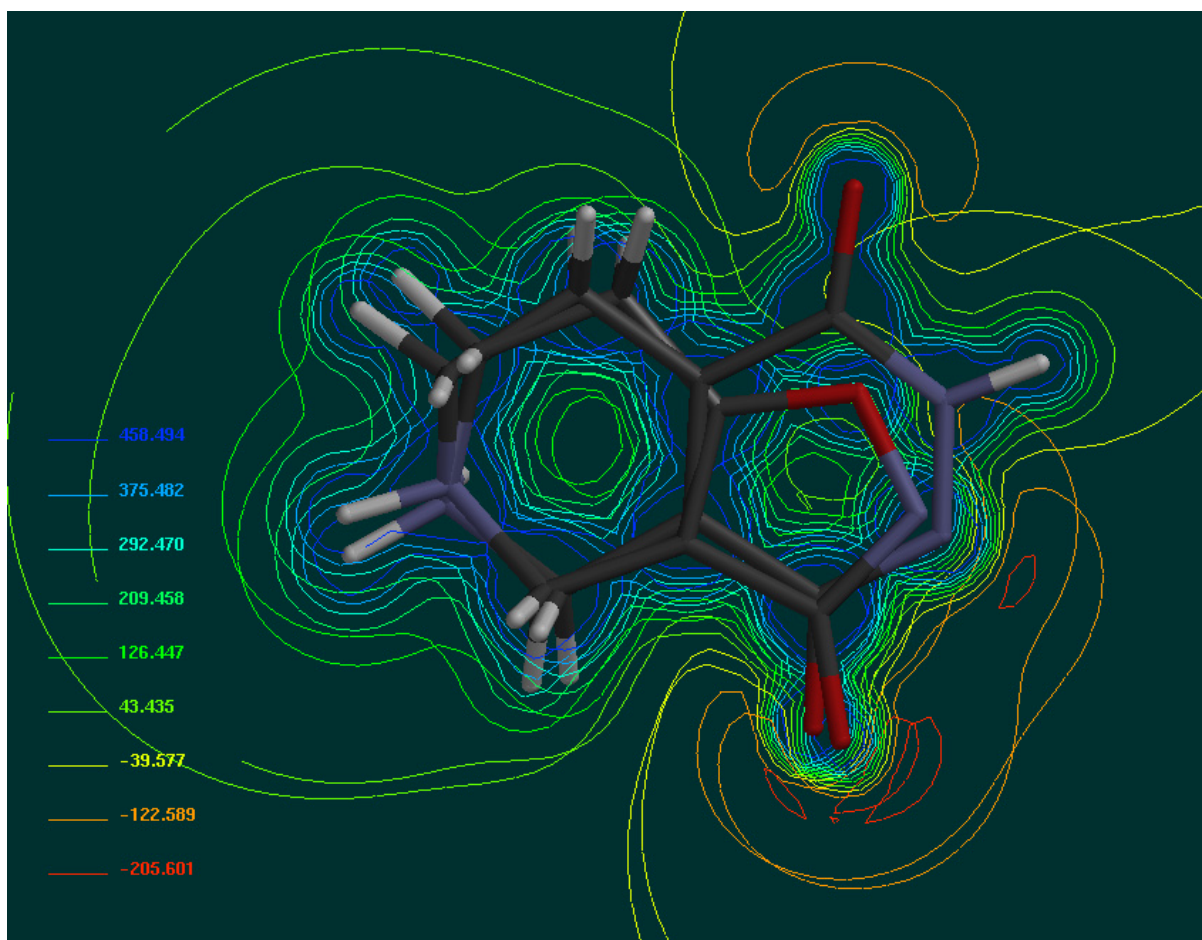


Figure 4.8 Overlay: 13, 19a

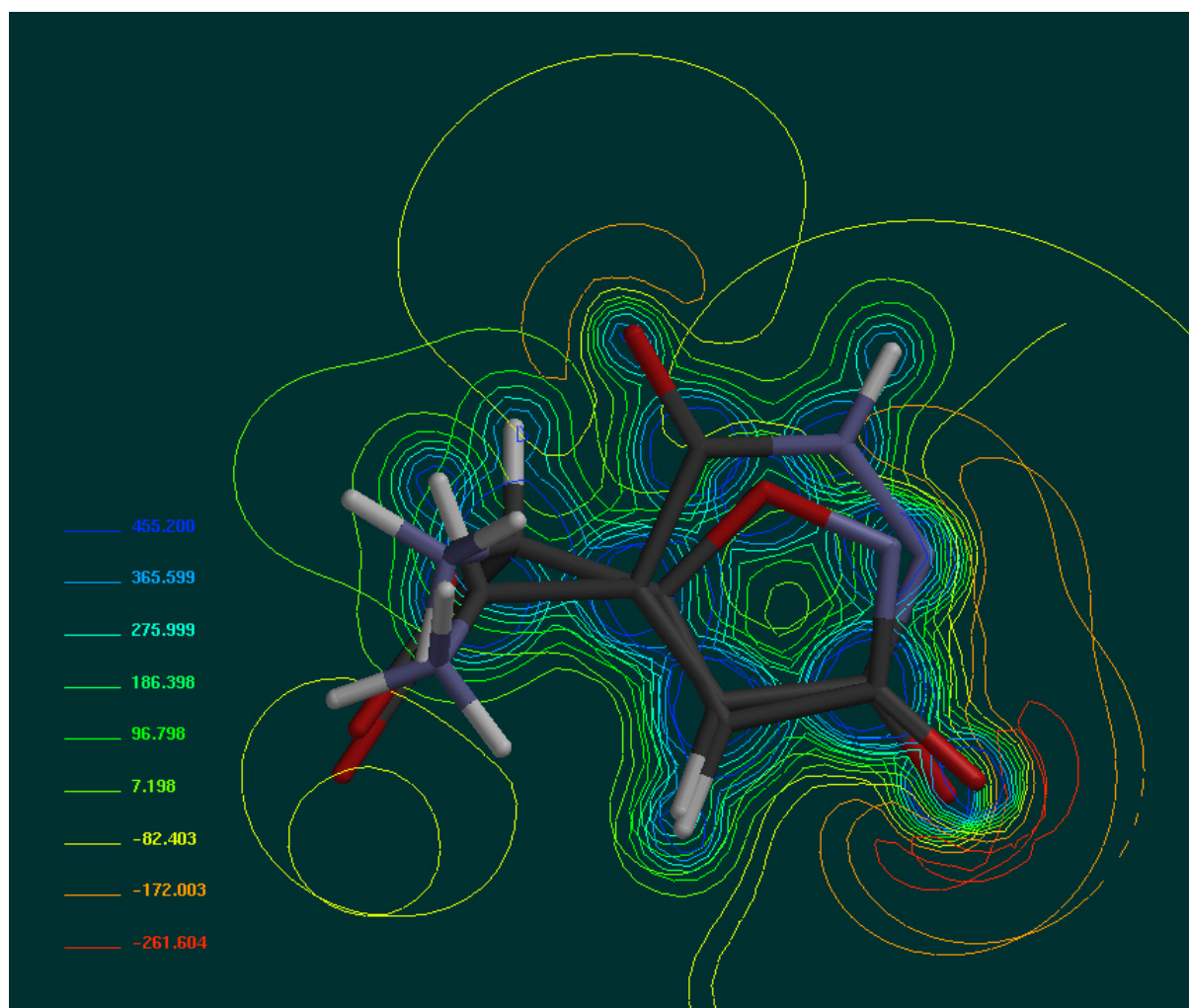


Figure 4.9 Overlay: 14, 19b

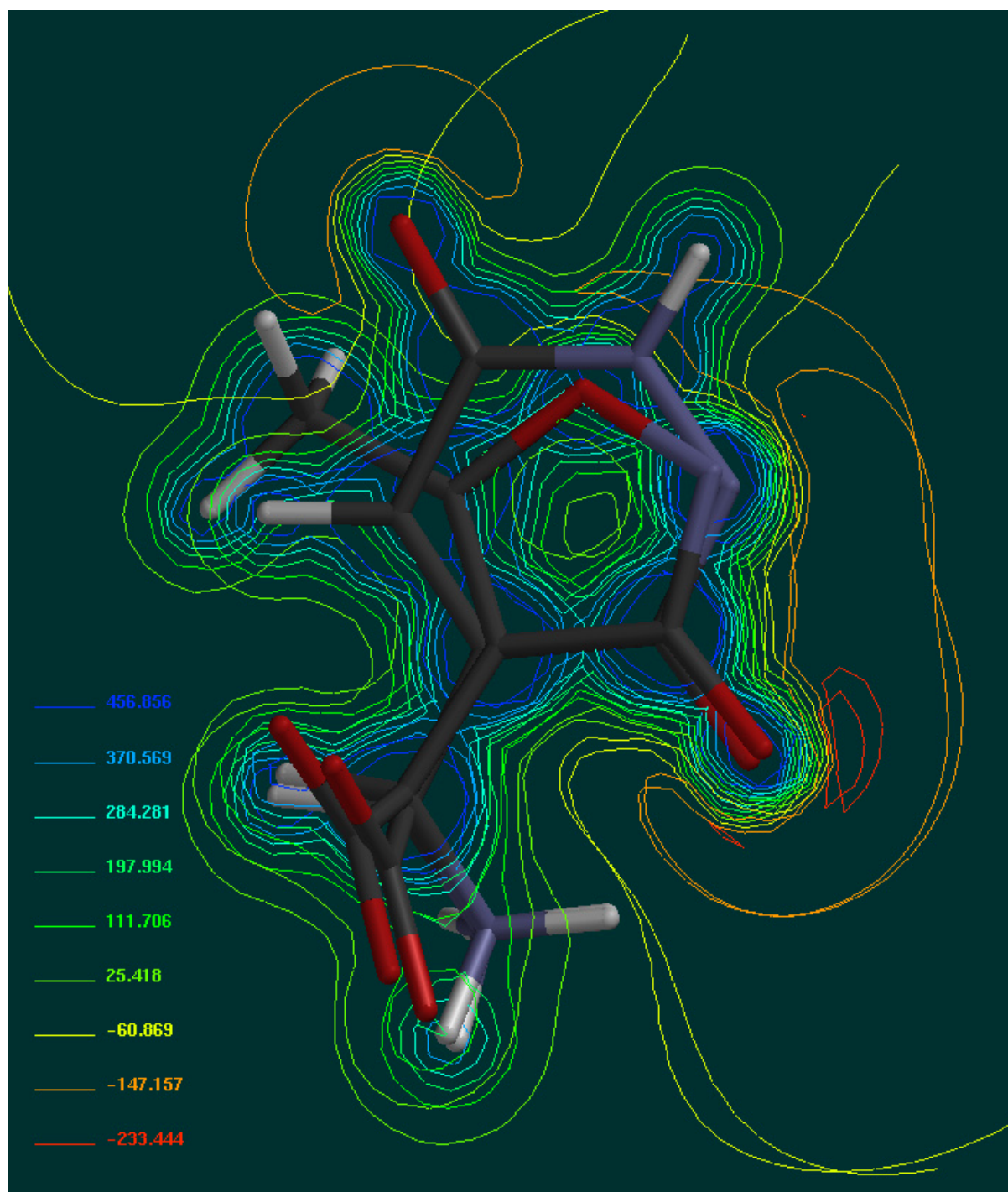


Figure 4.10 Overlay: 15, 20a

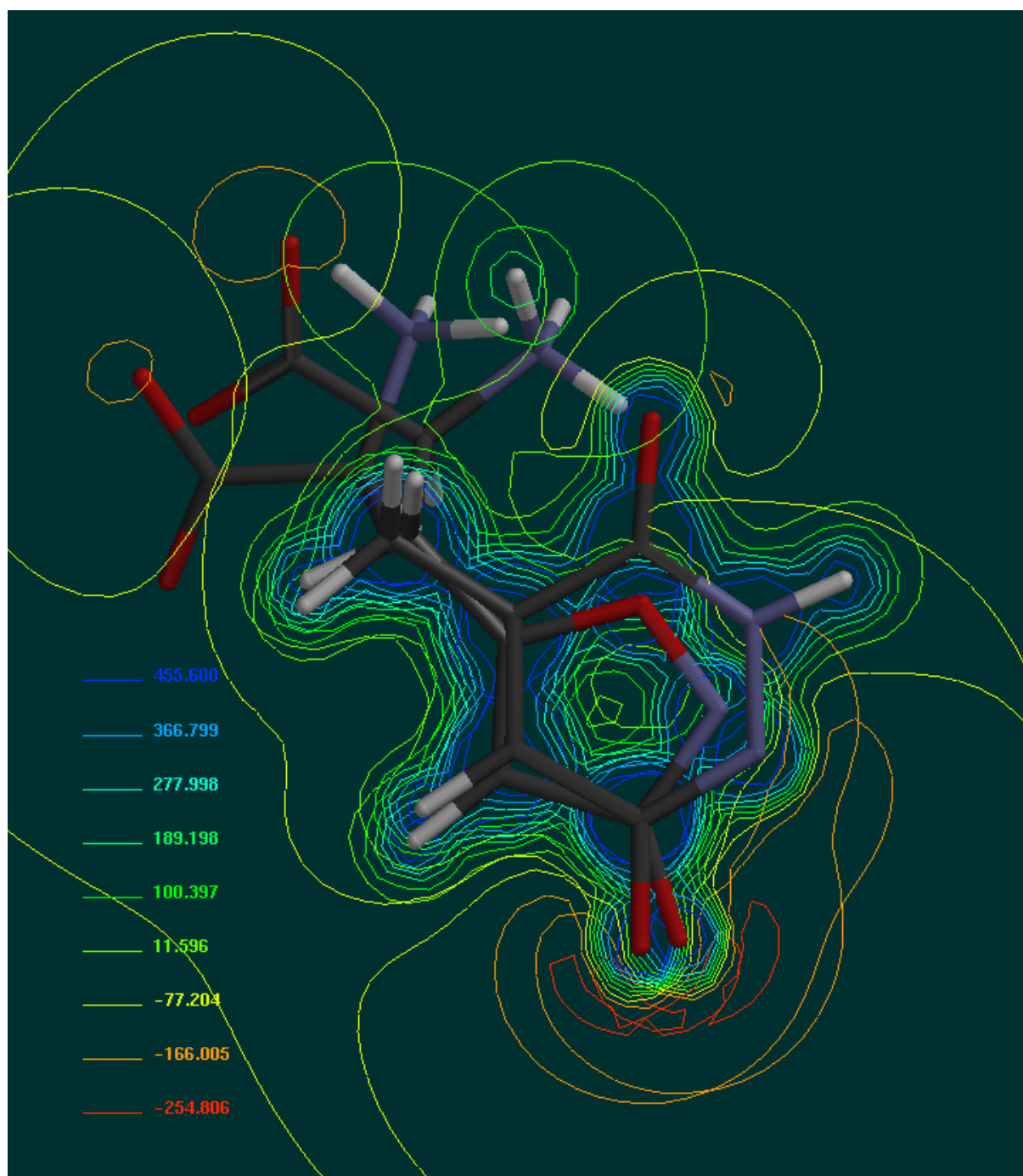
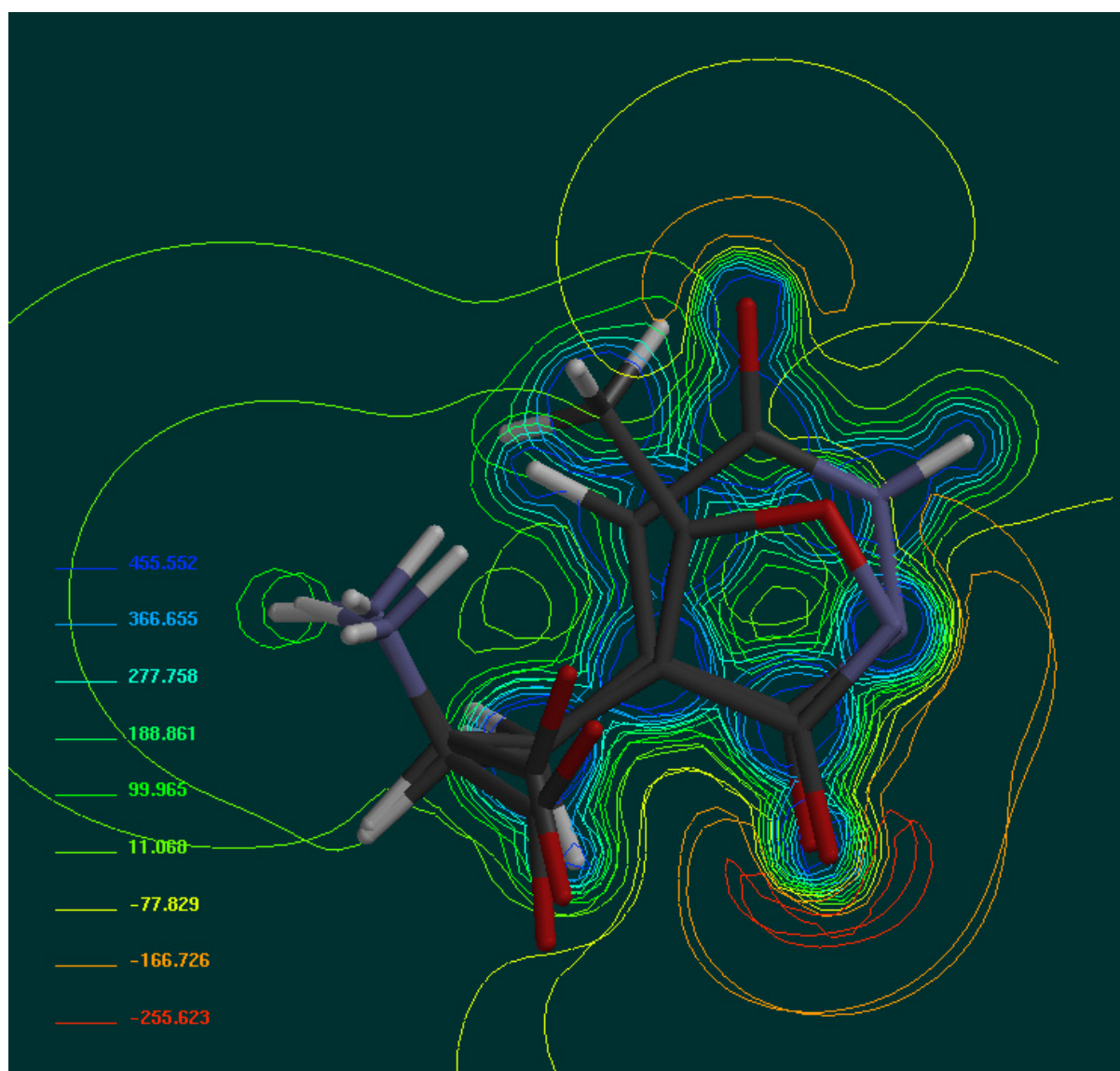


Figure 4.11 Overlay: 11, 20b



Chapter 4: Index of optimised geometries

3-isoxazolols	pyridazinones
muscimol (3)	4-aminomethyl-5-methyl-6-hydroxypyridazin-3(2H)-one (17a)
4-aminomethyl-5-methyl-3-isoxazolol (4)	4-methyl-5-aminomethyl-6-hydroxypyridazin-3(2H)-one (17b)
THIP (5)	1-hydroxy-5,6,7,8-tetrahydropyrido[3,4-d]pyridazin-4(3H)-one (18a)
THPO (6)	4-hydroxy-5,6,7,8-tetrahydropyrido[3,4-d]pyridazin-1(2H)-one (18b)
ibotenic acid (13)	2-Amino-2-(6-hydroxypyridazin-3(2H)-on-4-yl)ethanoic acid (19a)
AMAA (14)	2-Amino-2-(6-hydroxypyridazin-3(2H)-on-5-yl)ethanoic acid (19b)
HIBO (15)	2-Amino-3-(6-hydroxypyridazin-3(2H)-on-4-yl)propanoic acid (20a)
AMPA (11)	2-Amino-3-(6-hydroxypyridazin-3(2H)-on-5-yl)propanoic acid (20b)



© Copyright Nathan Wilson 1994

Amanita muscaria

5. Synthesis of pyridazine amino acids

Abstract

The attempted synthesis of the twelve target compounds proposed in [chapter 4](#) is described. Three aminomethyl pyridazines and three alanino pyridazines (muscimol and AMPA analogues) were readily produced via free-radical bromination of parent protected methyl pyridazines, followed by derivatisation to an amine or α -amino acid, and deprotection. An unusual *N*-methyl bromination product prompted the synthesis of another, *N*-substituted, alanino pyridazine. Three tetrahydro pyridopyridazinediones (THIP analogues) were readily produced by reduction of the hydrazides of pyridine-3,4-dicarboxylate. Three methods for producing pyridazinyl glycines (AMAA and HIBO analogues) were trialed: ring nucleophilic substitution, various aldehyde syntheses, and synthesis via an ethyl pyridazinyl acetate. The final method came within a step of completion, but α -amino acid decarboxylation during deprotection prevented the synthesis of the pyridazinedionyl glycine. In total, ten GABA and glutamate analogues were synthesised for pharmacological screening, described in [chapter 7](#).

Index

[5.1 Analogues of muscimol \(5-aminomethyl-3-isoxazolol\)](#)

[5.1.1 4-Aminomethylpyridazine-3,6\(1,2*H*\)-dione](#)

[5.1.2 2-Methyl-4-aminomethyl-6-hydroxypyridazin-3\(2*H*\)-one](#)

[5.1.3 2-Methyl-5-aminomethyl-6-hydroxypyridazin-3\(2*H*\)-one](#)

[5.2 Analogues of THIP \(4,5,6,7-tetrahydroisoxazolo\[5,4-*c*\]pyridine-3-ol\)](#)

[5.2.1 5,6,7,8-Tetrahydropyrido\[3,4-*d*\]pyridazine-1,4\(2,3*H*\)-dione](#)

[5.2.2 1-Hydroxy-3-methyl-5,6,7,8-tetrahydropyrido\[3,4-*d*\]pyridazin-4\(3*H*\)-one](#)

[5.2.3 2-Methyl-4-hydroxy-5,6,7,8-tetrahydropyrido\[3,4-*d*\]pyridazin-1\(2*H*\)-one](#)

[5.3 AMPA / HIBO analogues](#)

[5.3.1 2-Amino-3-\(pyridazine-3,6\(1,2*H*\)-dion-4-yl\)propanoic acid](#)

[5.3.2 2-Amino-3-\(2-methyl-6-hydroxypyridazin-3\(2H\)-on-4-yl\)propanoic acid](#)

[5.3.3 2-Amino-3-\(2-methyl-6-hydroxypyridazin-3\(2H\)-on-5-yl\)propanoic acid](#)

[5.3.4 2-Amino-3-\(6-hydroxypyridazin-3\(2H\)-on-2-yl\)propanoic acid](#)

5.4 AMAA / ibotenic acid analogues

[5.4.1 Pyridazine glycines via ring nucleophilic substitution](#)

[5.4.2 Pyridazine glycines via pyridazine aldehydes](#)

[5.4.3 Pyridazine glycines via ethyl 2-pyridazinyl acetates](#)

5.5 Conclusion

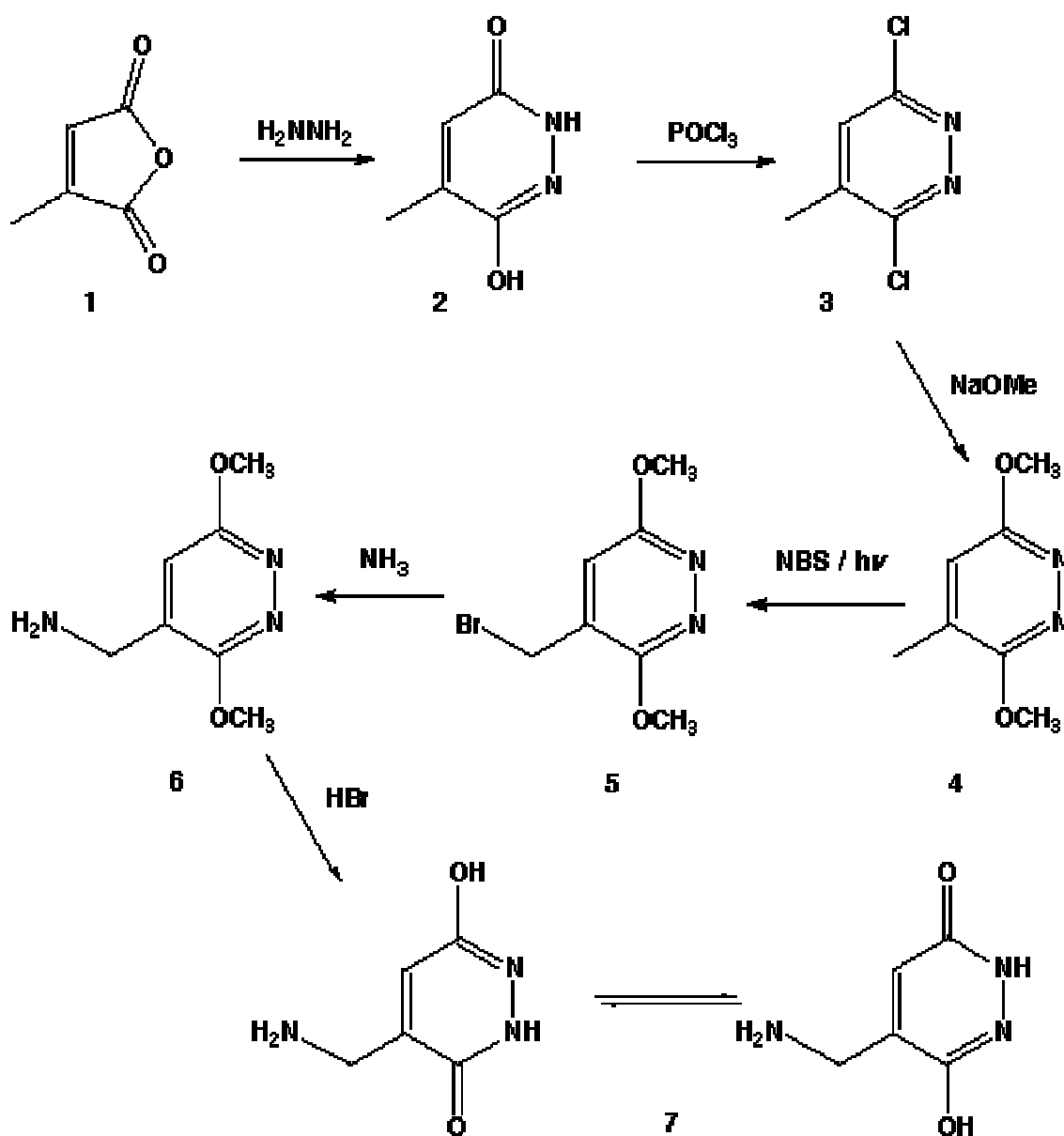
5.6 Experimental

5.7 Acknowledgments

5.8 References

5.1 Analogues of muscimol (5-aminomethyl-3-isoxazolol)

5.1.1 4-Aminomethylpyridazine-3,6(1,2*H*)-dione



Scheme 5.1 Synthesis of 4-aminomethylpyridazine-3,6(1,2*H*)-dione **7**, linked to experimental

A 3,6-diprotected 4-methyl pyridazine-3,6-dione was sought as a precursor to pyridazinedione muscimol analogues. An attempt at using a labile trimethylsilyl protecting group for the oxygens of citraconic hydrazide **2** was unsuccessful because of instability in the presence of even traces of moisture, hence the more robust dimethoxy derivative **4** was synthesised.

3,6-Dichloro-4-methyl-pyridazine **3** had been prepared by standard techniques from citraconic anhydride **1** via citraconic hydrazide **2** [1]. The dimethoxy derivative **4**, a known compound [2,3], was prepared by refluxing **3** with sodium methoxide in xylene. Bromination by *N*-bromosuccinimide (NBS) in CCl₄ afforded 36% of the bromomethyl derivative **5**, along with the dibromomethyl derivative. NBS had previously been used in the synthesis of AMPA and 4-methyl HIBO from 3-methoxy-4,5-dimethyl isoxazole [4], but its action on methoxy methyl pyridazines had not been reported. One account describes the success of the reaction on 2,4-dimethyl-6-phenylpyridazin-3(2*H*)-one [5].

Simple nucleophilic substitution of the activated bromide with ammonia in methanol at 0°C gave the protected amino acid **6**, which was demethylated to the muscimol analogue 4-aminomethyl pyridazin-3,6(1,2*H*)-dione **7** by reflux in concentrated HBr, conditions which have also been used to demethylate methoxy isoxazoles [4]. While the final product **7** resisted all attempts to obtain a crystalline material, it was purified by chromatography on ion exchange resin, followed by precipitation from a hot aqueous solution with ethanol. This compound is probably present in aqueous solution as a mixture of zwitterionic tautomers, and this may complicate the crystallisation procedure. TLC and n.m.r. evidence indicated greater than 95% purity.

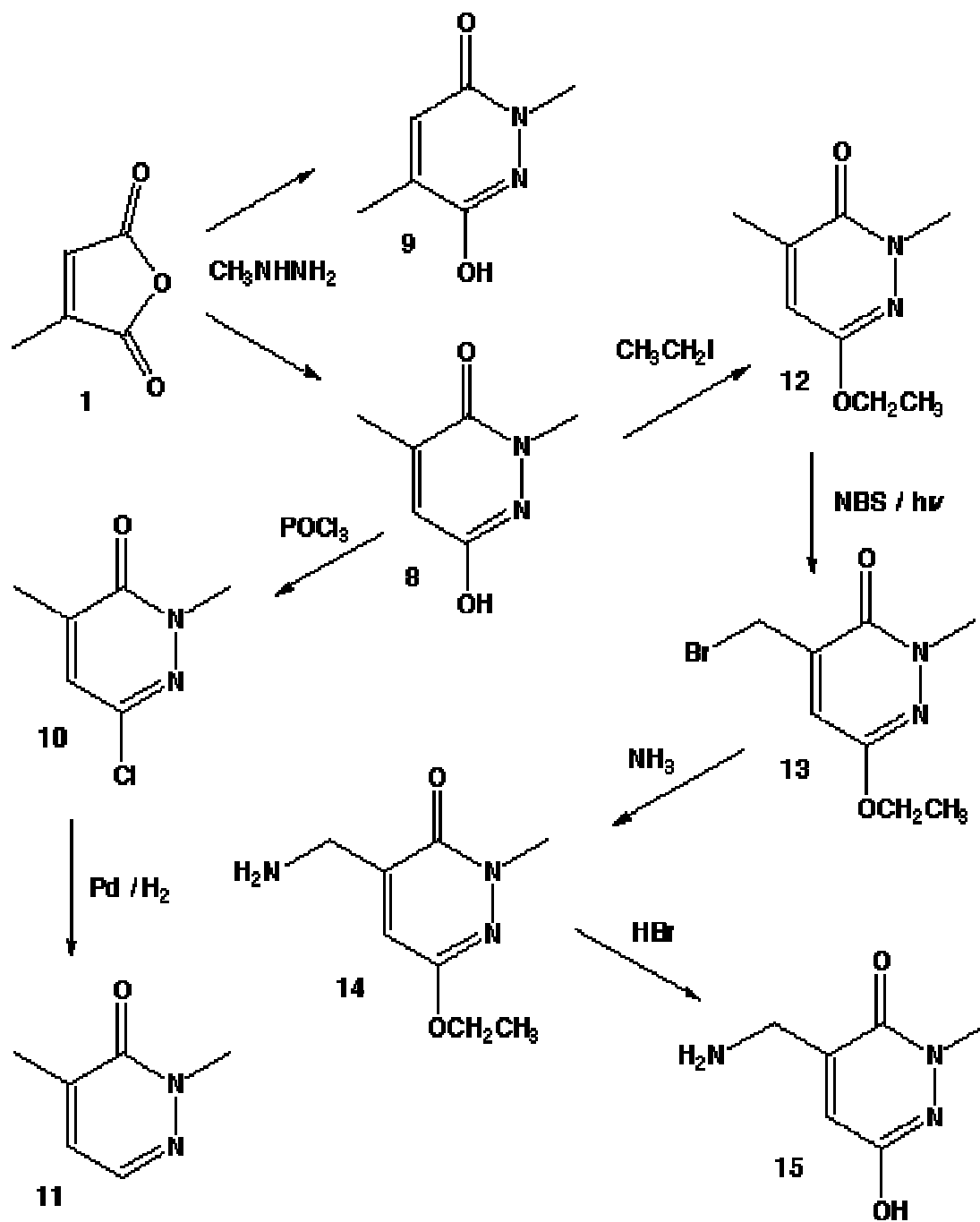
Attempts at further purification via the *t*-Boc derivative of **7** gave poor yields for insubstantial gain in purity.

An attempt at partial deprotection of the *t*-butyloxycarbonyl (*t*-Boc) derivative under gentler conditions (6M HCl) to produce 4-aminomethyl-6-methoxypyridazin-3(2*H*)-one and/or 5-aminomethyl-6-methoxypyridazin-3(2*H*)-one produced a

mixture of unclear composition, with at least three major components by TLC and n.m.r., showing little promise. This reaction also served to show that hydrolysis under harsher conditions with HBr is necessary for full deprotection of 3,6-dimethoxy pyridazines.

Attempts to produce the homologue of [7](#), i.e. the aminoethyl derivative, via nucleophilic substitution of [5](#) with cyanide, followed by reduction, were unsuccessful. The cyano group strongly activates the methylene, leading to further substitution and mixtures of dimeric products under gentle conditions in DMSO or acetonitrile/water solvents. Further attempts to synthesise analogues of homomuscimol (5-aminoethyl-3-isoxazolol) were abandoned when it later became apparent that pyridazine-3,6-diones held no promise as GABAergic agents (see [chapter 7](#)).

5.1.2 2-Methyl-4-aminomethyl-6-hydroxypyridazin-3(2H)-one



Scheme 5.2 Synthesis of 2-methyl-4-aminomethyl-6-hydroxypyridazin-3(2H)-one [15](#), linked to experiments

Several methods were tried to produce a 4-methyl-6-alkoxy-pyridazin-3(2*H*)-one, as a protected precursor for *N*-methyl derivatives. The action of dimethyl sulfate on citraconic hydrazide **2** produced complex mixtures with poor conversion, as did methyl iodide. However detailed chromatography and analysis of the products greatly assisted subsequent identification. Katrusiak and Baloniak subsequently described in detail the mixtures produced by the action of these methylating agents on the simpler maleic hydrazide system [6], testimony to the difficulty of this route. An attempt to isomerise **4** to give methyl ethers of **8** or **9** using *p*-toluenesulfonic acid at 170°C also failed, starting material and a complex mixture including degradation products resulting.

Condensation of citraconic anhydride **1** with *N*-methyl hydrazine producing the *N*-methyl derivatives of **2**, i.e. "citraconic methyl hydrazides", was successful following a method previously used for *N*-phenyl derivatives [7]. Separation of the two isomers **8** and **9**, produced in near equal amounts, was achieved by careful successive fractional crystallisation.

The isomer of higher R_f , lower melting point, and higher water solubility was identified by the following procedure: chlorination of the isomer using excess POCl_3 using a typical method for converting hydroxy pyridazines to their chlorides [8] produced only one compound of above baseline R_f , and despite a very poor yield from a difficult workup, in sufficient quantity after column chromatography for identification as the 6-chloro derivative, subsequently shown to be **10**.

Dehalogenation with hydrogen at 1 atm and palladium on carbon catalyst by a typical method [9] gave a product with a coupling constant with an ortho-arrangement of aromatic protons (J 4.1 Hz), but not ruling out a meta- arrangement. However only one of these protons was coupled with the methyl group (J 1.2 Hz). The Overhauser effect (n.O.e.) n.m.r. spectrum clearly showed one aromatic hydrogen rather than two proximal to the 4-methyl group, when this group was irradiated. This strongly indicated that the compound was 2,4-dimethylpyridazin-3(2*H*)-one **11**. Thus the hydrazide isomer of higher R_f was shown to be 2,4-dimethyl-6-hydroxypyridazin-3(2*H*)-one **8**. These two simple pyridazines **10** and **11**

are apparently previously unreported, perhaps because of the difficulties of separation and the chlorination reaction.

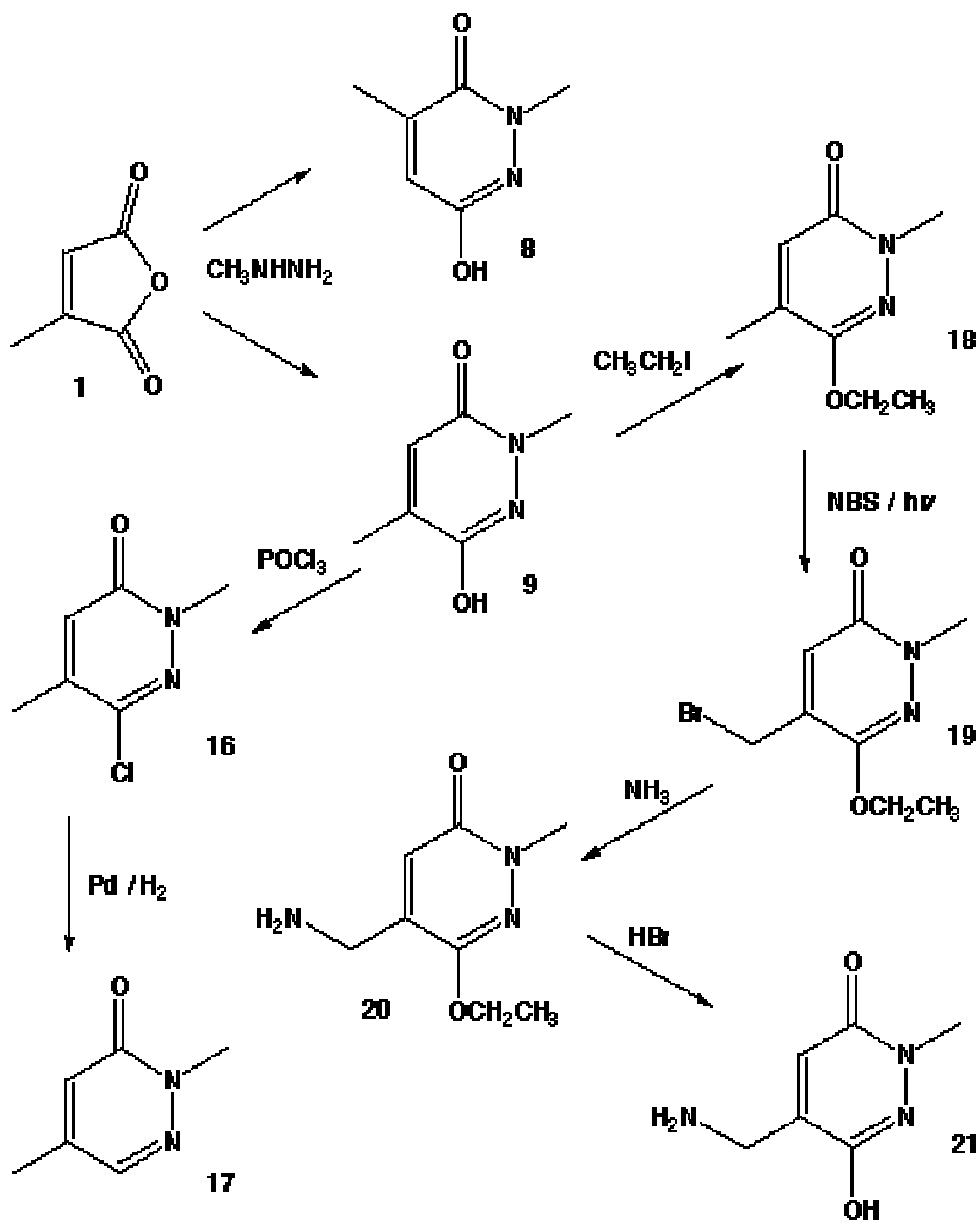
Prior to this synthesis, and n.O.e. experiments, the identities of the two isomers **8** and **9** had also been correctly predicted on the basis of theoretical calculations on their derivatives, as described in [Chapter 6](#).

After trying several methods of protecting the hydroxyl groups of **8** and **9**, as described in [Section 5.1.3](#), ethoxylation using ethyl iodide in ethanol / KOH was found to be the most convenient means of protection. It was applied to **8**, producing a good yield of 2,4-dimethyl-6-ethoxypyridazin-3(2*H*)-one **12**, which was easily recrystallised from petroleum ether or cyclohexane despite its low melting point.

The bromination of **12** using NBS was more difficult than that of **4**, there being a greater range of products, including the *N*-bromomethyl derivative as described in [Chapter 6](#). Nevertheless, the major product, recovered in acceptable yield, was 2-methyl-4-bromomethyl-6-ethoxypyridazin-3(2*H*)-one **13**.

Nucleophilic substitution with ammonia in methanol to produce 2-methyl-4-aminomethyl-6-ethoxypyridazin-3(2*H*)-one **14** was near quantitative, and deprotection by hydrolysis with concentrated HBr followed by ion exchange chromatography afforded 2-methyl-4-aminomethyl-6-hydroxypyridazin-3(2*H*)-one **15**, which resisted all attempts to recrystallise, but was of fair purity by n.m.r. and TLC, contaminated by about 2% starting material.

5.1.3 2-Methyl-5-aminomethyl-6-hydroxypyridazin-3(2H)-one



Scheme 5.3 Synthesis of 2-methyl-5-aminomethyl-6-hydroxy-pyridazin-3(2H)-one [20](#), linked to experimental

Of the two citraconic hydrazides [8](#), [9](#) whose preparation was described in [Section 5.2.1](#), the isomer of lower R_p , higher melting point, and lower water solubility was identified by the following procedure: chlorination of the isomer using excess POCl_3 produced only one compound of above baseline R_p , and despite a poor yield, in sufficient quantity after column chromatography for identification as the 6-chloro derivative [16](#). Straightforward dehalogenation with hydrogen at 1 atm and palladium on carbon catalyst gave a product, whose n.O.e. spectrum clearly showed two equidistant aromatic protons on irradiation of the 5-methyl group, i.e. 2,5-dimethylpyridazin-3(2*H*)-one [17](#). Thus the isomer of lower R_f was shown to be 2,5-dimethyl-6-hydroxypyridazin-3(2*H*)-one [9](#). Again, these simple pyridazinone derivatives [16](#) and [17](#) are apparently previously unreported.

In order to derivatise the 5-methyl position, it was necessary to protect the 6-hydroxy group. 6-Alkoxy pyridazines are intermediate in nature between an ester and an aromatic ether because of the lactim structure and the strongly acidic hydroxyl of the parent compound, and are thus easier to cleave than other aromatic ethers. A number of methods of achieving alkylation were tried. A *t*-butoxy derivative was attractive as being an easily removable group, in preference to an isopropoxy, in preference to a primary alkoxy derivative. Attempted *t*-butylation using isobutene / sulfuric acid in ether, returned starting material. Production of the 6-methoxy derivative using dimethyl sulfate as the alkylating agent, in methanol / potassium hydroxide, after the method of Druey *et al.* [[10](#)] which had been successfully applied to methylate the simpler 2-methyl-6-hydroxypyridazin-3(2*H*)-one, produced poor yields. The application of diethyl sulfate in ethanol / sodium ethoxide to make the ethoxy pyridazine fared somewhat better, producing the ethoxy derivative cleanly, but still with insufficient yield (36%). Turning to alkyl bromides, also previously used to alkylate pyridazinones [[11](#), [12](#)]: an attempt at alkylation by isopropyl bromide in a two phase system (aqueous sodium hydroxide / dichloromethane) with the phase transfer catalyst tetra-*n*-butylammonium hydrogen sulfate, produced no organic soluble products. Alkylation with isopropyl

bromide in dry DMF with potassium carbonate as the base produced a very low yield of the desired isopropoxy pyridazine. Using the more aggressive sodium isopropoxide base with isopropyl bromide in isopropanol also failed to produce the desired product, and there was indication from n.m.r. of rearrangement of the starting material, as evidenced by a significant movement of the Ar-H proton shift in the n.m.r.n.m.r. of the residues (7.04). Isopropylation in ethanol / potassium hydroxide [13] also failed, perhaps due to the volatility of isopropyl bromide vs. speed of reaction. Performing the same reaction in a bomb at higher temperature produced a low yield of the isopropoxy pyridazine. Several attempts to improve the yield gave mixed results. It was reasoned that the yield could be improved by employing a less hindered primary alkyl halide, a less volatile agent, and an iodide as a better leaving group. Butyl iodide in ethanol / potassium hydroxide produced a fair yield, but the product was of low melting point, hindering recrystallisation. Ethyl iodide in potassium hydroxide gave good yields (around 60%) of the ethoxy pyridazine 18 with facile recrystallisation. Ethyl iodide was used exclusively for preparations thereafter. The methoxy derivative 18a was also synthesised using methyl iodide, for the purposes of the comparisons with theoretical calculations described in Chapter 6.

The free radical bromination 18 proved particularly problematic. When the crude product of this reaction was reacted with ammonia in methanol, the major product was the 2-(methoxymethyl) derivative, the *N*-methyl bromide being particularly labile in the presence of methanol or moisture. This indicated a strong preference for the unexpected bromination at the 2-position over the 5-position. A close re-examination of the bromination of 12 also indicated the occurrence of 2-methyl bromination, but in this case, 4-methyl bromination was favoured. These results along with the results of a number of other methylpyridazine brominations which were being performed by co-workers, including the bromination of 2,4,5-trimethyl-6-methoxy-pyridazin-3(2*H*)-one, prompted the investigation which is presented in Chapter 6. The side reaction of *N*-methyl bromination was later used to synthesise an *N*-alanino pyridazine, as described in Section 5.3.4. No significant quantity of any aminomethyl derivatives could be separated after workup of the ammonia /

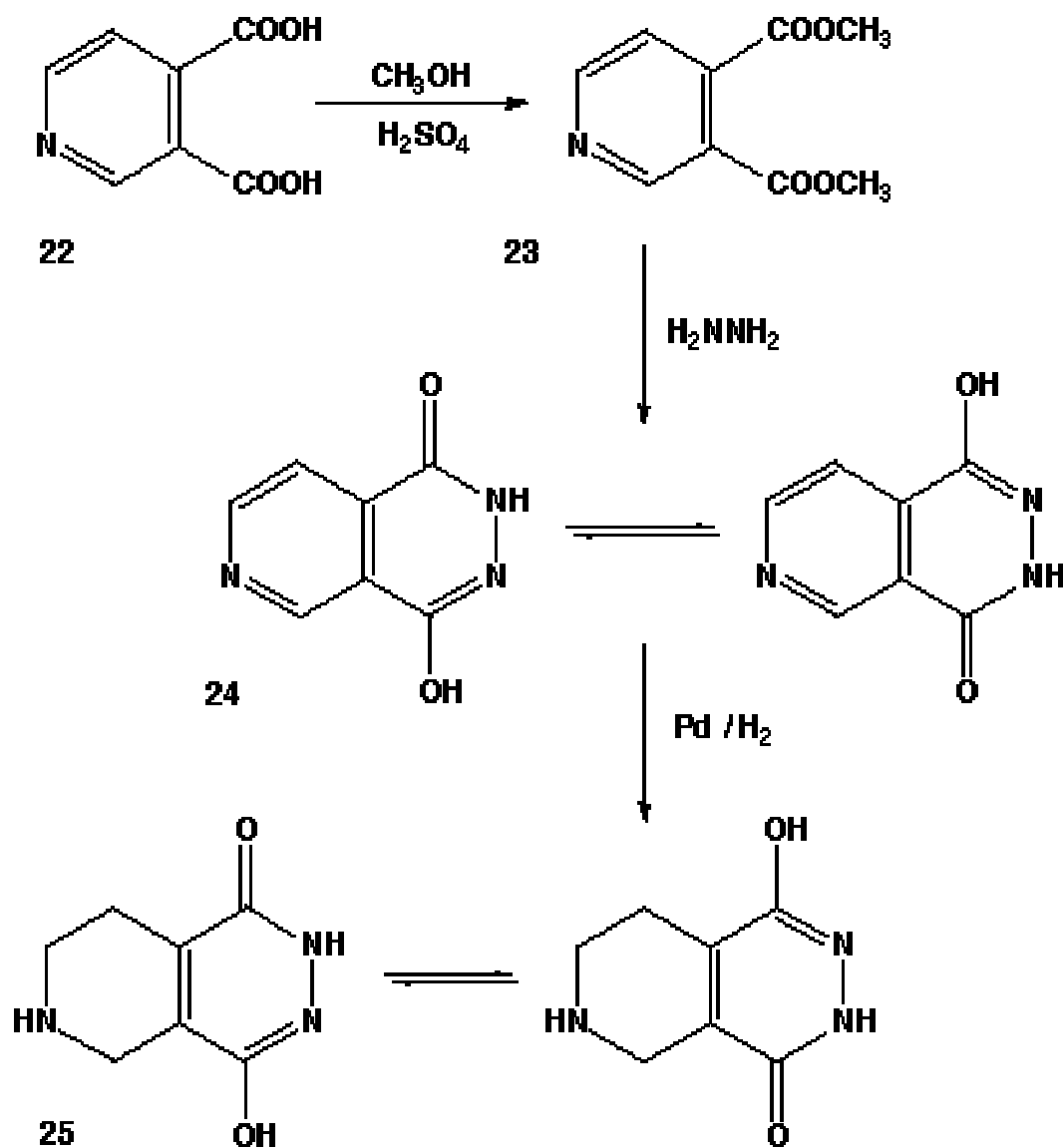
methanol treatment of the crude bromides of [18](#); a new *N*-aminomethyl GABA analogue was therefore not available.

Despite the very poor yields of the 5-bromomethyl compound [19](#) within the bromination mixture, the product was preferentially stable and separable under column chromatography, and a sufficient quantity could be synthesised to allow the production of the desired analogues in sufficient quantity for pharmacological screening, this being the main objective.

Thus, the purified 5-bromomethyl compound [19](#) was aminated in ammonia / methanol to produce the protected amino acid [20](#) in high yield. Furthermore, the deprotection of the hydroxyl using concentrated hydrobromic acid was also straightforward, and the conversion high, although recrystallisation could not be achieved. The product [21](#) was sufficiently pure after chromatography on ion exchange resin for screening for GABAergic activity.

5.2 Analogues of THIP (4,5,6,7-tetrahydroisoxazolo[5,4-c]pyridine-3-ol)

5.2.1 5,6,7,8-Tetrahydropyrido[3,4-d]pyridazine-1,4(2,3H)-dione



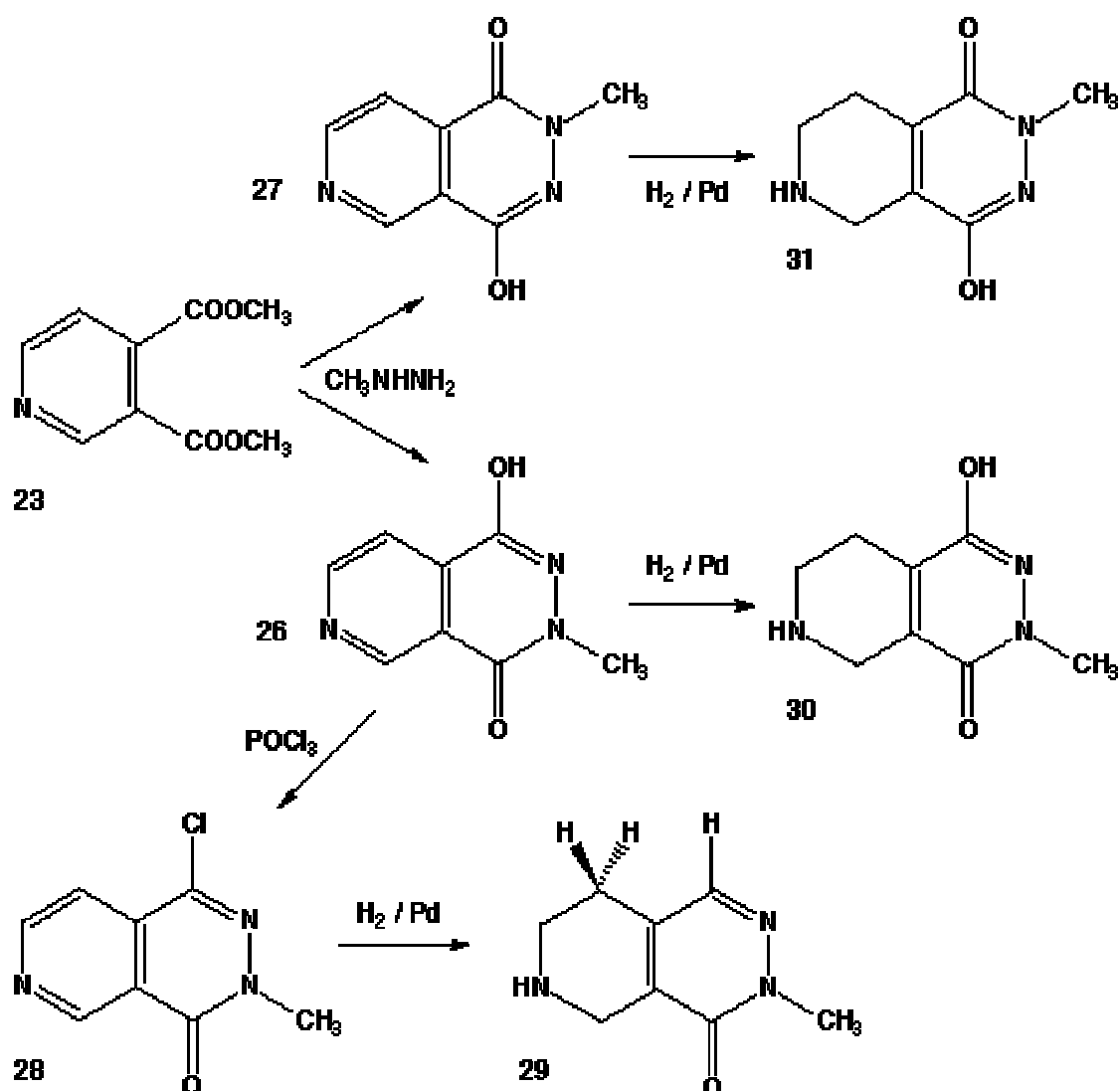
Scheme 5.4 Synthesis of 5,6,7,8-Tetrahydropyrido[3,4-d]pyridazine-1,4(2,3H)-dione [25](#), linked to experimental

Following the method of Silhankova *et al.* [14], the dimethyl pyridazinedicarboxylate **23** was prepared by refluxing the dicarboxylic acid **22** in sulfuric acid / methanol.

Condensation with hydrazine (after Jones [15]) gave the pyridopyridazinedione **24**. The tautomeric preference for this compound is not known but a mixture is likely. The two tautomers depicted differ by less than half a Kcal according to semi-empirical theories, the 1-hydroxy form being slightly favoured (depicted right).

Selective reduction of the pyridine ring of **24** with hydrogen and palladium on carbon catalyst (cf Kakimoto [16]) gave the tetrahydropyridazinedione THIP analogue **25**.

5.2.2 1-Hydroxy-3-methyl-5,6,7,8-tetrahydropyrido[3,4-*d*]pyridazin-4(3*H*)-one



Scheme 5.5. Synthesis of 1-hydroxy-3-methyl-5,6,7,8-tetrahydropyrido[3,4-*d*]pyridazin-4(3*H*)-one **30**, and 2-methyl-4-hydroxy-5,6,7,8-tetrahydropyrido[3,4-*d*]pyridazin-1(2*H*)-one **31**, linked to experimental

The dimethyl pyridinedicarboxylate **23** whose synthesis was described in [section 5.2.1](#) was condensed with methyl hydrazine, in analogous fashion with the synthesis of **8** and **9** ([section 5.1.2](#)), but under more gentle conditions [[15](#)]

Highly insoluble, the resulting mixture was carefully fractionally crystallised from a large volume of water, giving a nearly 50% yield of a highly pure isomer which later proved to be **26**.

In order to determine the identity of the products of this condensation, the following series of reactions was performed on the major, less soluble product: chlorination of the isomer with phosphorus oxychloride according to a method used on a pyrido[2,3-*d*]pyridazinedione [17] produced the chloropyridopyridazinone 28, and dehalogenation / ring reduction with hydrogen and palladium on carbon catalyst gave the tetrahydropyridopyridazinone 29. A Nuclear Overhauser Effect (n.O.e.) ¹H n.m.r. experiment on this compound, irradiating the aromatic 1-H, produced only a single low field enhancement, corresponding to the chemical shift of an allylic methylene, as opposed to an aminomethylene. This indicates the *peri*- interaction between the aromatic proton and the aliphatic methylene, thus proving the identity of 29, and hence 26 and 27.

The *N*-methyl hydroxypyridopyridazinone 26 was then easily reduced under the same conditions as the unmethylated 24, to produce the final desired tetrahydropyridazinone product 30, which was successfully purified by recrystallisation.

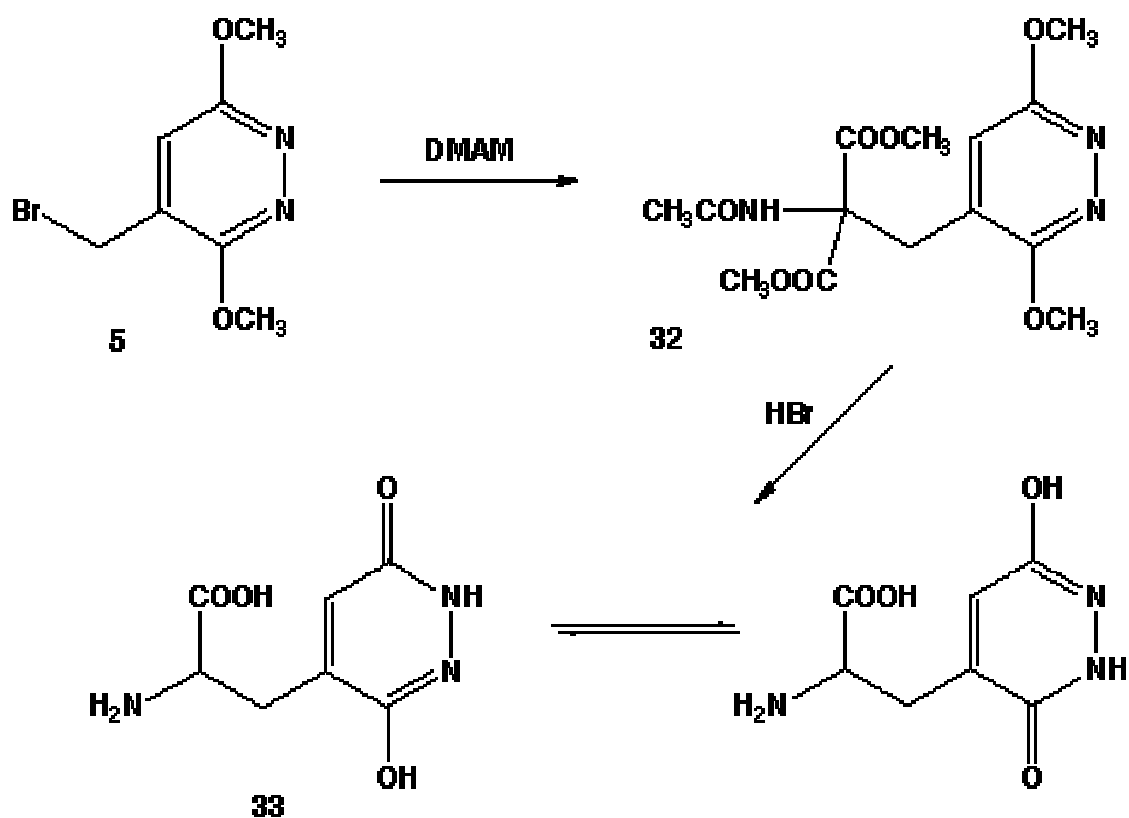
5.2.3 2-Methyl-4-hydroxy-5,6,7,8-tetrahydropyrido[3,4-*d*]pyridazin-1(2*H*)-one

See [scheme 5.5](#) for synthesis.

Whereas the pure the methyl hydrazide isomer 26, being of lower *R_f* and higher melting point, and the major product of condensation by a factor of two, proved easy to crystallise from the reaction of 23 with methyl hydrazine, the minor isomer 27 proved difficult to isolate. Fractional crystallisations of the remaining liquor could not improve on 85 : 15 co-crystallisation of 27 : 26. Fortunately, straightforward hydrogenation of this mixture produced a product containing mostly the desired tetrahydropyridazinone which was easily recrystallised to give the the isomer 31 only.

5.3 AMPA / HIBO analogues

5.3.1 2-Amino-3-(pyridazine-3,6(1,2H)-dion-4-yl)propanoic acid



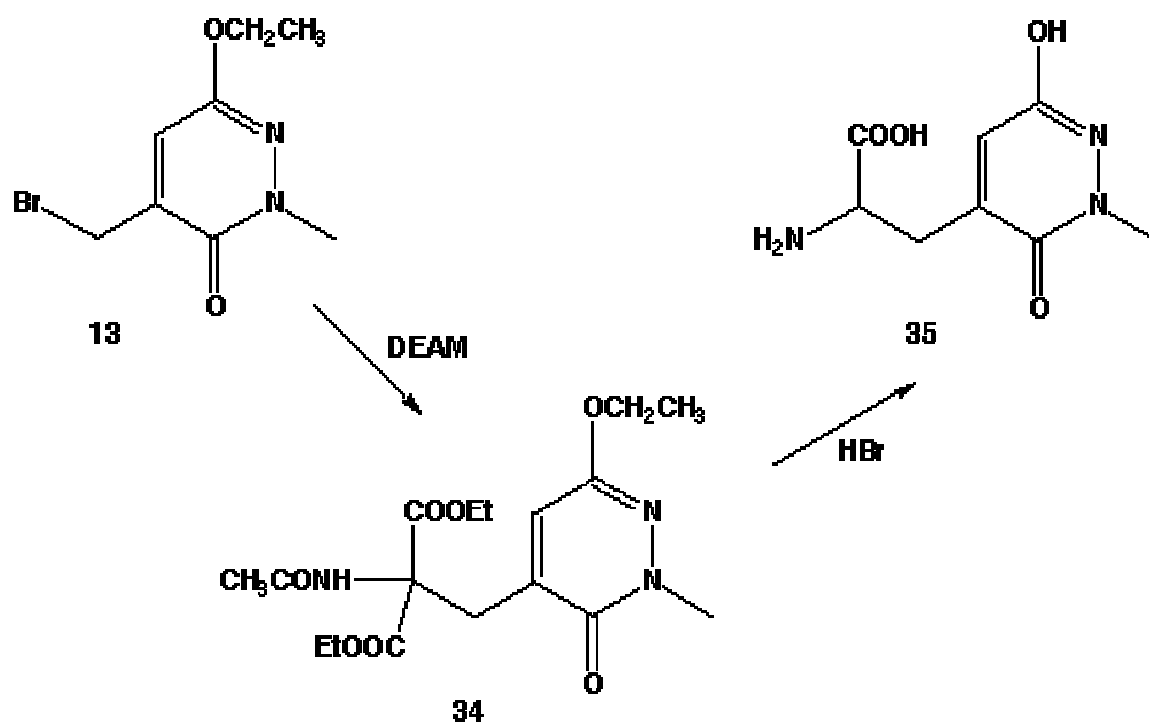
Scheme 5.6 Synthesis of 2-Amino-3-(pyridazine-3,6(1,2H)-dion-4-yl)propanoic acid [33](#) linked to experimental

The bromide [5](#), whose synthesis was described in [section 5.1.1](#), was the starting material for the synthesis of this alanino pyridazinone. The salts of dialkyl acetamidomalonates have long been used as convenient nucleophiles for amino acid synthesis [[18](#)], a method known as the Modified Sørensen Reaction. In this case the base of dimethyl acetamidomalonate (DMAM), rather than the more common diethyl derivative, was formed from sodium methoxide in methanol, to prevent transesterification and thus aid the purification of the intermediate [32](#). The reaction proceeded rapidly n.m.r. at room temperature, but two side products were isolated. The first, a methoxymethyl pyridazine, is the result of the competitive nucleophilic substitution by methoxide. It may be possible to reduce its presence by careful stoichiometric control and by the pre-formation of the DMAM anion prior to

addition of the bromide. The other byproduct was probably the result of small amounts of moisture in the reaction mixture. Partial hydrolysis of one of the methyl esters, followed by rapid decarboxylation, produces a partially decarboxylated compound which is in fact an intermediate between [32](#) and [33](#), and therefore useable. This compound was detected by TLC, isolated by column chromatography, and characterised by n.m.r. spectroscopy.

The full deprotection of [32](#), including decarboxylation, to produce the desired amino acid [33](#) was accomplished in a straightforward manner with concentrated HBr, as per the deprotection of the aminomethyl analogue [6](#). Purification was readily accomplished using acidic ion exchange resin.

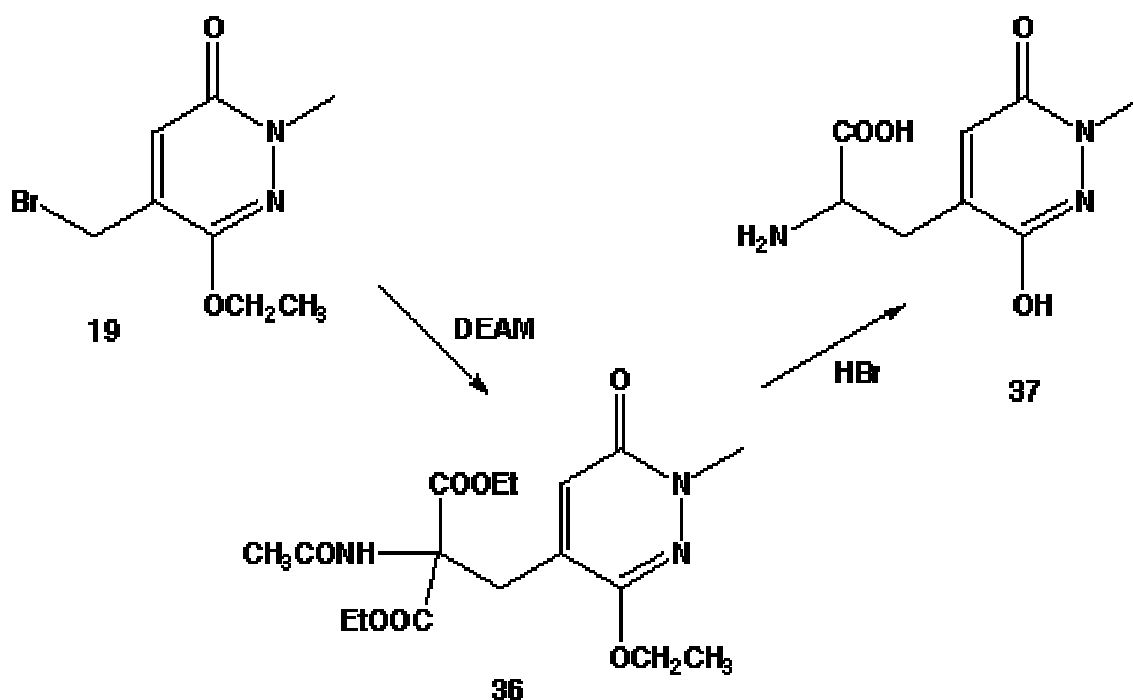
5.3.2 2-Amino-3-(2-methyl-6-hydroxypyridazin-3(2H)-on-4-yl)propanoic acid



Scheme 5.7 Synthesis of 2-amino-3-(2-methyl-6-hydroxypyridazin-3(2H)-on-4-yl)propanoic acid [35](#) linked to experimental

The bromide [13](#), whose synthesis was described in [section 5.1.2](#), was reacted with the base of a dialkyl acetamidomalonate to produce the protected amino acid [34](#). In order to avoid transesterification and subsequent difficulty of purification, sodium ethoxide in ethanol was used to produce the diethyl acetamidomalonate (DEAM) base. The reaction was clean and high yielding so long as it was scrupulously dry; small amounts of moisture producing traces of the partially hydrolysed, decarboxylated 2-acetamidoethyl propanoate derivative. The intermediate ([34](#)) was easily isolated and recrystallised. Hydrolysis by reflux with concentrated hydrogen bromide, followed by acid ion exchange resin chromatography gave the alanino pyridazinone [35](#) in good yield and purity by n.m.r. spectroscopy.

5.3.3 2-Amino-3-(2-methyl-6-hydroxypyridazin-3(2H)-on-5-yl)propanoic acid



Scheme 5.8 Synthesis of 2-amino-3-(2-methyl-6-hydroxypyridazin-3(2H)-on-5-yl)propanoic acid [37](#) linked to experimental

Synthesis of the AMPA analogue [37](#) proceeded from the bromide [19](#) whose synthesis and difficult isolation was described in [section 5.1.3](#). Though somewhat poorer yields were obtained from the nucleophilic substitution of [19](#) with DEAM anion compared with [13](#), the protected amino acid [36](#) was easily isolated in high purity and recrystallised. The hydrolysis of [36](#) by concentrated HBr was substantially more difficult than that of [34](#), presumably because of the steric hindrance of the proximal methylene. It was apparent that degradation was occurring after 12 hours of slow hydrolysis in three stages with purification and fresh HBr in between. The product resisted attempts to recrystallise from alcohol/water mixtures. The roughly 90% pure product was used for pharmacological screening, and when found to lack activity, no further attempt at purification was made.

N-methyl pyridazinones as well as provide a fourth kind of alanino pyridazindione for AMPA receptor screening. Most importantly, [43](#) is an isomer of the important natural AMPA agonist willardiine, which is also an *N*-alanino heteroaromatic dione, specifically the pyrimidine, 1-alanino uracil. [Chapter 8](#) covers in more depth the activities of the willardiines and azawillardiines. The ability to synthesise *N*-alanino heterocycles from readily accessible *N*-methyl compounds is therefore of potential importance.

The mono-methylated starting material [39](#) was chosen rather than attempt to functionalise the dimethyl pyridazinediones previously synthesised, in order to simplify the synthesis and the product. A long known compound [[19](#)], it was made by standard condensation of maleic anhydride [38](#) with methyl hydrazine. Its ethoxy derivative [40](#) which is also known [[19](#)] was readily produced by the same method using ethyl iodide which was successful for its 4- and 5- methyl derivatives [12](#) and [18](#).

As expected, the bromination reaction was successful, giving a fair yield of the *N*-bromomethyl compound [41](#) which could be isolated, and stored for long periods if kept cold and dry, although it readily decomposed in moist air at room temperature. The substitution with the base of DEAM in ethanol to give the protected amino acid [42](#) was straightforward and high yielding.

Deprotecting [42](#) proved highly problematical however. It soon became apparent that no amount of refluxing with concentrated hydrobromic acid could hydrolyse the ethoxy group, even though the amino acid function was readily deprotected. While HBr has been the reagent of choice for this kind of deprotection of heterocyclic phenols, it was found that refluxing with the stronger 57% hydriodic acid for 15 hours gave small amounts of the desired deprotected product [43](#), along with the partially deprotected ethoxy compound and some degradation. It being reasoned that the products of deprotection were diluting or altering the hydriodic acid, and possibly lowering the reflux temperature, the intermediate mixture was isolated on ion exchange resin with copious washings to remove traces of free iodine, and then re-refluxed with fresh acid for a further 9 hours whereupon the

reaction was complete. Remarkably, under such harsh conditions the compound was fairly stable, and a respectable yield was obtained. By contrast with the other amino acids synthesised, this compound was also readily purified by recrystallisation from ethanol/water.

5.4 AMAA / ibotenic acid analogues

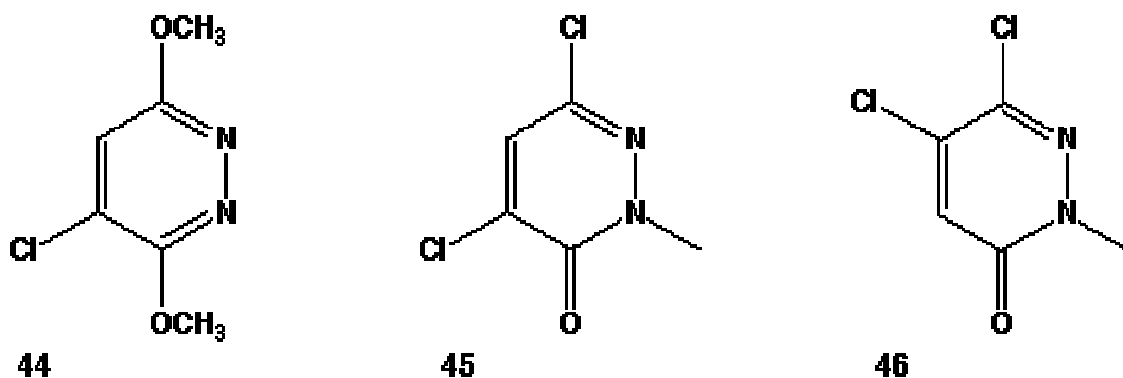
To complete the synthesis of the series of pyridazinones corresponding to the major types of isoxazolols active at amino acid receptors, it was desired to produce glycino-pyridazinones. Three possible routes were considered

5.4.1 Pyridazine glycines via ring nucleophilic substitution

Pyridazines, like other diazines, are electron deficient and susceptible to nucleophilic substitution [20]. In particular, 4- or 5- halopyridazines are strongly activated, relative to 3- or 6- halo substituents. The presence of a keto- or methoxy- is a deactivating influence. It was therefore considered worthwhile to test whether the Sørensen Reaction could be used to prepare pyridazine glycino pyridazinones as it was to prepare alanino pyridazinones.

A starting material for the attempted synthesis of the glycino pyridazine-3,6-diones was 3,6-dimethoxy-4-chloropyridazine **44**. This compound was prepared by chlorinating maleic hydrazide with phosphorous oxychloride, reacting with sodium methoxide to produce 3,6-dimethoxypyridazine, which is then converted to the *N*-oxide by hydrogen peroxide [21]. The *N*-oxide is converted to the 4-chloride by again chlorinating with phosphorous oxychloride [22].

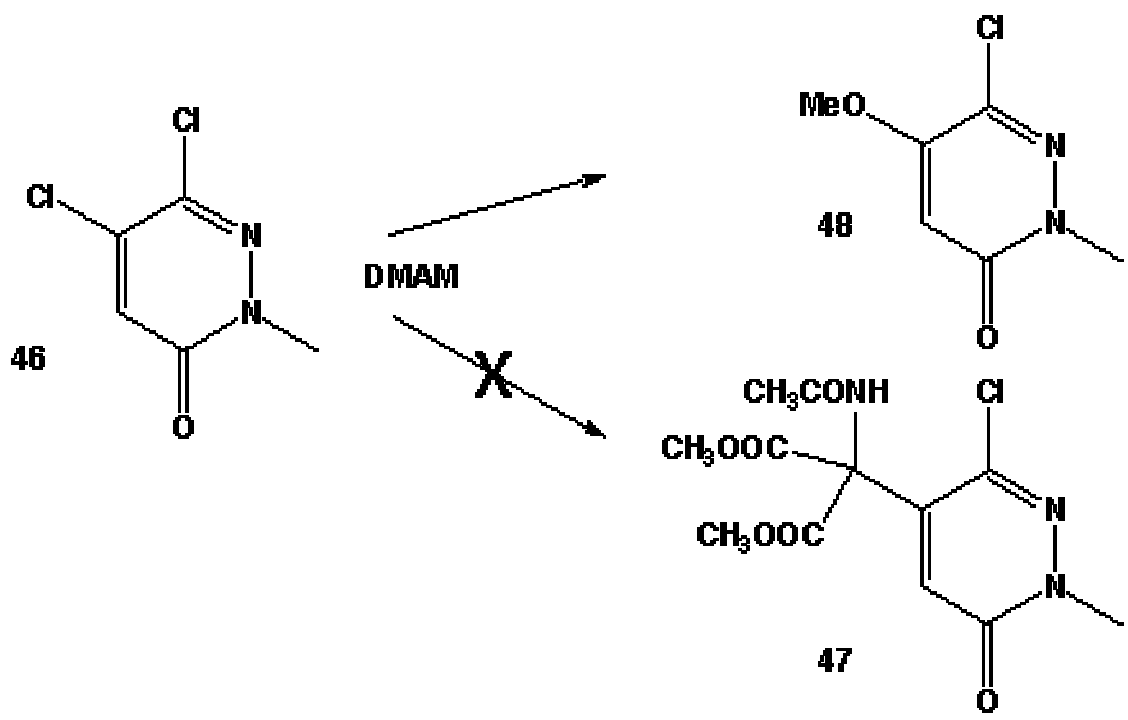
Starting materials for the attempted synthesis of the two *N*-methyl glycino-pyridazine-3,6-diones were 4,6- and 5,6-dichloro-2-methylpyridazin-3(2*H*)-one **45** and **46**. Chloromaleic anhydride is prepared from maleic anhydride by direct chlorination-dehydrochlorination [23]. Condensation with methylhydrazine gives the two chloro-2-methylpyridazinedione isomers. Chlorination with phosphorous oxychloride then gives the desired 4,6- and 5,6- dichloro compounds [24].



Scheme 5.10. Chloropyridazines synthesised as starting materials for ring nucleophilic substitution

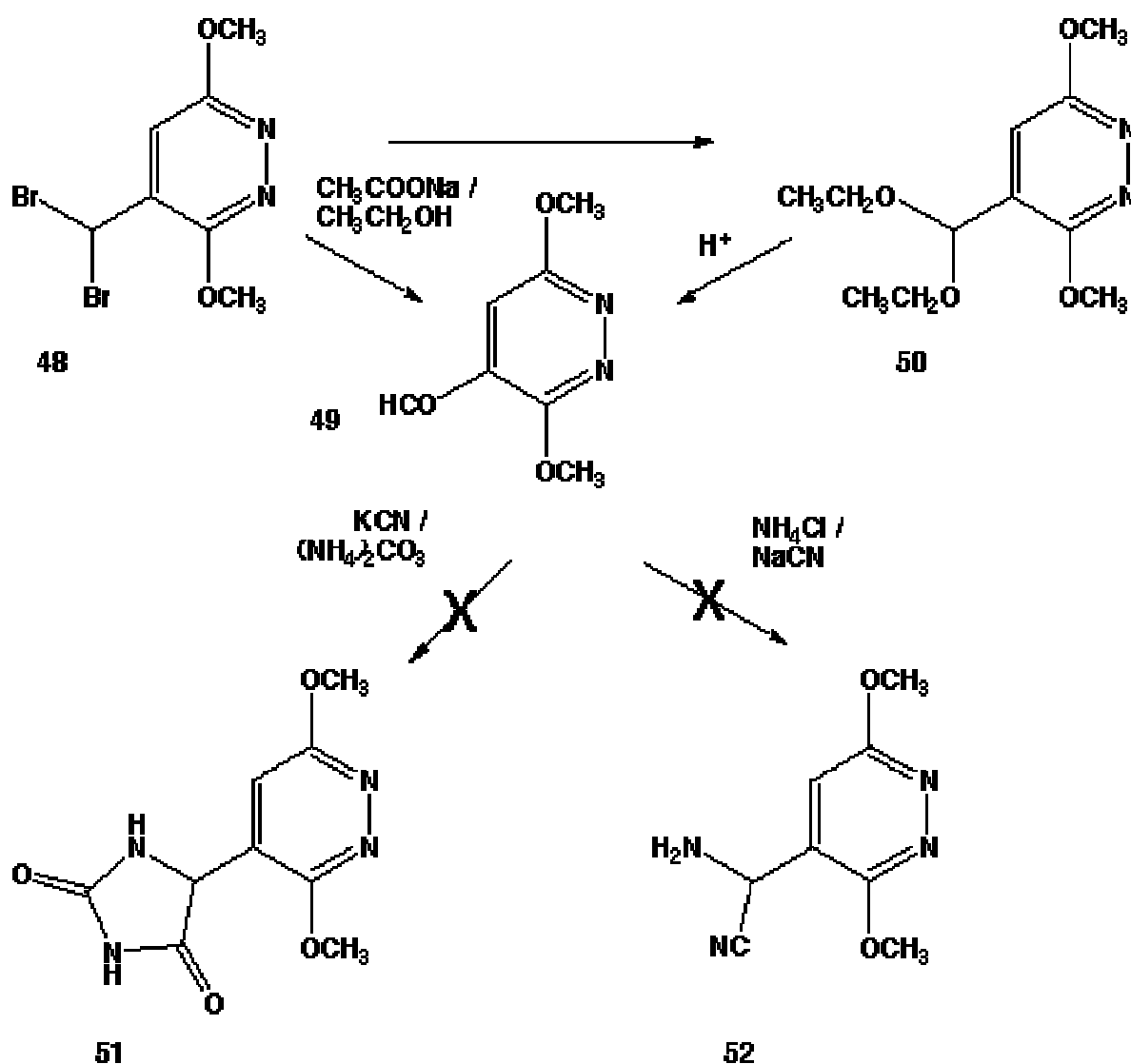
The reaction of 2-methyl-5,6-dichloropyridazin-3(2H)-one **46** with sodium DMAM in methanol produced quantitatively 2-methyl-5-methoxy-6-chloropyridazin-3(2H)-one **48**, rather than the protected amino acid **47**, showing the preference for substitution with a less hindered base. Producing the DMAM anion using sodium hydride in THF to prevent the presence of a competing nucleophile, slowly produced a small amount of the same product, along with degradation, presumably by slow degradation of DMAM to produce methoxide. Using DMF as a solvent fared no better, no product being formed at room temperature, and a complex mixture at reflux.

It was clear that ring substitution with such a hindered base was unfavourable, and this line was pursued no further.



Scheme 5.11 Failure of Modified Sørensen Reaction on ring halogen

5.4.2 Pyridazine glycines via pyridazine aldehydes



Scheme 5.12 Synthesis of a pyridazinyl aldehyde **49** but failure of α -amino acid syntheses.

Synthesis of aryl glycines has often been accomplished via the aryl aldehyde, for example methods such as the Bücherer-Bergs [25, 26] and Strecker [26] syntheses.

3,6-Dimethoxypyridazine-4-carboxaldehyde **49** would therefore be a desirable starting material for the synthesis of the glycino pyridazinedione. This compound proved remarkably difficult to synthesise, and once made, of poor stability. Simple underivatized pyridazine aldehydes are particularly rare in the literature [20]. Preparation of the pyridazine aldehyde directly, or the pyridazine carboxylic acid

by oxidation of the 4-methyl group in the hope of reduction to the aldehyde showed no promise. The adduct of hexamine with the bromomethyl derivative [5](#) (Sommelet reaction [\[27\]](#), a known aldehyde synthesis) was hydrolysed to form the aminomethyl pyridazine [6](#), but the aldehyde was not formed.

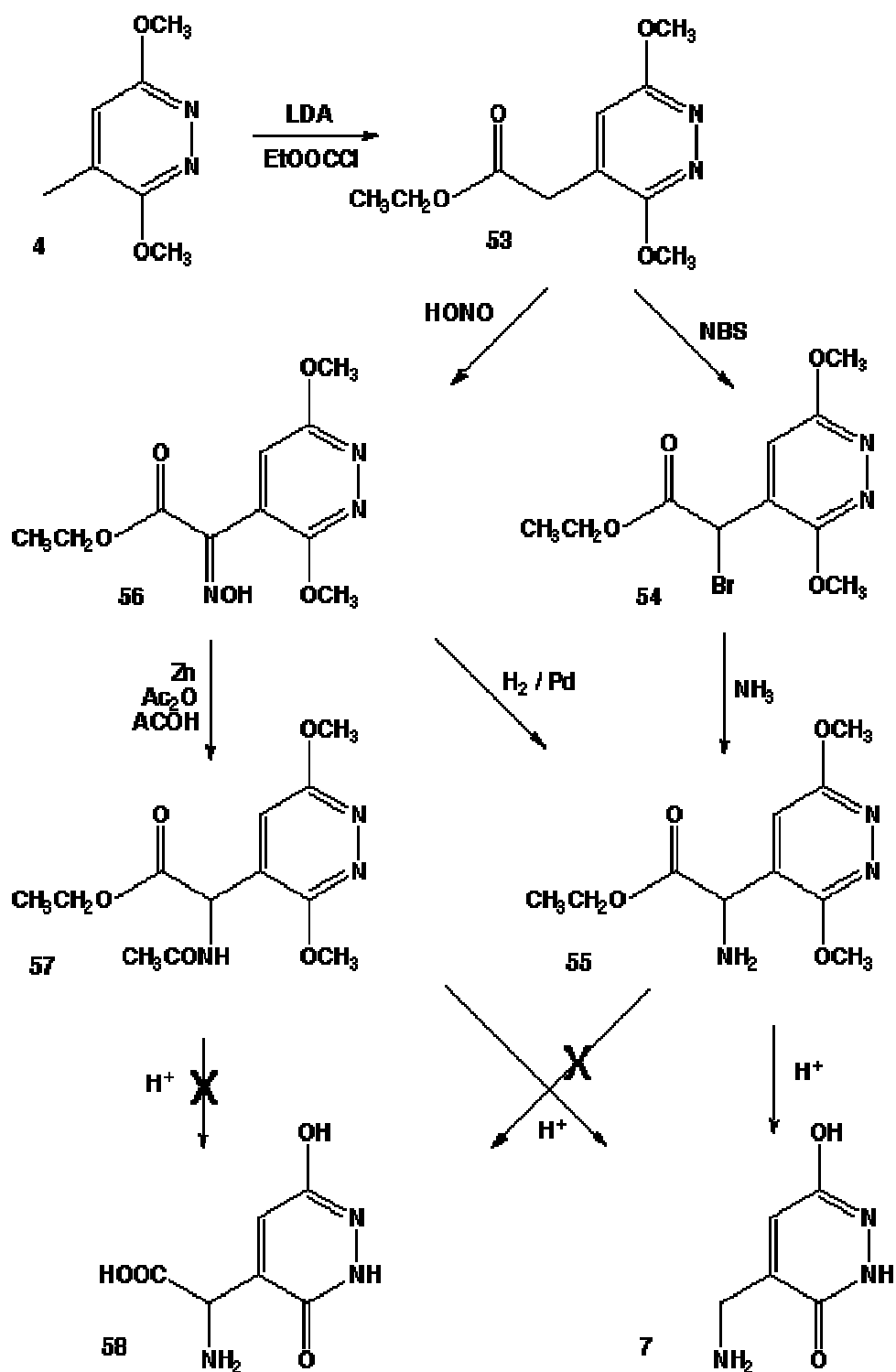
A reasonable method of production of a methoxy heteroaromatic aldehyde is the aqueous hydrolysis of the dibromomethyl compound [\[28\]](#). While 3,6-dimethoxy-4-(dibromomethyl)pyridazine [48](#) had already been synthesised as a byproduct in the preparation of [\(5\)](#), the material proved highly refractory to aqueous hydrolysis. Several conditions were tried; refluxing with sulfuric acid caused degradation. Calcium carbonate was tried as a base, as was dimethylaniline, and various dioxane/water and THF/water mixtures tried as solvent. Attempts to make a dimethyl acetal from the dibromide with sodium methoxide were unsuccessful.

Eventually, application of the method of Eliel *et al.* [\[29\]](#), employing a long reflux in ethanol/water with sodium acetate, followed by the mild acid hydrolysis of the diethoxy acetal [50](#) proved successful, although the yield was poor, and the product slightly contaminated by the acetal.

The feasibility of producing the 2-methyl-6-ethoxypyridazin-3(2H)-one-4-carboxaldehyde from a dibromide was tested, and found to be possible, although again, the yields were poor.

Unfortunately, all attempts to progress the small amounts of aldehyde to an amino acid or protected amino acid proved futile. Both Bücherer-Bergs ([51](#)) and Strecker ([52](#)) syntheses produced similar tars, apparently cyanides being incompatible with this substance. Aldehydes as a route to pyridazinonyl glycines were abandoned at this point.

5.4.3 Glycino pyridazinones via 2-(pyridazinyl)ethyl acetates



Scheme 5.13 Synthesis of an ethyl 2-(dimethoxypyridazinyl)acetate **53**, and its oxime and bromide, but failure of synthesis of glycino pyridazinone **58**.

In a fairly recent paper, Sitazmzé *et al.* [30], showed that certain 4-methyl pyridazines, including some 3-methoxy-4-methylpyridazines, could be metalated at the 4-position with lithium diisopropylamide (LDA), and subsequently alkylated with a variety of halides. It was reasoned that, could ethyl 2-(pyridazinonyl)acetates be made by this procedure, the activated aromatic methylene would be highly susceptible to further manipulation and hence provide a potential route to glycino pyridazinones. Lithiated methyl isoxazoles have previously been used in the synthesis of ibotenic acid analogues [31].

As shown in scheme 5.13, the metalation of 3,6-dimethoxy-4-methylpyridazine **4** with LDA and subsequent alkylation with ethyl chloroacetate gave a good yield of the ethyl 2-(3,6-dimethoxypyridazin-4-yl)acetate **53**. From this compound, two main routes were investigated on a test scale for feasibility.

Bromination of **53** with *N*-bromosuccinimide proceeded remarkably cleanly to give ethyl 2-bromo-2-(3,6-dimethoxy-pyridazin-4-yl)acetate **54**. However, the action of ammonia on this compound did not produce ethyl 2-amino-2-(3,6-dimethoxypyridazin-4-yl)acetate **55** cleanly. There was some n.m.r. evidence of dimerisation to a diketopiperazine byproduct.

Reduction of hydroximino esters has been recorded as an alternative route to α -amino acids [32]. The action of nitrous acid on **53** produced the oxime **56** in high yield, with some evidence of a cis-trans mixture by n.m.r. spectroscopy. Reduction to the amine **55** was promising, as was reduction/acetylation to a fully protected amino acid **57**, a preferred intermediate.

Hydrolysis under reasonably mild conditions (6M HCl) of the aminated products followed by ion exchange chromatography appeared to afford small amounts of **7**, along with methoxy derivatives. There was no evidence for the presence of **58** from TLC or n.m.r. This suggested that the decarboxylation of the α -amino acid was occurring more readily than the hydrolysis of the ring methoxy groups. At this point, the attempt to make a pyridazinyl glycine by this route was abandoned.

Although unsuccessful to date, the route described here offers the most promise of application to the synthesis of other glycino pyridazinones. The key factor is the potential for decarboxylation. If an appropriate leaving group could be found for ring-hydroxyl protection, hydrolysis could possibly be accomplished without decarboxylation. On the other hand, it may be that some or all pyridazine glycines are simply unstable under typical synthetic conditions; Goddfried Heinisch, a specialist in pyridazine medicinal chemistry, considered this a strong possibility [33]. It is worth noting in passing the care with which the deprotections of AMAA and ibotenic acid derivatives have been performed to avoid decarboxylation [31, 34] and that ibotenic acid apparently owes at least some of its *in vivo* activity to decarboxylation to muscimol [35].

5.5 Conclusion

This chapter has described the methods whereby a range of hydroxypyridazinone derivatives were synthesised. The central question being sought to be answered was: "How does replacement of a ring oxygen in a range of 3-isoxazolols, known to be archetypal agonists at GABA or EAA receptors, by either a ring amide or an *N*-methyl amide, to form a 6-hydroxypyridazin-3(2*H*)-one, affect potency at these receptors?". Synthesis was primarily a means to this end, all but three final products, the glycino pyridazines, being successfully made. As will become clear in [chapter 7](#), the results of activity screening were disappointing, and this line of investigation was abandoned. Hence, the experimental work was not taken up to the stage of full characterisation of purified compounds. The chemistry was challenging and the products were often very difficult to purify. n.m.r. spectroscopy and TLC behaviour gave good indications of the identities of the compounds and, considering the poor or nil activity of these various series of pyridazinones, it was considered that the large effort required for full characterisation would be better invested in the other areas. The most important advances of this work were increased understanding of synthetic methods pertaining to hydroxypyridazines, some of which were subsequently applied by co-workers in the synthesis of more potent glutamate analogues. Highlights of the synthetic program included the

convenient synthesis of an *N*-alanino pyridazine, the syntheses and realisation of the instability of pyridazine 4-carboxaldehydes, and the extension of the scope of the methylpyridazine metalation / alkylation reaction to include the formation of an ethyl pyridazinylacetate.

[Chapter 2](#) considered in detail the structure, tautomerism and pK_a of the hydroxypyridazine *N*-oxides. Some *N*-oxide derivatives which were synthesised by similar methods described here, were soon found to produce potent AMPA analogues. [Chapter 8](#) summarises their activity as well as the AMPA analogues synthesised in this chapter, along with other ring structures known to have been trialled in this capacity.

[5.6 Experimental](#)

5.6.6. 4-Aminomethyl-3,6-dimethoxypyridazine

Impure 4-bromomethyl-3,6-dimethoxypyridazine (1.144 g, 4.9 mmol, [5](#)) was dissolved in methanol (100 mL) saturated with gaseous ammonia at 0°C for 30 minutes. The mixture was allowed to stand loosely stoppered overnight at room temperature, then evaporated to give a pale yellow solid (1.228 g). The product was dissolved in 0.3M HCl (30 mL), washed twice with equal volumes CH₂Cl₂, made basic with excess 25% NH₃, and extracted four times with 30 mL CH₂Cl₂. The solvent was removed from the pooled extracts to leave 4-aminomethyl-3,6-dimethoxypyridazine (0.639 g, 3.8 mmol, 77%, [6](#)) as a waxy yellow solid. ¹H n.m.r. δ (CDCl₃) 3.78, d, *J* 1.1 Hz, 2 H, 4-CH₂NH₂; 4.04, s, 3 H, OCH₃; 4.07, s, 3 H, OCH₃; 6.95, t, *J* 1.1 Hz, 1 H, 5-H. ¹³C n.m.r. δ (CDCl₃=77.0) 40.5, 4-CH₂NH₂; 54.4, OCH₃; 54.5, OCH₃; 117.3, C(5)H; 136.5, C(4)CH₂; 160.4, COMe; 162.6, COMe. m.p. 89-91°C. Mass spectrum: *m/z* 170 (M+1, 100%), 153 (7%), 135 (6%).

5.6.7. 4-Aminomethylpyridazine-3,6(1,2*H*)-dione

4-Aminomethyl-3,6-dimethoxypyridazine (0.601 g, 3.55 mmol, [6](#)) was dissolved in 48% HBr (10 mL), and heated to reflux for 90 minutes. Removal of excess HBr under vacuum gave 1.192 g of an orange solid. TLC showed several spots, only one of

which (R_f 0.32, butanol/ acetic acid/ water 4:1:1) was ninhydrin positive. The impure product was absorbed onto Dowex 50W (H^+) ion-exchange resin, washed with several volumes of water, then eluted with 1M pyridine. The pyridine fractions were evaporated to leave 4-aminomethylpyridazine-3,6(1,2*H*)-dione (0.445 g, 3.15 mmol, 89%, **7**) as an orange gel. This could be converted to a yellow powder either by forming the hydrochloride or hydrobromide salt, or by precipitation from absolute ethanol. Recrystallisation from water and ethanol proved unsatisfactory. 1H n.m.r. δ (D_2O , DOH=4.81) 4.05, d, J 1.1 Hz, 2 H, N- CH_2 -; 6.98, t, J 1.1 Hz, 1 H, 5-H. ^{13}C n.m.r. δ (D_2O , dioxane=67.4) 39.2 (CH_2), 129.3 (CH), 137.0 (C), 157.3 (CO), 159.0 (CO). m.p. 244°C with gas evolution. Mass spectrum: m/z 142 ($M+1$, 100%), 125 (14%).

5.6.8. 2,4-dimethyl-6-hydroxypyridazin-3(2*H*)-one

5.6.9. 2,5-dimethyl-6-hydroxypyridazin-3(2*H*)-one

Hydrochloric acid (112 g, 32%, 1.0 mol), methyl hydrazine (41.5g, 0.9 mol) and water (200 mL) were heated to boiling in a 1 litre flask. Citraconic anhydride (100.9 g, 0.9 mol, **1**) was added. A white solid formed rapidly, which redissolved on further boiling. The mixture was held at reflux for four hours, cooled to a white solid gel, and then evaporated to a white paste. TLC showed 100% conversion to roughly equal amounts of the two isomers (R_f 0.33, 0.22, ethyl acetate). A first crystallisation from boiling water gave the lower isomer, later identified as 2,5-dimethyl-6-hydroxypyridazine-3(2*H*)-one (59.08 g, 0.42 mol, 42%, **9**). A second crystallisation gave the more soluble upper isomer, later identified as 2,4-dimethyl-6-hydroxypyridazine-3(2*H*)-one (20.67 g, 0.15 mol, 15%, **8**), only slightly contaminated by the lower isomer. The remaining liquor, containing mostly the upper isomer, with a proportion of the lower isomer, was retained for further fractional crystallisation. Attempted recrystallisations from various alcohols gave poorer separations than from water. Lower isomer: 1H n.m.r. δ (D_2O , DOH=4.81) 2.13, d, J 1.1 Hz, 3 H, 5- CH_3 ; 3.56, s, 3 H, N- CH_3 ; 6.85 q, J 1.1 Hz, 1 H, 4-H. m.p. subl. 268°C. Mass spectrum: m/z 141 ($M+1$, 100%). Upper isomer: 1H n.m.r. δ (D_2O ,

DOH=4.81) 2.11, d, *J* 1.1 Hz, 3 H, 4-CH₃; 3.58, s, 3 H, N-CH₃; 7.04 q, *J* 1.1 Hz, 1 H, 5-H. m.p. 178-9°C. Mass spectrum: *m/z* 141 (M+1, 100%).

5.6.10. 2,4-Dimethyl-6-chloropyridazin-3(2H)-one

2,4-dimethyl-6-hydroxypyridazin-3(1H)-one (2.0 g, 14.3 mmol, **8**) was dissolved in phosphorus oxychloride (30 mL), and heated with stirring at 80°C for 1 hour, producing a brown tar. Excess POCl₃ was distilled off under vacuum, and the resultant tar was allowed to cool, dissolved in dichloromethane (ca. 30 mL), and poured onto 100 mL of an ice/acetone mixture with stirring, and external cooling with an ice/salt/acetone bath. The mixture was allowed to assume room temperature, the organic layer separated, and evaporated, to leave 733 mg of brown tar. TLC on silica with ethyl acetate:toluene 1:4 showed the presence of the desired product, R_f 0.35. The tar was chromatographed on a silica column, eluting with the same solvent mixture, and evaporation of the desired fraction afforded 2,4-dimethyl-6-chloropyridazin-3(2H)-one (25 mg, 0.16 mmol, 1%, **10**), as a crystalline solid, around 95% pure by n.m.r. ¹H n.m.r. δ(CDCl₃) 2.22, d, *J* 1.3 Hz, 3 H, 5-CH₃; 3.75, s, 3 H, N-CH₃; 7.08, q, *J* 1.3 Hz, 1 H, 4-H.

5.6.11. 2,4-Dimethylpyridazin-3(2H)-one

2,4-Dimethyl-6-chloropyridazin-3(2H)-one (30 mg, 0.19 mmol, **10**) was dissolved in methanol (5ml), two drops conc. ammonia, and ca. 10 mg palladium on carbon catalyst added. The mixture was hydrogenated overnight at 1 atm, filtered, and evaporated. Column chromatography on silica, eluting with toluene : ethyl acetate 1:1, afforded 2,4-dimethylpyridazin-3(2H)-one (8 mg, 0.06 mmol, 34%, **11**).

Irradiation of 4-methyl peak in n.O.e. experiment gave a large enhancement of one of the two ring protons (d=7.04), but negligible enhancement of the other (d=7.63), confirming 2,4-dimethyl substitution. Enhancement height ratio of 8:1 corresponds to a distance ratio of 1:2 by square root of 6th power law, which is approximately correct for methyl to protons on 5 vs 6. ¹H n.m.r. δ(CDCl₃) 2.22, d, *J* 1.2 Hz, 3 H, 5-CH₃; 3.80, s, 3 H, N-CH₃; 7.04, dq, 1 H, 4-H; 7.63, d, *J* 4.1 Hz, 1 H, 3-H. n.O.e. irradiation at 2.22 ppm; enhancement at 7.04.

5.6.12. 2,4-Dimethyl-6-ethoxypyridazin-3(2H)-one

Potassium hydroxide (2.24 g, 40 mmol) was dissolved in absolute ethanol (30 g). 2,4-Dimethyl-6-hydroxypyridazin-3(2H)-one (2.80 g, 20 mmol **8**) was added with stirring. To this slurry was added ethyl iodide (6.24 g, 40 mmol), and the mixture heated at reflux with stirring overnight. The mixture was concentrated to a third its volume in vacuum, and water (20 mL) added. This procedure was repeated a further two times, followed by extraction three times with ethyl acetate (20 mL). The combined extracts were washed twice with brine, and twice with water, then evaporated to leave relatively pure 2,4-dimethyl-6-ethoxy-pyridazin-3(2H)-one (2.55 g, 15 mmol, 76%, **12**). Recrystallisation from petroleum ether gave 1.60 g product as large pale yellow crystals. ^1H n.m.r. δ (CDCl₃) 1.34, t, *J* 7.0 Hz, 3 H, -CH₂-CH₃; 2.18, d, *J* 1.1 Hz, 3 H, 4-CH₃; 3.65, s, 3 H, N-CH₃; 4.14, q, *J* 7.0 Hz, 2 H, -CH₂-CH₃; 6.76, q, *J* 1.1 Hz, 1 H, 5-H. ^{13}C n.m.r. δ (CDCl₃=77.0) 14.3, CH₂CH₃; 17.0, 4-CH₃; 39.5, N-CH₃; 62.4, CH₂; 123.3, CH; 142.5, C-CH₃; 152.2, C-OEt; 160.2, C=O. m.p. 43-5°C. Mass spectrum: *m/z* 169 (M+1, 100%), 141 (44%).

5.6.13. 2-Methyl-4-bromomethyl-6-ethoxypyridazin-3(2H)-one

2,4-Dimethyl-6-ethoxypyridazin-3(2H)-one (1.37 g, 8.2 mmol, **12**), *N*-bromo succinimide (1.52 g, 8.5 mmol), and CCl₄ (25 mL) were stirred together in a 50 mL flask fitted with a reflux condenser and irradiated for 25 minutes with an 800W "Lowel-Tota" high intensity lamp at a distance of 10 cm, by which time a surface layer of insoluble succinimide had formed. The mixture was allowed to cool, washed twice with equal volumes of water, dried over Na₂SO₄, and evaporated to 2.0g of yellow oil. This crude bromide could be used for further reaction without purification or purified by column chromatography on silica gel, eluting first with toluene/ethyl acetate 4:1 followed by pure ethyl acetate. Several fractions were recovered, including starting material, *N*-bromomethyl, and dibrominated compounds. The major fraction (*R_f* 0.56, toluene/ethyl acetate 1:1) was identified as the desired product, 2-methyl-4-bromomethyl-6-ethoxypyridazin-3(2H)-one (0.59 g, 2.4 mmol, 29%). This compound was easily recrystallised from petroleum ether. ^1H n.m.r. δ (CDCl₃) 1.37, t, *J*, 7.0 Hz, 3 H, -CH₂-CH₃; 3.68, s, 3 H, N-CH₃; 4.18, q, *J* 7.0 Hz,

2 H, -CH₂-CH₃; 4.38, d, *J* 0.9 Hz, 2 H, 4-CH₂Br; 7.08, t, *J* 0.9 Hz, 1 H, 5-H. m.p. 93-95°C. Mass spectrum: *m/z* 249 (M+1, 81%), 247 (M+1, 100%), 169 (M+2-Br, 65%), 167 (M-Br, 59%).

5.6.14. 2-Methyl-4-aminomethyl-6-ethoxypyridazin-3(2H)-one

2-Methyl-4-bromomethyl-6-ethoxypyridazin-3(2H)-one (500 mg, 2.03 mmol, **13**) was dissolved in methanol (20 mL), saturated with ammonia at 0°C, and allowed to stand loosely stoppered at room temperature for 24 hours. The solvent was removed, leaving 543 mg of orange powder. This was dissolved in dilute hydrochloric acid (20 mL, 0.25M), and washed twice with equal portions of dichloromethane, removing the orange colouring. The aqueous layer was basified with ammonia solution (2 mL, 25%), and extracted four times with 20 mL portions of dichloromethane. Evaporation gave 2-methyl-4-aminomethyl-6-ethoxypyridazin-3(2H)-one (333 mg, 1.81 mmol, 90%, **14**) as a white crystalline solid. ¹H n.m.r. δ (CDCl₃) 1.36, t, *J* 7.1 Hz, 3 H, -CH₂CH₃; 3.65, s, 3 H, N-CH₃; 3.77, d, *J* 1.3 Hz, 2 H, -CH₂NH₂; 4.17, q, *J* 7.1 Hz, 2 H, -CH₂-CH₃; 6.92, t, *J* 1.3 Hz, 1 H, 5-H. m.p. 72-4°C. Mass spectrum: *m/z* 184 (M+1, 100%), 167 (8%).

5.6.15. 2-Methyl-4-aminomethyl-6-hydroxypyridazin-3(2H)-one

2-Methyl-4-aminomethyl-6-ethoxypyridazin-3(2H)-one (304 mg, 1.66 mmol, **14**) was dissolved in 48% hydrobromic acid (10 mL), and heated to reflux for 90 minutes. The mixture was evaporated, leaving 511 mg of pale orange powder. This was dissolved in 10 mL water, absorbed onto a Dowex 50W H⁺ ion exchange resin column, eluted with 125 mL water, followed by 50 mL 1M pyridine. The pyridine fraction was evaporated to leave 295 mg pale orange residue, partly amorphous, partly crystallised, R_f 0.47 (butanol, acetic acid, water 4:1:1). The residue was suspended in 10 mL absolute ethanol, and evaporated to dryness to leave 2-methyl-4-aminomethyl-6-hydroxypyridazin-3(2H)-one (270 mg, 1.74 mmol, 105%, **15**) as a pale orange powder. Recrystallisation from water/ethanol was unsuccessful. The product was contaminated with a small amount (ca. 2%) of starting material. ¹H n.m.r. δ (D₂O, DOH=4.81) 3.56, s, 3 H, N-CH₃; 4.06, d, *J* 0.9 Hz, 2 H, -CH₂NH₂; 6.98, t,

J 0.9 Hz, 1 H, 5-H. ^{13}C n.m.r. δ (D_2O , dioxane=67.4) 39.7 (CH_2), 39.7 (N- CH_3), 131.5 (CH), 135.3 (C), 158.7 (CO), 161.8 (CO). m.p. 191°C, with gas evolution. Mass spectrum: m/z 156 (M+1, 100%), 139 (20%), 135 (11%), 127 (7%), 105 (5%).

5.6.16. 2,5-Dimethyl-6-chloropyridazin-3(2H)-one

2,5-Dimethyl-6-hydroxypyridazin-3(2H)-one (10.0 g, 71.4 mmol, **9**) was added to phosphorus oxychloride (60 mL), stirred and heated to 110°C for 40 minutes, by which time the starting material had fully dissolved, leaving a dark amber solution. The mixture was cooled, and the excess POCl_3 distilled off under vacuum. The remaining thick brown tar was poured onto a 200 mL mixture of conc. ammonia and ice with vigorous stirring. The mixture was filtered, the filtrate extracted with ether, and the residue triturated with CH_2Cl_2 . Both solvents were removed under vacuum, leaving 1.22 g and 2.63 g of residue respectively, which appeared to be of similar composition by TLC. The ether residue was chromatographed on silica, eluted with 4:1 toluene: ethyl acetate, and 0.646 g product recovered. The CH_2Cl_2 residue was treated the same way, with a recovery of 0.360 g. The product was 2,5-dimethyl-6-chloropyridazin-3(2H)-one (1.01 g, 6.34 mmol, 9%, **16**), and was used without further purification. ^1H n.m.r. δ (CDCl_3) 2.26, d, J 1.2 Hz, 3 H, 4- CH_3 ; 3.74, s, 3 H, N- CH_3 ; 6.80, q, J 1.2 Hz, 1 H, 5-H. Mass spectrum: m/z 161 (M+1, 34%), 159 (M+1, 100%), 125 (9%).

5.6.17. 2,5-Dimethylpyridazin-3(2H)-one

2,5-Dimethyl-6-chloropyridazin-3(2H)-one (50 mg, 0.315 mmol, **16**) and palladium on charcoal catalyst (10 mg) were added to methanol (5 mL) containing 0.5 mL ammonia solution. The mixture was stirred overnight under hydrogen at 1 atm. Slow absorption followed the initially rapid uptake of hydrogen over the first hour. The mixture was filtered, evaporated to dryness under vacuum, and partitioned between ethyl acetate and water (20 mL). The ethyl acetate layer was separated, washed with a little extra water, dried over Na_2SO_4 , and evaporated under vacuum to leave 2,5-dimethylpyridazin-3(2H)-one (23 mg, 0.19 mmol, 59%, **17**), sufficiently pure by n.m.r. for structure identification, there being a number of minor

components present up to around 5%. Irradiation of 5-methyl peak in n.O.e. experiment gave equal enhancements of both aromatic protons, consistent with the methyl being equidistant between ring protons and confirming 2,5-dimethyl-substitution. ^1H n.m.r. $\delta(\text{CDCl}_3)$ 2.21, d, J 1.2 Hz, 3 H, 4- CH_3 ; 3.76, s, 3 H, N- CH_3 ; 6.70, dq, 1 H, 5-H; 7.60, d, J 2.2 Hz, 1 H, 3-H. ^1H n.m.r. n.O.e. irradiation at 2.21 ppm; enhancements at 6.70 (int. 29.3); 7.60 (int. 29.1). Mass spectrum: m/z 125 ($M+1$, 100%), 111 (6%).

5.6.18. 2,5-Dimethyl-6-ethoxypyridazin-3(2H)-one

Potassium hydroxide (11.22 g, 200 mmol) was dissolved in absolute ethanol (100 mL). 2,5-dimethyl-6-hydroxypyridazin-3(2H)-one (14.02 g, 100 mmol, **9**) was added, the slurry stirred, and ethyl iodide (31.2 g, 200 mmol) added. The mixture was held at reflux with stirring overnight, whereupon most of the ethanol was removed in vacuum. Water (250 mL) was added, and the mixture evaporated once more. More water was added, and the aqueous suspension was extracted 4 times with 60 mL portions of ethyl acetate. The combined extracts were washed with 50 mL portions of brine and water, then evaporated to leave 10.79 g crude product. TLC (ethyl acetate) showed the majority of the product and minimal starting material to have been extracted. This product was recrystallised from 125 mL cyclohexane, with hot-filtration to remove the last of the starting material, to give 8.45 g and a second crop of 0.51 g 2,5-dimethyl-6-ethoxypyridazin-3(2H)-one (8.97 g total, 53 mmol, 53%, **18**) as large, slightly amber crystals. ^1H n.m.r. $\delta(\text{CDCl}_3)$ 1.37, t, J 7.0 Hz, 3 H, $-\text{CH}_2-\text{CH}_3$; 2.10, d, J 1.3 Hz, 3 H, 5- CH_3 ; 3.62, s, 3 H, N- CH_3 ; 4.18, q, J 7.0 Hz, 2 H, $-\text{CH}_2-\text{CH}_3$; 6.69, q, J 1.3 Hz, 1 H, 4-H. ^{13}C n.m.r. $\delta(\text{CDCl}_3=77.0)$ 13.9, CH_2CH_3 ; 15.4, 5- CH_3 ; 38.4, N- CH_3 ; 62.3, CH_2 ; 129.6, CH; 137.1, C- CH_3 ; 151.7, C-OEt; 159.3, C=O.

The methoxy derivative 2,5-Dimethyl-6-methoxypyridazin-3(2H)-one **18a** was synthesised by a similar method, but employing methyl iodide. ^1H n.m.r. $\delta(\text{CDCl}_3)$ 2.10, d, 3 H, 5- CH_3 ; 3.64, s, 3 H, N- CH_3 ; 3.83, s, 3 H, O- CH_3 ; 6.70, q, 1 H, 4-H.

5.6.19. 2-Methyl-5-bromomethyl-6-ethoxypyridazin-3(2H)-one

2,5-Dimethyl-6-ethoxypyridazin-3(2H)-one (17.20 g, 102 mmol, [18](#)) was dissolved in CCl₄ (300 mL), and *N*-bromosuccinimide (18.20 g, 102 mmol) added. The mixture was stirred in a 500 mL round-bottomed flask fitted with a reflux condenser for 30 minutes, under a high intensity UV source at a distance of 10 cm (800W Lowel-Tota lamp) which also heated the solution to reflux. A layer of floating succinimide indicated that the reaction had proceeded. The mixture was allowed to cool, was washed three times with 200 mL of water, dried over Na₂SO₄, and the CCl₄ removed in vacuum to leave 15.01 g of orange residue. TLC (ethyl acetate/toluene 1:1) showed several spots, indicating that the reaction had not proceeded cleanly. The mixture was chromatographed on a silica column, and the identity of some components in addition to starting material established by ¹H n.m.r. Among these were: (a) 2-bromomethyl-5-(dibromomethyl)-6-ethoxypyridazin-3(2H)-one (R_f 0.81); (b) 2,5-bis(bromomethyl)-6-ethoxypyridazin-3(2H)-one (R_f 0.73); (c) 2-bromomethyl-5-methyl-6-ethoxypyridazin-3(2H)-one (R_f 0.61) which was shown to be the major product (reaction of crude mixture with methanol saturated with ammonia at room temperature overnight produced the white crystalline solid 2-methoxymethyl-5-methyl-6-ethoxypyridazin-3(2H)-one, overall yield 37%, ¹H n.m.r. δ(CDCl₃) 3.45, s, 3 H, OCH₃; 5.29, s, 2 H, NCH₂O-; ¹³C n.m.r. δ(CDCl₃=77.0) 57.4, OCH₃; 80.2, NCH₂O-; Mass spectrum: *m/z* 199 (M+1, 22%); 167 (100%). The 2-bromomethyl product (¹H n.m.r. δ(CDCl₃) 5.75, s, 2 H, NCH₂Br) was difficult to characterise since it was unstable on silica and in moist air, and gave an extra TLC streak of low R_f perhaps from the *N*-hydroxymethyl derivative; (d) 2-methyl-5-bromomethyl-6-ethoxypyridazin-3(2H)-one (desired product, R_f 0.29, 2.218g, 8.98 mmol, 8.8%, [19](#)). ¹H n.m.r. δ(CDCl₃) 1.40, t, *J* 7.1 Hz, 3 H, -CH₂-CH₃; 3.64, s, 3 H, N-CH₃; 4.23, d, *J* 0.8 Hz, 2 H, 5-CH₂Br; 4.25, q, *J* 7.1 Hz, 2 H, -CH₂-CH₃; 6.96, t, *J* 0.8 Hz, 1 H, 4-H.

5.6.20. 2-Methyl-5-aminomethyl-6-ethoxypyridazin-3(2H)-one

2-Methyl-5-bromomethyl-6-ethoxypyridazin-3(2H)-one (300mg, 1.21 mmol, [19](#)) was dissolved in methanol (50 mL), chilled to 0°C, and saturated with anhydrous ammonia. The solution was allowed to stand overnight, then evaporated in vacuum

to leave 360 mg of an amorphous amber residue. This was dissolved in dilute HCl (30 mL, 0.3M), washed once with an equal volume of chloroform, basified with 1M sodium hydroxide, and extracted with equal volumes of chloroform four times. The combined extracts were dried over Na₂SO₄ and evaporated to leave 2-methyl-5-aminomethyl-6-ethoxypyridazin-3(2H)-one, as an amber liquid (150 mg, 0.82 mmol, 68%, **20**), which was pure by TLC and n.m.r. ¹H n.m.r. δ(CDCl₃) 1.38, t, *J* 7.1 Hz, 3 H, -CH₂CH₃; 3.64, s, 3 H, N-CH₃; 3.70, d, *J* 1.3 Hz, 2 H, -CH₂NH₂; 4.21, q, *J* 7.1 Hz, 2 H, -CH₂-CH₃; 6.87, t, *J* 1.3 Hz, 1 H, 4-H.

5.6.21. 2-Methyl-5-aminomethyl-6-hydroxypyridazin-3(2H)-one

2-Methyl-5-aminomethyl-6-ethoxypyridazin-3(2H)-one (150 mg, 0.82 mmol, **20**) was dissolved in conc. HBr (3 mL), the solution heated at 140°C for 1 hour, then evaporated. The brown residue was chromatographed on Dowex 50W (H⁺) ion exchange resin, washing with water and eluting with pyridine. Evaporation of the ninhydrin-positive pyridine fractions yielded solid 2-Methyl-5-aminomethyl-6-hydroxypyridazin-3(2H)-one, (36 mg, 0.23 mmol, 28%, **21**), contaminated with about 5% starting material and degradation products according to n.m.r. Recrystallisation from water-ethanol mixtures was unsuccessful, and due to the small quantity recovered from low-yielding reactions, further purification was not attempted. ¹H n.m.r. δ(D₂O, DOH=4.81) 3.54, s, 3 H, N-CH₃; 4.03, d, *J* 0.9 Hz, 2 H, -CH₂NH₂; 6.90, t, *J* 0.9 Hz, 1 H, 4-H.

5.6.23. Dimethyl pyridine-3,4-dicarboxylate

Pyridine-3,4-dicarboxylic acid (10.0 g, 59.8 mmol, **22**) was refluxed in H₂SO₄ (20 mL) and methanol (60 mL) for three hours. The mixture was poured onto ice (aprx. 200 mL) and 50 mL conc. ammonia solution was added to basify. On reaching room temperature, the mixture was extracted three times with 75 mL portions of CHCl₃, which were pooled, dried over Na₂SO₄, and evaporated to give dimethyl pyridine-3,4-dicarboxylate (10.29 g, 52.5 mmol, 88%, **23**) as a pale yellow oil, which very slowly darkened on standing. ¹H n.m.r. δ(D₂O, DOH=4.81) 3.93, s, 3 H, COOCH₃;

3.95, s, 3 H, COOCH₃; 7.66, d, *J* 5.1 Hz, 1 H, 5-H; 8.79, d, *J* 5.1 Hz, 1 H, 6-H; 8.97, s, 1 H, 2-H.

5.6.24. Pyrido[3,4-*d*]pyridazine-1,4(2,3*H*)-dione

Dimethyl pyridine-3,4-dicarboxylate (4.52 g, 23.2 mmol, [23](#)) and hydrazine hydrate (3.34 g, 70 mmol) were added to methanol (8 mL), and the mixture stirred at room temperature. Within minutes, yellow crystals appeared, and the reaction proceeded to completion overnight. The mixture was evaporated, dissolved in 30 mL hot water with 3 mL conc. ammonia solution, filtered hot, and the filtrate acidified with glacial acetic acid, giving a fine, yellow precipitate. This was filtered, and the residue washed with water, ethanol, ether, and dried, yielding pyrido[3,4-*d*]pyridazine-1,4(2,3*H*)-dione (2.915 g, 17.9 mmol, 77%, [24](#)). ¹H n.m.r. δ(D₂O, DOH=4.81) 7.89, dd, *J*_{8,7} 5.5 Hz, *J*_{8,5} 1.1 Hz, 1 H, 8-H; 8.81, d, *J*_{7,8} 5.5 Hz, 1 H, 7-H; 9.24, d, *J*_{5,8} 1.1 Hz, 1 H, 5-H.

5.6.25. 5,6,7,8-Tetrahydropyrido[3,4-*d*]pyridazine-1,4(2,3*H*)-dione

Pyrido[3,4-*d*]pyridazine-1,4(2,3*H*)-dione [3](#) (1.00 g, 5.98 mmol, [24](#)) was dissolved in 20 mL water with a few drops of conc. ammonia. Palladium on carbon catalyst (500 mg) was added, and the mixture stirred under hydrogen at atmospheric pressure for 24 hours. The catalyst was removed by filtration, and the mixture evaporated, to give 1.032 g of yellow residue. Recrystallisation from water gave 511 mg, followed by a second crop from water/ethanol of 337 mg, of 5,6,7,8-tetrahydropyrido[3,4-*d*]pyridazine-1,4(2,3*H*)-dione (848 mg, 5.07 mmol, 85%, [25](#)). ¹H n.m.r. δ(D₂O, DOH=4.81) 2.78, t, *J* 5.5 Hz, 2 H, C(8)H₂; 3.48, t, *J* 5.5 Hz, 2 H, C(7)H₂; 4.06, s, 2 H, C(5)H₂. ¹³C n.m.r. δ(D₂O, dioxane=67.4) 20.9, C(8)H₂; 40.8, CH₂; 41.1, CH₂; 131.8, C; 135.9, C; 159.9, CO; 160.6, CO.

5.6.26. 1-Hydroxy-3-methylpyrido[3,4-*d*]pyridazin-4(3*H*)-one

5.6.27. 2-Methyl-4-hydroxypyrido[3,4-*d*]pyridazin-1(2*H*)-one

A mixture of dimethyl pyridine-3,4-dicarboxylate (8.0 g, 41 mmol, [23](#)), methyl hydrazine (5.67 g, 113 mmol) and methanol (15 mL) was stirred at room

temperature in a sealed flask for seven days, by which time the reaction appeared to be near complete by TLC. The mixture was evaporated, to leave a yellow solid. This solid was dissolved in 20 mL hot water, with the addition of 2 mL conc. ammonia solution, and precipitated with 8 mL glacial acetic acid. By n.m.r., this was found to contain two isomers **26** and **27**, in roughly 2:1 proportions. The mixture was filtered, and the residue washed twice with small portions each of water, ethanol, and diethylether, leaving 6.29 g of yellow powder. This material was dissolved in 6000 mL boiling water, allowed to cool very slowly, and filtered, giving pure 1-hydroxy-3-methylpyrido[3,4-*d*]pyridazin-4(3*H*)-one (3.42 g, 19.3 mmol, 47%, **26**) as yellow-orange crystals. ¹H n.m.r. δ (D₂O, DOH=4.81) 3.58, s, 3 H, N-CH₃; 7.87, d, *J* 5.5 Hz, 1 H, 8-H; 8.85, d, *J* 5.5 Hz, 1 H, 7-H; 9.29, s, 1 H, 5-H. ¹³C n.m.r. δ (D₂O+NaOD, dioxane=67.4) 39.1, NCH₃; 119.5, C(8)H; 123.8, C; 136.0, C; 149.1, C(5)H; 151.6, C(7)H; 157.8, CO; 159.9, CO. Mass spectrum: *m/z* 178 (M+1, 100%). The filtrate was evaporated, and the residue recrystallised twice from water (600 mL and 400 mL). The concentration of **26** in the residues could not be decreased below 15% by fractional crystallisation. The residue from the final recrystallisation was 85% 2-methyl-4-hydroxypyrido[3,4-*d*]pyridazin-1(2*H*)-one (400mg total, aprx. 1.9 mmol, 5%, **27**). ¹H n.m.r. δ (D₂O, DOH=4.81) 3.60, s, 3 H, N-CH₃; 7.97, d, *J* 5.5 Hz, 1 H, 8-H; 8.81, d, *J* 5.5 Hz, 1 H, 7-H; 9.21, s, 1 H, 5-H. ¹³C n.m.r. δ (D₂O+NaOD, dioxane=67.4) 39.6, NCH₃; 119.5, C(8)H; 124.5, C; 134.9, C; 149.2, C(5)H; 150.4, C(7)H; 157.4, CO; 160.6, CO. Mass spectrum: *m/z* 178 (M+1, 100%), 162 (20%), 137 (43%), 119 (31%).

5.6.28. 1-Chloro-3-methylpyrido[3,4-*d*]pyridazin-4(3*H*)-one

A mixture of phosphorus oxychloride (1 mL, 11 mmol), phosphorus pentachloride (0.42 g, 2 mmol) and 1-hydroxy-3-methylpyrido[3,4-*d*]pyridazine-4(3*H*)-one (356 mg, 2 mmol, **26**) was refluxed for four hours. The mixture was poured into an ice / ethyl acetate slurry (50 mL aprx) and dilute ammonia added until basic while stirring. The ethyl acetate layer was separated, and evaporated to leave 37 mg of residue, showing a single spot by TLC, *R_f* = 0.53, ethyl acetate. This was recrystallised from boiling heptane to yield 1-chloro-3-methylpyrido[3,4-*d*]pyridazin-4(3*H*)-one (26 mg, 0.13 mmol, 7%, **28**). ¹H n.m.r. δ (CDCl₃) 3.85, s, 3 H,

N-CH₃; 7.76, d, *J* 5.3 Hz, 1 H, 8-H; 9.10, d, *J* 5.3 Hz, 1 H, 7-H; 9.72, s, 1 H, 5-H. ¹³C n.m.r. δ (CDCl₃=77.0) 39.5, NCH₃; 117.295, C(8)H; 134.1, C(9 or 10); 135.5, C(10 or 9); 150.9 C(5)H; 152.1 C(1); 153.2 C(7)H; 157.9 C(4). Mass spectrum: *m/z* 196 (M+1, 100%), 182 (10%), 160 (6%), 135 (6%).

5.6.29. 3-methyl-5,6,7,8-tetrahydropyrido[3,4-*d*]pyridazin-4(3*H*)-one

1-Chloro-3-methylpyrido[3,4-*d*]pyridazin-4(3*H*)-one (24 mg, 0.12 mmol, **28**) was hydrogenated for 18 hours at 1 atm, in a solution of 1.5 mL methanol, one drop of conc. ammonia, with 24 mg of palladium on carbon catalyst. The solution was filtered and evaporated to give a deep red residue, sufficient for n.m.r. identification as 3-methyl-5,6,7,8-tetrahydropyrido[3,4-*d*]pyridazin-4(3*H*)-one (23 mg, 80%, **29**), rather than its positional isomer, 2-methyl-5,6,7,8-tetrahydropyrido[3,4-*d*]pyridazin-1(2*H*)-one (not synthesised), by n.O.e. experiments. TLC (butanol/acetic acid/water 4:1:1) showed one ninhydrin active spot (*R_f* 0.22), and one minor contaminant (*R_f* 0.48). ¹H n.m.r. δ (CDCl₃) 3.04, d, *J* 5.8 Hz, 2 H, C(8)H₂; 3.47, d, *J* 5.8 Hz, 2 H, C(7)H₂; 3.80, s, 3 H, NCH₃; 4.20, s, 2 H, C(5)H₂; 7.63, s, 1H, C(1)H. n.O.e. irradiation at 7.63 ppm (Ar-H); significant enhancement at 3.03 ppm only (CH₂CH₂C).

5.6.30. 1-Hydroxy-3-methyl-5,6,7,8-tetrahydropyrido[3,4-*d*]pyridazin-4(3*H*)-one

1-Hydroxy-3-methylpyrido[3,4-*d*]pyridazin-4(3*H*)-one (1.00 g, 5.64 mmol, **26**), was dissolved in methanol (50 mL) with the addition of a few drops of conc. ammonia. Palladium on carbon catalyst was added (500 mg), and the mixture stirred under hydrogen at atmospheric pressure for 48 hours. The catalyst was removed by filtration, and the mixture evaporated, to leave 0.951 g. Recrystallisation from 15 mL water gave pale yellow crystals (102 mg). Second (92 mg) and third (307 mg) crops were obtained from water/ethanol, giving 1-hydroxy-3-methyl-5,6,7,8-tetrahydropyrido[3,4-*d*]pyridazin-4(3*H*)-one (501mg, 2.77 mmol, 49%, **30**). ¹H n.m.r. δ (D₂O, DOH=4.81) 2.75, tt, *J*₈₋₇ 6.3 Hz, *J*₈₋₅ 1.8 Hz, 2 H, 8CH₂; 3.45, t, *J*₇₋₈ 6.3 Hz, 2 H, 7CH₂; 3.51, s, 3 H, N-CH₃; 4.05, t, *J*₅₋₈ 1.8 Hz, 2 H, 5CH₂. ¹³C n.m.r. δ (D₂O,

dioxane=67.4) 21.5, C(8)H₂; 39.5, CH₃; 40.7, CH₂; 40.9, CH₂; 129.3, C; 136.9, C; 157.4, CO; 161.4, CO.

5.6.31. 2-Methyl-4-hydroxy-5,6,7,8-tetrahydropyrido[3,4-d]pyridazin-1(2H)-one

Impure 2-methyl-4-hydroxypyrido[3,4-d]pyridazin-1(2H)-one (400 mg, aprx. 85%, 1.9 mmol, [27](#)) was dissolved in methanol (20 mL), with the addition of a few drops of ammonia. Palladium on carbon catalyst (200 mg) was added, and the mixture stirred under hydrogen at atmospheric pressure for 48 hours. The catalyst was removed by filtration, and the mixture evaporated to leave 425 mg of residue. This was dissolved in 15 mL hot water, filtered hot, and 15 mL hot ethanol added to the filtrate. On slow cooling, there was crystallisation of pale yellow translucent plates of 2-methyl-4-hydroxy-5,6,7,8-tetrahydropyrido[3,4-d]pyridazin-1(2H)-one (191 mg, 1.05 mmol, aprx. 55%, [31](#)), without detectable contamination by [30](#). ¹H n.m.r. δ (D₂O, DOH=4.81) 2.78, t(br), J 6.3 Hz, 2 H, C(8)H₂; 3.47, t, J 6.3 Hz, 2 H, C(7)H₂; 3.54, s, 3 H, N-CH₃; 4.04, s(br), 2 H, 5CH₂. ¹³C n.m.r. δ (D₂O, dioxane=67.4) 20.7 C(8)H₂; 39.8, CH₃; 40.8, CH₂; 41.3, CH₂; 132.0 C; 133.9 C; 158.5 CO; 160.3 CO.

5.6.32. Methyl 2-acetamido-2-carbomethoxy-3-(3,6-dimethoxypyridazin-4-yl)propanoate

A dry sodium methoxide solution was prepared by dissolving sodium (690 mg, 30 mmol) in freshly dried and distilled methanol (30 mL). Of this solution, 1.5 mL was pipetted into a 5 mL flask fitted with a drying tube and stirring bar, and containing 3,6-dimethoxy-4-bromomethylpyridazine (212 mg, 0.91 mmol, [5](#)) and dimethyl acetamidomalonate (189 mg, 1.00 mmol). Within half an hour, the solids had dissolved to leave a clear, yellow solution. The mixture was left to stir at room temperature overnight, then the solvent removed under vacuum. The residue was suspended in 30 mL water, and extracted three times into equal volumes of ethyl acetate. The pooled extracts were washed with 10 mL water, dried with Na₂SO₄, and evaporated in vacuum to leave 220 mg of white solid. TLC showed three components (R_f 0.56, 0.23, and 0.07, ethyl acetate/toluene 1:1). The mixture was separated on a silica gel column, eluting with toluene/ethyl acetate (4:1) followed

by pure ethyl acetate. The first component, a white crystalline solid, was found to be a byproduct, 3,6-dimethoxy-4-methoxymethylpyridazine (43 mg, 0.23 mmol, 25%). ^1H n.m.r. δ (CDCl_3) 3.48, s, 3 H, CH_2OCH_3 ; 4.04, s, 3 H, OCH_3 ; 4.06, s, 3 H, OCH_3 ; 4.38, d, J 1.4 Hz, 2 H, CH_2OCH_3 ; 7.02, t, J 1.4 Hz, 1 H, 5-H. The second component, a white powder, was found to be the desired product, methyl 2-acetamido-2-carbomethoxy-3-(3,6-dimethoxypyridazin-4-yl)propanoate (148 mg, 0.43 mmol, 47%, **32**). ^1H n.m.r. δ (CDCl_3) 1.99, s, 3 H, COCH_3 ; 3.65, s, 2 H, 4- CH_2 ; 3.82, s, 6 H, $(\text{CO}_2\text{CH}_3)_2$; 3.99, s, 3 H, OCH_3 ; 4.02, s, 3 H, OCH_3 ; 6.55, s, 1 H, N-H; 6.64, s, 1 H, 5-H. ^{13}C n.m.r. δ ($\text{CDCl}_3=77.0$) 22.8, COCH_3 ; 32.2, 4- CH_2 ; 53.7, $(\text{CO}_2\text{CH}_3)_2$; 54.5, OCH_3 ; 54.8, OCH_3 ; 65.3, CH_2C ; 122.2, C(5)H; 129.5 C(4) CH_2 ; 160.9, COMe ; 162.2, COMe ; 167.7, $(\text{CO}_2\text{Me})_2$; 169.3, HNCO . m.p. 151-2°C. Mass spectrum: m/z 342 (M+1, 72%), 183 (16%), 155 (100%). The third component, a colourless crystalline residue, was found to be the partially hydrolysed and decarboxylated product, methyl 2-acetamido-3-(3,6-dimethoxypyridazin-4-yl)propanoate (4 mg, 0.014 mmol). ^1H n.m.r. δ (CDCl_3) 1.98, s, 3 H, COCH_3 ; 3.01, o, J_{AB} 13.9 Hz, J_{AX} 7.0 Hz, J_{AZ} 0.7 Hz, 1 H, $\text{RNHCH}_X\text{R}'\text{CH}_A\text{H}_B\text{R}''$; 3.12, o, J_{BA} 13.9 Hz, J_{BX} 6.1 Hz, J_{BZ} 0.7 Hz, 1 H, $\text{RNHCH}_X\text{R}'\text{CH}_A\text{H}_B\text{R}''$; 3.75, s, 3 H, CO_2CH_3 ; 4.03, s, 3 H, OCH_3 ; 4.06, s, 3 H, OCH_3 ; 4.86, o, 1 H, J_{XA} 7.0 Hz, J_{XB} 6.9 Hz, J_{XY} 7.4 Hz, $\text{RNH}_Y\text{CH}_X\text{R}'\text{CH}_A\text{H}_B\text{R}''$; 6.09, d(b), J_{YX} 7.4 Hz, 1 H, N- H_Y ; 6.74, t, J 0.7 Hz, 1 H, 5- H_Z .

5.6.33. 2-amino-3-(pyridazine-3,6(1,2H)-dion-4-yl)propanoic acid

Methyl 2-acetamido-2-carbomethoxy-3-(3,6-dimethoxypyridazin-4-yl)propanoate (70 mg, 0.205 mmol, **32**) was refluxed for 90 minutes in 1 mL 48% HBr. The mixture was evaporated in vacuum leaving 100 mg of amber liquid. This was absorbed onto Dowex 50W (H^+) ion exchange resin which was washed with several volumes of water, followed by elution with 1M pyridine. The pyridine fractions were collected and evaporated to leave 2-amino-3-(pyridazine-3,6(1,2H)-dion-4-yl)propanoic acid (40 mg, 0.188 mmol, 92%). An analytical sample was obtained by recrystallisation from water/ethanol. R_f 0.24 (Butanol/Acetic Acid/Water, 4:1:1). ^1H n.m.r. δ (D_2O , $\text{DOH}=4.81$) 3.04, q, J_{AB} 14.6 Hz, J_{AX} 7.6 Hz, 1 H, $\text{CH}_A\text{H}_B\text{CH}_X$; 3.18, q, J_{BX} 5.1 Hz, 1 H, $\text{CH}_A\text{H}_B\text{CH}_X$; 4.08, q, 1 H, $\text{CH}_A\text{H}_B\text{CH}_X$; 7.11, s, 1 H, 5-H. ^{13}C n.m.r. δ ($\text{D}_2\text{O}+\text{DCl}$,

dioxane=67.4) 31.8 (CH₂), 52.1 (CH), 130.4 (CH), 140.0 (C), 157.5 (CO), 160.2 (CO), 171.3 (CO₂H). m.p. >310°C with decomposition. Mass spectrum: *m/z* 200 (M+1, 100%), 183 (16%), 154 (16%), 139 (28%).

5.6.34. Ethyl 2-acetamido-2-ethoxycarbonyl-3-(2-methyl-6-ethoxypyridazin-3(2*H*)-on-4-yl)propanoate

A sodium ethoxide solution was prepared by dissolving sodium (0.369 g, 16.1 mmol) in 20 mL freshly dried ethanol. From this solution, 1.05 mL (0.84 mmol ethoxide) was added to 2-methyl-4-bromomethyl-6-ethoxypyridazin-3(2*H*)-one (203 mg, 0.82 mmol, **13**) and diethyl acetamidomalonate (176 mg, 0.81 mmol) under dry conditions. Within a few minutes of stirring, a slightly yellow milky precipitate had formed. The mixture was allowed to stir overnight, the ethanol evaporated, and the products suspended in 20 mL water. Extraction twice into equal volumes of ethyl acetate, drying over Na₂SO₄, and removal of solvent gave 300 mg of crude product. This was recrystallised from 15-20 mL petroleum ether to give ethyl 2-acetamido-2-ethoxycarbonyl-3-(2-methyl-6-ethoxypyridazine-3(2*H*)-on-4-yl)propanoate (245 mg, 0.64 mmol, 79%, **34**). ¹H n.m.r. δ(CDCl₃) 1.28, t, *J* 7.1 Hz, 6 H, (CO₂CH_AH_BCH₃)₂; 1.34, t, *J* 7.1 Hz, 3 H, 6-OCH₂CH₃; 2.00, s, 3 H, COCH₃; 3.56, s, 2 H, 4-CH₂; 3.60, s, 3 H, N-CH₃; 4.13, q, *J* 7.1, 2 H, 6-OCH₂CH₃; 4.264, qq, *J*_{AX3} 7.1 Hz, *J*_{AB} 10.7 Hz, 2 H, (CO₂CH_AH_BCH₃)₂; 4.306, qq, *J*_{BX3} 7.1 Hz, *J*_{BA} 10.7 Hz, 2 H, (CO₂CH_AH_BCH₃)₂; 6.75, s, 1 H, 5-H; 7.04, s, 1 H, N-H. ¹³C n.m.r. δ(CDCl₃=77.0) 13.9, (CO₂CH₂CH₃)₂; 14.2, 6-OCH₂CH₃; 22.9, COCH₃; 34.0, 4-CH₂; 39.6, NCH₃; 62.7, 6-OCH₂CH₃; 62.8, (CO₂CH₂CH₃)₂; 65.3, CH₂C; 126.7, C(5)H; 140.0, C(4)CH₂; 152.1, CO; 159.9, CO; 167.6, (CO₂Et)₂; 169.3, HNCO. m.p. 123-5°C. Mass spectrum: *m/z* 384 (M+1, 70%), 218 (11%), 197 (15%), 169 (100%). The byproduct ethyl 2-acetamido-3-(2-methyl-6-ethoxypyridazin-3(2*H*)-on-4-yl)propanoate, which is also hydrolysable to the glycine derivative, was detected in the crude product. ¹H n.m.r. δ(CDCl₃) 1.25, t, *J* 7.2 Hz, 3 H, CO₂CH₂CH₃; 1.35, t, *J* 7.0 Hz, 3 H, OCH₂CH₃; 2.00, s, 3 H, COCH₃; 3.02, m, 2 H, 4-CH₂CH; 3.67, s, 3 H, N-CH₃; 4.16, q, *J* 7.0 Hz, 2 H, OCH₂CH₃; 4.19, q, *J* 7.2 Hz, 2 H, CO₂CH₂CH₃; 4.67, m, 1 H, 4-CH₂CH; 6.80, s, 1 H, 5-H; 7.66, d(b), *J* 6.6 Hz, 1 H, NHCOCH₃.

5.6.35. 2-Amino-3-(2-methyl-6-hydroxypyridazin-3(2H)-on-4-yl)propanoic acid

Ethyl 2-acetamido-2-ethoxycarbonyl-3-(2-methyl-6-ethoxypyridazine-3(2H)-on-4-yl)propanoate (466 mg, 1.22 mmol, **34**) was dissolved in 3 mL 48% hydrobromic acid and held at reflux for 90 minutes. The acid was removed in vacuum to leave 375 mg of orange foamy residue. Ethyl 2-acetamido-3-(2-methyl-6-ethoxypyridazin-3(2H)-on-4-yl)propanoate (144 mg, 0.46 mmol) was treated in the same way to leave 167 mg of residue. These combined products were absorbed onto Dowex 50W (H⁺) ion exchange resin, washed with several volumes of water, and eluted with 1M pyridine. The pyridine fractions were evaporated to leave 2-amino-3-(2-methyl-6-hydroxypyridazine-3(2H)-on-4-yl)propanoic acid (281 mg, 1.32 mmol, 79%) as an off-white powder. ¹H n.m.r. δ (D₂O, DOH=4.81) 3.05, q, J_{AB} 14.6 Hz, J_{AX} 7.1 Hz, 1 H, CH_AH_BCH_X; 3.19, q, J_{BX} 4.9 Hz, 1 H, CH_AH_BCH_X; 3.64, s, 3 H, N-CH₃; 4.07, q, 1 H, CH_AH_BCH_X; 7.13, s, 1 H, 5-H. ¹³C n.m.r. δ (D₂O, dioxane=67.4) 32.9, CH₂; 40.5, NCH₃; 54.3, CH₂CH; 127.6, C(5)H; 141.5, C(4); 154.8, CO; 161.5, CO; 173.6, CO₂H. m.p. 256-9°C. Mass spectrum: *m/z* 214 (M+1, 100%), 197 (12%), 168 (16%).

5.6.36. Ethyl 2-acetamido-2-ethoxycarbonyl-3-(2-methyl-6-ethoxypyridazin-3(2H)-on-5-yl)propanoate

Sodium (552 mg, 24 mmol) was dissolved in 40 mL dry ethanol. 2 mL of this solution was added to diethyl acetamidomalonate (261 mg, 1.20 mmol), and the mixture stirred. 2-Methyl-5-bromomethyl-6-ethoxypyridazin-3(2H)-one (300 mg, 1.21 mmol, **19**) was added, whereupon the stirred solution turned dark instantly. After stirring overnight, the solvent was removed in vacuum, the residue suspended in 20 mL water, and extracted three times with 20 mL ethyl acetate. The combined extracts were evaporated in vacuum to leave 555 mg of a crystalline solid, which was recrystallised from cyclohexane to yield 220 mg of white crystals. The residue after crystallisation was chromatographed on silica, eluting with ethyl acetate:toluene, 1:1, affording a further 13 mg of ethyl 2-acetamido-2-ethoxycarbonyl-3-(2-methyl-6-ethoxypyridazin-3(2H)-on-5-yl)propanoate (total yield 233 mg, 0.61 mmol, 51%, **36**). ¹H n.m.r. δ (CDCl₃) 1.28, t, J 7.1 Hz, 6 H, (CO₂CH_AH_BCH₃)₂; 1.34, t, J 7.0 Hz, 3 H, 6-OCH₂CH₃; 2.01, s, 3 H, COCH₃; 3.55, s, 2 H,

5-CH₂; 3.61, s, 3 H, N-CH₃; 4.14, q, *J* 7.05, 2 H, 6-OCH₂CH₃; 4.22, qq, *J*_{AX3} 7.1 Hz, *J*_{AB} 10.7 Hz, 2 H, (CO₂CH_AH_BCH₃)₂; 4.32, qq, *J*_{BX3} 7.1 Hz, *J*_{BA} 10.7 Hz, 2 H, (CO₂CH_AH_BCH₃)₂; 6.60, s, 1 H, 4-H; 6.61, s(b), 1 H, NHCOCH₃. ¹³C n.m.r. δ (CDCl₃=77.0) 13.9, (CO₂CH₂CH₃)₂; 14.1, 6-OCH₂CH₃; 22.9, COCH₃; 31.5, 4-CH₂; 39.0, NCH₃; 62.9, (CO₂CH₂CH₃)₂; 63.2, 6-OCH₂CH₃; 65.6, CH₂C; 132.4, C(5)H; 135.2, C(4)CH₂; 151.5, CO; 159.1, CO; 167.2, (CO₂Et)₂; 169.2, HNCO.

5.6.37. 2-Amino-3-(2-methyl-6-hydroxypyridazin-3(2H)-on-5-yl)propanoic acid

Ethyl 2-acetamido-2-ethoxycarbonyl-3-(2-methyl-6-ethoxypyridazin-3(2H)-on-5-yl)propanoate (223 mg, 0.58 mmol, **36**) was dissolved in 3 mL conc. HBr, and heated at 140°C for a total of 12 hours, in three stages, between each of which the HBr was evaporated and the product purified on Dowex 50W (H⁺) ion exchange resin, eluting with pyridine, and the progress of the reaction followed by TLC (butanol:acetic acid:water 4:1:1). Whilst hydrolysis of the acetamide and ethyl esters was rapid, hydrolysis of the ring ethoxide was slow, incomplete, and by 12 hours it was apparent that substantial degradation was occurring. The product was evaporated and chromatographed on Dowex 50W. Removal of the pyridine in vacuum yielded crude 2-amino-3-(2-methyl-6-hydroxypyridazin-3(2H)-on-5-yl)propanoic acid (105 mg, 0.49 mmol, 85%, **37**), as a beige powder, contaminated with aprx. 8% 6-ethoxy derivative. *R*_f 0.24 (Butanol/Acetic Acid/Water, 4:1:1). ¹H n.m.r. δ (D₂O, DOH=4.81) 3.00, q, *J*_{AB} 14.5 Hz, *J*_{AX} 7.7 Hz, 1 H, CH_AH_BCH_X; 3.16, q, *J*_{BX} 5.2 Hz, 1 H, CH_AH_BCH_X; 3.59, s, 3 H, N-CH₃; 4.07, q, 1 H, CH_AH_BCH_X; 6.92, s, 1 H, 4-H.

5.6.39. 2-Methyl-6-hydroxypyridazin-3(2H)-one

Maleic anhydride (9.8 g, 0.1 mol, **38**) and conc. hydrochloric acid (11.2 g, 0.1 mol) were mixed in a 100 mL flask, and methyl hydrazine (4.6 g, 0.1 mol) was added dropwise with caution. The mixture was heated at 100°C for three hours, cooled and filtered. The residue was washed with several volumes of cold water, collected, and dried to leave 8.25 g white crystals. The combined filtrates were concentrated, yielding a second crop of 0.17 g 2-methyl-6-hydroxypyridazin-3(2H)-one (8.42 g,

0.067 mol, 67%, **39**). ^1H n.m.r. δ (D₂O, DOH=4.81) 3.60, s, 3 H, 1-CH₃; 7.03, d, *J* 9.7 Hz, 1 H, 5-H; 7.20, d, *J* 9.7 Hz, 1 H, 4-H.

5.6.40. 2-Methyl-6-ethoxypyridazin-3(2H)-one

2-Methyl-6-hydroxypyridazin-3(2H)-one (8.00 g, 63 mmol, **39**), potassium carbonate (21.92 g, 317 mmol, 2.5 eq.), ethyl iodide (20.3 mL, 254 mmol, 4 eq.), and 150 mL absolute ethanol were added to a 500 mL flask. The slurry was stirred and heated at reflux (80°C) for 24 hours, cooled, and filtered. The residue was washed with ethanol, and the filtrates evaporated to leave 14.10 g pale yellow residue.

Recrystallisation from 75 mL heptane, including hot filtration, yielded large off-white oily crystals of 2-methyl-6-ethoxypyridazin-3(2H)-one (8.64 g, 56 mmol, 88%, **40**). ^1H n.m.r. δ (CDCl₃) 1.37, t, *J* 7.1 Hz, 3 H, OCH₂CH₃; 3.65, s, 3 H, NCH₃; 4.18, q, *J* 7.1 Hz, 2 H, OCH₂CH₃; 6.89, s, 2H, 4,5-H (coincident).

5.6.41. 2-Bromomethyl-6-ethoxypyridazin-3(2H)-one

2-Methyl-6-ethoxypyridazin-3(2H)-one (8.00 g, 52 mmol, **40**), *N*-bromosuccinimide (9.24 g, 52 mmol), and 200 mL CCl₄, were stirred in a 500 mL flask fitted with a reflux condenser. The mixture was irradiated for 30 minutes with a high intensity UV source (800W Lowel-Tota lamp), at a distance of around 10 cm. The mixture was washed twice with equal volumes of water to remove the floating succinimide layer, dried over Na₂SO₄, and evaporated, to leave 8.78 g yellow residue. 60 mL of a 3:1 mixture of heptane and toluene was added, the mixture boiled, and decanted from an insoluble orange oily layer. On cooling, 2-bromomethyl-6-ethoxypyridazin-3(2H)-one was recovered as soft, yellow oily crystals (4.72 g, 20 mmol, 39%, **41**). This compound showed rapid degradation in moist air, presumably to the 2-hydroxymethyl derivative (based on n.m.r. data, ^1H n.m.r. δ (CDCl₃) 5.54, s, 2H, NCH₂OH) conversion being substantially complete in 24 hours. Only minor degradation was visible after 12 months in a sealed container at -15°C. ^1H n.m.r. δ (CDCl₃) 1.39, t, *J* 7.1 Hz, 3 H, -CH₂-CH₃; 4.24, q, *J* 7.1 Hz, 2 H, -CH₂-CH₃; 5.75, s, 2 H, N-CH₂Br; 6.87, d, *J* 9.8 Hz, 1 H, 5(or 4)-H; 6.93, d, *J* 9.8 Hz, 1 H, 4(or 5)-H. ^{13}C n.m.r.

δ (CDCl₃=77.0) 14.1, CH₃; 46.1, CH₂Br; 63.5, OCH₃; 128.7, CH; 132.5, CH; 153.1, CO; 158.4, CO.

5.6.42. Ethyl 2-acetamido-2-ethoxycarbonyl-3-(6-ethoxypyridazin-3(2H)-on-2-yl)propanoate

A sodium ethoxide solution was prepared by dissolving sodium (0.99 g, 43 mmol) in 100 mL dry ethanol. Diethyl acetamidomalonate (2.33 g, 10.7 mmol) was dissolved in 25 mL of this solution in a 50 mL flask fitted with a drying tube, and allowed to stir for a few minutes. 2-Bromomethyl-6-ethoxypyridazin-3(2H)-one (2.50 g, 10.7 mmol, **41**) was added, and rapidly dissolved, whereupon the solution turned to a pale orange-pink, and a mild exotherm was noted. The solution was stirred for 18 hours, evaporated, suspended in 100 mL water, and extracted three times with equal volumes of ethyl acetate. Drying of the ethyl acetate over Na₂SO₄, followed by evaporation, gave 3.87 g residue, which was recrystallised from 200 mL heptane containing a few mL of toluene to leave fluffy white needles of ethyl 2-acetamido-2-ethoxycarbonyl-3-(6-ethoxy-pyridazin-3(2H)-on-2-yl)propanoate (2.87 g, 7.77 mmol, 73%, **42**). ¹H n.m.r. δ (CDCl₃) 1.31, t, *J* 7.1 Hz, 6 H, (CO₂CH_AH_BCH₃)₂; 1.34, t, *J* 7.1 Hz, 3 H, 3-OCH₂CH₃; 1.98, s, 3 H, COCH₃; 4.09, q, *J* 7.1, 2 H, 3-OCH₂CH₃; 4.271, qq, *J*_{AX3} 7.1 Hz, *J*_{AB} 10.7 Hz, 2 H, (CO₂CH_AH_BCH₃)₂; 4.332, qq, *J*_{BX3} 7.1 Hz, *J*_{BA} 10.7 Hz, 2 H, (CO₂CH_AH_BCH₃)₂; 4.91, s, 2 H, N-CH₂-; 6.59, s (br), 1 H, NHCOCH₃; 6.83, d, *J* 9.8 Hz, 1 H, 5(or 4)-H; 6.87, d, *J* 9.8 Hz, 1 H, 4(or 5)-H. ¹³C n.m.r. δ (CDCl₃=77.0) 13.9, (CO₂CH₂CH₃)₂; 14.2, 6-OCH₂CH₃; 22.8, COCH₃; 51.8, N-CH₂; 62.8, 6-OCH₂CH₃; 62.8, (CO₂CH₂CH₃)₂; 64.6, CH₂C; 127.0, CH; 132.5, CH; 152.4, CO; 159.4, CO; 166.9, (CO₂Et)₂; 169.0, HNCO.

5.6.43. 2-Amino-3-(6-hydroxypyridazin-3(2H)-on-2-yl)propanoic acid

Ethyl 2-acetamido-2-ethoxycarbonyl-3-(6-ethoxypyridazine-3(2H)-on-2-yl)propanoate (2.5 g, 6.77 mmol, **42**) was dissolved in hydroiodic acid (10 mL, 57%), and refluxed 15 hours. Evaporation of excess acid, followed by chromatography on Dowex 50W (H⁺ ion-exchange resin, eluting with pyridine, and evaporation of the pyridine fractions, gave 1.13 g of buff-coloured solid. TLC (butanol/acetic

acid/water, 4:1:1) and n.m.r. showed that only a modest proportion the material was fully deprotected (R_f 0.24), with the major product being 2-amino-3-(6-ethoxy-pyridazine-3(2*H*)-on-2-yl)propanoic acid (R_f 0.31) along with some degradation. ^1H n.m.r. δ (D_2O , $\text{DOH}=4.81$) 1.34, t, J 7.1, 3 H, $-\text{OCH}_2\text{CH}_3$; 4.19, dd, 1 H, $\text{NCH}_\text{A}\text{H}_\text{B}\text{CH}$; 4.23, q, J 7.1, 2 H, $6-\text{OCH}_2\text{CH}_3$; 4.46, dd, 1 H, $\text{NCH}_\text{A}\text{H}_\text{B}\text{CH}$; 4.64, dd, 1 H, $\text{NCH}_\text{A}\text{H}_\text{B}\text{CH}$; 7.03, d, J 9.9 Hz, 1 H, 5(or 4)-H; 7.18, d, J 9.9 Hz, 1 H, 4(or 5)-H. This material was redissolved in 10 mL fresh hydroiodic acid, and refluxed for a further 9 hours, by which time conversion appeared substantially complete by TLC, and the free amino acid was recovered as before by ion-exchange chromatography, leaving 771 mg of residue. This was recrystallised from 30 mL of boiling ethanol/water (1:1), yielding fluffy white needles of 2-Amino-3-(6-hydroxypyridazin-3(2*H*)-on-2-yl)propanoic acid (612 mg, 3.07 mmol, 45% overall, **43**). R_f 0.28 (Butanol/Acetic Acid/Water, 4:1:1). ^1H n.m.r. δ (D_2O , $\text{DOH}=4.81$) 4.21, dd, J_{XB} 3.8 Hz, J_{XA} 6.9 Hz, 1 H, $\text{NCH}_\text{A}\text{H}_\text{B}\text{CH}_\text{X}$; 4.50, dd, J_{AX} 6.9 Hz, J_{AB} 14.8 Hz, 1 H, $\text{NCH}_\text{A}\text{H}_\text{B}\text{CH}_\text{X}$; 4.56, dd, J_{BX} 3.8 Hz, J_{BA} 14.8 Hz, 1 H, $\text{NCH}_\text{A}\text{H}_\text{B}\text{CH}_\text{X}$; 7.08, d, J 9.9 Hz, 1 H, 5(or 4)-H; 7.23, d, J 9.9 Hz, 1 H, 4(or 5)-H. ^{13}C n.m.r. δ (D_2O , dioxane=67.4) 51.1, NCH_2 ; 54.6, CH_2CH ; 129.2, CH; 133.5, CH; 155.2, CO; 161.8, CO; 172.0 CO_2H .

5.6.48. 3,6-Dimethoxy-4-(dibromomethyl)pyridazine

3,6-Dimethoxy-4-methylpyridazine (11.56 g, 75 mmol, **4**) was dissolved in CCl_4 (200 mL) and *N*-bromosuccinimide (26.70 g, 150 mmol) added. The stirred mixture was fitted with a reflux condenser, and irradiated for 40 minutes with an 800W "Lowel-Tota" high intensity lamp at a distance of 10 cm. The mixture was allowed to cool, filtered to remove excess succinimide, washed once with water (200 mL) and evaporated to leave 23.6 g dark residue. The residue was triturated with three approximate 50 mL volumes of hot heptane, discarding a tarry residue. The heptane extracts were pooled, and allowed to stand. Further tar being deposited, the extract was filtered, evaporated, and recrystallised from heptane to give 3,6-dimethoxy-4-(dibromomethyl)pyridazine (13.09 g, 42 mmol, 56%, **48**) as large soft pale beige waxy crystals. ^1H n.m.r. δ (CDCl_3) 4.08, s, 3 H, OCH_3 ; 4.14, s, 3 H, OCH_3 ; 6.70, d, J 1.1

Hz, 1 H, 5-H; 7.39, d, *J* 1.1 Hz, 1 H, CHBr₂. ¹³C n.m.r. δ (CDCl₃=77.0) 31.5, CHBr₂; 54.8, OCH₃; 55.2, OCH₃; 119.9, C(5)H; 134.0, C(4); 156.0, COMe; 162.0, COMe.

5.6.49. 3,6-Dimethoxy-4-carboxaldehyde

Attempted hydrolysis of the methyl pyridazine dibromide in water, THF/water, dioxane/water, or alcohol/water, with or without the addition of mineral acids or bases, with prolonged reflux, generally either returned starting material or baseline products, along with traces of the aldehyde. The following was the best of several methods trialled: 3,6-dimethoxy-4-(dibromomethyl)pyridazine (13.1 g, 42 mmol, **48**) was dissolved in ethanol (80 mL) and sodium acetate trihydrate (14.3 g, 105 mmol) added. Upon heating, the mixture became homogeneous, and reflux was maintained for five days. TLC (toluene/EtOAc 4:1) indicated substantial destruction of starting material (*R_f* 0.55), the presence of 3,6-dimethoxypyridazine-4-carboxaldehyde **49** and its diethoxy acetal **50** (*R_f* 0.30 and 0.33 respectively) along with baseline or low *R_f* material. Addition of water (200 mL) and extraction twice into ether (200 mL) followed by vacuum removal of the ether afforded 3.89 g of pale yellow liquid residue. ¹H n.m.r. indicated that the ratio of diacetal to aldehyde was 5:1. Dilute hydrochloric acid (0.1M, 100 mL) was added, and the mixture shaken for ten minutes at 70°C, converting most of the diacetal to the aldehyde, with some degradation. The mixture was again evaporated, and the residue chromatographed on silica (toluene/EtOAc 9:1) to give crude 3,6-dimethoxypyridazine-4-carboxaldehyde (819 mg, 4.8 mmol, 12%, **49**) as a somewhat volatile and low-melting white crystalline solid, the major contaminant being the diethoxy acetal. This mixture could be further purified by repeating the hydrolysis step, and triturating the residue with chloroform, with reduced yields due to further degradation. The aldehyde is unstable at room temperature in air, but can be maintained sealed at lower temperatures for reasonable periods. *R_f* 0.38 (toluene/ethyl acetate, 4:1). ¹H n.m.r. δ (CDCl₃) 4.10, s, 3 H, OCH₃; 4.21, s, 3 H, OCH₃; 7.30, s, 1 H, 5-H; 10.37, s, 1 H, 4-CHO. ¹³C n.m.r. δ (CDCl₃=77.0) 55.11, OCH₃; 55.14, OCH₃; 118.0, C(5)H; 125.1, C(4)CH; 160.0, COMe; 163.1, COMe; 188.2, 4-CHO. The acetal appears more stable, and the relative success of the reaction in ethanol

vs. other solvents, and with mildly basic buffered conditions may be attributed to its formation. 3,6-Dimethoxy-4-(diethoxymethyl)pyridazine **50**: R_f 0.43 (toluene/ethyl acetate, 4:1). ^1H n.m.r. δ (CDCl_3) 1.23, t, J 7.1 Hz, 6 H, $(\text{OCH}_2\text{CH}_3)_2$; 3.59, qq, J_{AX} 7.1 Hz, J_{AB} 9.3 Hz, 2 H, $(\text{OCH}_A\text{H}_B\text{CH}_3)_2$; 3.64, qq, J_{BX} 7.1 Hz, 2 H, $(\text{OCH}_A\text{H}_B\text{CH}_3)_2$; 4.05, s, 3 H, OCH_3 ; 4.09, s, 3 H, OCH_3 ; 5.54, d, J 0.75 Hz, 1 H, 4- $\text{CH}(\text{OEt})_2$; 7.16, d, J 0.75 Hz, 5-H. ^{13}C n.m.r. δ ($\text{CDCl}_3=77.0$) 15.1, $(\text{OCH}_2\text{CH}_3)_2$; 54.5, OCH_3 ; 54.7, OCH_3 ; 62.4, $(\text{OCH}_2\text{CH}_3)_2$; 95.7, 4- $\text{CH}(\text{OEt})_2$; 118.1, C(5)H; 131.7, C(4)CH; 159.7, COMe; 162.6, COMe. Mass spectrum: m/z 243 (M+1, 100%), 229 (12%), 213 (23%), 197 (48%).

5.6.53. Ethyl 2-(3,6-dimethoxypyridazin-4-yl)acetate

A dry 100 mL 3-neck flask was prepared under nitrogen. Freshly distilled THF (30 mL) was introduced by syringe, as was diisopropylamine (0.56 mL, 405 mg, 4 mmol) which had been freshly distilled from calcium hydride. The mixture was cooled to -30°C . Butyl lithium in hexane, recently titrated at 2.2M with 2,5-dimethoxybenzaldehyde, was added (1.82 mL, 4 mmol). The mixture was stirred 30 minutes at 0°C and then cooled to -70°C . A solution of carefully dried 3,6-dimethoxy-4-methylpyridazine (308 mg, 2 mmol, **4**) in 10 mL dry THF was introduced, whereupon a pale yellow colour developed. The temperature was maintained below -50°C and stirred for 90 minutes. Freshly distilled ethyl chloroacetate (0.19 mL, 217 mg, 2 mmol) in 10 mL dry THF was introduced, whereupon a deep red colour developed, and the solution was allowed to warm slowly to 0°C . 15 mL 1M HCl was added to quench, the solution returning to pale yellow, followed by 10 mL ethanol. The solution was neutralised with saturated sodium bicarbonate solution, and rotary evaporated. The residue was extracted twice with chloroform (50 mL portions), dried over sodium sulfate, and evaporated to leave 413 mg. The crude product was recrystallised from heptane, to give ethyl 2-(3,6-dimethoxypyridazine-4-yl)acetate (244 mg, 1.3 mmol, 65%, **53**). ^1H n.m.r. δ (CDCl_3) 1.26, t, 3 H, J 7.1 Hz, OCH_2CH_3 ; 3.55, d, 2 H, J 0.8 Hz, ArCH_2 ; 4.04, s, 3 H, OCH_3 ; 4.05, s, 3 H, OCH_3 ; 4.18, q, 2 H, J 7.1 Hz, OCH_2CH_3 ; 6.87, t, 1 H, J 0.8 Hz, ArH .

^{13}C n.m.r. δ ($\text{CDCl}_3=77.0$) 14.1, OCH_2CH_3 ; 35.0, ArCH_2 ; 54.5, OCH_3 ; 54.7, OCH_3 ; 61.3 OCH_2CH_3 ; 120.9, $\text{C}(5)\text{H}$; 128.4, $\text{C}(4)\text{R}$; 160.6, COMe ; 162.1, COMe ; 169.1, COOEt .

5.6.54. Ethyl 2-bromo-2-(3,6-dimethoxy-pyridazin-4-yl)acetate

Ethyl 2-(3,6-dimethoxy-pyridazin-4-yl)acetate (55 mg, 0.24 mmol, [53](#)) was dissolved in 2 mL CCl_4 , and *N*-bromosuccinimide added (43.3 mg, 0.24 mmol). The mixture was stirred, and irradiated for 20 minutes with an 800W "Lowel-Tota" high intensity UV lamp at a distance of 10 cm. A layer of floating succinimide indicated the reaction had proceeded, and TLC indicated clean conversion. The mixture was filtered, and evaporated, to leave crude ethyl 2-bromo-2-(3,6-dimethoxy-pyridazin-4-yl)acetate (82 mg, (112%), [54](#)). ^1H n.m.r. δ (CDCl_3) 1.30, t, J 7.1, 3 H, OCH_2CH_3 ; 4.07, s, 3 H, OCH_3 ; 4.09, s, 3 H, OCH_3 ; 4.26, q, J 7.1 Hz, 2 H, OCH_2CH_3 ; 5.42, s, 1 H, CHBr ; 7.28, s, 1 H, Ar-H .

5.6.56. Ethyl 2-hydroximino-2-(3,6-dimethoxy-pyridazin-4-yl)acetate

Ethyl 2-(3,6-dimethoxy-pyridazin-4-yl)acetate (49 mg, 0.22 mmol, [53](#)), was dissolved in acetic acid (330 mg, 5.5 mmol) and stirred at 0°C . A solution of sodium nitrite (84 mg, 1.2 mmol) in 2 mL water was slowly added dropwise over a 20 minute period. The solution turned pale yellow, and a creamy solid began to form. The mixture was maintained at 0°C for several hours. After stirring overnight, 10 mL water was added, and the solution extracted three times with 5 mL portions of CHCl_3 . The pooled extracts were evaporated to give a very pale yellow liquid which crystallised on standing to a yellow solid: ethyl 2-hydroximino-2-(3,6-dimethoxy-pyridazin-4-yl)acetate (48 mg, 0.18 mmol, 85%, [56](#)) of fair purity by TLC and n.m.r. ^1H n.m.r. δ (CDCl_3) 1.31, t, J 7.1 Hz, 3 H, OCH_2CH_3 ; 4.04, s, 3 H, OCH_3 ; 4.08, s, 3 H, OCH_3 ; 4.33, q, J 7.1 Hz, 2 H, OCH_2CH_3 ; 6.99, s, 1 H, Ar-H ; 8.8 (aprx), s (broad), 1 H, CNOH . ^{13}C n.m.r. δ ($\text{CDCl}_3=77.0$) 14.0, CH_2CH_3 ; 54.8, OCH_3 ; 55.0, OCH_3 ; 62.5, OCH_2CH_3 ; 121.4, $\text{C}(5)\text{H}$; 123.0, $\text{C}(4)\text{R}$; 144.4, CNOH ; 158.3, CO ; 161.7, COMe ; 161.9, COMe .

5.7 Acknowledgments

The laboratory assistance and support of Dr Hue Tran, Dr Rujee Duke, and most especially Dr Ken Mewett in facilitating these syntheses is gratefully acknowledged.

5.8 References

1. S Linholter, AAB Kristensen, R Rosenørn, SE Nielsen, H Kaaber, *Acta Chem. Scand.*, **15**(8), 1660 (1961)
2. T Nakagome, *Yakugaku Zasshi*, **83**, 934 (1963)
3. J Druey, K Meier, J Eichenberger, *Helv. Chim. Acta*, **37**, 121 (1954)
4. T Honoré, J Lauridsen, *Acta Chem. Scand.*, **B 34**, 235-240 (1980)
5. G Leclerc, C Wermuth., *C. R. Acad. Sci. Paris, Ser. C*, **267**(19), 1242-1244 (1968).
6. A Katrusiak, S Baloniak, *Acta Poloniae Pharmaceutica - Drug Research*, **51**, 4-5, 403-405 (1994)
7. J Druey, A Hüni, D Ringier, A Staehelin, *Helv. Chim. Acta*, **37**, 510 (1954)
8. T Nakagome, A Misaki, T Komatsu, *Chem. Pharm. Bull.*, **14**(10), 1082-1090 (1966)
9. R Schönbeck, *Monatsch Chem.*, **90**(2), 284-296 (1959)
10. K Eichenberger, A Staehelin, J Druey, *Helv. Chim. Acta*, **37**, 837 (1954)
11. S Hünig, K Oette, *Justus Leibigs Ann. Chem.*, **640**, 98 (1961)
12. P Coad, RA Coad, J Hyepock, *J. Org. Chem.*, **29**, 1751 (1964)
13. NG PH Buu-Hoï, H Le Bihan, F Binon, *Rec. Trav. Chim. (Recueil)*, **70**, 1099 (1951)
14. A Silhankova, D Doskocilova, M Ferles, *Collection Czech. Chem. Commun.*, **34**, 1976-1984 (1969)
15. RG Jones, *J. Am. Chem. Soc.*, **78**, 159-163 (1956)
16. S Kakimoto, S Tonooka, *Bull. Chem. Soc. Japan*, **40**, 153-159 (1967)
17. I Matsuura, F Yoneda, Y Nitta, *Chem. Pharm. Bull.*, **14**(9), 1010-1016 (1966)
18. H Hellmann, F Lingens, *Zeitschrift für Physiologische Chemie*, **297**, 283-287 (1954)
19. K Eichenberger, A Staehelin, J Druey, *Helv. Chim. Acta*, **37**, 837 (1954)
20. RN Castle, *Pyridazines, The Chemistry of Heterocyclic Compounds*, Wiley Interscience, **28**, (1973)
21. T Itai, H Igeta, *Yakugaku Zasshi*, **75**, 996 (1955)
22. H Igeta, *Chem. Pharm. Bull.*, **8**, 368 (1960)

23. YA Baskakov, NN Melnikov, *Zh. Obshch. Khim.*, **24**, 1216 (1954)
24. T Nakagome, A Misaki, T Komatsu, *Chem. Pharm. Bull.*, **14**(10), 1082-1090 (1966)
25. TN Johansen, K Frydenvang, B Ebert, P Krogsgaard-Larsen, U Madsen, *J. Med. Chem.*, **37**, 3252 (1994)
26. RD Allan, JR Hanrahan, TW Hambley, GAR Johnston, KN Mewett, AD Mitrovic, *J. Med. Chem.*, **33**(10), 2911 (1990)
27. SJ Angyal, RC Rassack, *J. Chem. Soc.*, 2700-2706 (1949)
28. TN Johansen, K Frydenvang, B Ebert, P Krogsgaard-Larsen, U Madsen, *J. Med. Chem.*, **37**, 3252-3262 (1994)
29. EL Eliel, KW Nelson, *J. Chem. Soc.*, 1628-1629 (1955)
30. J-M Sitazmzé, A Mann, C-G Wermuth, *Heterocycles*, **39**(1), 271 (1994)
31. JJ Hansen, P Krogsgaard-Larsen, *J. Chem. Soc. Perkin Trans. I.*, 1826-1833 (1980)
32. DJ Drinkwater, PWG Smith, *J. Chem. Soc.*, 1305-1307 (1971)
33. G Heinisch, Personal communication, 2 October (1996)
34. TN Johansen, K Frydenvang, B Ebert, P Krogsgaard-Larsen, U Madsen, *J. Med. Chem.*, **37**, 3252 (1994)
35. J Mann, *Murder Magic and Medicine*, Oxford University Press (1992)

6. Theoretical studies on the free-radical bromination of methyl pyridazines

Abstract

Free-radical bromination by *N*-bromosuccinimide has been performed on a range of methyl 3-methoxypyridazine derivatives. Depending on the substitution pattern, various products and selectivities have been observed, including atypical *N*-methyl bromination. The hypothesis that selectivity is dependent primarily on the stability of the free-radical intermediate formed in the reaction is examined, and a range of semi-empirical and *ab initio* molecular orbital methods used to calculate these stabilities and evaluated for agreement with experiment. Semi-empirical calculations using the PM3 Hamiltonian gave the best qualitative predictions of the methods trialed, thus providing a rapid method for predicting the selectivity of reactions used in the synthesis of novel heterocyclic analogues of the neurotransmitters GABA and glutamate.

"Theoretical studies on free-radical bromination of methyl pyridazines in the synthesis of novel heterocyclic analogues of neurotransmitters", JR Greenwood, G Vaccarella, HR Capper, KN Mewett, RD Allan, GAR Johnston. *Journal of Molecular Structure (Theochem)* 368, 235-243 (1996)

Index

[6.1 Introduction](#)

[Scheme 6.1 Mechanism of the Wohl-Ziegler reaction](#)

[6.2 Method](#)

[6.3 Results](#)

[Table 6.1 experimental products](#)

[Table 6.2 relative and absolute energies](#)

[Table 6.3 heats of reaction](#)

[Index of optimised geometries](#)

[6.4 Discussion](#)

[Figure 6.1 Image and PM3 energies of 9\(2\), 9\(4\), 10\(2\), 10\(5\)](#)

[Figure 6.2 Wavefunction map of HOMO of 9\(2\), 9\(4\), 10\(2\), 10\(5\)](#)

[6.5 Experimental](#)

[6.6 Calculation Details](#)

[6.7 Conclusion](#)

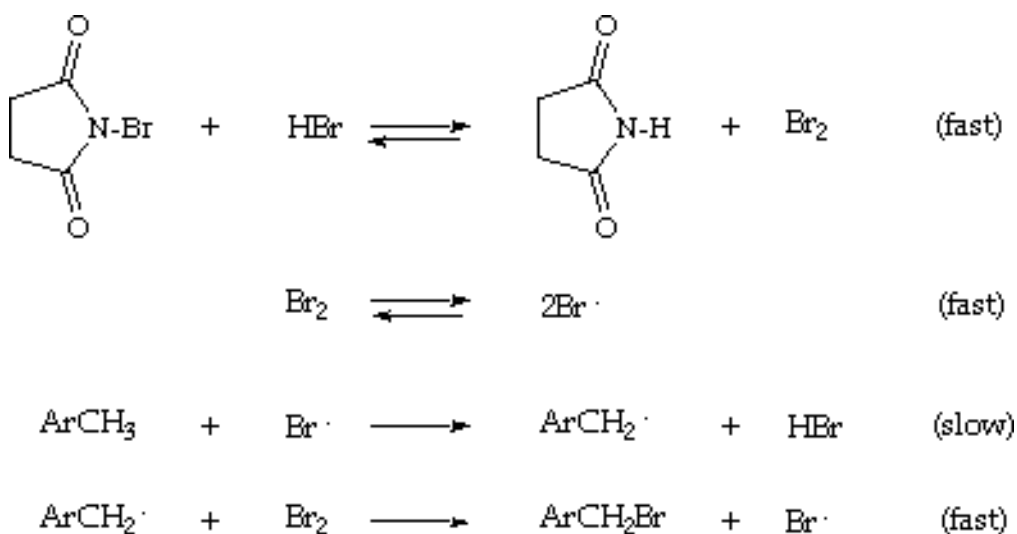
[6.8 Acknowledgments](#)

[6.9 References](#)

6.1 Introduction

The Wohl-Zeigler reaction has long been used as a general means of brominating unsaturated compounds at an allyl or aromatic methyl position [1].

This reaction is believed to take place by a free-radical mechanism [2], is generally conducted in carbon tetrachloride as a solvent, and is catalysed by light and peroxides. *N*-bromosuccinimide is used as a source of low-concentration bromine, which produces bromine radicals which initiate the reaction. [3]



Scheme 6.1: Mechanism of the Wohl-Zeigler reaction

The rate limiting step is believed to be the formation of the aromatic methylene free-radical, and the stability of this radical and the ease of breaking the carbon-hydrogen bond are crucial to the ease of bromination and the selectivity of the

reaction [4], outweighing other factors such as steric effects. The focus of the calculations presented here is on predicting the thermodynamics of this step as the best indicator of the course of the overall reaction.

The Wohl-Ziegler reaction has been used to produce intermediates for the synthesis of conformationally restricted bioactive analogues of the neurotransmitters GABA and glutamic acid [5]. In the course of the synthesis of such analogues, based on the pyridazine heterocycle, of which there were a number of examples in [Chapter 5](#), it has been found that this essential step is unreliable; unexpected products have been formed, and some compounds fail to brominate. In particular, the formation of *N*-bromomethyl derivatives of methyl pyridazinones (9,10,11) appears unprecedented. The single account found of the bromination of a similar system, 2,4-dimethyl-6-phenyl-3(2*H*)-pyridazinone, describes the formation of the 4-bromomethyl derivative [6], although the elemental analysis and infra-red spectroscopy employed to identify the product may not have detected the presence of a 2-bromomethyl substituted derivative.

The aim of this work is to study these reactions further by comparing experimental results with a variety of computational methods, and develop a convenient and preferably rapid theoretical means of predicting selectivity.

6.2 Method

In order to study the stability of the free-radical intermediates in the Wohl-Ziegler reaction by theoretical calculations, an appropriate theory and method must be chosen.

Since the reaction being considered is a neutral one, and since the solvent used is non-polar, it is a fair assumption that solvent effects will be minimal, and gas-phase calculations will reflect properties of species in solution.

Semi-empirical theories provide rapid results, which although unlikely to be quantitatively accurate, may provide useful qualitative information, especially when relative energies are compared with one another, so as to cancel out as far as

possible inherent errors. Among commonly used semi-empirical parametrisations, the PM3 Hamiltonian has previously been found to give the most reliable results for calculations on pyridazinones [7]. Here, the results of AM1, MNDO and PM3 are compared with experimental observations for all the systems studied.

High level *ab initio* calculations, while much more computationally demanding, hold the promise of definitive and quantitative results. Wong and Radom [8] suggest that large basis sets and advanced correlation methods such as UQCISD(T) are necessary for accurate descriptions of the energy barriers and enthalpies in radical reactions. Since methyl-pyridazines are relatively large molecules, such calculations are at present prohibitively expensive. *Ab initio* optimisations have been carried out on all of the systems studied, with restricted Hartree-Fock theory (RHF) for singlet species, and unrestricted Hartree-Fock theory (UHF) for doublets, using the 3-21G or 3-21G(d) basis sets. In addition, optimisations have been performed on pyridazinone systems of particular interest (9,10) with restricted open-shell Hartree-Fock theory (ROHF) and second-order Møller-Plesset perturbation theory (MP2), using the 6-31G(d) basis set.

6.3 Results

[Table 6.1](#) summarises the experimental products observed for each of the bromination reactions considered, and correlates mono-brominated derivatives with free-radical intermediates. Secondary bromination reactions, producing di-bromides as minor products, have not been considered.

[Table 6.2](#) lists the relative energies of these radicals and the heats of formation or total energies of parent species, calculated by MOPAC [11] and Gaussian [12]. Also included for reference are the same calculations performed on hydrogen bromide and bromine radicals.

[Table 6.3](#) lists the heats of reaction, calculated by subtracting the calculated energy of formation of bromine radicals from hydrogen bromide, from the calculated relative energies of the free-radical intermediates.

[Geometries](#) optimised at HF / PM3 are available in Protein Data Bank (.pdb) format.

6.4 Discussion

In the case of the methoxy pyridazines ([1](#), [2](#), [3](#), [4](#)) and pyridazine *N*-oxides ([5](#), [6](#), [7](#), [8](#)) studied experimentally, bromination of methyls ortho to the methoxy substituent is consistently favoured. Every theoretical method trialled on these systems predicted the greater stability of methylene radicals at the ortho vs. the meta position, with a typical energy difference for parallel reactions being around 1-4 Kcal. Of the semi-empirical methods, PM3 gave magnitudes for the heat of reaction in closest agreement with *ab initio* results. PM3 also gave relative radical stabilities calculated from total energies (E(R.)-E(RH)) in closest agreement with HF / 3-21G.

The chlorinated methoxy pyridazines ([2](#), [3](#), [4](#)) react normally with NBS, although a significant amount of tar is produced from [2](#) and [3](#) indicating that side-reactions are occurring. Most importantly, [3](#) is observed to react at approximately five times the rate of [2](#). This is reflected in the relatively small (1-3 Kcal) differences in the calculated heats of reaction for these species. This modest energy difference appears to be sufficient to ensure the selective bromination of [3](#) at position 5, and shows the sensitivity of this theory for predicting selectivity.

The methods trialed did not fully describe the observed failure of 3-methoxy-5-methylpyridazine *N*-oxide ([6](#)) to react in a normal fashion. The most reliable semi-empirical method, PM3, gave a larger heat of reaction for this species than for any other, although HF / 3-21G did not. Also, the reaction of [6](#) was found to be generally more unfavourable compared with [5](#) than was the case for the other parallel systems. Since ring bromination has been observed in this case, it seems likely that the methylene radical at position 4 is sufficiently high in energy for a more favoured ring radical species to be produced, possibly involving rearrangement. This hypothesis is further supported by the fact that while the calculated energetics of the more substituted [7](#) are very similar to those of [5](#) and [6](#),

traces of the 5-bromomethyl product, but no ring brominated products were observed in this case, implicating the 4-position of [6](#) in the side reaction.

The observed reactivities of the *N*-methyl pyridazinones studied ([9](#), [10](#), [11](#)) were not well reproduced, particularly by *ab initio* SCF calculations. Experimentally, the unexpected *N*-bromomethyl products were formed in all cases to some extent, and in the case of [10](#), this product predominates, although a mixture is formed. No method gave energies which entirely reflect the observed product distributions, although PM3 performs well, according to which [10\(2\)](#) and [10\(5\)](#) are very close in energy, suggesting a mixture. This method also gave good qualitative agreement with experiment for [11](#). While all SCF methods correctly predicted [9\(4\)](#) to be favoured over [9\(2\)](#), the large differences in energy observed, particularly for HF / 3-21G and HF / 6-31G(d), do not reflect the substantial proportion of the *N*-bromomethyl product formed in this reaction. On the other hand, all methods favour [9\(4\)](#) over [10\(5\)](#), as well as [11\(4\)](#) over [11\(2\)](#) and [11\(5\)](#), in agreement with experiment.

The greater ability of semiempirical methods to qualitatively predict selectivity compared with *ab initio* Hartree-Fock calculations in these cases may be attributed to the implicit consideration of electron correlation inherent in the empirical parametrisation of these methods. The post-SCF calculations performed indicate that electron correlation leads to substantially increased stability of *N*-methylene radicals. MP2 / 6-31G(d) // HF / 6-31G(d) single point energies, with or without the inclusion of zero-point energies, give [9\(2\)](#) and [10\(2\)](#) as more stable than [9\(4\)](#) and [10\(5\)](#). However, these calculations also attribute [9\(2\)](#) greater stability vs. [9\(4\)](#) than [10\(2\)](#) vs. [10\(5\)](#), in conflict with experiment. This trend appears to be reversed under geometry optimisation at MP2 / 6-31G(d), and therefore presumably an artefact of the Hartree-Fock geometry, but convergence failure for *N*-methylene radical structures has prevented inclusion of these results. It would appear likely that MP2 is overcompensating for deficiencies in the Hartree-Fock model, and higher level correlation is required.

The fact that substituting ROHF theory for UHF greatly increases the stability of *N*-methylene radicals vs. 4- or 5- methylene radicals, in closer agreement with the observed products, indicates that spin contamination may be significantly contributing to the failure of Hartree-Fock theory to model these systems. The UHF calculations show high spin contamination, and S^2 is generally within the range 0.8-1.2. UHF is known to greatly overestimate spin-polarisation, which is neglected by ROHF theory, and hence UHF may be overestimating the stability of allylic radicals of high spin polarisation. Significantly, the MP2 calculations show reduced spin contamination, concurrent with destabilisation of [9\(4\)](#) and [10\(5\)](#).

In summary, PM3 gave the best qualitative predictions of the methods trialed.

[Figure 6.1 Image and PM3 energies of 9\(2\), 9\(4\), 10\(2\), 10\(5\)](#)

[Figure 6.2 Wavefunction map of HOMO of 9\(2\), 9\(4\), 10\(2\), 10\(5\)](#)

6.5 Experimental

Method A exemplified for [9](#):

2,4-Dimethyl-6-methoxy-3(2*H*)-pyridazinone (100 mg, 0.65 mmol) ([9](#)) was dissolved in carbon tetrachloride (2 ml), and *N*-bromosuccinimide (115 mg, 1 equivalent) added. The mixture was stirred in a round-bottomed flask fitted with a reflux condenser for 30 minutes, under a high intensity light source (800W Lowel-Tota lamp). A layer of floating succinimide indicated that the reaction had proceeded.

Method B exemplified for [2](#):

3-Chloro-4-methyl-6-methoxypyridazine (3.18 g, 20 mol) ([2](#)) was dissolved in carbon tetrachloride (250 ml), and *N*-bromosuccinimide (3.60 g, 1 equivalent), and benzoyl peroxide (25 mg) were added. The mixture was stirred at reflux until no NBS remained and a layer of floating succinimide indicated completion of the reaction.

Both methods:

The reaction mixtures were allowed to cool, filtered to remove most of the succinimide and evaporated rapidly under vacuum, except in the case of the *N*-oxides, where products and starting material co-precipitated with succinimide. Instead, *N*-oxides were purified by column chromatography.

Components of the crude reaction mixtures were identified by ¹H n.m.r. spectroscopy.

Isolation of all individual products was generally not attempted since some components, particularly *N*-bromomethyl compounds, were found to be very susceptible to hydrolysis. More stable components could be separated by column chromatography on silica, eluting with ethyl acetate/toluene, dichloromethane, or dichloromethane/hexane.

Ambiguities in the interpretation of the spectra of isomeric products were resolved by a combination of derivatisation of the bromides (4, 11) or precursors (9, 10), nuclear Overhauser effect (n.O.e.) ¹H n.m.r. spectroscopy experiments (1, 4, 7, 8, 9, 10), and X-ray crystallography (11).

6.6 Calculation Details

Structures were initially modelled using Chem-X [9], which, together with RasMol [10], was also used for post-calculation visualisation. Semi-empirical geometry optimisations were performed using Mopac 6.0 [11]. The gradient norm (GNORM) requirement was set at 0.01 throughout, and the SCF criterion (SCFCRT) was set at 10⁻⁶. *Ab initio* geometry optimisations were performed using Gaussian 92/DFT for Windows, Gaussian 94/DFT for Windows, and Gaussian 94 [12]. Symmetry was constrained to C_s for all *ab initio* calculations, other than 9(2) and 10(2), where a slightly pyramidal N-CH₂ (dihedral angles ~ 10°) induced a loss of symmetry with 6-31G(d) basis set. Minima up to HF / 6-31G(d) were checked with analytical frequency calculations. Polarisation (d) functions were added to the 3-21G basis set for chlorine atoms only. RHF and UHF theories were used for the calculation of

singlet and doublet species respectively throughout, except where ROHF is specified for doublets. The platforms used were an Intel Pentium 66 with 16 Mb RAM and 800 Mb scratch space under Windows 3.1, an IBM RS/6000 with 24 Mb RAM and 1.8 Gb scratch space under AIX 3.2, and a Silicon Graphics Power Challenge with 8 R8000 processors under IRIX 6.2.

6.7 Conclusion

The selectivity of free-radical brominations of methyl 3-methoxy-pyridazine derivatives via the Wohl-Ziegler reaction is confirmed to be related to the stability of the free-radicals formed in the rate-limiting step.

Studying these intermediates is difficult experimentally, but is amenable to theoretical calculations.

Semi-empirical calculations using the PM3 Hamiltonian generally give relative energies which qualitatively reproduce the selectivities observed experimentally. Thus, a rapid method for predicting the selectivity of these reactions has been found. This technique has application to the syntheses of novel heterocyclic neurotransmitter analogues.

Small to moderate basis set *ab initio* Hartree-Fock calculations do not reproduce experimental trends reliably, particularly with respect to the pyridazinones studied. Spin contamination is high for these systems. MP2 theory performs better, but appears to over-correct HF deficiencies. Higher level calculations incorporating large basis sets and further electron configuration interaction may be necessary for quantitative results.

6.8 Acknowledgments

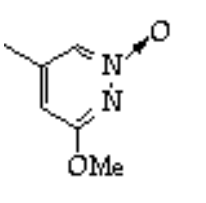
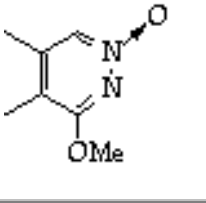
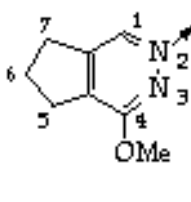
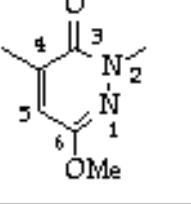
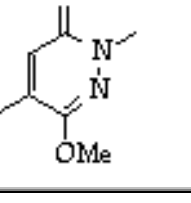
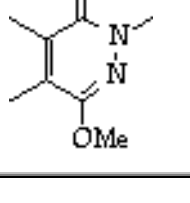
This work would not have been possible without the technical assistance of [Malcolm Gillies](#). All experimental data, summarised in [Table 6.1](#) and described in [Section 6.5](#) were provided by [Dr Ken Mewett](#) and [Dr Graziano Vaccarella](#) for compounds other than [9](#) and [10](#).

6.9 References

1. C Djerassi, *Chem. Rev.*, **43**, 271-317 (1948)
2. JK Kochi, FF Rust, *J. Am. Chem. Soc.*, **84**, 3946 (1962)
3. J Adam, PA Gosselain, P Goldfinger, *Nature*, **171**, 704 (1953)
4. CJM Stirling, *Radicals in Organic Chemistry*, *Oldbourne Chemistry Series*, 53-57 (1965)
5. T Honoré, J Lauridsen, *Acta Chem. Scand., Ser. B*, **B34**, 235-240 (1980)
6. G Leclerc, C Wermuth, *C. R. Acad. Sci. Paris, Ser. C*, **267**(19), 1242-1244 (1968)
7. WMF Fabian, *J. Computational Chem.*, **12**, 17-35 (1991)
8. MW Wong, L Radom, *J. Phys. Chem.*, **99**, 8582-8588 (1995)
9. *CHEM-X* (PC and Macintosh versions). Chemical Design Ltd. Oxford UK (April 1995)
10. *RasMol* Version 2.6. for Windows, R Sayle, Glaxo Wellcome Research and Development, Stevenage, Hertfordshire, U.K. (1995)
11. NE Heimer, JT Swanson, JP Stewart, *MOPAC: Protected Mode Version 6.0* for IBM. Frank J. Seiler Research Laboratory. U.S. Air Force Academy. Colorado Springs, Colorado. 80840. USA (1993)
12. *Gaussian 94*, Gaussian Inc. Carnegie Office Park, Building 6. Pittsburg, PA 15106 USA.
13. G Vaccarella, RD Allan, unpublished data; G Vaccarella, *Synthesis and Activity of Pyridazine Analogues of Glutamic Acid*, PhD thesis, Department of Pharmacology, University of Sydney (1998)
14. KN Mewett, RD Allan, Department of Pharmacology, University of Sydney, unpublished data
15. JR Greenwood, RD Allan, Department of Pharmacology, University of Sydney, unpublished data (Ibid. [Chapter 5](#))

Table 6.1. Summary of the experimental products of bromination reactions

No	Structure	Method	Products ^a	Ratio (%)	Radical Intermediate	Reference
1		A	starting material	-		
			4	80	1(4)	[14]
			5	15	1(5)	
2		B ^b	starting material	22		
			4	15	2(4)	[14]
			4,4	16		
			^c			
3		B ^b	starting material	38		
			5	36	3(5)	[14]
			5,5	26		
4		A	starting material	11		
			4	10	4(4)	[14]
			5	79	4(5)	
5		B	starting material	10		
			4	60-70	5(4)	[14]
			4,4	10		

6		B	starting material	10		
			5	- ^d	6(5)	[14]
7		A	starting material	12		
			4	81	7(4)	[13]
			5	4-6	7(5)	
8		A	starting material	10-15		
			5	major (~65%) ^e	8(5)	[13]
			7	-	8(7)	
9		A	starting material	23		
			2	21	9(2)	[15]
			4	38	9(4)	
			2,4	10		
			4,4	8		
10		A	starting material	8-12		
			2	48 ^e	10(2)	[15]
			5	8-10	10(5)	
			2,2	6		
			2,5	6		
11		A	starting material	12		
			2	5-8	11(2)	[13]
			4	65	11(4)	
			5	4-6	11(5)	
			polybromo	12-17		

Notes:

^a Reaction products as determined by ¹H NMR; position of mono- or di- bromo methyls

^b (2) NBS consumed in 96 hours; (3) NBS consumed in 18 hours

^c substantial (~ 45%) degradation products

^d ring substitution, polymerization with heating

^e unstable to air/moisture

Table 6.2: Energies relative to singlet species (and heats of formation or total energies)

$H_f - H_f[\text{RH}]$ ($H_f[\text{RH}]$) MOPAC, Kcal/mol

$E - E[\text{RH}]$ ($E[\text{RH}]$) Gaussian, Hartree

Reactant	Product	Method								
		HF / AM1	HF / MNDO	HF / PM3	HF / 3-21G(d)	ROHF / 3-21G(d)	HF / 6-31G(d)	ROHF / 6-31G(d)	MP2 / 6-31G(d) // HF / 6-31G(d)	Best ^a
	HBr	0 (-10.50)	0 (3.64)	0 (5.31)	0 (-2560.62078)	0 (-2560.62078)	0 (-2570.46555)	0 (-2570.46555)	0 (-2570.58099)	0 (-2570.57462)
Br.		37.24	23.10	21.43	0.58016	0.58022	0.59910	0.60259	0.62516	0.61878
1		0 (2.40)	0 (-14.44)	0 (-1.44)	0 (-415.11051)					
	1(4)	24.10	19.88	25.71	0.59637					
	1(5)	25.33	21.15	27.00	0.60131					
2		0 (4.34)	0 (-15.66)	0 (0.19)	0 (-870.06901)					
	2(4)	25.39	21.25	26.36	0.60085					
3		0 (4.81)	0 (-15.31)	0 (1.44)	0 (-870.06918)					
	3(5)	23.87	19.89	25.28	0.59571					
4		0 (-1.70)	0 (-19.26)	0 (-7.07)	0 (-908.89074)					
	4(4)	24.68	20.39	27.27	0.59872					
	4(5)	23.93	19.52	25.49	0.59621					
5		0 (27.47)	0 (6.21)	0 (2.34)	0 (-487.61144)					
	5(4)	17.51	12.14	25.39	0.57142					
6		0 (26.51)	0 (6.18)	0 (0.45)	0 (-487.61112)					
	6(5)	22.52	15.11	28.85	0.58459					
7		0 (20.13)	0 (1.67)	0 (-6.40)	0 (-526.43421)					
	7(4)	17.48	11.11	25.32	0.57204					
	7(5)	22.01	15.01	28.68	0.58507					
8		0 (25.94)	0 (-0.32)	0 (-0.62)	0 (-564.08960)					
	8(5)	16.36	9.37	21.16	0.57181					
	8(7)	20.21	12.55	23.42	0.58180					
9		0 (-18.99)	0 (-45.37)	0 (-37.70)	0 (-526.54045)	0 (-526.54045)	0 (-529.49803)	0 (-529.49803)	0 (-531.06189)	0 (-530.87845)
	9(2)	25.23	24.77	25.83	0.62109	0.62879	0.62536	0.63115	0.65986	0.64285
	9(4)	20.79	17.75	22.32	0.59801	0.62423	0.60322	0.62663	0.66154	0.64526
10		0 (-18.99)	0 (-44.95)	0 (-37.00)	0 (-526.53879)	0 (-526.53879)	0 (-529.49644)	0 (-529.49644)	0 (-531.06018)	0 (-530.876750)
	10(2)	25.59	24.81	25.92	0.62114	0.62875	0.62540	0.63112	0.66111	0.64412
	10(5)	24.84	20.37	25.83	0.60339	0.62532	0.60716	0.62751	0.66247	0.64624
11		0 (-24.61)	0 (-48.47)	0 (-44.38)	0 (-565.36271)					
	11(2)	24.32	24.82	25.91	0.62101					
	11(4)	19.93	18.01	20.82	0.59654					
	11(5)	22.61	19.05	24.66	0.60155					

^a Best energy = ZPE(HF / 6-31G(d)) + E(MP2 / 6-31G(d) // HF / 6-31G(d))

Table 6.3: Heats of Reaction (Kcal/mol)
E(R.) + E(HBr) - E(RH) - E(Br.)

Reactant	Product	Method								
		HF / AM1	HF / MNDO	HF / PM3	HF / 3-21G (d)	ROHF / 3-21G(d)	HF / 6-31G(d)	ROHF / 6-31G(d)	MP2 / 6-31G(d) // HF / 6-31G(d)	Best ^a
1	1(4)	-13.14	-3.22	4.28	10.17					
	1(5)	-11.91	-1.95	5.57	13.27					
2	2(4)	-11.85	-1.85	4.93	12.98					
	3(5)	-13.37	-3.21	3.85	9.76					
4	4(4)	-12.56	-2.71	5.85	11.64					
	4(5)	-13.31	-3.58	4.06	10.07					
5	5(4)	-19.73	-10.96	3.96	-5.48					
	6(5)	-14.73	-7.99	7.42	2.77					
7	7(4)	-19.77	-11.99	3.89	-5.1					
	7(5)	-15.23	-8.09	7.25	3.08					
8	8(5)	-20.89	-13.73	-0.27	-5.24					
	8(7)	-17.03	-10.55	1.99	1.03					
9	9(2)	-12.01	1.67	4.41	25.68	30.48	16.55	18.42	21.77	15.1
	9(4)	-16.45	-5.35	0.89	11.2	27.61	2.59	15.09	22.83	16.62
10	10(2)	-11.65	1.71	4.49	25.72	30.45	16.6	18.44	22.56	15.9
	10(5)	-12.4	-2.73	4.4	14.58	28.3	5.06	15.64	23.41	17.23
11	11(2)	-12.92	1.73	4.48	25.63					
	11(4)	-17.31	-5.09	-0.61	10.28					
	11(5)	-14.63	-4.05	3.23	13.42					

^a Best energy = ZPE(HF / 6-31G(d)) + E(MP2 / 6-31G(d) // HF / 6-31G(d))

Figure 6.1 Image and PM3 energies of 9(2), 9(4), 10(2), 10(5)

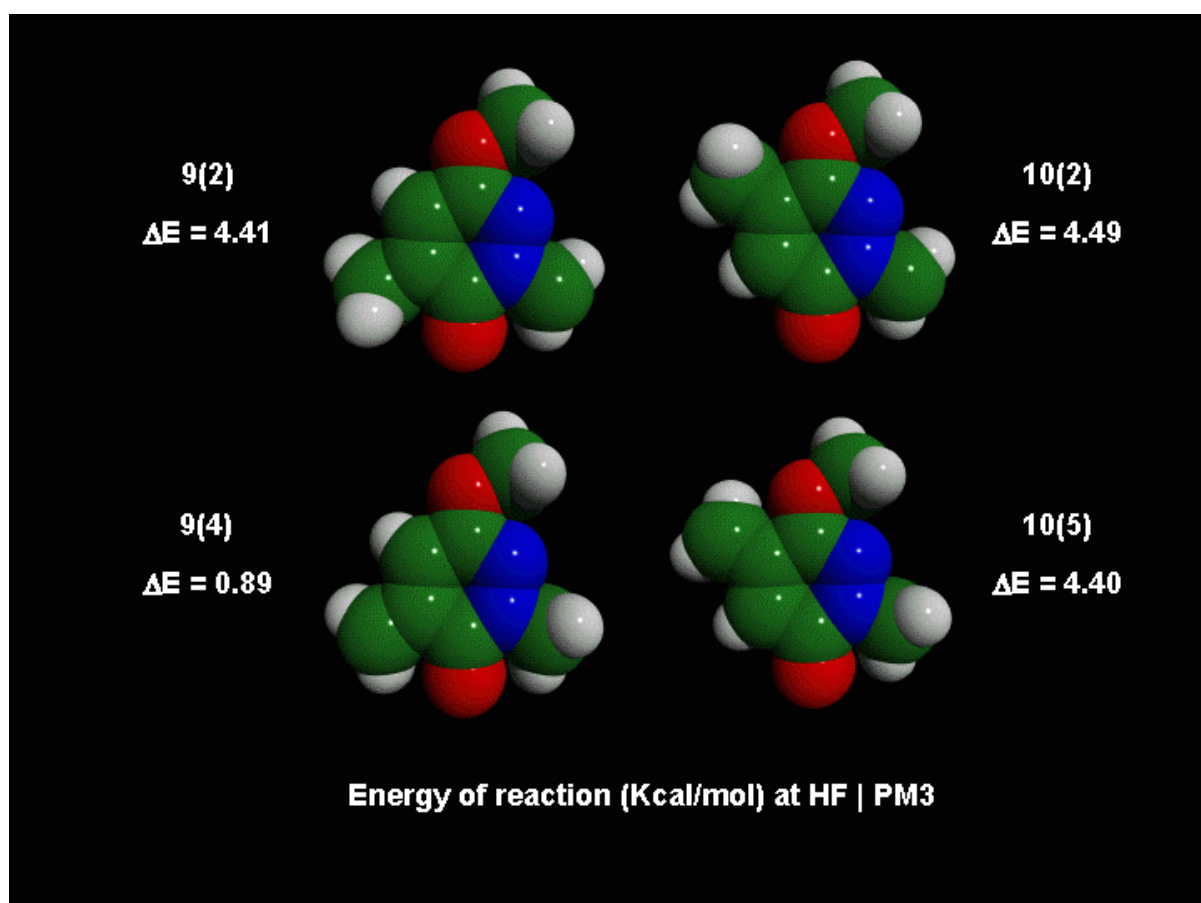
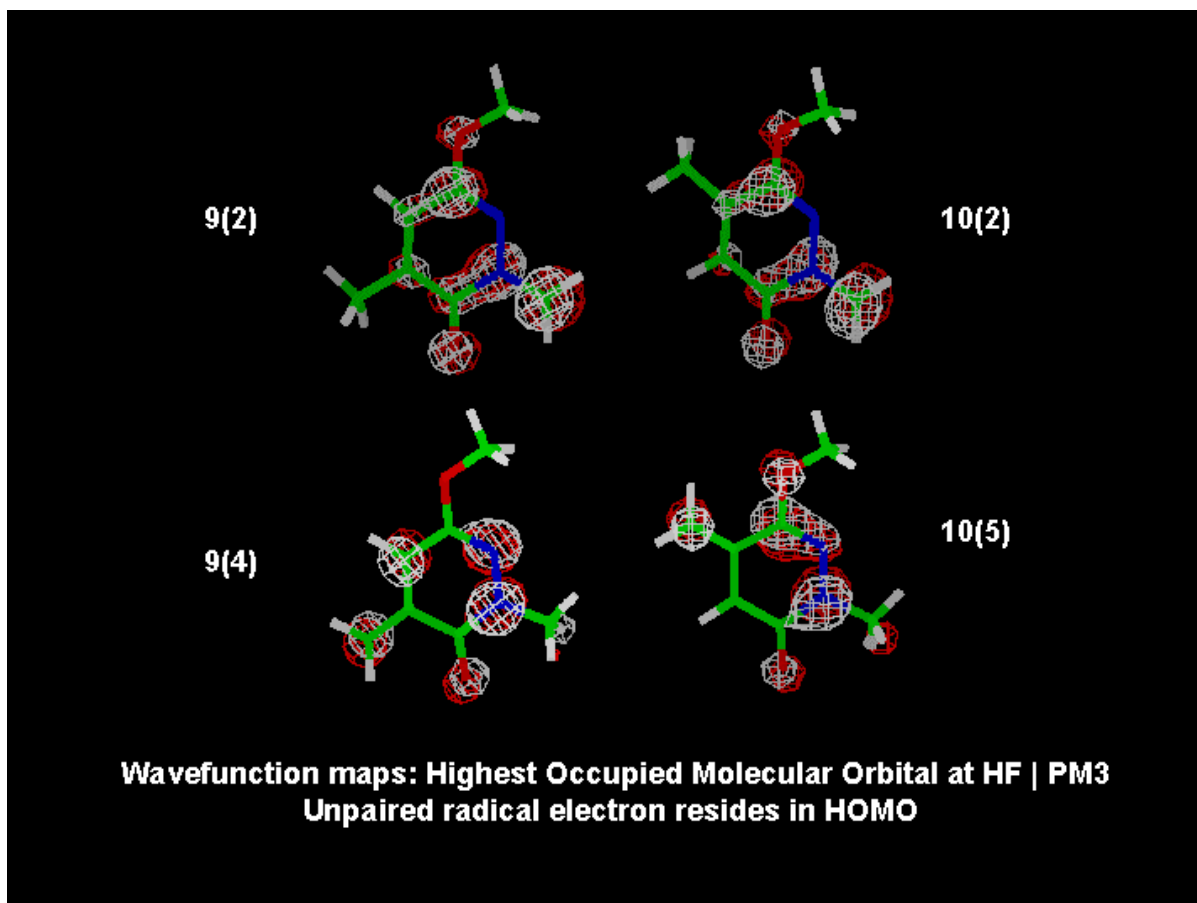


Figure 6.2 Wavefunction map of HOMO of 9(2), 9(4), 10(2), 10(5)



Chapter 6. pdb files of structures, optimised at HF / PM3

[1.pdb](#)

3-methoxy-4,5-dimethyl-pyridazine

[1\(4\).pdb](#)

4-methylene radical

[1\(5\).pdb](#)

5-methylene radical

[2.pdb](#)

3-chloro-4-methyl-6-methoxy-pyridazine

[2\(4\).pdb](#)

4-methylene radical

[3.pdb](#)

3-chloro-5-methyl-6-methoxy-pyridazine

[3\(5\).pdb](#)

5-methylene radical

[4.pdb](#)

3-chloro-4,5-dimethyl-6-methoxy-pyridazine

[4\(4\).pdb](#)

4-methylene radical

[4\(5\).pdb](#)

5-methylene radical

[5.pdb](#)

3-methoxy-4-methyl-pyridazine 1-oxide

[5\(4\).pdb](#)

4-methylene radical

[6.pdb](#)

3-methoxy-5-methyl-pyridazine 1-oxide

[6\(5\).pdb](#)

5-methylene radical

[7.pdb](#)

3-methoxy-4,5-dimethyl-pyridazine 1-oxide

[7\(4\).pdb](#)

4-methylene radical

[7\(5\).pdb](#)

5-methylene radical

[8.pdb](#)

3-methoxy-6,7-dihydro-5*H*-cyclopenta[d]pyridazine 1-oxide

[8\(5\).pdb](#)

5-methylene radical

[8\(7\).pdb](#)

7-methylene radical

[9.pdb](#)

2,4-dimethyl-6-methoxy-3(2*H*)-pyridazinone

[9\(2\).pdb](#)

2-methylene radical

[9\(4\).pdb](#)

4-methylene radical

[10.pdb](#)

2,5-dimethyl-6-methoxy-3(2*H*)-pyridazinone

[10\(2\).pdb](#)

2-methylene radical

[10\(5\).pdb](#)

5-methylene radical

[11.pdb](#)

2,4,5-trimethyl-6-methoxy-3(2*H*)-pyridazinone

[11\(2\).pdb](#)

2-methylene radical

[11\(4\).pdb](#)

4-methylene radical

[11\(5\).pdb](#)

5-methylene radical

7. Pharmacological screening *in vitro*

Abstract

The ten pyridazine-3,6-dione amino acid analogues whose design was proposed in [Chapter 4](#) and synthesis described in [Chapter 5](#) were screened for activity: three analogues [1,2,3](#) of muscimol [4](#), three analogues [5,6,7](#) of THIP [8](#), and four analogues [9,10, 11, 12](#) of AMPA [13](#) and HIBO [14](#). The muscimol and THIP analogues were screened for GABA_A activity using a guinea-pig ileum preparation, and found to be inactive. Additionally, two compounds [1](#) and [5](#) were tested for GABA_C activity at receptors expressed in *Xenopus* oocytes and found to be inactive. The glutamate analogues were tested for NMDA and AMPA activity on rat cortical wedge preparation. Compound [9](#) was found to be a weak non-specific EAA receptor agonist. Compound [10](#), although weaker still, was more specific for the AMPA receptor.

Index

[7.1 GABA_A activity: Guinea-pig isolated ileum preparation](#)

[7.1.1 Results](#)

[7.1.2 Discussion](#)

[7.1.3 Experimental](#)

[7.2 EAA activity: Cortical wedge preparation](#)

[7.2.1 Results](#)

[7.2.2 Discussion](#)

[7.2.3 Experimental](#)

[7.3 GABA_C activity](#)

[7.4 Conclusion](#)

[7.5 Acknowledgments](#)

[7.6 References](#)

7.1 GABA_A activity: Guinea-pig isolated ileum preparation

7.1.1 Results

The guinea-pig isolated ileum preparation is a standard assay for activity at the GABA_A class of GABA receptors [[1,2,3,4](#)], a receptor at which both muscimol [4](#) and THIP [8](#) are known to have high potency as agonists [[5](#)]

Compounds [1,2,3,5,6,7](#) were tested on this assay, as described in [Section 7.1.3](#), following the method described by Ong and Kerr [[4](#)] and Apostopoulos [[6](#)].

No evidence for either agonist activity of these compounds was found at a bath concentration of 1000 µM, ten times the concentration of GABA producing a maximal tissue response. No evidence of antagonist activity was found, although weak antagonist activity cannot strictly be ruled out on the basis of the experiments conducted.

Traces:

- [Trace 7.1](#) [1](#) followed by GABA
- [Trace 7.2](#) [2](#) followed by GABA
- [Trace 7.3](#) [3](#) followed by GABA
- [Trace 7.4](#) [5](#) followed by GABA
- [Trace 7.5](#) [6](#) followed by GABA
- [Trace 7.6](#) [7](#) followed by GABA
- [Trace 7.7](#) GABA followed by TACA

7.1.2 Discussion

It is concluded that these pyridazinedione analogues of muscimol [4](#) and THIP [8](#) are inactive at GABA_A receptors. The pyridazine-3,6-dione base does not mimic carboxylate at this receptor in the way that the 3-isoxazolol base does. Given that little is known about the precise environment of the GABA_A receptor, it is difficult to pin-point the reason for the loss of activity on exchange of a ring oxygen

heteroatom for a lactam. One possibility is that the pyridazine-3,6-dione is simply too large to be accommodated in the receptor. Another is that the position of the extra carbonyl group is disturbing the electronic complementarity of the ring for the receptor.

This lack of activity may be considered in the light of previous attempts to find heterocyclic carboxylate bioisosteres other than 3-isoxazoles with activity at this receptor. Close analogues of muscimol [4](#), such as dihydromuscimol [15](#) and thiomuscimol [16](#) retain moderate to high agonist potency [\[7\]](#). More substantial changes, e.g. replacing ring oxygen with nitrogen (azamuscimol [17](#)) or transposing oxygen and nitrogen (isomuscimol [18](#)) result in a considerable loss of potency [\[7\]](#).

Departing further from the isoxazole structure, is quisqualamine [19](#), which is closely related to the potent EAA agonist quisqualate [20](#), and may be considered an analogue of the weakly active homomuscimol [21](#), as well as of THIP [8](#). It is described in the Tocris Catalogue (<http://www.tocris.com>) as a weak GABA_A agonist, based on the work of Evans *et al.* [\[8\]](#), and Herrero [\[9\]](#). Quisqualamine is derived from the strongly acidic five-membered heterocycle, 2-methyl-3,5-dioxo-1,2,4-oxadiazolidine, which has structural and electronic similarity to 3-isoxazolol ([see Chapter 8](#)). It is also, like the pyridazinediones, a doubly oxygen-substituted heterocycle. A hydantoin analogue [22](#) of quisqualamine is inactive [\[7\]](#), suggesting receptor sensitivity to small changes in structure.

Another muscimol analogue with reported GABAergic activity is kojic amine [23](#), derived from the six-membered heterocycle, 3-hydroxy-4H-pyran-4-one. [\[1,10\]](#). This structure is of particular interest, because it is the only known active 6-membered hydroxy-heterocycle, and like the pyridazine-3,6-diones and quisqualamine [19](#), is doubly oxygen substituted. Little information is available about this compound; it is unknown whether its activity is sensitive to bicuculine antagonism (GABA_A). Atkinson *et al.* [\[10\]](#) report a range of modifications, all leading to a loss of activity: homologisation to the aminoethyl derivative [24](#), substitution of nitrogen for the ring oxygen forming pyridone derivatives [25](#), [26](#), and shifting the position of the hydroxyl substituent ortho- to the aminomethyl chain [27](#).

These examples serve to underscore the very particular and still poorly understood requirements for carboxylate bioisosterism at the GABA_A receptor. There is considerable scope for further investigation in this area, including the incorporation of ortho- and meta- substituted dioxo-pyridazines, whose electronic and tautomeric properties were described in detail in [Chapters 2 and 3](#). In particular, the fact that kojic amine [23](#) appears to show GABAergic activity suggests that the GABA_A receptor may accommodate six-membered dioxo-heterocycles, and that such structures are worthy of further investigation.

7.1.3 Experimental

Guinea pig isolated ileum preparation, from the descriptions of Ong and Kerr [\[4\]](#) and Apostopoulos [\[6\]](#):

Three female guinea-pigs weighing 500 g, 570 g, and 660 g were killed by cervical dislocation. Segments of distal ileum approximately 3 cm in length, taken at least 10 cm from the ileo-caecal valve were removed, emptied of their contents using a syringe, and allowed to relax in Krebs solution for at least two hours at room temperature, or refrigerated overnight. When ready, the segments were mounted vertically in a 20 mL organ bath containing modified Krebs-bicarbonate solution of composition (mM): Na⁺ 151.0, K⁺ 4.6, Mg²⁺ 0.6, Ca²⁺ 2.5, Cl⁻ 134.9, HCO₃⁻ 24.9, H₂PO₄⁻ 1.3, SO₄²⁻ 0.6, glucose 7.7, (pH 7.4 at 35°C). The Krebs solution was continuously gassed with a mixture of 95% O₂ and 5% CO₂.

The effects of drug treatments were examined on resting tissue. Isotonic contractions of the longitudinal muscle were recorded using a Curken polygraph recorder. Tissues were placed under a resting tension of 1g and left to equilibrate for 30 - 60 min before drugs were applied. A standard solution of GABA, 2 mg/mL was used to test the tissue, a 100 µL injection corresponding to a bath concentration of 100 µM, and producing a rapid spontaneous contraction, followed by relaxation. The potent GABA_A agonist, trans-4-aminocrotonic acid (TACA) 20 mg/mL, 100 µL, 1000 µM bath concentration, was tested for comparison.

Tissue response to known agonists having been established, [1,2,3](#) and [5,6,7](#) were tested at least 3 times on separate preparations in the following manner: 100 μ L of a 200 mM solution was injected, for a bath concentration of 1000 μ M. After 3 minutes, 100 μ M GABA solution was introduced, the response recorded, and the preparation washed twice and allowed to re-equilibrate for at least 10 minutes. In this fashion, test compounds were rapidly screened for agonist activity, and also for any indication of potent antagonist activity.

7.2 EAA activity: Cortical wedge preparation

7.2.1 Results

A standard assay for activity at NMDA and AMPA classes of EAA receptors is the cortical wedge preparation [[11,12](#)].

Compounds [9,10,11,12](#) were tested on this assay, as described in [Section 7.2.3](#)

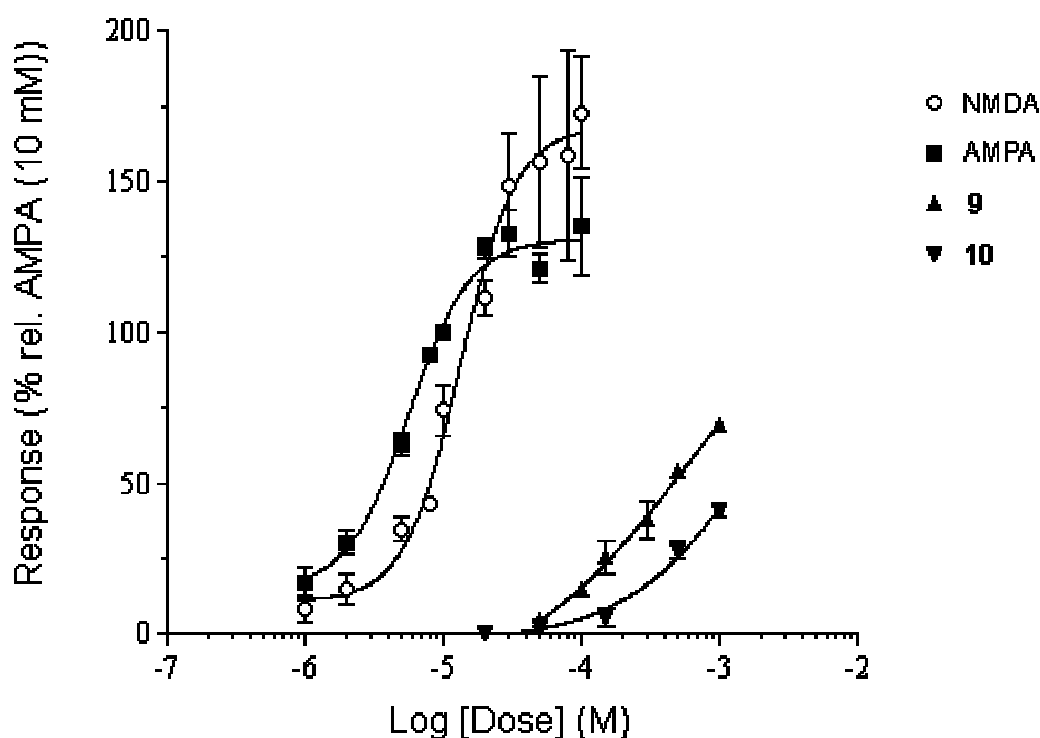
Compound [12](#) showed no agonist response at concentrations up to 1000 μ M, nor inhibition of 10 μ M NMDA or 5 μ M AMPA responses at 500 μ M, and is concluded to be without activity.

Compound [11](#) caused a slight attenuation in spontaneous activity of the wedge at 1000 μ M, but this effect on spontaneous activity was sufficiently weak as to be unquantifiable. No antagonist activity was observed, and the substance is presumed to be without significant activity.

Compound [9](#) was found to be a weak non-specific EAA agonist. At 500 μ M, its activity was almost completely blocked by 10 μ M CPP, and attenuated by 5 μ M CNQX, potent and selective antagonists for NMDA and AMPA respectively. An EC_{50} value of 481 μ M was determined for [9](#). It was not found to decrease tissue response to AMPA or NMDA, except in as much as it appeared to be cumulatively toxic to the tissue at levels above 500 μ M. Its low activity did not allow the maximum response to be determined, but there is no clear evidence for antagonist activity based on these experiments.

Compound **10** was found also to be a very weak agonist at EAA receptors, with an EC_{50} greater than 1000 μ M. At these concentrations, lack of solubility, and toxicity to the tissue hampered investigation, as previously found with poorly active pyridazinones [13]. Its response showed little or no change with CPP (10 μ M), but was attenuated by CNQX (5 μ M), indicating greater activity at AMPA receptors compared with NMDA receptors.

Neither **9** nor **10** were capable, at the highest doses tested (1000 μ M), of producing a maximal depolarisation, compared with high doses of NMDA or AMPA.



Graph 7.1. log[Dose] - response curves for compounds **9** and **10**, compared with AMPA and NMDA (including data from Vaccarella [14])

Traces:

- [Trace 7.8](#) **9**
- [Trace 7.9](#) CPP plus **9**
- [Trace 7.10](#) CNQX plus **9**

- [Trace 7.11](#) **10**
- [Trace 7.12](#) CPP plus **10**
- [Trace 7.13](#) CNQX plus **10**

7.2.2 Discussion

The AMPA receptor structure-activity implications of the observed lack of activity of **11** and **12**, and the poor activity of **9** and **10**, are discussed in detail in [Section 8.4.3](#), in the context of modelling a range of AMPA agonists. Their activity is compared with a number of other alanino-pyridazinones in [Table 8.1](#).

The NMDA activity of **9** is worthy of note. This compound is capable of existing in two tautomeric forms in solution; which of the two predominates is not possible at present to determine. A number of other alanino-heterocycle EAA agonists having mixed AMPA / NMDA activity are known ([Table 8.1](#)), quisqualate **20** being one example. So it may simply be the case that only one of the tautomeric forms of **9** is active, and this form is of non-specific activity. On the other hand, it is possible that one tautomer is largely responsible for the NMDA activity, and the other is responsible for AMPA activity. This hypothesis is supported by the observation that the *N*-methylated **10**, with fixed position of carboxylate-like function, shows a loss of NMDA activity. It should also be noted that alanino-hydroxy heterocycles are known to have varying specificity depending on stereochemistry, and the current work has considered racemic mixtures of pyridazinediones only. The fact that the other isomer, **11**, is inactive at both AMPA and NMDA, is presumed to be a result of an unfavourable hydrophobic interaction between the *N*-methyl group and these receptors.

The lack of activity of **12** can be attributed to the unfavourable orientation of the carboxylate-like region with respect to the alanine substituent.

- [Chart 7.2](#) AMPA (**13**), AMAA (**14**), and tested glutamate analogues

7.2.3 Experimental

Rat cortical wedge preparation, following the methods described by Harrison and Simmonds [11], Allan *et al.* [12] and Apostopoulos [6]:

Slices of rat neocortex and corpus callosum were obtained from Sprague-Dawley rats weighing 200 - 300 g, as previously described [11,12]. A minimum of three preparations from each of three separate animals was used to screen for activity. Cerebral wedges were prepared and placed between layers of absorbent fibre supported on an inclined block at room temperature, superfused with a magnesium-free Krebs solution oxygenated with 95% oxygen and 5% carbon dioxide, at a rate of 1 mL / min. DC potentials between the cingulate cortex and corpus callosum were monitored by Ag / AgCl electrodes via agar / saline bridges and a high impedance DC amplifier and were displayed on a chart recorder. All compounds tested were made up in magnesium-free Krebs buffer. Testing for agonist activity involved application to the cortex for a period of one minute. Testing for antagonist activity involved application to the cortex for four minutes, followed by one minute of a solution containing the test compound plus a standard agonist (10 μ M NMDA). Testing for selectivity involved application of an antagonist compound (10 μ M CPP for NMDA receptor, 5 μ M CNQX for AMPA receptor) to the cortex for four minutes, followed by application for one minute of a solution containing the test compound plus the antagonist. With this arrangement, recording cortex against corpus callosum, activity was measured as a depolarising response (an upward deflection from the baseline in which amplitude was measured in mV). The attenuation of repetitive spontaneous discharge of the tissue was also noted as evidence of agonist activity.

7.3 GABA_C activity

Compounds **1** and **5** were tested by Dr Mary Collins on the GABA_C (ρ 1) receptor [15] expressed in *Xenopus* oocytes as part of a routine screening program at this receptor. Whereas muscimol **4** and THIP **8** are active at GABA_C, the compounds showed no activity and no further investigation was warranted.

7.4 Conclusion

The observed lack of activity at GABA_A receptors of [1,2,3](#) and [5,6,7](#) has ended the pursuit of pyridazine-3,6-diones as GABA analogues. Further attempts to find novel heterocyclic derivatives binding at GABA_A receptors would better be directed towards 6-membered structures with ortho- or meta- dioxo substitution, and hydroxy- or dioxo- 5-membered structures. The increasing range of heterocycles known to yield active AMPA analogues ([see Chapter 8](#)) provides several untested leads in this regard.

The lack of activity of [11,12](#) and poor activity of [9,10](#) at EAA receptors has contributed to abandoning the evaluation of pyridazine-3,6-diones as glutamate analogues. However, this study has taken place within the context of the evaluation of a range of pyridazinone-derived structures for EAA activity, and has assisted in leading research towards AMPA analogues with higher potencies. This research is examined in detail in [the next chapter](#).

7.5 Acknowledgments

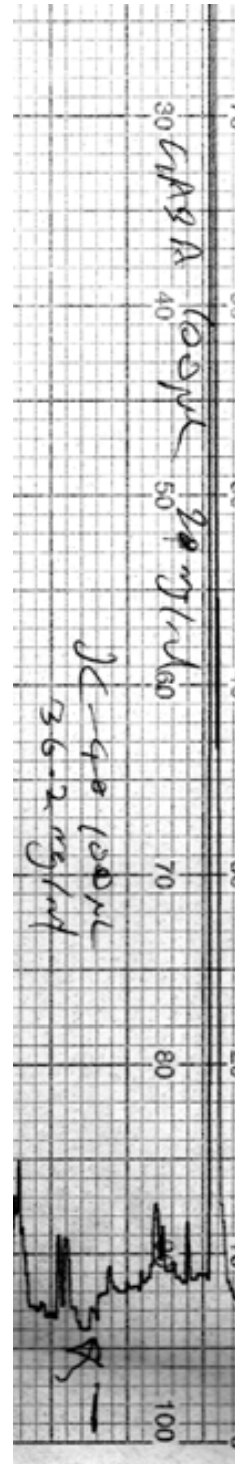
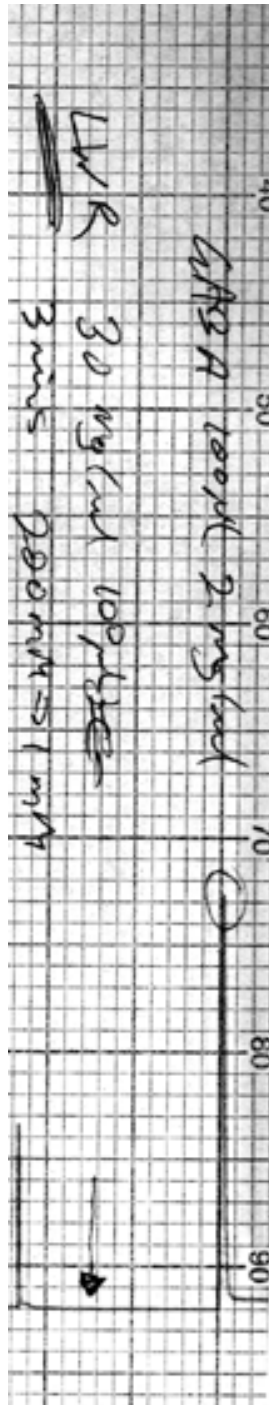
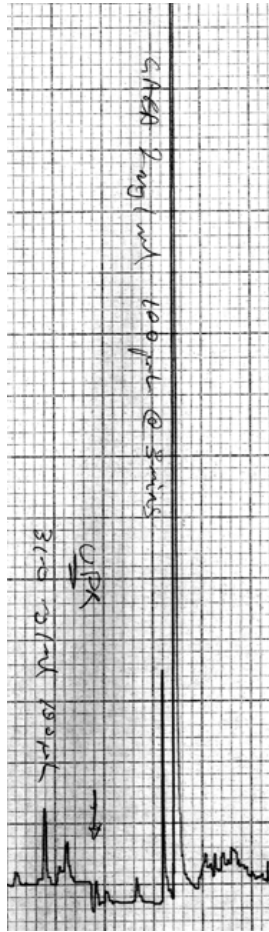
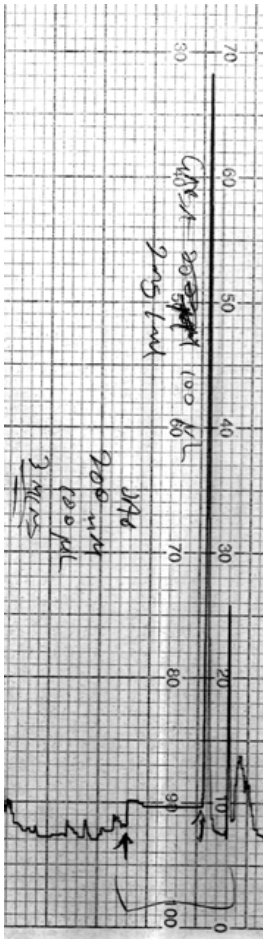
Thanks to Dr Ann Mitrovic for guidance and assistance with the cortical wedge preparation, Dr Hue Tran for guidance and assistance with the guinea pig ileum preparation, Dr Graziano Vaccarella for log[dose] - response analysis and provision of some AMPA and NMDA cortical wedge data, and Dr Mary Collins for GABA_C screening.

7.6 References

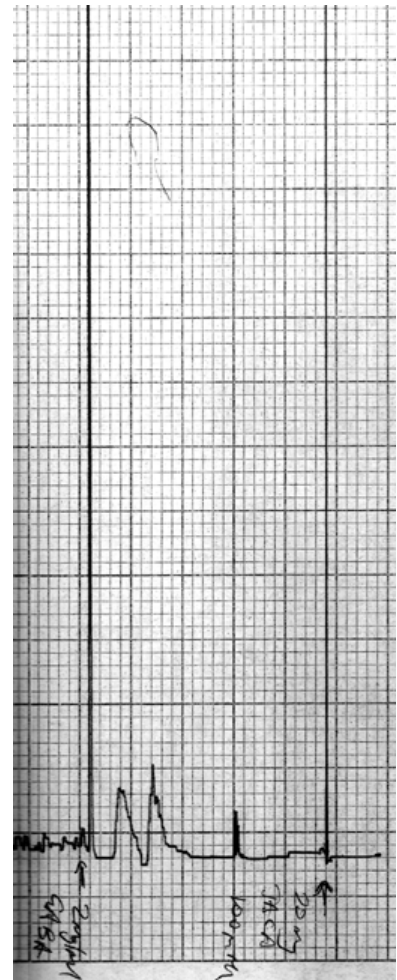
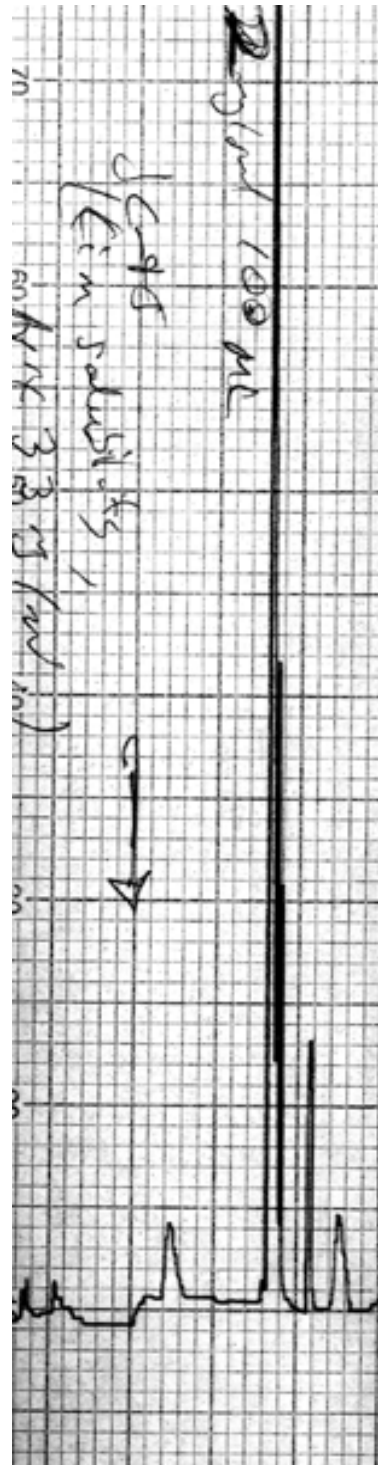
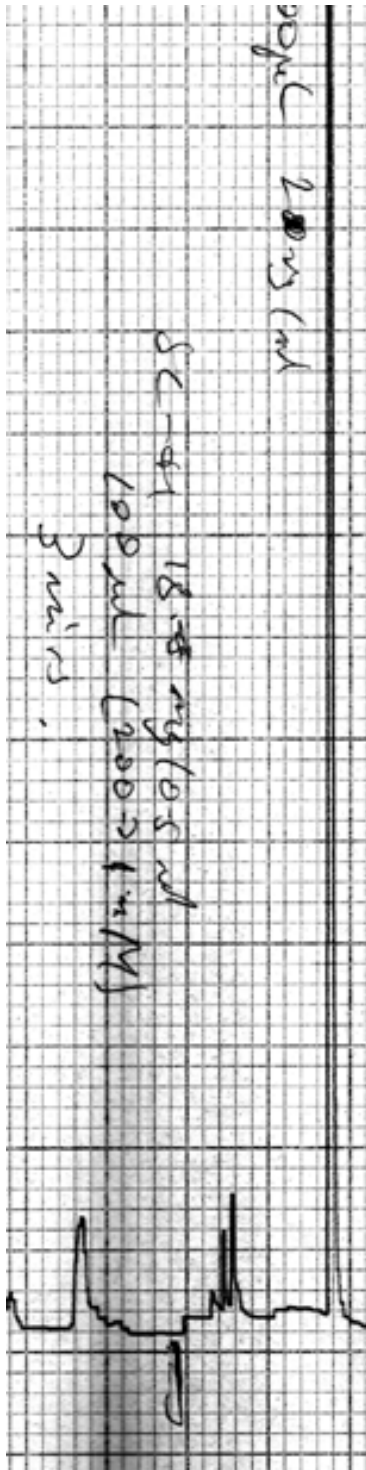
1. RD Allan, GAR Johnston, Synthetic analogues for the study of GABA as a neurotransmitter, *Medicinal Research Reviews*, **3**, 2, 91-118 (1983)
2. A Krantis, M Costa, JB Furness, J Orback, γ -Aminobutyric acid stimulates intrinsic inhibitory and excitatory nerves in the guinea-pig intestine, *Eur. J. Pharmacol.*, **67**, 461 (1980)
3. A Krantis, DIB Kerr, GABA induced excitatory responses in the guinea-pig small intestine are antagonised by bicuculine, picrotoxinin and chloride ion blockers, *Naunym-Schmiedeberg's Arch. Pharmakol.*, **317**, 257 (1981)
4. J Ong, DIB Kerr, GABA_A and GABA_B receptor-mediated modification of intestinal motility, *Eur. J. Pharmacol.*, **86**, 9-17 (1983)

5. DIB Kerr, J Ong, GABA Agonists and Antagonists, *Medicinal Research Reviews*, **12**(6), 593-636 (1992)
6. C Apostopoulos, *Medicinal Chemistry Studies of GABA_A Antagonists and Cyclic Glutamate Analogues*, PhD thesis, Department of Pharmacology, University of Sydney (1993)
7. GAR Johnston, RD Allan, SME Kennedy, B Twitchin, Systematic Study of GABA Analogues of Restricted Conformation, GABA-Neurotransmitters, *Alfred Benzon Symposium* **12**, Munksgaard (1978)
8. RH Evans, AA Francis, K Hunt, MR Martin, JC Watkins, Quisqualamine, a novel γ -aminobutyric acid (GABA)-related depressant amino acid, *J. Pharm. Pharmacol.*, **30**, 364-367 (1978)
9. JF Herrero. GABAergic activity of quisqualamine and homoquisqualamine in hemisected spinal cord *in vitro* preparation, *Revista Espanola de Fisiologia*, **50**(1), 11-18 (1994)
10. JG Atkinson, Y Girard, J Rokach, CS Rooney, CS McFarlane, A Rackham, NN Share, Kojic amine - a novel γ -aminobutyric acid analogue, *J. Med. Chem.*, **22**(1), 99-106 (1979)
11. NL Harrison, MA Simmonds, Quantitative studies on some analogues of N-methyl-D-aspartate in slices of rat cerebral cortex, *Br. J. Pharmacol.*, **84**, 381-391 (1985)
12. RD Allan, JR Hanrahan, TW Hambley, GAR Johnston, KN Mewett, AD Mitrovic, Synthesis and activity of a potent N-methyl-D-aspartic acid agonist, trans-1-aminocyclobutane-1,2-dicarboxylic acid, and related phosphinic and carboxylic acids, *J. Med. Chem.*, **33**, 2905 - 2915 (1990)
13. W Binder, *Activity of pyridazine derivatives on glutamate receptors*, Honours Thesis, Department of Pharmacology, University of Sydney (1993)
14. G Vaccarella, *Synthesis and Activity of Pyridazine Analogues of the Excitatory Neurotransmitter, Glutamic Acid*, PhD thesis, Department of Pharmacology, University of Sydney (1998).
15. GAR Johnston. GABA_C receptors relatively simple transmitter-gated ion channels? *Trends Pharmacol.Sci.*, **17**, 319-323 (1996).

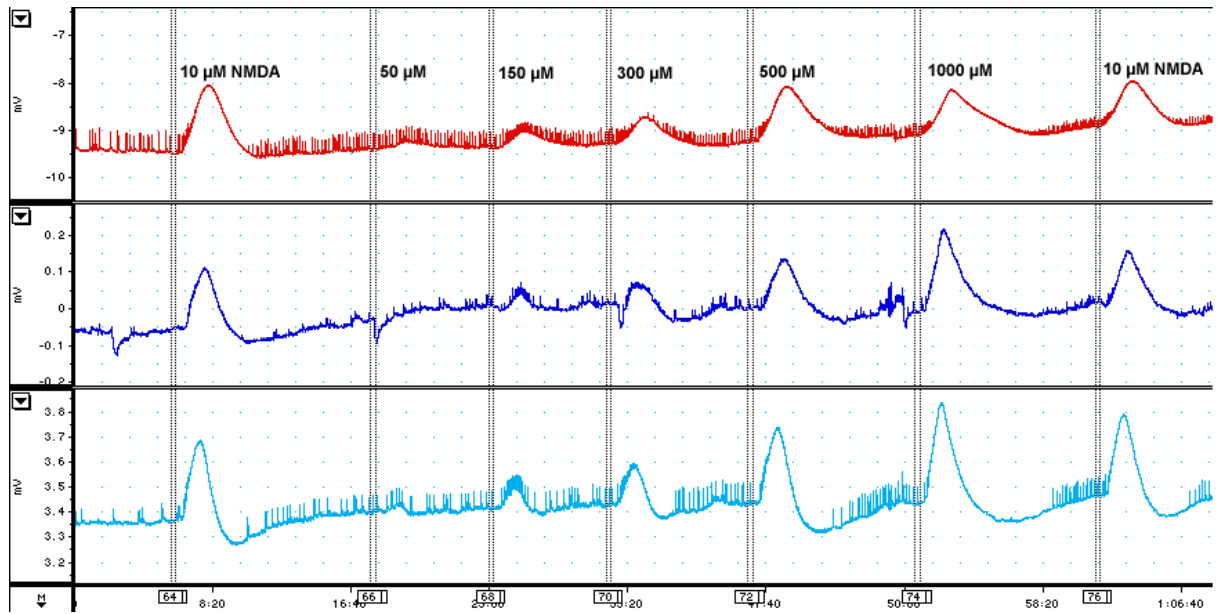
Trace 7.1 1 followed by GABA; **Trace 7.2** 2 followed by GABA;
Trace 7.3 3 followed by GABA; **Trace 7.4** 5 followed by GABA



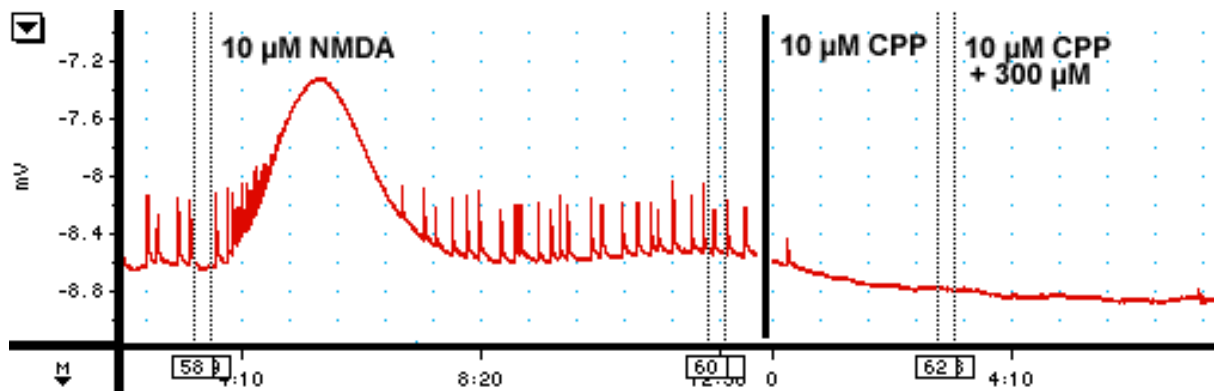
Trace 7.5 6 followed by GABA; **Trace 7.6** 7 followed by GABA;
Trace 7.7 GABA followed by TACA



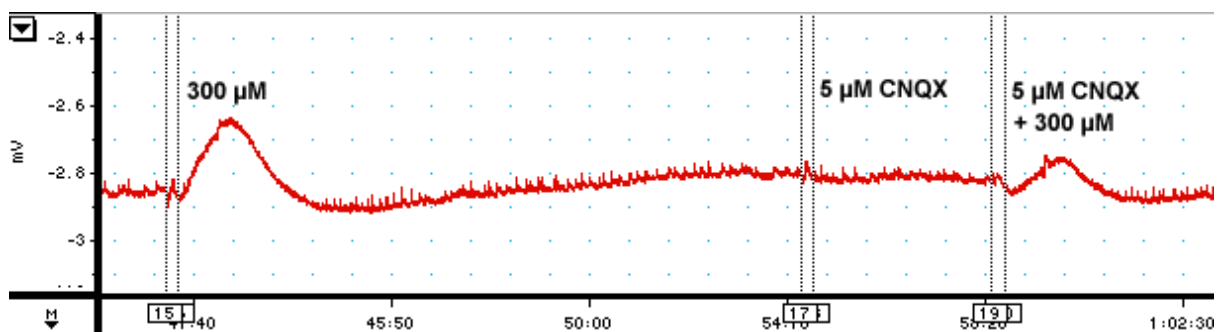
Trace 7.8 9



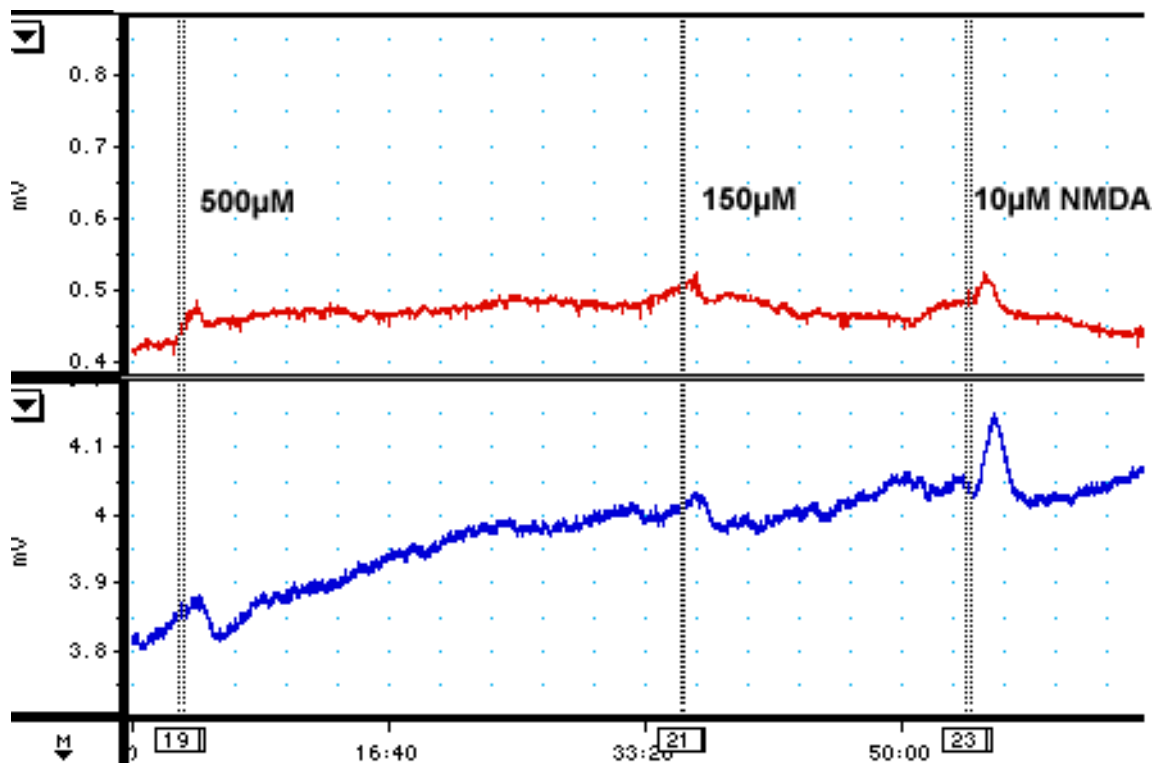
Trace 7.9 CPP plus 9



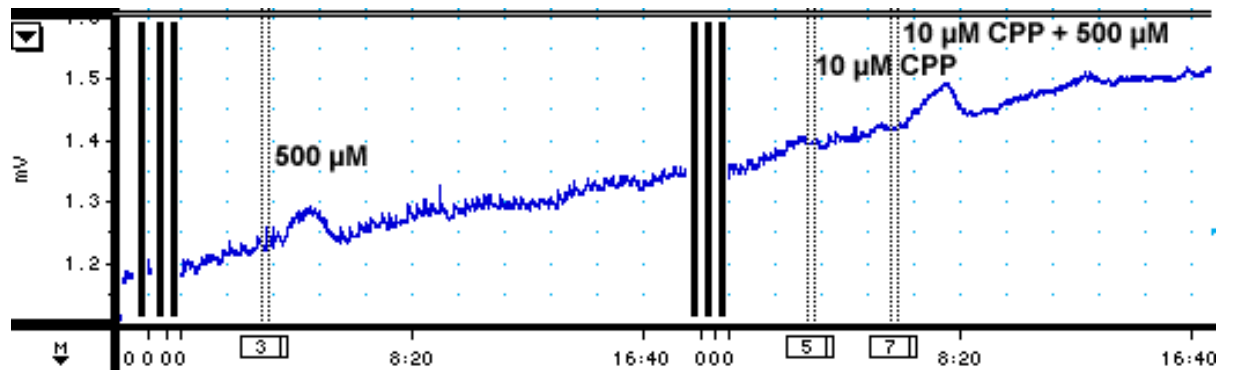
Trace 7.10 CNQX plus 9



Trace 7.11 10



Trace 7.12 CPP plus 10



Trace 7.13 CNQX plus 10

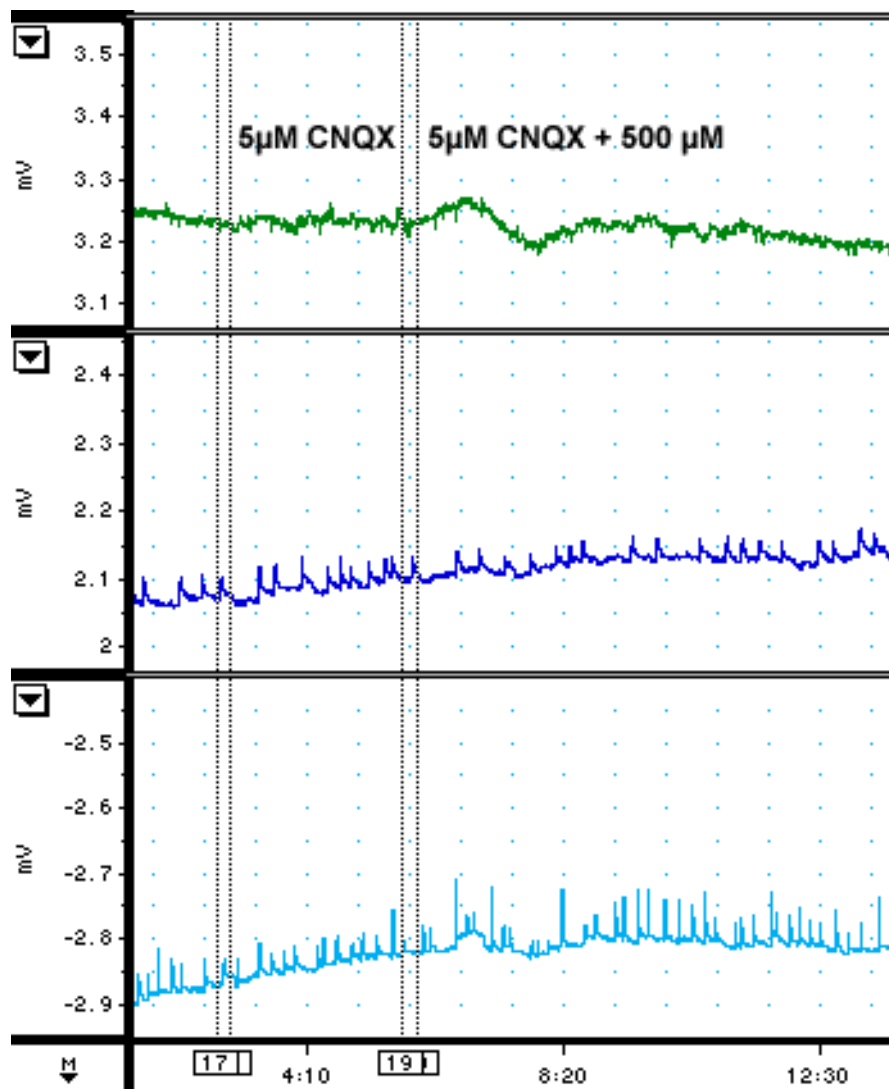


Chart 7.1 muscimol (4), THIP (8), and tested GABA analogues

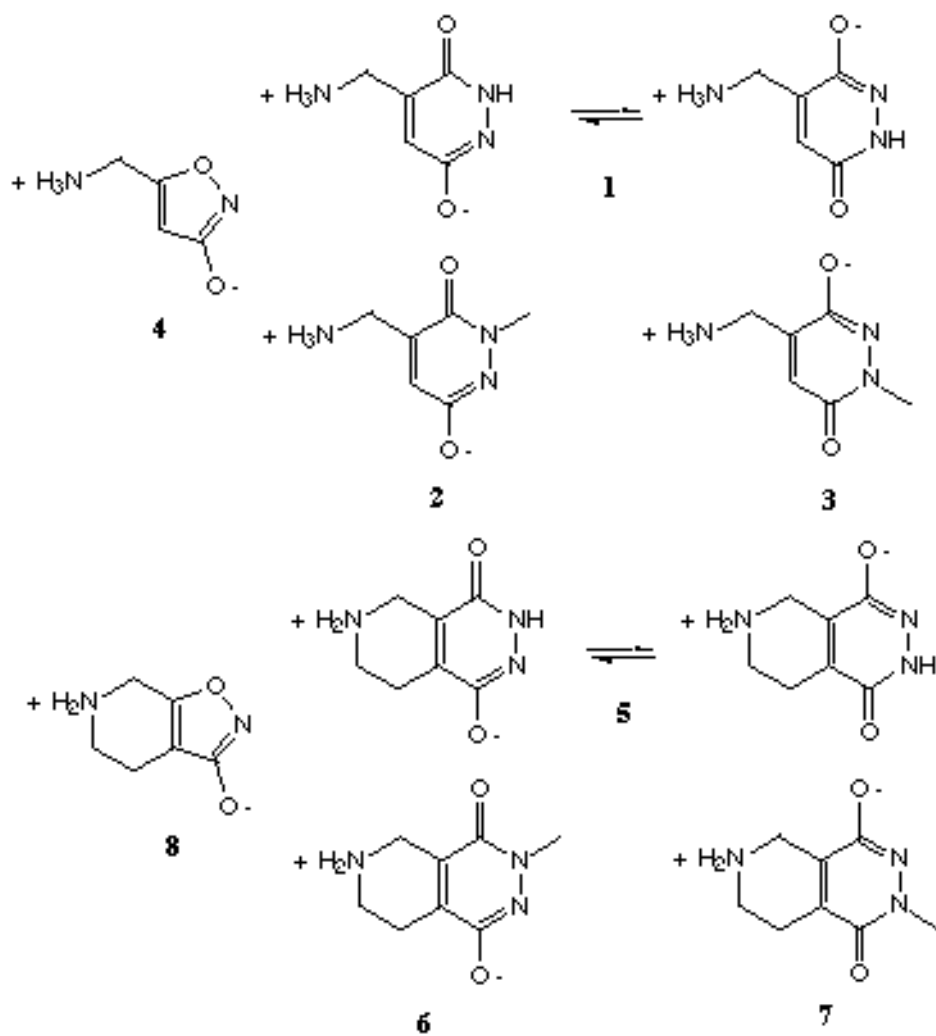


Chart 7.2 AMPA, AMAA, and glutamate analogues tested

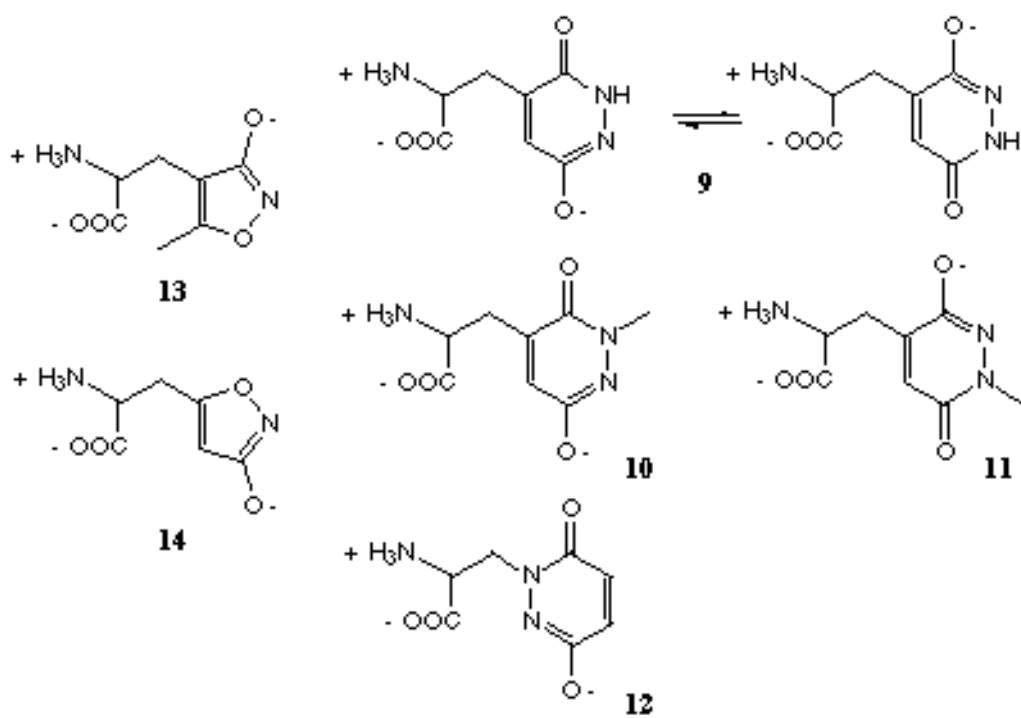
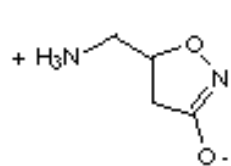
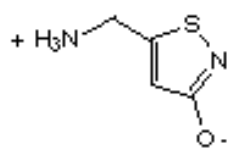


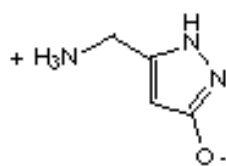
Chart 7.3 other analogues referred to



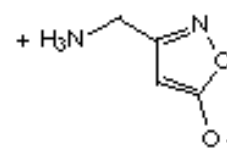
15



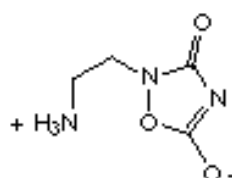
16



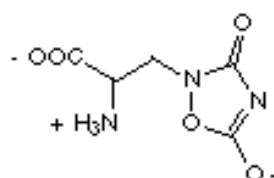
17



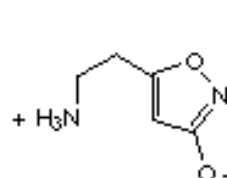
18



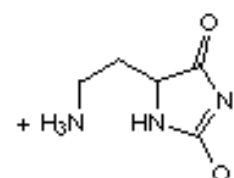
19



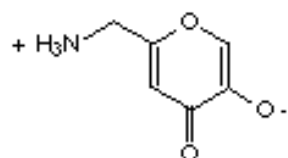
20



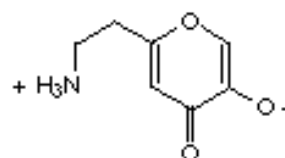
21



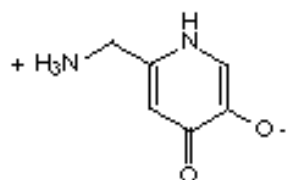
22



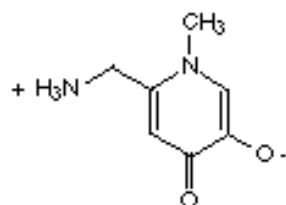
23



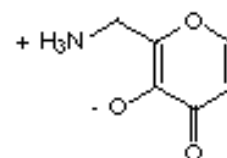
24



25



26



27

8. Heterocycles as bioisosteres for the α -carboxylate moiety of glutamate in AMPA receptor agonists: A review and theoretical study.

Abstract

(S)-2-Amino-3-(3-hydroxy-5-methylisoxazol-4-yl)propionic acid (AMPA) is the prototypical selective agonist for the AMPA subtype of excitatory amino acid (glutamate) receptors. Several 3-hydroxy-isoxazole analogues are known to have activity at this receptor, as do a number of other alanine-substituted heterocyclic phenols, the acidic heterocycles being bioisosteres for the α -carboxylate moiety of glutamate. The increasingly diverse range of known AMPA agonists is reviewed, including a number of novel pyridazine-based analogues. By removal of a common glycine unit, the parent heterocycles 3-hydroxy-4,5-dimethylisoxazole, 3-hydroxy-4,5-dimethylisothiazole, 4-methyl-5-isoxazolone, 3-hydroxy-4-methyl-1,2,5-thiadiazole, 2-methyl-3,5-dioxo-1,2,4-oxadiazolidine, 1-methyl uracil, 6-aza-1-methyl uracil, and 3-hydroxy-4-methylpyridazine 1-oxide are modelled as representative of the known α -carboxylate bioisosteres. In addition, heterocyclic fragments of inactive hydantoin and 3,5-dioxotriazole quisqualate analogues, and pyridazinone fragments with derivatives of varying potency are considered. These structures and their conjugate bases are subjected to high level *ab initio* calculations up to G2(MP2) theory, and semi-empirical aqueous phase calculations using the AM1-SM2 model. Their tautomerism and aqueous pK_a behaviour are studied in detail, and compared with experimental data. Molecular geometries and electrostatic potential-derived charge distributions are presented. Electrostatic properties at the Van der Waals surface are compared. Calculated properties are discussed with respect to structural requirements for AMPA receptor activity. Tridentate models of AMPA receptor binding are presented.

"Heterocycles as bioisosteres for the α -carboxylate moiety of glutamate in AMPA receptor agonists: A review and theoretical study" JR Greenwood, G Vaccarella, HR Capper, RD Allan, and GAR Johnston. [Internet Journal of Chemistry](#) 1, 38 (1998)

Index

8.1. Introduction

[8.1.1 Carboxylate bioisosterism and drug design](#)

[8.1.2 EAA and AMPA receptors](#)

[8.1.3 Alanino heterocycles active at AMPA receptors](#)

[8.1.4 The theoretical study of heterocycles related to AMPA receptors](#)

8.2. Methods and results

[8.2.1 Choice of model compounds](#)

[8.2.2 Structure determination](#)

[8.2.3 Gas phase thermochemistry and tautomerism](#)

[8.2.4 Point charges and dipoles](#)

[8.2.5 Aqueous phase modelling and tautomerism](#)

[8.2.6 pK_a estimation](#)

8.3. Key to tables, graphs, charts and figures

8.4. Discussion

[8.4.1 Tautomerism](#)

[8.4.2 pK_a behaviour](#)

[8.4.3 Observations on the requirements for carboxylate bioisosterism at the AMPA receptor](#)

8.5. Conclusion

8.6. Calculation details

8.7. Acknowledgements

8.8. References

8.1. Introduction

8.1.1 Carboxylate bioisosterism and drug design

The concept and study of bioisosterism is a central theme in drug design and development [1]. It has been defined as "groups of molecules which have chemical and physical similarities producing broadly similar biological properties" [2]. Both major reviews of the subject [1,2] discuss bioisosteres for carboxylic acids, and in particular 3-isoxazolols (26) as bioisosteres for the ω -carboxylate moiety of the inhibitory neurotransmitter γ -aminobutyric acid (GABA), the latter work also drawing attention to the potential carboxylate bioisosterism of 3,5-dioxo-1,2,4-oxadiazolidines (30). It is now known that both of these heterocycles, when appropriately substituted, among several others, display carboxylate bioisosterism at Excitatory Amino Acid (EAA) receptors [3,4]. The current work examines heterocyclic carboxylate bioisosterism at the AMPA subclass of EAA receptors. In particular it examines the agonist pharmacophore. The range of structures known to possess carboxylate-like properties at this receptor, as evidenced by their binding constants and potency as agonists is reviewed and expanded. Theoretical calculations on these structures are presented with a view to increasing the understanding of structure-activity relationships and aiding the design of novel ligands.

8.1.2 EAA and AMPA receptors

Glutamate is the major excitatory neurotransmitter in the brain [3]. EAA receptors, which bind (*S*)-glutamate, consist of a number of subtypes. Three main ionotropic subtypes have been classified on the basis of neurochemistry, pharmacology, and molecular biology: NMDA, AMPA, and kainate receptors. Much effort has been directed towards the production of specific ligands for these receptors, both as research tools, and as potential leads to novel therapeutic compounds for use in the treatment of disorders in which EAA receptors are believed to play a role, for example excitotoxicity caused by cerebral ischaemia, and neurodegenerative

conditions such as Huntington's Chorea, AIDS-related dementia, and schizophrenia. [4,5,6]

AMPA receptors are named after the highly selective potent agonist (*S*)-2-amino-3-(3-hydroxy-5-methylisoxazol-4-yl)propionic acid (**1a**) (Chart 8.1). This compound is a conformationally restricted analogue of glutamate, in which the acidic 3-isoxazolol heterocycle behaves as a bioisostere for the α -carboxylate moiety. An extensive and expanding series of 3-isoxazolol derivatives have subsequently been found to have agonist or antagonist activity at AMPA receptors (Table 8.1) [4].

Structure-activity studies have revealed that modifications of the α -carboxylate group of AMPA substantially reduces or abolishes activity at these receptors [3]. Likewise, little modification of the amino group is tolerated, other than incorporation into a bicyclic system. By contrast, several analogues with various heterocycle replacements for the 3-isoxazolol of AMPA retain activity. Such derivatives are a fertile area in the search for receptor characterisation tools and novel therapeutics.

8.1.3 Alanino heterocycles active as agonists at AMPA receptors

AMPA agonists of this type are alanine- and oxygen- substituted acidic heterocycles, with or without further ring substitution or other modification. The following classes are representative of the known spectrum of heterocycles from which potent AMPA receptor ligands may be formed: AMPA and derivatives (**1**), and homoibotenic acid (HIBO) and derivatives (**2**), from 3-isoxazolol; isothiazole analogues of AMPA and HIBO (**3,4** respectively), TAN-950A and its derivatives from 5-isoxazolol (**5**); LY-262466 from 3-hydroxy-1,2,5-thiadiazole (**6**); quisqualic acid from 3,5-dioxo-1,2,4-oxadiazolidine (**7**); willardiine and derivatives from uracil (**10**); 6-aza willardiine and derivatives from 6-aza uracil (**14, 15**), and 2-amino-3-(3-hydroxypyridazin-1-oxide-4-yl)propionic acid and other derivatives of 3-hydroxypyridazine (**9**). The structures of these compounds are presented in Charts 8.1 along with closely related less active or inactive heterocycles in Chart 8.2. Their

activities are summarised in [Table 8.1](#). Where possible, both binding data and electrophysiology have been included for comparison.

The lack of a single standard assay for AMPA activity across all tested structures hampers direct comparison, but qualitative trends may be perceived by comparing values obtained from different preparations, electrophysiology and binding assays.

8.1.4 The theoretical study of heterocycles related to AMPA receptors

With the fairly recent proliferation of structures tested as AMPA receptor ligands, it is of interest to make a uniform and detailed study of the various heterocycles which are now known to act as ω -carboxylate bioisosteres at this receptor. In particular, it is hoped that accurate geometrical and electrostatic data for known ligands, previously unavailable but now accessible via quantum chemical simulations, will benefit future ligand design, and lay the groundwork for modelling such as QSAR, 3D-QSAR (CoMFA) and molecular dynamics simulations.

The theoretical study of heterocycles has long been a challenge for quantum chemistry, since relatively expensive calculations involving large basis sets and thorough treatment of electron correlation are required in order to consistently treat aromatic and semi-aromatic ring atoms of unusual or variable atom hybridisation, and capable of complex tautomerism [7]. The treatment of aromatic anions is even more problematic. The study of heterocyclic tautomerism has been historically been pursued by a variety of experimental techniques on account of the major importance of heterocycles in biological systems, as well as being a rich chemical discipline in its own right [8]. This chapter employs *ab initio* gas phase molecular orbital methods in conjunction with semi-empirical aqueous phase calculations to characterise the range of heterocycles known to produce active AMPA receptor agonists. The study of tautomeric preferences, both gas and aqueous phase behaviour, pK_a , and electronic structure, are considered useful for understanding these compounds and their activity.

8.2. Methods and results

8.2.1 Choice of model compounds

In order to simplify computation, and facilitate comparison of different ω -carboxylate bioisosteres over the range of known AMPA agonists, a representative simplest set of heterocyclic structures was chosen. Removal of the α -amino acid function of prototypical ligands, that is a glycine unit, being common to all structures (1–25), leaves a series of methyl- substituted heterocycles forming such a set (26–38, neglecting some duplicate heterocycles differing only by a methyl group). This approach was originally adopted for this kind of system by Jackson *et al.* [9], to simplify theoretical comparisons between quisqualate analogues (7, 8, 9), and it is a reasonable first assumption that the removal of the glycine unit has only modest impact on the properties of the heterocyclic fragment. A similar approach (glycine or alanine removal) was recently adopted by Frydenvang *et al.* in their stimulating *ab initio* and X-ray crystallography study of 3-isoxazolol and 3-isothiazolol as carboxylate bioisosteres [10].

It is well established from pK_a data that at physiological pH, glutamate is tri-ionised [11]. The heterocyclic analogues under consideration here also appear to be predominantly tri-ionised. It cannot be said for certain that the anionic base is the heterocyclic form interacting with the AMPA receptor, since localised effects within the receptor such as desolvation in a low dielectric environment are largely unknown and a proton might be transferred to the ligand on binding. On the other hand, the variety of strong tautomeric preferences of the heterocycles under consideration would suggest that proton transfer at a particular position to an anion would be favourable for some structures but not for others.

Therefore, it is of particular interest to model the anionic conjugate bases, present in solution. It is also of interest to model the tautomerism and pK_a behaviour of the neutral conjugate acids. Regardless of the form involved in binding and activation, it is likely that transport across membranes, and hence to some extent *in vivo* activity of these amino acids depends on the neutral forms [12]. Frydenvang *et al.*

[10] emphasise the importance of the interaction between the anion and the receptor, and hence the study of pK_a .

Thus, the base of 4,5-dimethyl-3-isoxazolol ([26-](#)) is a model compound for both AMPA ([1a](#)) and its derivatives, and 4-methyl homoibotenic acid ([2b](#)) and its derivatives. The base of 4,5-dimethyl-3-isothiazolol ([27-](#)) is used as a model for isothiazole-based ligands ([3-4](#)). 4-Methyl-5-isoxazolol base ([28-](#)) represents the known 5-isoxazolol ligands ([5](#)), 3-hydroxy-4-methyl-1,2,5-thiadiazole base ([29-](#)) represents LY-262466 ([6](#)), 2-methyl-3,5-dioxo-1,2,4-oxadiazolidine base ([30-](#)) represents quisqualate ([7](#)), 1-methyl uracil base ([31-](#)) represents the willardiine series ([10,11-13](#)), 6-aza-1-methyl uracil base ([32-](#)) represents the aza willardiines ([14,15](#)) and 3-hydroxy-4-methyl-pyridazine 1-oxide base ([33-](#)) represents newly discovered ligands derived from this structure ([16-17,18](#)). In addition, we have examined a number of less active heterocyclic systems tested at AMPA receptors: the bases of 2-methyl-3,5-dioxotriazole ([34a-](#)) and 1-methyl hydantoin ([35a-](#)) representing the apparently inactive quisqualate analogues ([8-9](#)), 2,4,5-trimethyl-6-hydroxy-pyridazine-3(2*H*)-one base ([36-](#)) representing a series of weakly active analogues based on pyridazine-3,6-dione ([21-23](#)), 6-hydroxy-7-methyltetrazolo[1,5-*b*]pyridazine base ([37-](#)) for alanino heterocycles derived from this ring system ([19-20](#)), and 4,5-dimethylpyridazin-3(2*H*)-one base ([38-](#)) representing the alanino pyridazin-3(2*H*)-ones ([24-25](#)). These thirteen anionic structures are presented in [Chart 8.3](#).

Well established [[7,13,14,15,16](#)] theoretical techniques were used to model these structures as follows:

8.2.2 Structure determination

Gas-phase geometries were determined by optimisation at MP2 / 6-31G(d,p) *ab initio* theory. The structures are illustrated in [Charts 8.3](#) and [8.4](#), and have geometries as follows (.pdb format):

26-	26a	26b	
27-	27a	27b	
28-	28a	28b	28c
29-	29a	29b	29c
30-	30a	30b	30c
31-	31a	31b	31c
32-	32a	32b	32c
33-	33a	33b	33c
34a-	34b-		
35a-	35b-		
36-	36a	36b	
37-	37a	37b	
38-	38a	38b	

8.2.3 Gas phase thermochemistry and tautomerism

Optimisation and frequency calculations were performed at RHF / 6-31G(d), to calculate zero point energy and thermochemical parameters at 298.15 K, using a frequency scaling factor of 0.8929.

Single point energies were calculated at MP2 / 6-311+G(3df,2p) // MP2 / 6-31G(d,p), a large basis set, including diffuse functions for improved treatment of anions. The combination of these results with thermochemistry calculations for systems [26–33](#) are presented in [Table 8.2a](#). Relative energies of tautomers of systems [34–38](#) are discussed in [Section 8.4.1.9](#).

Single point energies were calculated at QCISD(T) / 6-311G(d,p) // MP2 / 6-31G(d,p) for anions [26-](#) to [33-](#), as well as neutral tautomers of [27](#), [28](#), [29](#), [31](#), [32](#) and [33](#). The energies at 0 K and free energies at 298.15 K according to G2(MP2) theory [14] for [27](#), [28](#), [29](#), [31](#), [32](#) and [33](#) calculated from these results are presented in [Table 8.2b](#).

Due to the expense of QCISD(T) calculations on relatively large molecules in C_1 symmetry, G2 theory energies were calculated using a double- ζ rather than triple- ζ reduced basis set, i.e. QCISD(T) / 6-31G(d,p) // MP2 / 6-31G(d,p) for some tautomers of [26](#) and [30](#). This theory is intermediate in level between G2(MP2) theory [[14](#)], and the G2(MP2, SVP) theory of Curtiss *et al.* [[17](#)]. The higher-level correction energy (HLC) for this reduced basis set has not been published, and so while [26](#) and [30](#) may be compared, having equal numbers of alpha and beta valence electrons, direct comparison with the other systems can not be made from the results presented in [Table 8.2c](#).

8.2.4 Point charges and dipoles

Gas phase point charges and dipoles derived from the molecular electrostatic potential were calculated using the Merz-Kollman-Singh scheme [[18,19](#)]. These results, as well as molecular geometries, are depicted for anions [26-](#) to [38-](#) in [Figures 8.1.26 – 8.1.38](#).

8.2.5 Aqueous phase modelling and tautomerism

The AM1-SM2 theory of Cramer and Truhlar [[20](#)] was used to predict free energies of solvation for systems [26–33](#). Whereas gas phase geometries are considered sufficiently accurate for aqueous phase calculations on neutral species, and indeed likely to yield more accurate results for unusual systems such as these due to poor AM1 geometries, the same is not necessarily true of ionic species [[16,21](#)].

Accordingly, the free energies of solvation of neutral species were calculated as single point energy differences between AM1 and AM1-SM2 theory using MP2 /6-31G(d,p) optimised geometries, whereas free energies of solvation for anions were calculated using semi-empirical geometry optimisation. These results are summarised in [Tables 8.2a – 8.2c](#).

AM1-SM2 theory was used to generate electrostatic potential contour plots in the heterocyclic ring planes, and electrostatic potential maps at the Van der Waals surface of anions [26-](#) to [38-](#), and these results are presented in [Figures 8.2.26 – 8.2.38](#).

Electrostatic potential contour plots of [26-](#) to [33-](#) calculated by this method and superimposed are depicted in [Figure 8.3](#).

Aqueous phase tautomeric behaviour of [26](#) to [38](#) is summarised in [Chart 8.4](#), as determined from theory and some experiments as discussed in [Section 8.4.1](#).

8.2.6 pK_a estimation

[Table 8.3](#) reports free energies of solvation and pK_a estimation for systems [26–33](#). Relative pK_a values, calculated entirely from theory, and corrected for 1-methyl-uracil = 9.75, are compared with an empirical pK_a determination technique [[22,23](#)], and experimental literature values for the systems under investigation, or their near analogues. Comparisons of pK_a predictions are shown in [Graphs 8.1–8.3](#). For those structures for which the pK_a is unknown experimentally, the next nearest structure's pK_a is used.

8.3. Key to tables, graphs, charts and figures

Table 8.1	Summary of AMPA analogue activities
Table 8.2	Energies and tautomerism of model heterocycles
Table 8.3	Solvation energies, pK _a predictions and literature values
Graph 8.1	Experimental pK _a s vs. <i>ab initio</i> predictions
Graph 8.2	Experimental pK _a s vs. empirical predictions
Graph 8.3	pK _a s: <i>ab initio</i> vs. empirical predictions
Chart 8.1	Structures with moderate to high potency
Chart 8.2	Structures with reduced or abolished potency
Chart 8.3	Model des-glycino heterocyclic conjugate base anions
Chart 8.4	Tautomerism of model heterocycles
Chart 8.5	The tridentate binding hypothesis of heterocycles at the AMPA receptor, illustrated for AMPA (1a) and two possible models of tridentate binding of bromo-HIBO (2c) and bromo- willardiine (10d).
Chart 8.6	A plausible tridentate binding of bromo- willardiine (10d) to the bidentate hydrogen bond donor arginine and another hydrogen bond donor. Two possible modes of binding of AMPA (1a) to the same residues, with and without the mediation of a water molecule.

Figure 8.1.26	<p>Conjugate base anions of model acidic heterocycles (26- to 38-) are presented as CPK models, with MP2/6-31G(d,p) optimised geometry. From electrostatic properties calculated at MP2/6-311+G(3df,2p)//MP2/6-31G(d,p), point charges assigned using the Merz-Kollman-Singh method [18,19] are indicated in yellow. The dipole and its magnitude calculated at this level of theory are indicated as a yellow arrow, displaced by 1.5 Å in the z- direction for visibility. The most favoured position of protonation is indicated by H⁺, and the magnitude of the point charge on the proton calculated by the above method for the neutral species indicated. The methyl group(s) at which glycine substitution results in an AMPA analogue is indicated by white GLY-, there being two such positions in the case of the isoxazol-3ol 26- and isothiazol-3ol 27-. Thio 4-methyl-homoibotenic acid is apparently unknown, although both 4-unsubstituted and 4-bromo derivatives are tested, hence 27- is taken to model both series 3 and 4, as 26- models both 1 and 2 in the present work. Similarly, 31- represents uracils 11-13 as well as 10. 32- represents aza-uracils 14 and 15. 33- may be considered as representative not only of 16a, but the analogues 16b, 17 and 18, allowing for varying position of methyl substitution. Likewise 36-, being desglycino 22b, may be taken to represent the ring structures of series 21-23, 37- to represent 19 and 20, and 38- to represent 24 and 25.</p>
Figure 8.1.27	
Figure 8.1.28	
Figure 8.1.29	
Figure 8.1.30	
Figure 8.1.31	
Figure 8.1.32	
Figure 8.1.33	
Figure 8.1.34	
Figure 8.1.35	
Figure 8.1.36	
Figure 8.1.37	
Figure 8.1.38	

<p>Figure 8.2.26</p> <p>Figure 8.2.27</p> <p>Figure 8.2.28</p> <p>Figure 8.2.29</p> <p>Figure 8.2.30</p> <p>Figure 8.2.31</p> <p>Figure 8.2.32</p> <p>Figure 8.2.33</p> <p>Figure 8.2.34</p> <p>Figure 8.2.35</p> <p>Figure 8.2.36</p> <p>Figure 8.2.37</p> <p>Figure 8.2.38</p>	<p>Conjugate base anions of model acidic heterocycles (26- to 38-), presented as wire-frame models, with MP2/6-31G(d,p) optimised geometry. The Van der Waals surface is depicted, with electrostatic potential calculated using AM1-SM2 mapped onto the surface in colour. The electrostatic potential in the plane of the ring (or near plane for puckered 30-) is shown by colour contour plot.</p>
<p>Figure 8.3</p>	<p>Conjugate base anions (26- to 33-) are overlaid such that regions of similar electrostatic potential coincide. Electrostatic potentials in the ring planes are depicted by coloured contour plot. The orientation of 26- and 27- is chosen to correspond to AMPA (1a) and thio-AMPA (3a) with respect to overlap of side chain.</p>
<p>Figure 8.4</p>	<p>1-methyl uracil anion (31-), methyl guanidinium cation (arginine fragment), and methanol (serine fragment), optimised as a complex, using AM1-SM2 theory, as a model of direct residue tridentate binding of willardiine to the AMPA receptor. Electrostatic potential is mapped on to a dot representation of the Van der Waals surface.</p>
<p>Figure 8.5</p>	<p>4,5-dimethyl-3-isoxazolol anion (26-), methyl-guanidinium cation, water, and methanol, optimised as a complex, using AM1-SM2 theory, as model of water-mediated tridentate binding of AMPA (1a) or 4-methyl-HIBO (2b)</p>

8.4. Discussion

8.4.1 Tautomerism of model heterocyclic phenols

The tautomerism of systems [26](#) to [38](#), taking into account both literature and theoretical predictions, is summarised in [Chart 8.4](#). Several of these systems, or closely related ones, have been experimentally studied by a variety of means [\[8\]](#). The predicted tautomeric behaviour from *ab initio* and semi-empirical calculations is presented in [Tables 8.2a, 8.2b and 8.2c](#). Systems [34](#) and [35](#) are exceptional, being capable of anionic tautomerism, as presented.

The significance of tautomerism to AMPA receptor binding is an open question: whether or not and at what position heterocycles might be protonated upon binding to the receptor remains unknown. The plasma form of glutamate analogues are believed to be anionic, that is immediately prior to binding, whereas neutral tautomers are probably involved in transport across membranes.

However, the study of heterocyclic tautomerism is a challenging application for theoretical chemistry in its own right. Tautomerism is complimentary to the study of pK_a . It is likely to effect *in vivo* transport behaviour of these molecules, as well as providing insight into preferred sites and strengths of hydrogen bonding interactions or protonation within the receptor.

8.4.1.1 3-hydroxy-4,5-dimethylisoxazole ([26](#))

3-Isoxazolols are widely reported to prefer a hydroxy ([26a](#)) over a keto ([26b](#)) structure, with an experimental $pK_T = -0.72 \pm 0.07$ reported for the dimethyl derivative ([26](#)) [\[8, 24\]](#), however the authors stress that this is most likely an underestimate. Woodcock *et al.* [\[25\]](#) report that the unmethylated 3-isoxazolol is favoured by 7.1 Kcal at MP4/6-31G(d,p)//3-21G, and also examine SCRF, PCM, and free energy perturbation theories as means of estimating aqueous phase properties, finding the latter two in good agreement and the former overestimating the effect of large dipole on solvation. The calculations presented here give a difference of 2.96 Kcal in favour of the hydroxy form at the highest level of theory

trialed, being the reduced-basis set G2(MP2) calculation, corresponding to $pK_T = 2.2$ in the aqueous phase. Refining these figures to G2(MP2) theory was not attempted because of the high cost of QCISD(T) calculations on C_1 symmetry structures, however better treatment of electron correlation may further lower the energy of the keto tautomer (c.f. [27](#)).

8.4.1.2 3-hydroxy-4,5-dimethylisothiazole ([27](#))

Elguero [\[8\]](#) describes the tautomerism of the parent structure, 3-hydroxyisothiazole, citing the UV and NMR studies of Chan et al. [\[26\]](#), and also SCF-LCAO calculations [\[27\]](#). The hydroxy form is claimed to be favoured in non-polar solutions, with the NH ketone becoming more prominent as the polarity increases ($K_{T(aq)} = 0.3$). The current results at G2(MP2) theory for the dimethyl derivative are in very good agreement with this data, the hydroxy form ([27a](#)) being strongly favoured in the gas phase ($K_{T(gas)} = 280$) and the two forms being very close in energy in the aqueous phase ($K_{T(aq)} = 1.5$). Of particular note is the sensitivity of geometries of both the OH and NH tautomers with respect to increased basis size, the NH tautomer ([27b](#)) preferring a puckered structure at MP2/6-31G(d,p), but a planar structure at MP2/6-311+G(3df,2p). The structural preference of both tautomers is predicted to be planar in gas phase and aqueous solution.

8.4.1.3 4-methyl-5-isoxazolone ([28](#))

The tautomerism of the 5-hydroxy isoxazoles is less clear, despite this heterocycle being heavily studied by experimental and *ab initio* methods [\[7,25\]](#). NH, (4)CH and OH tautomers must all be considered, and apparently the position of equilibrium is strongly dependent on solvent [\[8\]](#). Generally, for 5-hydroxy-isoxazoles, polar solvents tend to favour NH tautomers over CH tautomers, and the occurrence of OH tautomers is rare. However, 4- substitution decreases the stability of CH tautomers. The aqueous behaviour of the 4-methyl derivative ([28](#)) is not reported, however the presence of the NH form only ([28a](#)) is reported in aqueous sulfuric acid [\[8,28\]](#), and a mixture of [28a](#) and [28b](#) reported in cyclohexane (ratio 1:3) and chloroform. Cramer and Truhlar [\[7\]](#) provide an extensive theoretical study and

review the tautomerism of methyl- and unsubstituted 5-isoxazolones. High level calculations (up to 345 basis functions with a triple- ζ basis set, and CCSD treatment of electron correlation) were applied to the parent compound, as well as aqueous phase modelling using semi-empirical (AM1-SM2, SM1a) and cavity models. Methyl derivatives were examined using semi-empirical corrections applied to the parent compound, and **(28)** was concluded in aqueous solution to prefer the NH **(28a)** tautomer over the CH **(28b)** tautomer using AM1-SM2, and CH over NH using AM1-SM1a, with the 5-OH **(28c)** tautomer substantially less favourable. Their results are generally in accordance with known experimental trends, but doubt exists as to the tautomeric behaviour of **28**. They noted fairly poor convergence of gas phase calculations with respect to increasing levels of theory and basis size, emphasising the need for high quality calculations. The G2(MP2) calculations on **28** reported here are of comparable level to those of Cramer and Truhlar [7] on 5-hydroxy-isoxazole. Without the inclusion of higher-level electron correlation (QCISD(T)), the results suggest a mixture of all three tautomers, in proportions NH>OH>CH in aqueous phase, and CH>OH>NH in gas phase. However, at G2(MP2) theory, the OH tautomer proves substantially less favourable, in accordance with experiment. An increase in stability of the NH tautomer with respect to the CH tautomer from gas to aqueous phase is also noted, in accordance with experiment. These results suggest a mixture of tautomers in the aqueous phase, the CH tautomer being favoured by half a Kcal, within the expected error range for this method. Further experimental and theoretical work would be necessary to establish more accurately proportions of these two tautomers in aqueous solution.

8.4.1.4 3-hydroxy-4-methyl-1,2,5-thiadiazole **(29)**

There is little experimental or theoretical data available on this compound. The synthesis and pK_a of **29** are known [29,30], and the claim is made on the basis that there is no carbonyl peak observed in the IR spectrum in CHCl₃, that the preference is for a hydroxy tautomer **(29a)**. The zwitterionic (5)NH structure suggested by Elguero *et al.* [8] was found to be highly unfavourable energetically for **29** at

MP2/6-31G(d,p) (by 33 Kcal) and not considered further. The results at G2(MP2) theory support the experimental conclusion that [29a](#) is the predominant tautomer in the gas phase. However, an increase in the relative stability of the NH tautomer ([29b](#)) in water indicates that it may play a role in the aqueous behaviour of this system. Significant quantities of [29b](#) would not be expected in non-polar solution.

8.4.1.5 2-methyl-3,5-dioxo-1,2,4-oxadiazolidine ([30](#))

This unusual ring system seems to have been poorly studied, despite the well-known activity of the natural product derived from it, quisqualate ([7](#)). Jackson *et al.* [[9](#)] describe in detail X-ray crystal data of [7](#), and use [30](#) as a model for theoretical studies in a similar fashion to the present work. They describe MNDO calculations of the energy barrier of inversion of [30a](#). The current calculations support their experimental and theoretical conclusions that [30](#) prefers a non-planar structure, the substituted nitrogen being markedly pyramidal. Using reduced-basis set G2(MP2) theory, it is predicted that the dioxo tautomer [30a](#) is strongly preferred over either OH tautomers, [30b](#) and [30c](#), in gas and aqueous phases, in accordance with the X-ray crystal structure.

8.4.1.6 1-methyl uracil ([31](#))

The tautomerism of 1-methyl uracil is well studied and understood, as would be expected from its biological importance [[8,31,30,33](#)]. The dioxo tautomer [31a](#) has been firmly established as strongly preferred in solution and solid phases. The present study strongly supports only the presence of [31a](#) in appreciable quantities in the gas phase and in aqueous solution.

8.4.1.7 1-methyl 6-azauracil ([32](#))

Elguero *et al.* [[8](#)] conclude that the tautomeric behaviour of 1-methyl 6-azauracil ([32](#)) in solution closely parallels that of 1-methyl uracil ([31](#)), i.e. a preference for the 3-NH tautomer [32a](#), citing [[34](#)]. A diketo structure was proposed and the pK_a of [32](#) determined by Gut *et al.* [[35](#)]. The crystal structure of 6-azauracil is known to be a diketone [[36](#)], supporting the presence of [32a](#) in the solid phase. 6-Azauracil was the

subject of quantum chemical studies as early as 1962 [37], and was included in an *ab initio* tautomerism study [38] concluding the (3)NH tautomer to be preferred over the 4-OH tautomer in the gas phase by 10.2 Kcal/mol uncorrected. The G2(MP2) theory calculations gave a preference of 9.9 Kcal/mol for the corresponding 1-methyl structures [32a](#) vs. [32c](#). in the gas phase. Despite the fact that these aqueous calculations show substantial preferential stabilisation of hydroxy tautomers, there is no indication that any structure other than the diketo [32a](#) is present in any phase.

8.4.1.8 3-hydroxy-4-methylpyridazine 1-oxide ([33](#))

Despite the superficial similarity between [31](#) and [33](#), these two systems are found to have quite different tautomeric behaviour. The parent compound 3-hydroxypyridazine 1-oxide has been extensively studied experimentally [[39,40,41](#)]. A thorough *ab initio* investigation of this unmethylated heterocycle [[15](#)] was presented in [Chapter 2](#), supporting the 3-OH tautomer as most favoured in gas phase and in solution. The tautomerism of [33](#) is previously unexamined, although the compound is known synthetically [[42,43](#)]. It is found here to be very similar in behaviour to 3-hydroxy-pyridazine 1-oxide, i.e. that the hydroxy tautomer [33a](#) is substantially more favourable than the N-OH ([33b](#)) or NH ([33c](#)) tautomers.

8.4.1.9 Model systems [34–38](#)

Thorough analysis of the tautomerism of these structures is beyond the scope of this work. The tautomerism of the triazole [34](#) is particularly complex, and its conjugate base, [34-](#) is capable of tautomerism. The (4)NH dioxo tautomer [34a-](#) is predicted to be preferred over the (1)NH dioxo tautomer [34b-](#) by 0.99 Kcal in the gas phase at MP2/6-311+G(3df,2p)//MP2/6-31G(d,p), in accordance with the available literature [[44](#)]. Likewise, the conjugate base of the hydantoin, [35-](#), is capable of tautomerism. The (5)CH₂ dioxo tautomer [35a-](#) is favoured by 15.72 Kcal over the (5)CH, (3)NH dioxo tautomer [35b-](#) at the same level, in accordance with the literature [[8](#)]. Pyridazine-3,6-diones ([36](#)) are well known to prefer a lactam-lactim structure [[45,46](#)], as examined in detail in [Chapter 3](#), and *N*-methylation fixes the position of the ketone and hydroxy substituents. The planar hydroxy-keto form [36a](#)

is found to be preferred over the non-planar keto-keto form [36b](#) by 7.96 Kcal at MP2/6-31G(d,p). The tetrazole [37](#) would be expected by analogy to prefer a hydroxy tautomer, and this is found to be the case, the hydroxy form [37a](#) being preferred by 6.23 Kcal over the keto form [37b](#) at MP2/6-311+G(3df,2p)//MP2/6-31G(d,p). However [38](#) is believed from previous work to strongly favour the keto (2)NH tautomer [38a](#) [[46,47,48](#)], and a preference of 5.73 Kcal over [38b](#) is found at this level of theory.

8.4.2 pK_a prediction, behaviour and activity

[Table 8.3](#) compares *ab initio*, empirical, and experimental predictions of pK_a for the model compounds [26–33](#), corresponding to the ring structures known to give rise to the most potent AMPA agonists. To a certain extent, interpretation of [Table 8.3](#) is hampered by the fact that the experimental literature is incomplete with respect to pK_a determination of the compounds under investigation. Moreover, inconsistencies often occur between different methods applied to the same compound by different authors. The development of easily applied and consistent approaches to determining aqueous pK_a is an ongoing area of research.

In their extensive study of compounds from series [1–4](#), several results of which have been incorporated into [Tables 8.1](#) and [8.3](#), Matzen *et al.* [[12](#)] devoted considerable attention to determining and analysing the pK_as of these analogues. Their method of determining pK_a was ¹³C nmr titration. Their conclusion was that "no simple correlation... was apparent" between pK_a and *in vitro* activity. On the other hand, a slightly more recent theoretical paper from the same group by Frydenvang *et al.* [[10](#)] states "it appears that the difference in the acidity is the primary factor affecting the activity" of isoxazolols vs. isothiazolols. Unfortunately, it now seems that some early measurements underestimated the potency of the isothiazolols [[49](#)] and thus these conclusions may need revision. The question of the relationship between pK_a and AMPA receptor activity remains wide open.

All of the structures considered by Matzen *et al.* [[12](#)], and Frydenvang *et al.* [[10](#)] are predicted to be substantially ionised at physiological pH, the highest pK_as for amino

acids being for thio-AMPA (**3a**) and thio-ATPA (**3b**), i.e. $pK_a = 7.0$, and for heterocyclic fragments, 7.54 for 4-methyl 3-isothiazolol. This is in accordance with the hypothesis that it is the tri-ionised anionic species which proceeds to interact with the AMPA receptor. The suggestion is also made [12] that the observed disparity between trends in the *in vitro* data and the *in vivo* data (uncertainty regarding the activity of the isothiazolols notwithstanding) namely that the thio analogues are apparently more active *in vivo* as convulsants vs. the isoxazolols than would be expected from electrophysiology, is the result of the fact that compounds of higher α -carboxylate bioisostere pK_a may more easily cross lipid membrane barriers such as the blood-brain barrier (BBB), due to the greater ease of formation of neutral species. Significant proportions of the isothiazolol amino acids will be present as neutral zwitterions in plasma.

The major anomaly with respect to activity and pK_a , evident from [Tables 8.1](#) and [8.3](#), is willardiine (**10a**). Based on literature pK_a s, the heterocycle portion of willardiine is *not* expected to be substantially ionised at physiological pH. The literature pK_a of methyl-uracil (**31**) is 9.75 [50], meaning that it is not expected to ionise to a significant degree in plasma. The published pK_a s of willardiine are 9.3 or 9.97 for the ring proton, and 7.98 for the amino group [51,52]. If this is to be believed, it would indicate that the tri-ionised anion should never exist at any pH in appreciable quantities. One possible explanation is that the pK_a measurements are inaccurate, or that the order of protolysis has been confused; the pK_a of glutamate amino group being 9.7. While willardiine itself is of moderate potency, when substituted with electron withdrawing groups, the potency is greatly increased. It should also be noted that substitution of willardiine with electron withdrawing groups (**10b–10i**), which decrease pK_a , generally results in considerable increases in *in vitro* activity, with some correspondence between the degree of electron withdrawal and the activity. It may be the case then, that the ionisation of willardiine is borderline for activity, and that analogues with pK_a s above this are unlikely to be active.

At the other end of the scale, there are strongly active analogues with pK_a s around 4. Glutamate itself has a pK_a of 4.2, and aspartate 3.9. We do not yet have any indication of what the lower limit of the pK_a of the α -carboxylate bioisostere is for retaining activity.

In summary, the current results lend support to the conclusions of Matzen *et al.* [12] regarding the AMPA receptor, i.e. that no clear relationship between pK_a and activity has yet been found. Better experimental data are needed. Compounds with pK_a s between 4 and 8 are known to be active. With respect to the design of AMPA-targetted pharmaceuticals, *in vivo* activity is likely to be higher with higher pK_a ; design of a prodrug being an alternative strategy in this regard.

The claim is made of ACD/pKa [23], the empirical package used to estimate pK_a s in [Table 8.3](#), "The accuracy of calculation is usually better than ± 0.2 pK_a units (for very complex structures, better than ± 0.5)" [23]. These results, compared with experimental data, do not bear out this claim - there are substantial disparities between pK_a s predicted by this method, and experimental values, most notably for the isoxazole (26) and oxadiazole (30). Although the precise method of empirical calculation is not discussed by the manufacturer, it is clear that it is based on a database of experimental compounds. Given that every heterocycle is a new story with respect to pK_a , the poor performance of an empirical scheme for heterocycles outside its database is to be expected. The RMS deviation for the empirical method vs. experiment was found to be approximately 2.0 ([Graph 8.2](#)), allowing for incomplete experimental data. By comparison, the *ab initio* theoretical methods fare slightly worse, with an RMS value of 2.4 ([Graph 8.1](#)), and in particular do a poor job with the triazole (32). The deviation between empirical and theoretical methods is substantially poorer at 3.5 ([Graph 8.3](#)).

The fact that both empirical and theoretical methods perform particularly poorly for the oxadiazole may be attributed to the unusual character of this anion, with its clear preference for a non-aromatic non-planar structure. It should also be noted, that the authors expressed ambiguity in their experimental determination of the pK_a of quisqualate (7) by potentiometric titration [53].

To the credit of the empirical method, it is able to evaluate absolute rather than relative pK_a s, and for compounds included in its database such as 1-methyl uracil (31) the results are in good agreement with experiment, whereas theoretical technique employed is applicable only to relative estimates within a homologous series. However, neither method may be judged sufficiently reliable in order to predict pK_a data to the accuracy required for activity relationships to be determined. With regard to the theoretical calculations, the main source of error resides in the consistency of the treatment of the anions. The quoted RMS error in anion solvation by AM1-SM2 is 4.0 Kcal [54], but the relative treatments of analogous anions is probably better than this. The treatment of anionic electron rich heterocycles is known to require very large basis sets and extensive treatment of correlation; inconsistencies in this treatment across heterocycles are most likely where the bulk of the error lies. It may be hoped that as the quality of the calculations able to be performed on heterocycles of this kind increases with increased computing power, and with improved aqueous phase modelling, the theoretical approach will become more viable for the *ab initio* prediction of pK_a .

8.4.3 Observations on the requirements for π -carboxylate bioisosterism at the AMPA receptor: a tridentate model.

Being a trans-membrane protein, the 3D structure of the AMPA receptor and its agonist binding site are unlikely to be solved within the near future. Attempts to map the agonist binding site based on ligand properties must necessarily be considered speculative. Previous work on AMPA agonists has tended to consider only one or other class of heterocycles at a time. It is worthwhile making some qualitative observations here, based on the whole range of bioisosteres, in expectation of a more thorough future quantitative treatment.

Noting that known AMPA ligands (other than endogenous excitatory amino acids aspartate and glutamate) are generally heterocyclic and exhibit charge delocalisation, might suggest that a complementary receptor moiety would be a positively charged heterocycle, such as a protonated histidine residue. In addition to electrostatic interactions, such a model would suggest π - π stacking interaction

between adjacent heterocyclic rings. Preliminary studies using AM1-SM2 calculations have not shown this kind of interaction to be favourable, the histidine residue preferring to lie co-planar rather than parallel to the anionic heterocycle.

An examination of [Figures 8.2.26 – 8.2.33](#), and especially [Figure 8.3](#), being an overlay of the electrostatic potentials of these structures [26–33](#) which represent the classes of heterocyclic phenols from which the most potent AMPA agonists known are derived, indicate three main regions of electrostatic minima. Most clearly seen in [Figures 8.2.30, 8.2.31 and 8.2.33](#), are three co-linear minima near the Van der Waals surface of the heterocycles. Those active heterocycles carrying only one oxygen substituent, [26–29](#), show a deep negative potential well surrounding this atom, and a broader region in the space corresponding to the other two minima of the dioxo- heterocycles, but with steric and electrostatic properties favourable for interaction with more than one electropositive group. Proposed, therefore, is a tridentate binding model hypothesis, involving three electropositive complements, $\delta+1$, $\delta+2$ and $\delta+3$, corresponding to the three co- linear electrostatic minima observed, for example three proton interactions with the AMPA receptor (see [Chart 8.5, Chart 8.6](#)), with or without actual proton transfer to the anion. Previous authors have tended to consider only one or two points of binding interaction with the ring.

The interactions between 3- and 5-isoxazolol ions and methyl guanidinium cations (as arginine residue fragments) were studied in detail using semi-empirical methods by Boulanger *et al.* [\[55\]](#), in connection with the inhibitory GABA_A receptor, which shows many parallels with EAA receptors. Their work suggested a bidentate interaction of the GABA_A receptor with these heterocycles. A tridentate binding model at the AMPA receptor could be satisfied by an arginine as a bidentate complementary residue, and in addition a third hydrogen bond donor. A flexible, neutral hydrogen bond donor, for example serine, would accommodate both the monoxo- and dioxo- heterocycles producing powerful agonists. Another possibility which would assist in explaining both the binding of singly and doubly oxygen-substituted heterocycles is the presence or absence of a binding site water molecule mediating hydrogen bonding at position $\delta+1$. These two possibilities are illustrated

in [Chart 8.6](#). An optimised complex between [31](#)-, methyl-guanidinium, and methanol, is depicted in [Figure 8.4](#), as an example of the tridentate binding model without water mediation. [Figure 8.5](#) depicts an optimised complex between [26](#)-, methyl-guanidinium, water and methanol, an example of the water-mediated tridentate binding model. This kind of ligand-water- residue mediation of binding is well documented in other systems, e.g. the binding of dihydrofolate to dihydrofolate reductase [[56](#)].

Preliminary studies of complexes between [26–33](#) and hydrogen bond donors using geometry optimisation and AM1-SM2 theory are promising (e.g. [Figures 8.4, 8.5](#)) indicating a preference for hydrogen bonding interactions within a few degrees of the plane of the heterocyclic ring.

A binding model must not only be consistent with the activities of the closely homologous singly oxygen-substituted series [1, 3, 5, 6](#), and the doubly substituted series [7, 10, 14, 15, 16](#) and [17](#) for which an oxygen substituent lies α - to the alanino substituent, it must also be consistent with those systems for which the alanino substituent lies β - to an oxygen substituent, e.g. series [2](#) and [4](#).

[Chart 8.5](#) illustrates two possible models of the way in which these two homologies may be reconciled, namely that there are two possible orientations of the heterocyclic ring of known potent ligands which satisfy tridentate binding. Both models assume consistent (*S*) stereochemistry about the chiral centre. Model 1 places importance on the consistent interactions of δ^{+2} and δ^{+3} with strongly electronegative regions of the carboxylate bioisostere, presuming that conformational flexibility will allow the α -amino acid portion of the molecule to align with its receptor complement despite the difference in relative substitution position. Model 2 places more importance on the relative position of alanino substitution with respect to δ^{+2} and δ^{+3} , and less importance on dipole direction. [Chart 8.5](#) compares the potent agonists bromo-willardiine ([10d](#)) and bromo-HIBO ([2c](#)) with AMPA. The binding orientation of willardiines is ambiguous under Model 1, a reason to prefer Model 2; [10d](#) is depicted here with bromine substituent isosteric with that of [2c](#).

The tridentate hypothesis should also be consistent with, and assist in explaining the reduction in activity observed with other compounds in [Table 8.1](#). Firstly, the decreased electronegativity surrounding the sulfur atom in the thio- analogues of AMPA and HIBO, [3](#) and [4](#), and the decreased hydrogen bond accepting character of the isothiazoles, is consistent with the reported decrease in *in vitro* activity observed for these compounds ([Figure 8.2.27](#)). The hydantoin [9](#), although ostensibly capable of accepting three hydrogen bonds, probably owes its lack of activity to its high pK_a and hence, lack of ionisation *in vivo*, and lack of aromatic character or electron delocalisation. [8](#), While fairly acidic ($pK_a = 4.7$ [[53](#)]), prefers an anionic tautomer with a proton in position to interrupt binding ([Figure 8.2.34](#)), and a dipole in an unfavourable direction for receptor alignment ([Figure 8.1.34](#)).

The reduced activity of [18](#) vs. [17](#) and [16](#) is not necessarily expected from Model 1, but lends weight to Model 2 by confirming the importance for activity of the positioning of the α -amino acid moiety with respect to the electronegative regions of the molecule. While the activity of [17](#) is less than [16](#), it is still fairly active for a compound without hydrophobic substituent, c.f. [2b](#), [2a](#), [5a](#) *et al.*

While the tetrazoles [19](#) and [20](#) appear to potentially support tridentate interaction ([Figures 8.1.37](#), [8.2.37](#)), their activities are low. Whether this is because these bicyclic systems are approaching the size limit which may be accommodated by the AMPA receptor binding pocket, whether because of unfavourable electrostatic interaction, or because of insufficiently low pK_a , is unknown. It is worth noting that the degree of negative charge assigned to the tetrazole nitrogen attached to the pyridazine ring nitrogen from electrostatic potential derived charges ([Figure 8.1.37](#)) is substantially lower than that assigned for the homologous *N*-oxide ([Figure 8.1.33](#)). The relative positions of the alanino substituent and anionic regions of [19](#) vs. [20](#) are reflected in their activities in analogous fashion to [16b](#) vs [18](#).

The pyridazine-3,6-dione AMPA analogues, series [21–23](#), are particularly interesting illustrations of the requirements for activity. The non-*N*-methylated compounds [21a](#) and [21c](#), are weak and non-specific glutamate agonists [[67](#), [Chapter 7](#)]; two hydrogen bond acceptor regions are available in these cases, but the

presence of a protonated ring nitrogen prevents a third point of binding. Their weak activity as NMDA agonists may be related to the alternate tautomeric forms available to the anions, and may be compared with the lack of specificity of quisqualate (7). The second ring oxygen substituent, situated para- to the first, is poorly placed to interact with the AMPA receptor under the tridentate hypothesis. N-methylation para- to the alanino substituent (21b) completely abolishes activity, despite the superficial similarity between this compound and 1a, the difference being replacement of ring oxygen with methyl-lactam. This clearly indicates that the AMPA receptor cannot tolerate a hydrophobic group in this region, i.e. $\delta+1$. The low and moderate activities of 22a and 22b parallel the reduced activity of 18 vs 16b, and compared with 21b, seem to indicate a greater tolerance for hydrophobic substituents close to position $\delta+3$ than for position $\delta+1$. None the less, the potency of 22b is unexpectedly high under the present hypothesis, and may indicate some latitude of binding orientation. The orientation of the regions of electrostatic potential minima of 23 vs the location of the amino acid substituent correspond very poorly with the current models of the AMPA receptor, and unsurprisingly, this compound is without activity.

The pyridazin-3-ones 25 and particularly 24 also fit within the tridentate binding hypothesis, but show poor or nil activity. The electrostatics appear favourable (Figures 8.1.38 and 8.2.38), but most likely it is the relatively high $pK_a = 10.5$ [57] of this heterocycle which is preventing binding. It would be most interesting to examine the effect of ring substitution with an electron withdrawing group on activity. As with 18 vs. 16, shifting the position of the alanino substituent reduces activity, in this case abolishing it entirely.

8.5. Conclusion

The available literature on the activities of alanino heterocycles as agonists at the AMPA excitatory amino acid receptor has been summarised, and structure-activity data on novel pyridazinone AMPA analogues presented. This catalogue of structures is expected to continue to proliferate in the future.

Des-glycino parent heterocycles of AMPA active compounds have been modelled using high level *ab initio* gas phase and semi-empirical aqueous phase calculations. Structure, tautomerism, electrostatic properties, and pK_a behaviour have been modelled and discussed with respect to experimental literature. Neither empirical nor *ab initio* methods of pK_a determination are yet satisfactory for confident extrapolation to novel heterocycles. Models of a tridentate binding hypothesis of ω -carboxylate bioisosteres at the AMPA receptor have been presented, as a means to rationalising the whole range of alanino heterocycles known to activate the receptor.

The design of new ω -carboxylate bioisosteres based on hydroxy heterocycles should take into consideration tautomerism and pK_a behaviour such that ionisation at physiological pH is significant and structure favours hydrogen bonding interactions. The tridentate binding hypothesis suggests that the presence of steric, neutral, or positive groups in any of the three binding regions is likely to decrease potency. All known bioisosteres are five- or six-membered heterocycles possessing two or more adjacent heteroatoms, monoxo- or dioxo- substituted, with a heteroatom α - to an oxygen substituent.

8.6. Calculation details

QCISD(T) energies were calculated using Molpro 96 [58]. All other *ab initio* calculations were performed using Gaussian 94, revision D.3 [59]. AM1-SM2 calculations were performed using AMSOL 5.4 [54] and Spartan 4 [60]. Empirical pK_a estimates were calculated with ACD/pKa [23]. Platforms used were SGI R4000 O2 and SGI R10000 Power Challenge (IRIX 6.2) and IBM RS6000 (AIX 3.2). Visualisation and rendering were performed with Spartan 4, and Povray [61].

8.7. Acknowledgments

The special assistance of Povl Krogsgaard-Larsen in providing biological activity data is gratefully acknowledged. The support of the [NSW Centre for Parallel Computing](#) is also appreciated. Thanks to Chris Cramer for his advice regarding semi-empirical solvation theories.

8.8. References

1. CA Lipinski, Bioisosterism in drug design, Ch 27, *Annual reports in Medicinal Chemistry*, **21**, (1986)
2. CW Thornber, *Chem. Soc. Rev.*, **8**, 563 (1979)
3. JJ Hansen, P Krogsgaard-Larsen, *Medicinal Research Reviews*, **10**(1), 55-94 (1990)
4. P Krogsgaard-Larsen, B Ebert, TM Lund, H Bräuner-Osborne, FA Sløk, TN Johansen, L Brehm, U Madsen, *Eur. J. Med. Chem.*, **31**, 515-537 (1996).
5. MB Brennan, *Chemical and Engineering News*, May 13, (1996)
6. GJ Lees, *CNS Drugs*, Jan 5(1), (1996)
7. CJ Cramer, DG Truhlar, *J. Am. Chem. Soc.*, **115**, 8810-8817 (1993)
8. J Elguero, C Marzin, AR Katritzky, P Linda, *The Tautomerism of Heterocycles, Advances in Heterocyclic Chemistry, Supplement 1* (1976)
9. DE Jackson, BW Bycroft, TJ King, *Journal of Computer-Aided Molecular Design*, **2**, 321-328 (1988)
10. K Frydenvang, L Matzen, P-O Norrby, FA Sløk, T Liljefors, P Krogsgaard-Larsen, JW Jaroszewski, *J. Chem Soc., Perkin Trans. 2*, 1783-1791 (1997)
11. G Zubay, *Biochemistry*, Addison-Wesley Publishing Company, Inc. (1993)
12. L Matzen, A Engesgaard, B Ebert, M Didriksen, B Frølund, P Krogsgaard-Larsen, JW Jaroszewski, *J. Med. Chem.*, **40**, 520-527 (1997)
13. JB Foresman, A Frisch, *Exploring Chemistry with Electronic Structure Methods*, 2nd Edition. Gaussian Inc., (1995-6).
14. LA Curtiss, K Raghavachari, JA Pople, *J. Chem. Phys.*, **98**, 1293 (1993)
15. JR Greenwood, HR Capper, RD Allan, GAR Johnston, *Proceedings, Third Electronic Computational Chemistry Conference, J. Molec. Struct. (Theochem)* **419**, 97-111 (1997)
16. WJ Hehre, *Practical Strategies for Electronic Structure Calculations*, Wavefunction Inc., (1995)
17. LA Curtiss, PC Redfern, BJ Smith, L Radom, *J. Chem. Phys.*, **104**(13), 5148-5152 (1996)
18. BH Besler, KM Merz, Jr., PA Kollman, *J. Comp. Chem.*, **11**, 431 (1990)
19. UC Singh, PA Kollman, *J. Comp. Chem.*, **5**, 129 (1984)
20. CJ Cramer, DG Truhlar, *Science*, **256**, 213- 217 (1992)
21. CJ Cramer, Personal Communication (1996)

22. HH Jaffe, *Chem. Rev.*, **53**, 191 (1953)
23. ACD/pKa by Advanced Chemistry Labs, Inc. <http://www.acdlabs.com> (1997)
24. AJ Boulton, AR Katritzky, A Majid- Hamid, S Øksne. *Tetrahedron*, **2**, 2835-2840 (1964)
25. S Woodcock, DVS Green, MA Vincent, IH Hillier, MF Guest, P Sherwood, *J. Chem. Soc Perkin Trans. 2*, 2151- 2154 (1992)
26. AWK Chan, WD Crow, I Gosney, *Tetrahedron*, **26**, 2497 (1970)
27. JR Christie, B Selinger, *Aust. J. Chem.*, **21**, 1113 (1968)
28. F De Sarlo, G Dini, *J. Heterocyclic Chem.*, **4**, 533 (1967)
29. LM Weinstock, PI Pollak, *Advan. Heterocycl. Chem.*, **9**, 27 (1968)
30. LM Weinstock, P Davis, B Handelsman, R Tull, *J. Org. Chem.*, **32**, 2823 (1967)
31. R Shapiro, S Kang, *Biochemica Et Biophysica Acta*, **232**, 1-4 (1971)
32. K Nakanishi, N Suzuki, F Yamazaki, *Chem. Bull. Soc. (Japan)*, **34**(1), 53-57 (1961)
33. PA Levene, LW Bass, HS Simms, *J. Biol. Chem.*, **70**, 229 (1926)
34. J Pitha, J Beranek, *Collections Czech. Chem. Commun.*, **28**, 1507-1515 (1963)
35. J Gut, M Prystas, J Jonas, F Sorm, *Collections Czech. Chem. Commun.*, **26**, 974-985 (1961)
36. P Singh, DJ Hodgson, *Acta Crystallogr., Sect. B*, **30**, 1430 (1974)
37. R Zahradnik, J Koutecky, J Jonas and J Gut, *Collections Czech. Chem. Commun.*, **28**, 1499-1506 (1963)
38. A Les, I Ortega-Blake, *International Journal of Quantum Chemistry*, **30**, 225-237 (1986)
39. T. Itai, Pyridazine N-oxides, *The Chemistry of Heterocyclic Compounds*, Interscience, **28**(8), 721 (1973)
40. H Igeta, *Chem. Pharm. Bull. (Tokyo)*, **7**, 938 (1959)
41. H Igeta, T Tsuchiya, M Nakajima, H Yokogawa, *Chem. Pharm. Bull (Tokyo)*, **17**(4), 763-769 (1969)
42. T Nakagome, *Yakugaku Zasshi*, **82**, 1005 (1962)
43. M Yanai, T Kinoshita, *Yakugaku Zasshi*, **87**, 114 (1967)
44. AA Gordon, AR Katritzky, FD Popp, *Tetrahedron, Suppl.*, **7**, 213 (1966)
45. NA Burton DVS Green, IH Hiller, PJ Taylor, MA Vincent, S Woodcock, *J. Chem. Soc. Perkin Trans. 2* , 331-335 (1993)

46. WMF Fabian, *J. Computational Chem.*, **12**, 17-35 (1991)
47. L Lapinski, *Spectrochimica Acta*, **46A** (7), 1087-1096 (1990)
48. L Lapinski, *J. Phys. Chem.*, **96**, 6250- 6254 (1992)
49. P Krogsgaard-Larsen, Personal Communication, 26 April (1998)
50. JL Wong, DS Fuchs, *J. Org. Chem.*, **36**(6), 848-850 (1971)
51. RA Hill, LJ Wallace, DD Miller, DM Weinstein, G Shams, H Tai, RT Layer, D Willins, NJ Uretsky, SN Danthi, *J. Med. Chem.*, **40**, 3182-3191 (1997)
52. MY Lidak, IV Dipan, RA Paégle, YP Stradyn, *Chem. Heterocyclic Compounds*, **5**, 644-648 (1972)
53. P Boden, BW Bycroft, SR Chhabra, J Chiplin, PJ Crowley, RJ Grout, TJ King, E McDonald, P Rafferty, PNR Usherwood, *Brain Research*, **385**, 205-211 (1986)
54. GD Hawkins, GC Lynch, DJ Giesen, I Rossi, JW Storer, DA Liotard, CJ Cramer, DG Truhlar, *AMSOL v-5.4, QCPE Program 606* (1995); based on DA Liotard, EF Healy, JM Ruiz, and MJS Dewar, *AMPAC, version 2.1, QCPE Program 506* (1989)
55. T Boulanger, DP Vercauteren, F Durant, J-M Andre, *International Journal of Quantum Chemistry: Quantum Biology Symposium*, **15**, 149-165 (1988)
56. A Itai, N Tomoika, Y Kato, *QSAR and Drug Design - New Developments and Applications*, Elsevier Science, 3-48 (1995)
57. A Albert, JN Phillips, *J. Chem. Soc.*, 1294 (1956)
58. H-J Verner, PJ Knowles *MOLPRO 96.1*, <http://www.t.c.bham.ac.uk/molpro/molpro.htm> . *Chem. Phys. Lett.* **190**, 1 (1992)
59. *Gaussian 94, Revision D.3*, MJ Frisch, GW Trucks, HB Schlegel, PMW Gill, BG Johnson, MA Robb, JR Cheeseman, T Keith, GA Petersson, JA Montgomery, K Raghavachari, MA Al-Laham, VG Zakrzewski, JV Ortiz, JB Foresman, J Cioslowski, BB Stefanov, A Nanayakkara, M Challacombe, CY Peng, PY Ayala, W Chen, MW Wong, JL Andres, ES Replogle, R Gomperts, RL Martin, DJ Fox, JS Binkley, DJ Defrees, J Baker, JP Stewart, M Head-Gordon, C Gonzalez, and JA Pople, Gaussian, Inc., Pittsburgh PA, (1995)
60. WJ Hehre. *Spartan 4.1.2*. Wavefunction Inc., 18401 Von Karman, Suite 370, Irvine, California 92715 (1996)
61. *Persistence of Vision ray-tracing*. <http://www.povray.org/>
62. P Krogsgaard-Larsen, T Honore, JJ Hansen, *Nature*, **284**, 64-66 (1980)
63. V Birch, KN Mewett, RD Allan, Honours thesis, Dept. Pharmacology, University of Sydney (1994)
64. T Iwama, Y Nagai, N Tamura, S Harada, A Nagaoka, *Eur. J. Pharmacol.*, **197**, 187-192 (1991)

65. A Mitrovic, RD Allan, Honours thesis, Dept. Pharmacology, University of Sydney (1987)
66. J Hanrahan, RD Allan, Honours thesis, Dept. Pharmacology, University of Sydney (1988)
67. G Vaccarella, RD Allan, unpublished data; G Vaccarella, *Synthesis and Activity of Pyridazine Analogues of Glutamic Acid*, PhD thesis, Department of Pharmacology, University of Sydney (1998)
68. B Bang-Andersen, SM Lenz, N Skjærbaek, Karina K Søby, HO Hansen, Bjarke Ebert, KP Bøgesø, P Krogsgaard-Larsen, *J. Med. Chem.*, **40**, 2831-2842 (1997)
69. FA Sløk, B Ebert, Y Lang, P Krogsgaard-Larsen, SM Lenz, U Madsen, *Eur. J. Med. Chem.*, **32**, 329-338 (1997)
70. N Skjærbaek, B Ebert, E Falch, L Brehm, P Krogsgaard-Larsen, *J. Chem. Soc. Perkin Trans I*, 221-225 (1995)
71. B Ebert, S. Lenz, L Brehm, P Bregnedal, J. Hansen, K. Frederiksen, K Bøgesø, P Krogsgaard-Larsen, *J. Med. Chem.*, **37**, 878-884 (1994)
72. IT Christensen, B Ebert, U Madsen, B Nielsen, L Brehm, P Krogsgaard-Larsen, *J. Med. Chem.*, **35**, 3512-3519 (1992)
73. TN Johansen, K Frydenvang, B Ebert, P Krogsgaard-Larsen, U Madsen, *J. Med. Chem.*, **37**, 3252-3262 (1994)
74. TN Johansen, B Ebert, E Falch, P Krogsgaard-Larsen, *Chirality*, **9**, 274-280 (1997)
75. TN Johansen, B Ebert, H Bräuner- Osbourne, M Didriksen, IT Christensen, KK Søby, U Madsen, P Krogsgaard-Larsen, *J. Med. Chem.*, **41**, 930-939 (1998)
76. PL Ornstein, unpublished data
77. H. Shinozaki, I. Shibuya, *Neuropharmacology*, **13**, 665-672 (1974),
78. TJ Biscoe *et al.*, *Nature*, **255**, 166-167 (1975)
79. DK Patneau, Mayer ML, *J. Neuroscience*, **10**, 2385-2399 (1990)
80. N Subasinghe, M Schulte, RJ Roon, JF Koerner, RL Johnson, *J. Med. Chem.*, **35**, 4602-4607 (1992)
81. RH Evans, AW Jones, JC Watkins, *Proc. Physiology Society*, **308**, 71-72P (1980)
82. DK Patneau, ML Mayer, DE Jane, JC Watkins, *J. Neuroscience*, Feb 1992, **12**(2), 595-606 (1992)
83. LM Hawkins, KM Beaver, DE Jane, PM Taylor, DC Sunter, PJ Roberts, *Neuropharmacology*, **34**(4), 405-410 (1995)
84. LA Wong, ML Mayer, DE Jane, JC Watkins, *J. Neuroscience*, **14**(6), 3881-3897 (1994)
85. LM Hawkins, DE Jane, PJ Roberts, *Br. J. Pharmacol. Proc. Suppl.*, **117**, 332P (1995)

86. DE Jane, K Hoo, R Kamboj, M Deverill, D Bleakman, A Mandelzys, *J. Med. Chem.*, **40**, 3645-3650 (1997)
87. JM Pinkney, P Ahluwalia, WP Kingston, P C-K Pook, DE Jane, JC Watkins, *Br. J. Pharmacol.*, **118**, 50P (1996)
88. JR Greenwood, RD Allan, unpublished data; JR Greenwood, PhD Thesis [chapter 7](#), Dept. Pharmacology, University of Sydney (1999)
89. W Binder, KN Mewett, RD Allan, Honours thesis, Dept. Pharmacology, University of Sydney (1993)
90. NL Harrison, MA Simmonds, *Br J. Pharmacol.*, **84**, 381-391 (1985)
91. RD Allan, JR Hanrahan, TW Hambley, GAR Johnston, KN Mewett, AD Mitrovic, *J. Med. Chem.*, **33**, 2905-2915 (1990)
92. LS Moltzen, E Falch, KP Boegessoe, P Krogsgaard-Larsen, *PCT Int. Appl. WO 95 12,587*; *Chem. Abstr.* **123**: 112056n (1995)
93. U Madsen, K Schaumburg, L Brehm, DR Curtis, P Krogsgaard-Larsen, *Acta Chem. Scand. B*, **40**, 92-97 (1986)
94. R Slack, KRH Wooldridge, *Adv. Heterocyclic Chem.*, **4**, 107 (1965)
95. J Jonas, J Gut, *Collections Czech. Chem. Commun.*, **27**, 716-723 (1962)

Table 8.1. Activities of alanine-substituted heterocycle AMPA analogues

Structure ^a , Class	Substituents (Chart 1.2)	Activity, electrophysiology ^b	Activity, binding ^c	Selectivity and stereoselectivity	References
3-isoxazolols					
1a	R = Me	3.5 μM^1 5.4 μM^1 5.4 μM^{II} 1 μM^{III}	0.040 μM^* 0.02 μM^{S}^* 76 μM^{R}^* 0.28 & 14.23 $\mu\text{M}^{\text{S}}^{**}$ 82.80 $\mu\text{M}^{\text{R}}^{**}$	AMPA >> NMDA, KAIN (S) >> (R)	[3, 4, 12, 62, 63, 64, 65, 66, 67, 68, 69]
1b	R = H	900 μM^1	0.27 μM^*	AMPA >> NMDA, KAIN	[69]
1c	R = Et	2.3 μM^1	0.03 μM^*	AMPA >> NMDA, KAIN	[70]
1d	R = C(CH ₃) ₃	34 μM^1 ~50 μM^1	2.1 μM^* 10 μM^*	AMPA >> NMDA, KAIN	[3, 12, 70] [72]
1e	R = Pr	5.0 μM^1	0.09 μM^*	AMPA >> NMDA, KAIN	[69]
1f	R = CH(CH ₃) ₂	9.0 μM^1	0.19 μM^*	AMPA >> NMDA, KAIN	[69]
1g	R = cyclopropyl	5.5 μM^1	0.035 μM^*	AMPA >> NMDA, KAIN	[70]
1h	R = (CH ₂) ₃ CH ₃	32 μM^1	1.0 μM^*	AMPA >> NMDA, KAIN	[69]
1i	R = CH ₂ CH(CH ₃) ₂	23 μM^1	0.61 μM^*	AMPA >> NMDA, KAIN	[69]
1j	R = C(CH ₃) ₃	34 μM^1 ~50 μM^1	2.1 μM^* 10 μM^*	AMPA >> NMDA, KAIN	[3, 12, 70] [72]
1k	R = (CH ₂) ₂ CH(CH ₃) ₂	>1000 μM^1	>100 μM^*		[69]
1l	R = CH ₂ C(CH ₃) ₃	420 μM^1	55 μM^*	AMPA >> NMDA, KAIN	[69]
1m	R = phenyl	230 μM^{S}^1 (R) is weak antagonist	6 μM^{S}^*	AMPA >> NMDA, KAIN (S) AMPA, KAIN antagonist (R)	[71]
1n	R = CH((CH ₂) ₂ CH ₃) ₂	>1000 μM^1	99 μM^*		[69]
1o	R = benzyl	>1000 μM^1	>100 μM^*		[69]
1p	R = CH ₂ Br	13 μM^1	0.03 μM^*		[3, 73]
1q	R = thiazole, -2-yl ^d	2.3 μM^1	0.094 μM^*	AMPA > KAIN > NMDA	[68]
1r	R = imidazole, -2-yl	550 μM^1	48 μM^*	AMPA > KAIN > NMDA	[68]
1s	R = imidazole, 1-methyl-2-yl	> 1000 μM^1	> 100 μM^*	KAIN > AMPA, NMDA	[68]
1t	R = 1,2,4-triazole, -3-yl	63 μM^1	1.5 μM^*	AMPA > KAIN > NMDA	[68]
1u	R = 1,2,4-triazole, 2-methyl-3-yl	93 μM^1	5.8 μM^*	AMPA, KAIN > NMDA	[68]
1v	R = 1,2,4-triazole, 1-methyl-3-yl	11 μM^1	0.7 μM^*	AMPA >> KAIN, NMDA	[68]
1w	R = tetrazole, 5-yl	> 1000 μM^1	72 μM^*	AMPA > KAIN, NMDA	[68]
1x	R = tetrazole, -1-methyl-5-yl	> 1000 μM^1	54 μM^*	AMPA > KAIN, NMDA	[68]
1y	R = tetrazole, -2-methyl-5-yl	0.92 μM^1	0.03 μM^*	AMPA > KAIN > NMDA	[68]
1z	R = pyridin-2-yl ^e	7.4 μM^1 4.5 μM^{S}^1 (R) is weak antagonist	0.57 μM^* 0.19 μM^{S}^*		[74]

2a	R = H	370µM ^I	1.5µM *	AMPA>>NMDA, KAIN (S) >> (R)	[4,12,62]
2b	R = Me	~20µM ^I	0.6µM *		[62, 72]
2c	R = Br	22µM ^I 23µM ^I 21µM (S) ^I >1000 (R) ^I	0.65µM * 0.60µM * 0.34 µM(S) * 32µM(R) *		[12,62,75]
2d	R = (CH ₂) ₃ CH ₃	~40µM ^I 37µM ^I 17µM (S) ^I >1000 (R) ^I	2µM * 1.8µM * 0.48µM (S)* >1000 (R) ^I	AMPA >> NMDA,KAIN	[72,75]
2e	R = CH ₂ CH ₂ OH	~90µM ^I	2µM *	AMPA >> NMDA,KAIN	[72]
3-isothiazolols					
3a	R = Me	15µM ^I	1.8µM *		[12]
3b	R = C(CH ₃) ₃	14µM ^I	0.63µM *		[12]
4a	R = H	380µM ^I	5.8µM *		[12]
4b	R = Br	500µM ^I	17µM *		[12]
5-isoxazolols					
5a	R = H	300µM ^{III}	0.28µM *	AMPA>KAIN>NMDA (S) NMDA>AMPA>KAIN (R)	[4,64]
5b	R = Me	1µM ^{III}	0.30µM *		[64]
5c	R = Et	1µM ^{III}	0.67µM *		[64]
5d	R = cyclopropyl	0.3µM ^{III}	0.12µM *		[64]
5e	R = cyclopentyl	0.3µM ^{III}	0.31µM *		[64]
5f	R = isopropyl	3µM ^{III}	3.8µM *		[64]
5g	R = phenyl	30µM ^{III}	15µM *		[64]
3-hydroxy-1,2,5-thiadiazole					
6		"potent"		AMPA	[4,49,76]
3,5-dioxo-1,2,4-oxadiazolidine					
7		8µM ^{II} 0.9 µM(S) ^{IV} 25 µM ^V 15 µM (S) ^V 120 µM (R) ^V	0.0086 µM * 0.26µM (S) **	AMPA,KAIN>NMDA	[53, 64, 65, 66, 77, 78, 79]
3,5-dioxo-1,2,4-triazole					
8		nil at 1000 µM ^V			[53]
hydantoin					
9		nil at 1000 µM ^V "potent" ^g		"depolarisation in the mammalian EAA system" ^g	[53] [51, 80]
uracils					
10a	R = H	1/3 to 1/2 vs 7a ^{VI} 44.8µM (S) ^{IV}	3.40µM(S) ** > 1000µM(R) **	AMPA,KAIN >>NMDA (S)>>(R)	[4,81,82,83, 84]
10b	R = F	1.47µM (S) ^{IV}	0.02 & 30.39µM(S) **		[4,82,83, 84]
10c	R = Cl	7.28µM (S) ^{IV}	0.39µM(S) **		[82,83, 84]
10d	R = Br	8.82µM (S) ^{IV}	0.56µM(S) ** 41.00µM(R) **		[82,83, 84]
10e	R = I	19.2µM (S) ^{IV}	19.45µM(S) ** > 1000µM(R) **		[82, 83, 84]
10f	R = NO ₂	4.10µM (S) ^{IV}	0.20µM(S) **		[82, 83, 84]
10g	R = CN	3.75µM (S) ^{IV}	1.64µM(S) **		[83, 84]
10h	R = CF ₃	4.00µM (S) ^{IV}	0.37µM(S) **		[83, 84]
10i	R = CH ₃	251µM (S) ^{IV}	68.5µM(S) **		[83, 84]
11			23.46µM**		[83]
12			> 1000µM **		[83]
13			> 1000µM **		[83]

6-aza-uracils					
14a	R = H	3.99 (S) ^{VI} 3645 (R) ^{VI}	1.6µM(S) >1000µM(R)**	KAIN,AMPA >> NMDA (S)>>(R)	[85, 86, 87]
14b	R = Cl	0.07 (S) ^{VI}	53.0µM(S)**	KAIN,AMPA >> NMDA	[85, 86, 87]
14c	R = Br	0.08 (S) ^{VI}	19.0µM(S)**	KAIN,AMPA >> NMDA	[85, 86, 87]
14d	R = I	0.15 (S) ^{VI}	0.5µM(S)**	KAIN,AMPA >> NMDA	[85, 86, 87]
14e	R = Me	1.90 (S) ^{VI}	2.5µM(S)**	KAIN,AMPA >> NMDA	[85, 86, 87]
15		4.62 (RS) ^{VI}	5.4µM(RS)**	KAIN,AMPA >> NMDA	[85,87]
3-hydroxy-pyridazine 1-oxides					
16a	R = H	9.28µM ^{II}		AMPA>>NMDA	[63,67]
16b	R = Me	8.74µM ^{II}		AMPA>>NMDA	[67]
17		65µM ^{II}			[63,67]
18	R = Me	588µM ^{II}			[67]
6-hydroxy-tetrazolo[1,5- b]pyridazines					
19		299µM ^{II}		AMPA>>NMDA	[67, 89]
20		610µM ^{II}		AMPA,NMDA	[67, 89]
pyridazine-3,6-diones					
21a (=22c)^h	R ₁ = R ₂ = H	481µM ^{II}		AMPA, NMDA	[67, 88]
21b	R ₁ = H R ₂ = Me	nil at 1000 µM ^{II}			[67, 88]
21c (=22d)^h	R ₁ = Me R ₂ = H	289µM ^{II}		AMPA, NMDA	[67, 88]
22a	R ₁ = H R ₂ = Me	low (1000 µM) ^{II}		AMPA>>NMDA	[67, 88]
22b	R ₁ = R ₂ = Me	81.4µM ^{II}		AMPA>>NMDA	[67, 88]
23		nil at 1000µM ^{II}			[67, 88]
pyridazine-3-ones					
24		837µM ^{II}			[67]
25		nil at 1000 µM ^{II}			[67]

^a unless otherwise indicated, values refer to racemic mixture.

^b electophysiological assays

^I EC₅₀, cortical wedge preparation, Krogsgaard-Larsen et al. [\[12, 68, 70, 73, 72, 90\]](#)

^{II} EC₅₀, cortical wedge preparation, Vaccarella, Allan, et al. [\[67, 90, 91\]](#)

^{III} Minimum effective concentration required to excite rat hippocampal CA1 neurones in vitro [\[64\]](#)

^{IV} Steady-state EC₅₀ values, whole-cell recording from mouse embryonic hippocampal neurons [\[82, 84\]](#)

^V Equipotency of inhibition of retractor unguis muscle of *Schistocerca gregaria* vs L-glutamate at 100 µM [\[53\]](#)

^{VI} Depolarisation of motoneurons from ventral roots of hemisected spinal-cord preparations [\[81\]](#). Equieffective molar concentrations relative to (S)-AMPA=1 [\[87\]](#)

^c IC₅₀, µM, inhibition of AMPA binding.

* (RS)[³H]AMPA. One site model, in the presence of KSCN. [\[64, 70, 83\]](#) et al.]

** (S)[³H]AMPA. One or two site models, in the absence of KSCN. [\[83\]](#).

^d The thiophene-2-yl isomer of [1q](#) is reportedly active, EC₅₀ of 5.8 μM; and the furan-2-yl isomer apparently also known. [[49](#), [92](#)]

^e The pyridin-3-yl isomer of [1z](#) is reportedly inactive, and the pyridin-4-yl isomer a weak agonist. [[74](#)]

^f [3a](#) has apparently been found to be substantially more active than the published figures suggest [[49](#)]

^g While inactive in the locust glutamatergic system [[53](#)], [7c](#) potentiates depolarisation by L-AP4 in mammalian hippocampal CA1 neurones, and is suggested to act via the AMPA receptor [[51](#), [80](#)]

^h Structures [21a](#) and [21c](#) may be regarded also as structures [22c](#), [22d](#) by tautomerism.

Table 8.2a. 26–33 at MP2/6- 311+G(3df,2p)//MP2/6-31G(d,p)

Structure	Symmetry	E_0^a	$G_{298, \text{gas}}^b$	Gas phase Ratio c	G_{aq}^d	Aqueous Ratio e
26a	C_s	-344.27	-343.44	99.97%	- 276.66	99.98%
26b	C_1	-339.53	-338.70	0.03%	- 271.59	0.02%
27a	C_s^e	-344.46	-344.17	99.99%	-284.27	98.90%
27b	C_s^f	-338.58	-338.41	0.01%	-281.61	1.10%
28a	C_1	-327.64	-326.53	5.62%	- 268.80	55.36%
28b	C_1	-329.13	-327.99	65.68%	- 269.06	8.92%
28c	C_s	-328.33	-327.50	28.71%	- 267.98	35.72%
29a	C_s	-335.64	-334.87	100.00%	- 279.13	100.00%
29b	C_s	-325.57	-325.20	0.00%	- 271.92	0.00%
30a	C_1	-326.59	-326.04	100.00%	- 271.03	100.00%
30b	C_1	-311.48	-310.86	0.00%	- 259.06	0.00%
30c	C_1	-309.95	-309.28	0.00%	- 256.70	0.00%
31a	C_s	-344.53	-343.70	100.00%	- 282.59	100.00%
31b	C_s	-326.00	-325.17	0.00%	- 268.39	0.00%
31c	C_s	-334.29	-333.12	0.00%	- 274.48	0.00%
32a	C_s	-334.22	-332.11	100.00%	- 272.13	99.99%
32b	C_s	-319.34	-318.28	0.00%	- 262.86	0.00%
32c	C_s	-324.97	-323.33	0.00%	- 266.28	0.01%
33a	C_s	-330.96	-330.21	99.78%	- 276.36	100.00%
33b	C_s	-322.66	-322.02	0.00%	- 270.16	0.00%
33c	C_s	-327.63	-326.60	0.22%	- 268.25	0.00%

Table 8.2b. Tautomerism at G2(MP2) theory

Structure	Symmetry	E ₀ ^g	G _{298, gas} ^b	Gas phase Ratio ^c	G _{aq} ^d	Aqueous Ratio ^c
27a	C _s ^e	-345.22	-344.93	99.64%	- 285.04	60.45%
27b	C _s ^f	-342.03	-341.59	0.36%	- 284.79	39.55%
28a	C ₁	-331.96	-330.85	0.54%	- 273.38	28.13%
28b	C ₁	-335.09	-333.94	99.36%	- 273.93	71.23%
28c	C _s	-330.67	-329.84	0.10%	- 271.14	0.64%
29a	C _s	-336.65	-335.88	100.00%	- 280.15	99.71%
29b	C _s	-330.33	-339.96	0.00%	- 276.68	0.29%
31a	C _s	-346.55	-345.71	100.00%	- 284.61	100.00%
31b	C _s	-338.14	-337.31	0.00%	- 270.52	0.00%
31c	C _s	-336.19	-335.02	0.00%	- 276.38	0.00%
32a	C _s	-336.58	-334.48	100.00%	- 274.50	100.00%
32b	C _s	-321.78	-320.72	0.00%	- 265.30	0.00
32c	C _s	-326.65	-325.01	0.00%	- 267.96	0.00
33a	C _s	-332.91	-332.16	99.18%	- 278.31	100.00%
33b	C _s	-324.73	-324.10	0.00%	- 272.24	0.00%
33c	C _s	-330.36	-329.32	0.82%	- 270.98	0.00%

Table 8.2c. Tautomerism at reduced basis set G2(MP2) theory

Structure	Symmetry	E_0^h	$G_{298, \text{gas}}^b$	Gas phase Ratio ^c	G_{aq}^d	Aqueous Ratio ^c
26a	C _s	-345.06	-344.22	99.33%	- 277.45	99.62%
26b	C ₁	-342.09	-341.26	0.67%	- 274.15	0.38%
30a	C ₁	-328.56	-328.00	100.00%	- 272.99	100.00%
30b	C ₁	-314.13	-313.51	0.00%	- 261.70	0.00%
30c	C ₁	-312.86	-312.19	0.00%	- 259.61	0.00%

^a $E_{\text{elec}} = E\{\text{MP2}/6\text{-}311+\text{G}(3\text{df},2\text{pd})//\text{MP2}/6\text{-}31\text{G}(\text{d},\text{p})\}$

$E_0 = E_{\text{elec}} + 0.8929*\text{ZPE}\{\text{HF}/6\text{-}31\text{G}(\text{d})\}$

All energies in Kcal/mol, relative to conjugate base anion

^b $G_{298} = E_{\text{elec}} + E_{\text{thermal}} + RT - TS$

Thermochemistry calculated at HF/6-31G(d) minima, 298.15 K.

^c $\text{HA}_i \rightleftharpoons \text{HA}_j$; $K_{ji} = [\text{HA}_j]/[\text{HA}_i] = \exp((G_i - G_j)/RT)$; $\sum_i [\text{HA}] = 1$

^d For neutral species:

$G_{\text{aq}} = G_{298} + E\{\text{AM1-SM2}//\text{MP2}/6\text{-}31\text{G}(\text{d},\text{p})\} - E\{\text{AM1}//\text{MP2}/6\text{-}31\text{G}(\text{d},\text{p})\}$

For anions:

$G_{\text{aq}} = G_{298} + E\{\text{AM1-SM2}\} - E\{\text{AM1}\}$

^e Minimum in C_s symmetry at MP2/6-31G(d,p). C_s symmetry is not a minimum at HF/6-31G(d). C₁ structure used for thermochemistry calculation.

^f C₁ optimised structure favoured over C_s optimised structure at MP2/6-31G(d,p) by 0.21 Kcal. However, C_s symmetry favoured by 0.10 Kcal at MP2/6-311+G(3df,2pd)//MP2/6-31G(d,p). C₁ optimised structure used for thermochemistry.

^g Modified G2(MP2) theory [14] incorporating optimisation at MP2/6-31G(d,p):

$E_{\text{elec}} = E\{\text{MP2}/6\text{-}311+\text{G}(3\text{df},2\text{pd})//\text{MP2}/6\text{-}31\text{G}(\text{d},\text{p})\}$

+ $E\{\text{QCISD}(\text{T})/6\text{-}311\text{G}(\text{d},\text{p})//\text{MP2}/6\text{-}31\text{G}(\text{d},\text{p})\}$

- $E\{\text{MP2}/6\text{-}311\text{G}(\text{d},\text{p})//\text{MP2}/6\text{-}31\text{G}(\text{d},\text{p})\}$

+ ΔE^{HLC}

$E_0 = E_{\text{elec}} + 0.8929*\text{ZPE}\{\text{HF}/6\text{-}31\text{G}(\text{d})\}$

^h Reduced basis set G2(MP2) theory (cf [14, 17]), neglecting ΔE^{HLC} :

$E_{\text{elec}} = E\{\text{MP2}/6\text{-}311+\text{G}(3\text{df},2\text{pd})//\text{MP2}/6\text{-}31\text{G}(\text{d},\text{p})\}$

+ $E\{\text{QCISD}(\text{T})/6\text{-}31\text{G}(\text{d},\text{p})//\text{MP2}/6\text{-}31\text{G}(\text{d},\text{p})\}$

- $E\{\text{MP2}/6\text{-}31\text{G}(\text{d},\text{p})\}$

$E_0 = E_{\text{elec}} + 0.8929*\text{ZPE}\{\text{HF}/6\text{-}31\text{G}(\text{d})\}$

Table 8.3. Solvation energies, pK_a predictions and literature values*

Structure	ΔG_{solv} single point ^a	ΔG_{solv} optimised ^b	$G_{298, \text{aq}}$ ^c	ΔpK_a theoretical ^d	pK _a empirical ^e	pK _a experimental	reference
26-	-74.62	-75.41	- 398.74839	4.41	8.05 ± 0.44	4.8 ^f 5.12 ^f 5.07 ^g 5.85 ^h	[93] [11] [11] [10]
26a	-8.64	-8.84	- 399.19032				
27-	-73.09	-74.45	- 721.39789	9.99	9.84 ± 0.42	8.15 ⁱ 7.00 ^j 6.69 ^k 7.54 ^l	[94] [12] [12] [10]
27a	-14.56	-17.62	- 721.85213				
27b	-17.64	-23.93	- 721.85173				
28-	-67.11	-67.21	- 359.53390	1.80	5.80 ± 0.50	4.5	[28]
28a	-9.74	-9.72	- 359.96957				
28b	-7.21	-7.22	- 359.97045				
28c	-8.52	-8.85	- 359.96599				
29-	-74.18	-74.71	- 698.23865	6.48	6.35 ± 0.44	5.1	[30]
29a	-18.97	-19.64	- 698.68509				
29b	-21.43	-25.56	- 698.67956				
30-	-67.26	-66.53	- 450.75033	1.23	7.41 ± 0.40	4.2 ^m	[53]
30a	-11.52	-11.67	- 451.18534				
31-	-73.85	-75.07	- 452.89612	9.75 ^d	9.24 ± 0.40	9.75 9.3 ⁿ 9.97 ⁿ	[50] [51] [52]
31a	-13.96	-14.93	- 453.34967				
31b	-18.28	-18.94	- 453.32723				
31c	-16.43	-16.54	- 453.33656				
32-	-71.43	-72.12	- 468.92181	2.34	7.69 ± 0.40	6.99	[95]
32a	-12.15	-12.79	- 469.35925				
32b	-16.70	-17.21	- 469.34459				
32c	-15.07	-15.25	- 469.34884				
33-	-67.54	-66.69	- 452.78955	5.14	6.31 ± 0.45	4.1 ^o	[40]
33a	-12.84	-12.09	- 453.23307				
33b	-14.83	-15.91	- 453.22339				
33c	-8.35	-8.39	- 453.22139				

* See also [Graphs 1- 3](#).

^a Free energy of solvation at MP2/6-31G(d,p) geometry in Kcal / mol
 $\Delta G_{\text{solv}} = E\{\text{AM1-SM2} // \text{MP2/6-31G(d,p)}\} - E\{\text{AM1} // \text{MP2/6-31G(d,p)}\}$

^b Free energy of solvation at semi-empirical geometry in Kcal / mol
 $\Delta G_{\text{solv}} = E\{\text{AM1-SM2}\} - E\{\text{AM1}\}$

^c Absolute $G_{298,\text{aq}}$ free energies in Hartree, from modified G2(MP2) theory, thermochemistry at HF/6-31G(d), and AM1-SM2 solvation energy as follows
 $E_{\text{elec}} = E\{\text{MP2/6-311+G(3df,2pd)} // \text{MP2/6-31G(d,p)}\} + E\{\text{QCISD(T)/6-311G(d,p)} // \text{MP2/6-31G(d,p)}\} - E\{\text{MP2/6-311G(d,p)} // \text{MP2/6-31G(d,p)}\} + \Delta E^{\text{HLC}}$
 $E_0 = E_{\text{elec}} + 0.8929 * \text{ZPE}\{\text{HF/6-31G(d)}\}$
 $G_{298} = E_{\text{elec}} + E_{\text{thermal}} + RT - TS$

Thermochemistry calculated at HF/6-31G(d) minima, 298.15 K.

For neutral species:

$G_{298,\text{aq}} = G_{298} + E\{\text{AM1-SM2} // \text{MP2/6-31G(d,p)}\} - E\{\text{AM1} // \text{MP2/6-31G(d,p)}\}$

For anions:

$G_{298,\text{aq}} = G_{298} + E\{\text{AM1-SM2}\} - E\{\text{AM1}\}$

^d $\Delta \text{pK}_a = \Delta(-\log_{10}(\exp(-\Delta G_{298,\text{aq}}/RT)))$, Relative to pK_a (31) = 9.75

Where more than one tautomer is significant, i.e. 28, 29, 30, free energy at equilibrium is determined as a weighted average:

$\Delta G_{298,\text{aq}} = \sum a_i G_{298,\text{aq},i} - G_{298,\text{aq},\text{anion}}$; such that $\sum a_i = 1$

^e Modified Jaffe method [22] of estimating parameters for the Hammett equation, as implemented in ACD/pKa program [23]

^f pK_a of AMPA (1a)

^g pK_a of HIBO (2a)

^h pK_a of 3-isoxazolol

ⁱ pK_a of 4-methyl-3-isothiazolol

^j pK_a of thio-AMPA (3a)

^k pK_a of thio-HIBO (4a)

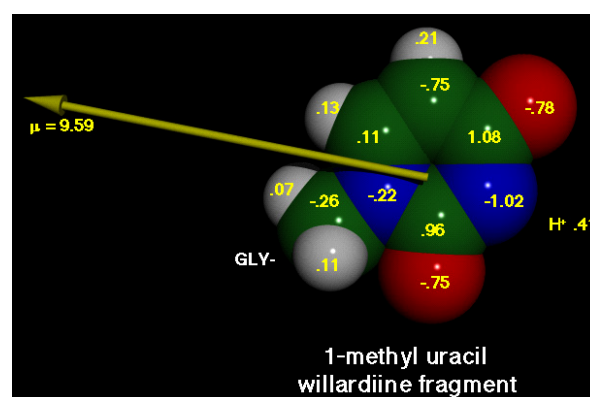
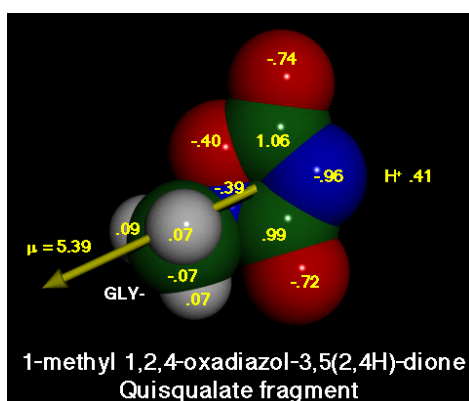
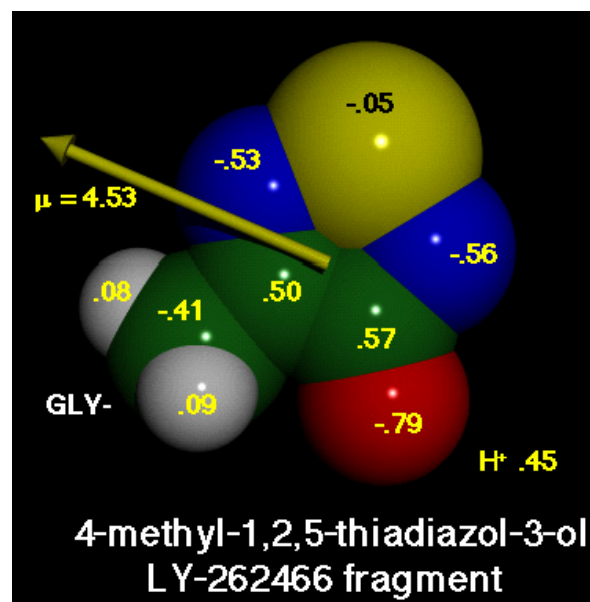
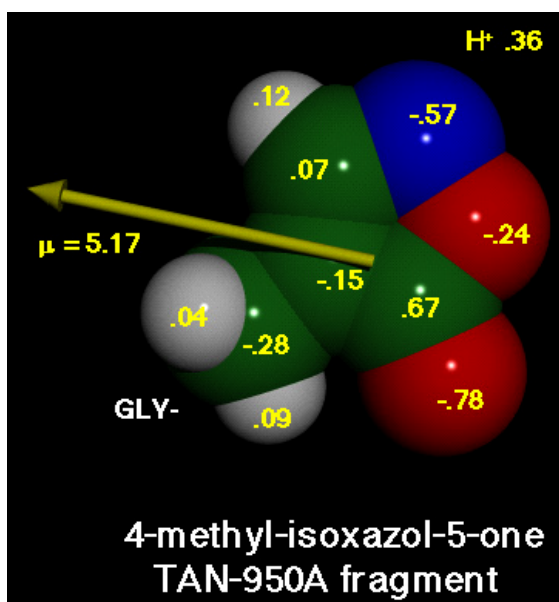
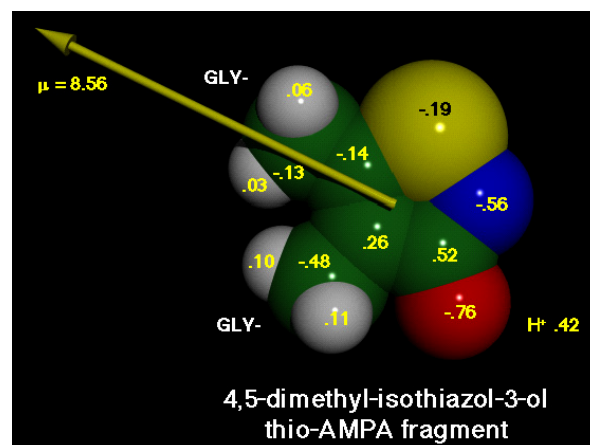
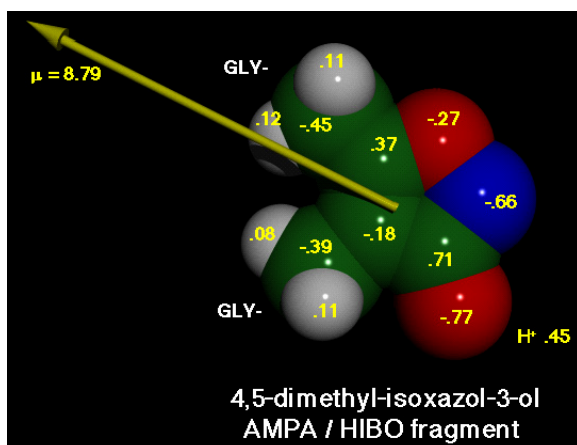
^l pK_a of 3-isothiazolol

^m pK_a of quisqualate (7) as determined by Boden et al. [53] and apparently misquoted as 4.5 by Hill et al. [51]

ⁿ pK_a of willardiine (10a) as determined by Lidak et al [51] and Hill et al. [52] respectively. Interestingly, Lidak also quotes ammonium protolysis $\text{pK}_{\text{NH}_3^+}$ for willardiine as 7.98.

^o pK_a of 3-hydroxy-pyridazine 1-oxide

Figures 8.1.26 to 8.1.31 Conjugate base anions of model acidic heterocycles, CPK rendering, point charge distributions



Figures 8.1.32 to 8.1.37 Conjugate base anions of model acidic heterocycles

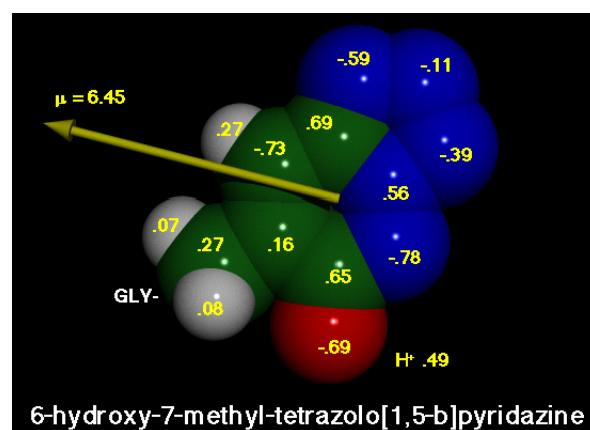
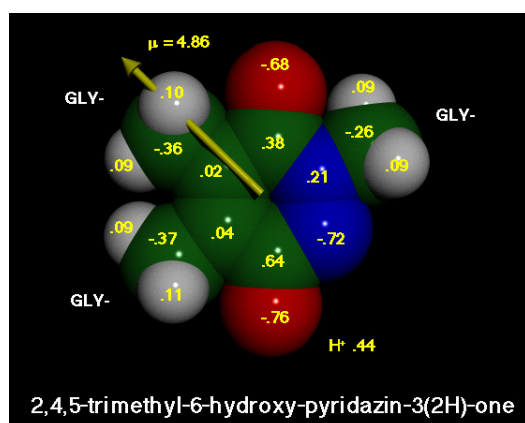
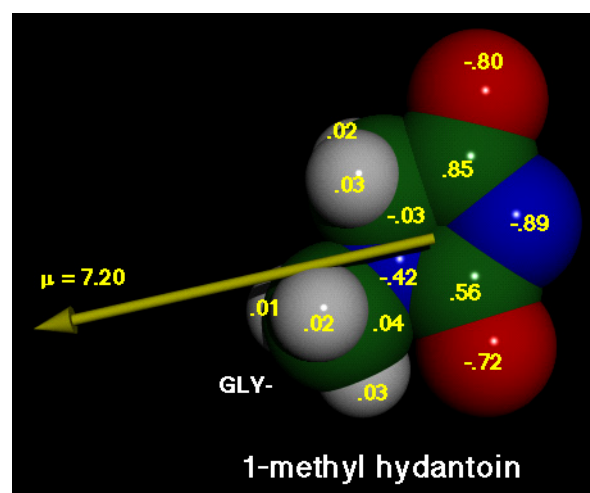
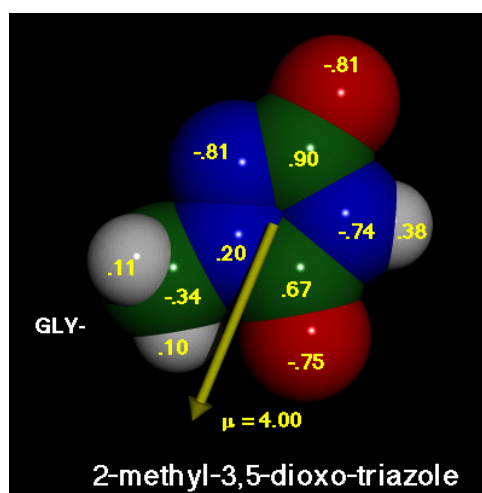
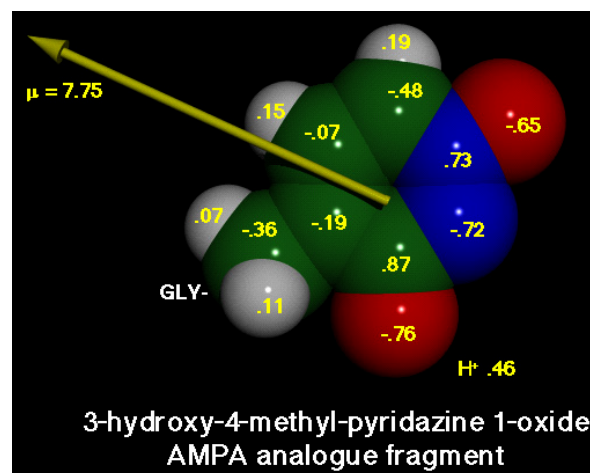
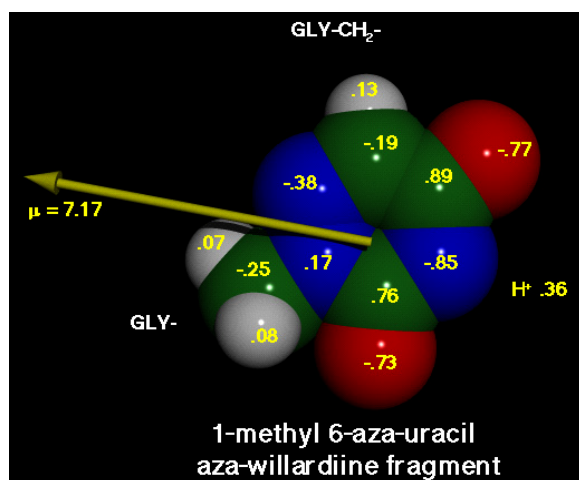
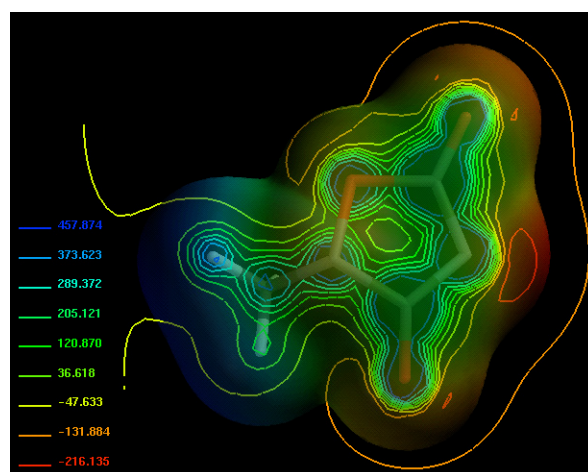
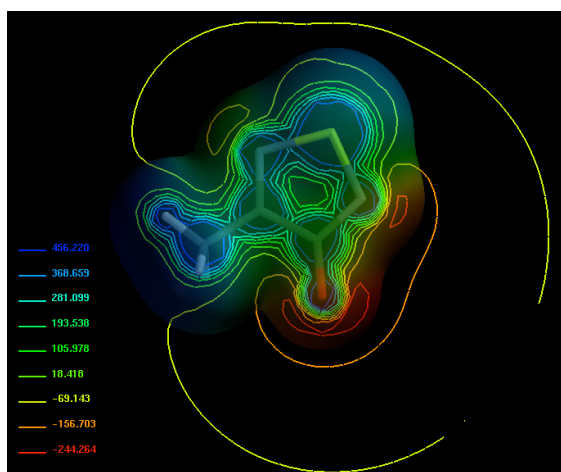
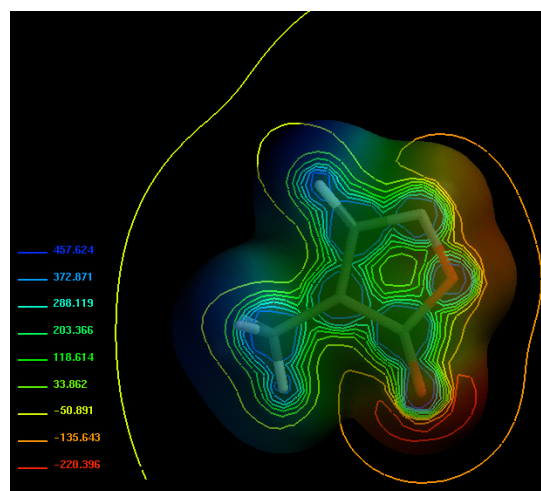
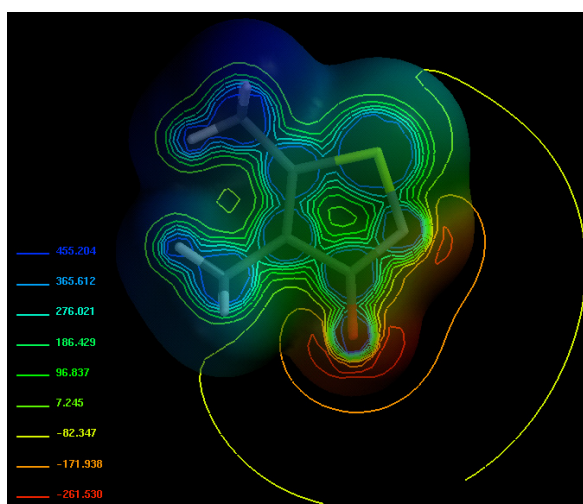
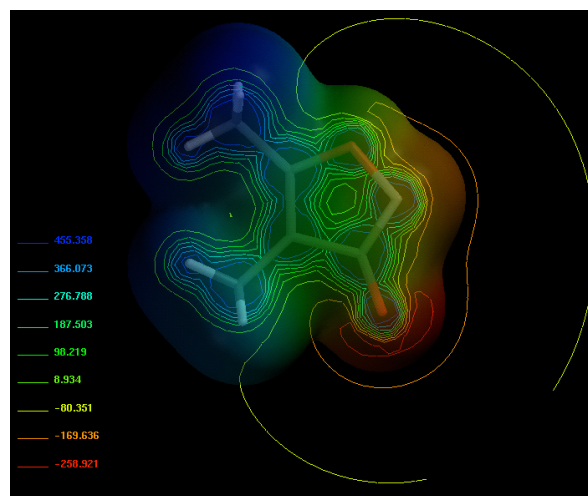
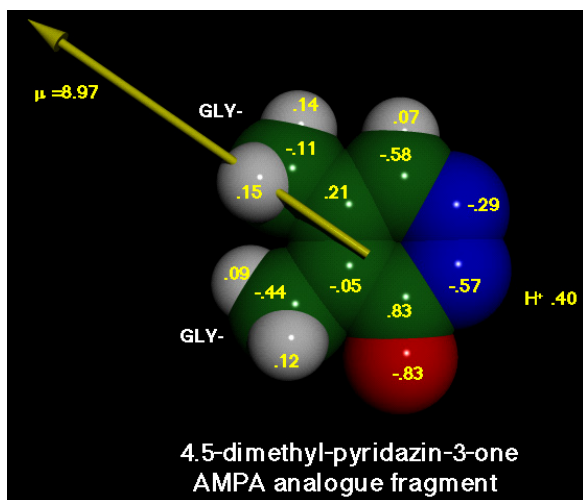
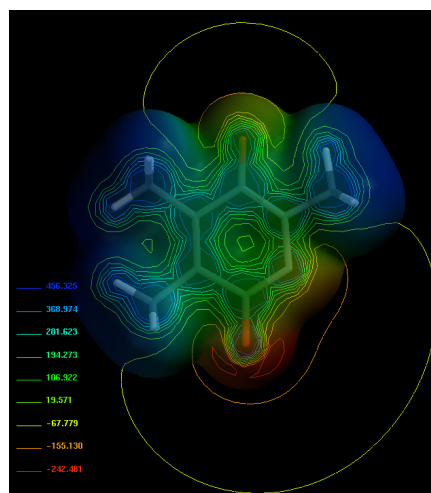
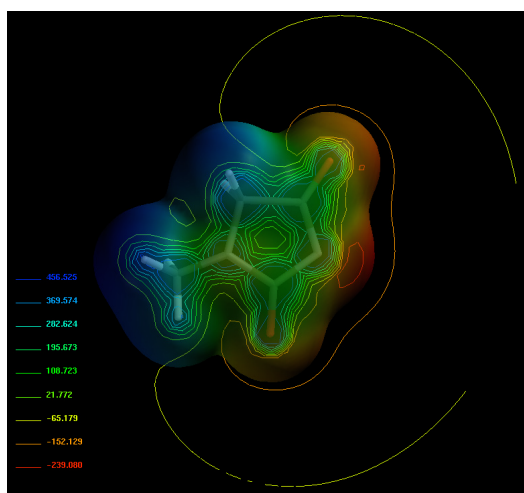
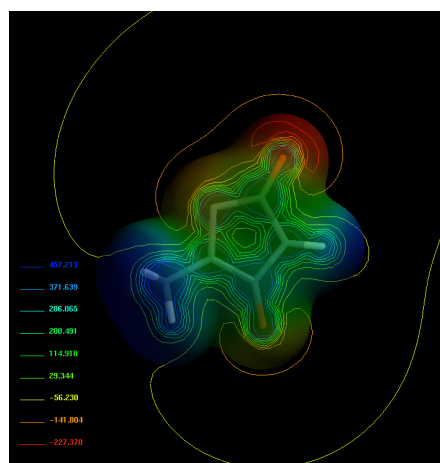
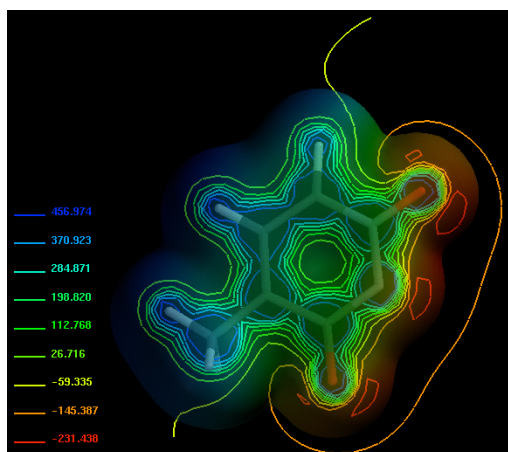
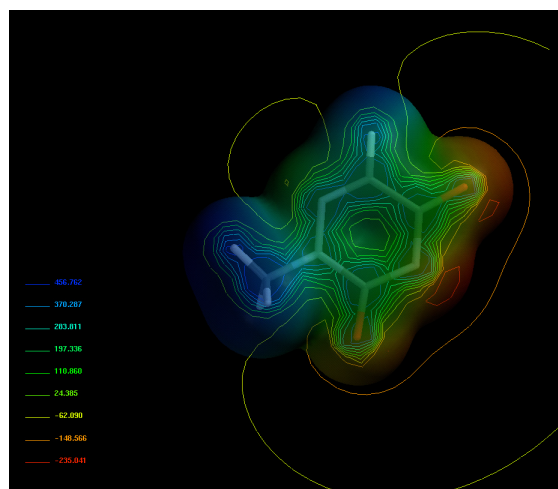
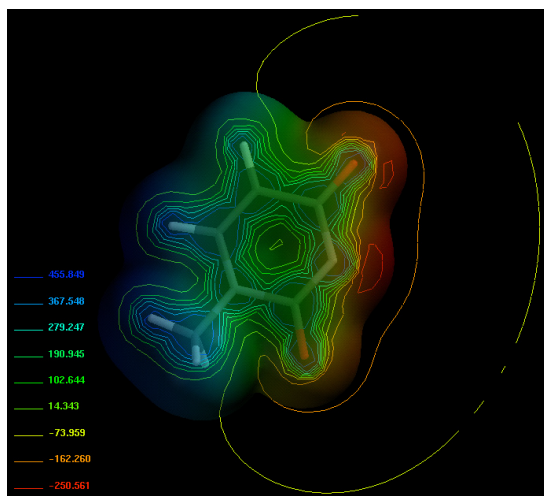


Figure 8.1.38, Figures 8.2.26 to 8.2.30 Conjugate base anions of model acidic heterocycles, Van der Waals surfaces, electrostatic potentials



Figures 8.2.31 to 8.2.36 Conjugate base anions of model acidic heterocycles, Van der Waals surfaces, electrostatic potentials



Figures 8.2.37 to 8.2.38 Conjugate base anions of model acidic heterocycles, Van der Waals surfaces, electrostatic potentials

Figure 8.3 Conjugate base anions 26- to 33- overlaid

Figure 8.4 1-methyl uracil anion, methyl guanidinium cation, and methanol complex

Figure 8.5 4,5-dimethyl-3-isoxazolol anion, methyl-guanidinium cation, water, and methanol complex

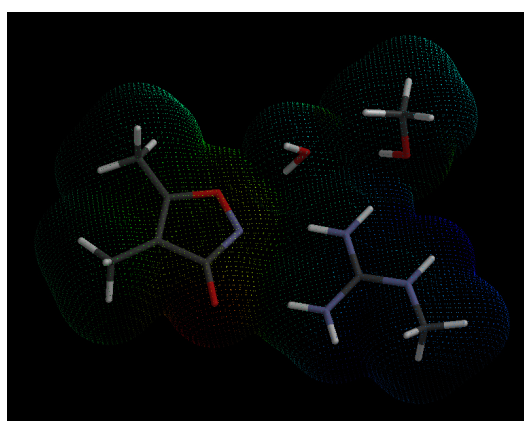
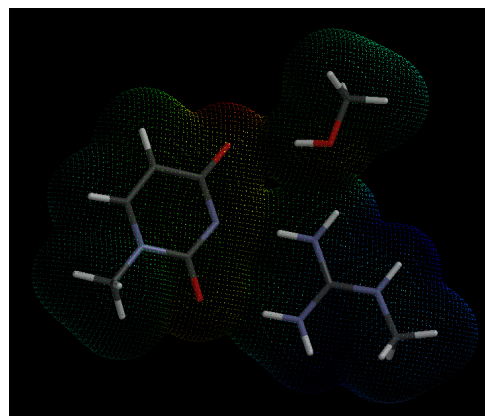
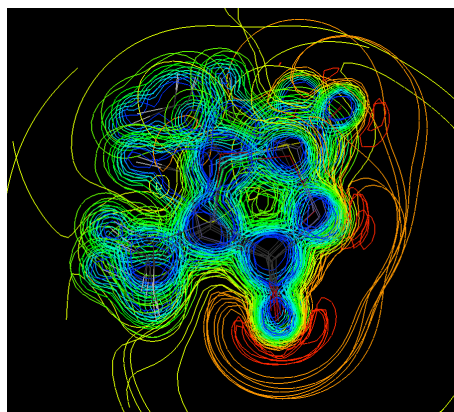
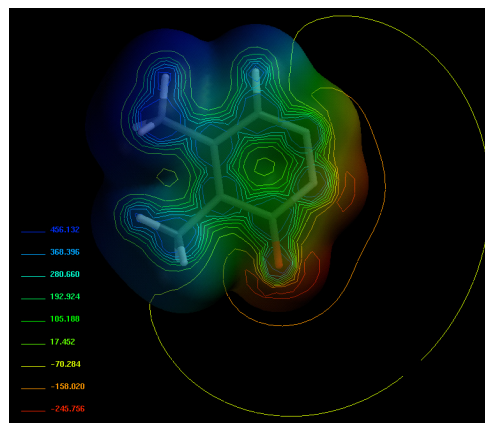
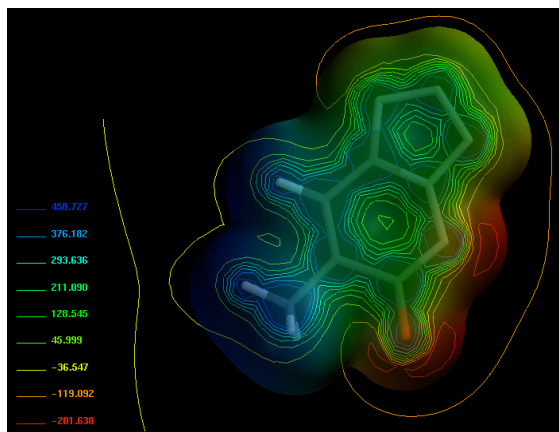


Chart 8.1. Alanino hydroxy-heterocycles with moderate to high agonist activity at AMPA receptors

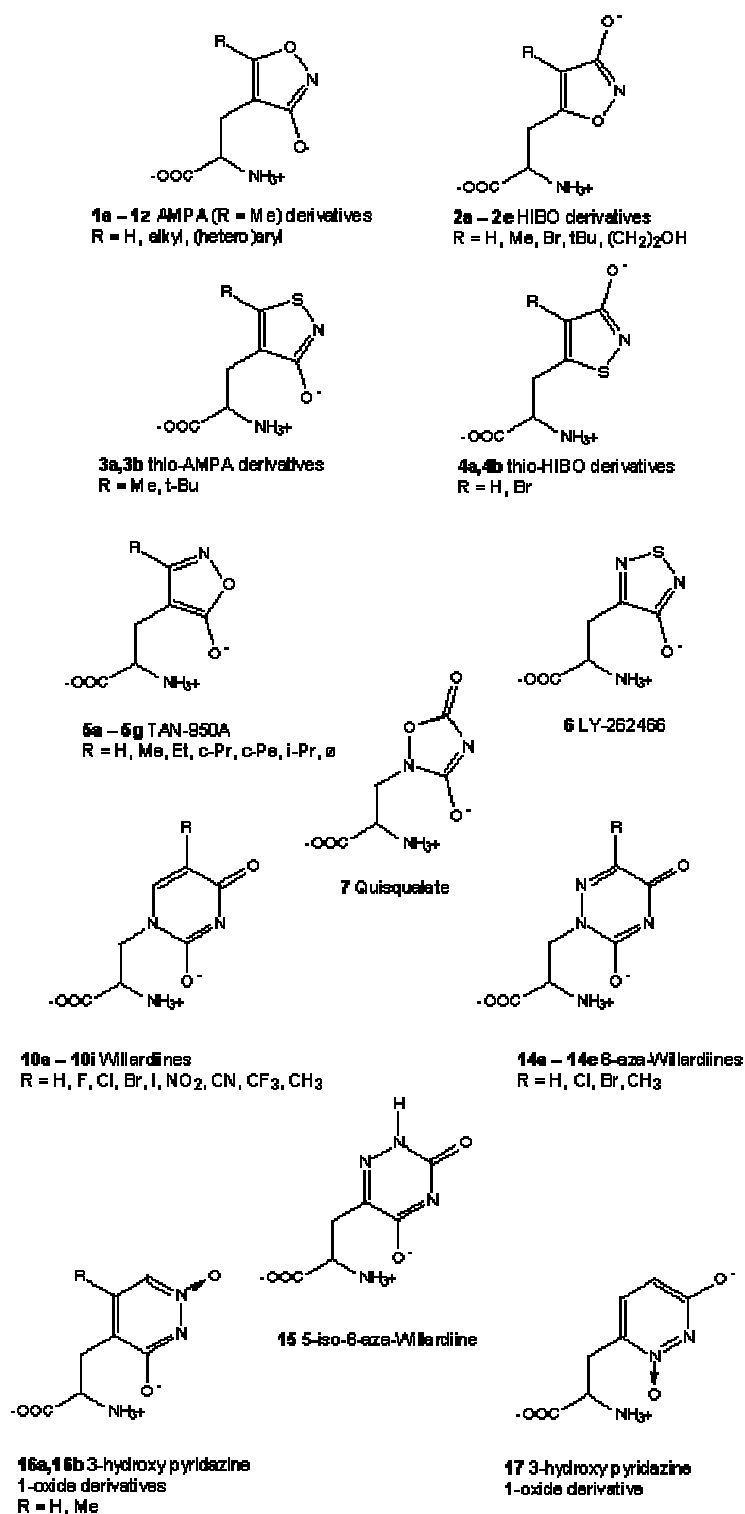


Chart 8.2. Alanino hydroxy-heterocycles showing reduced or abolished activity at AMPA receptors

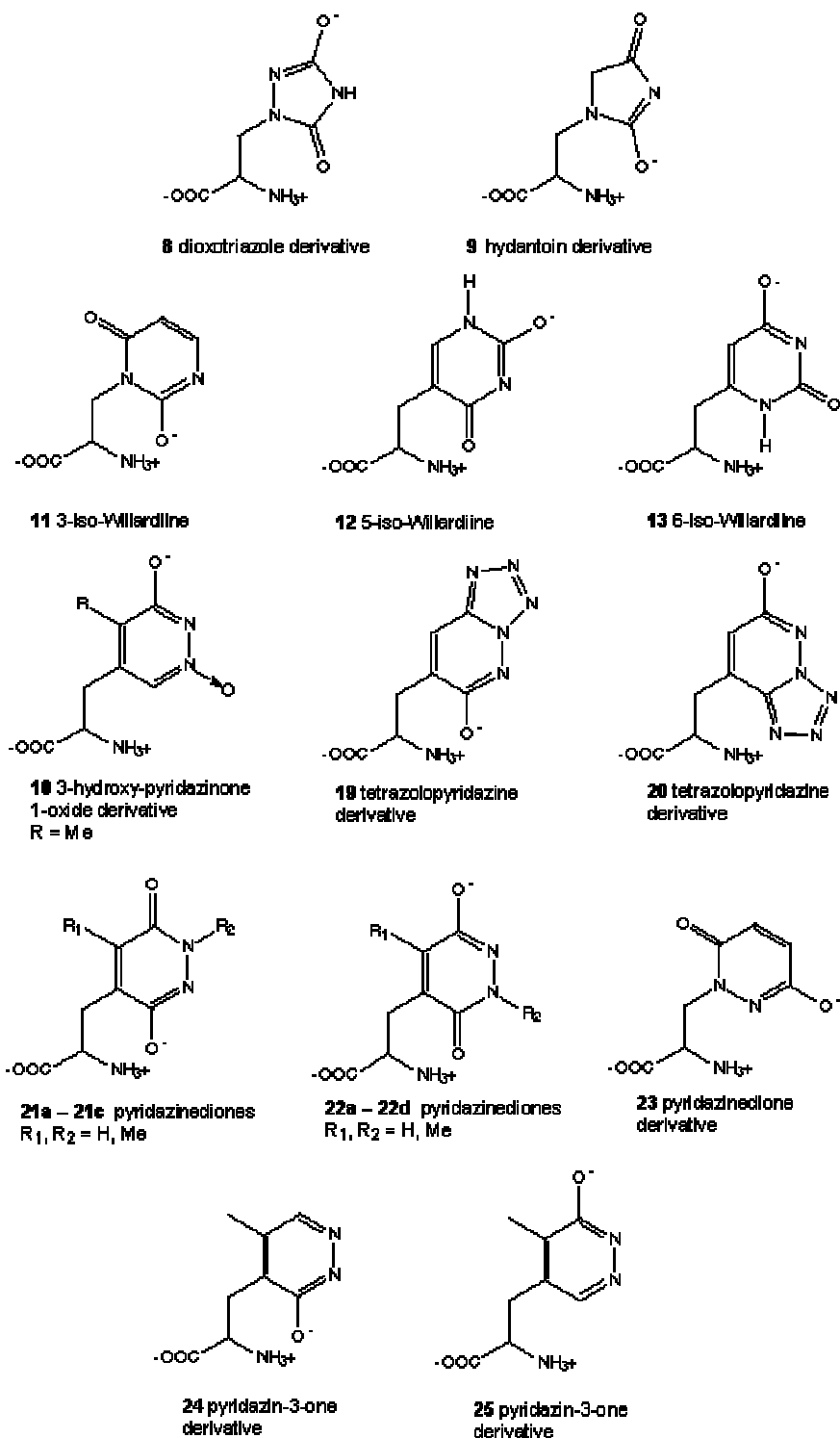
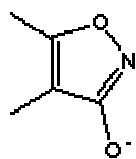
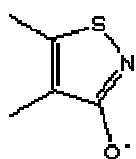


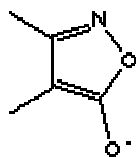
Chart 8.3. Model heterocyclic conjugate bases



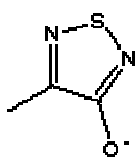
26-



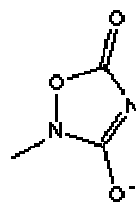
27-



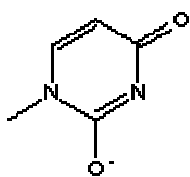
28-



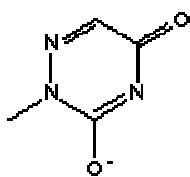
29-



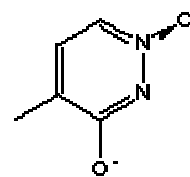
30-



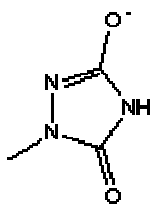
31-



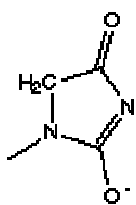
32-



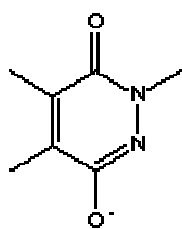
33-



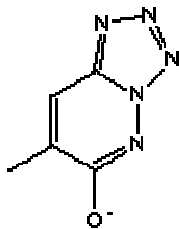
34a-



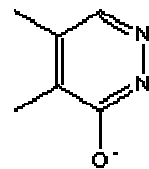
35a-



36-



37-



38-

Chart 8.4. Tautomerism of model heterocycles

Optimised geometries at MP2/6-31G(d,p) linked

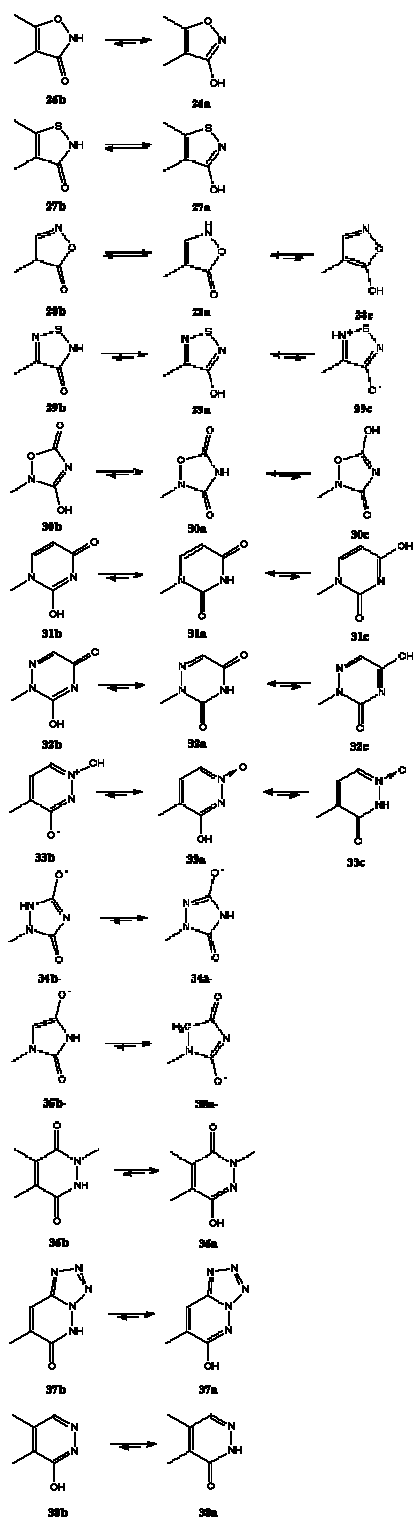
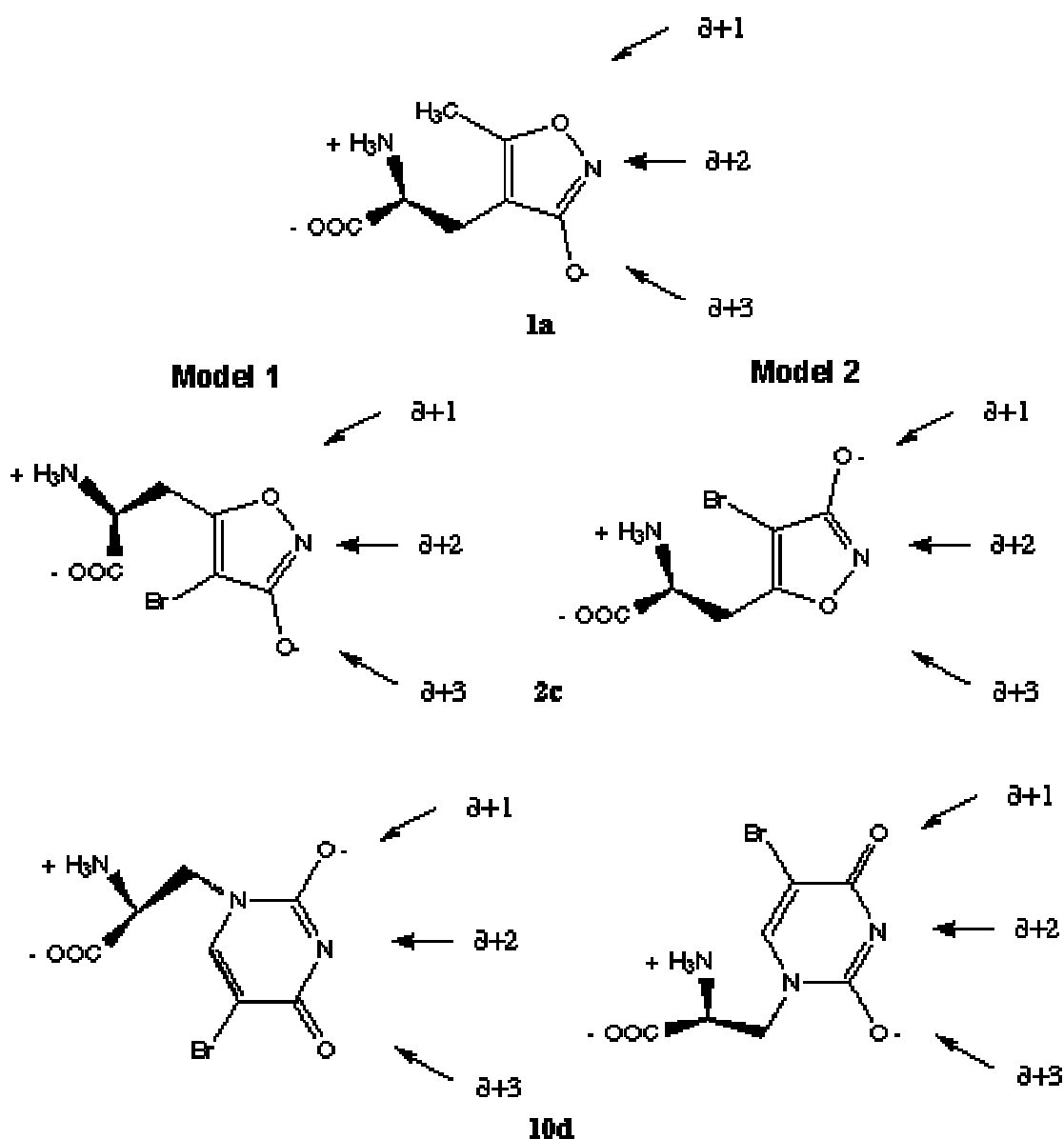
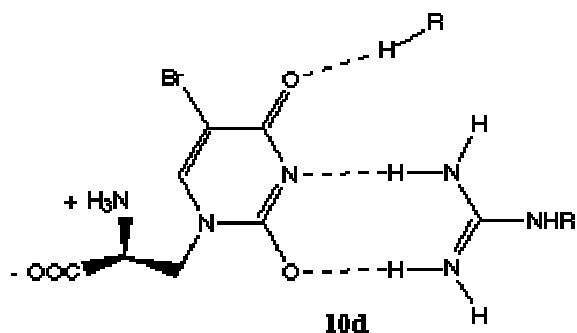


Chart 8.5. Tridentate binding models at AMPA receptors



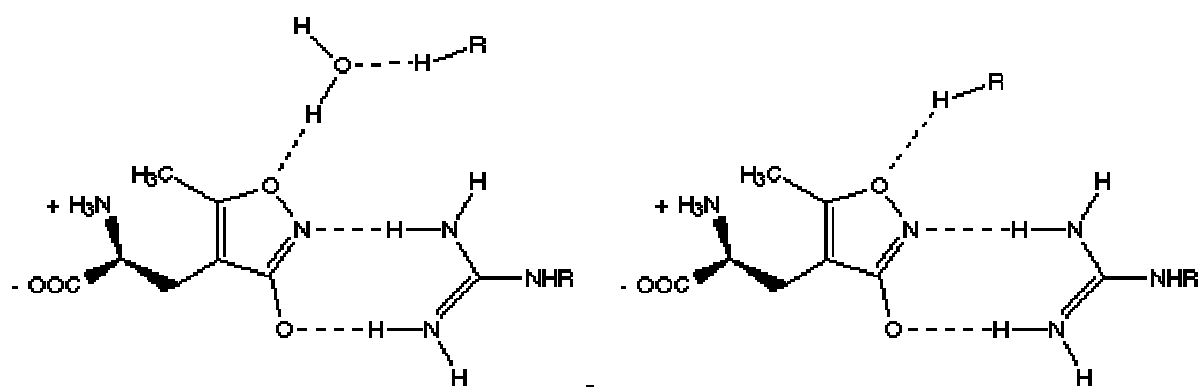
The tridentate binding model hypothesis suggests two possible binding orientations of heterocyclic domains.

Chart 8.6. Tridentate binding to two putative residues, with and without water mediation



10d

Residue tridentate binding

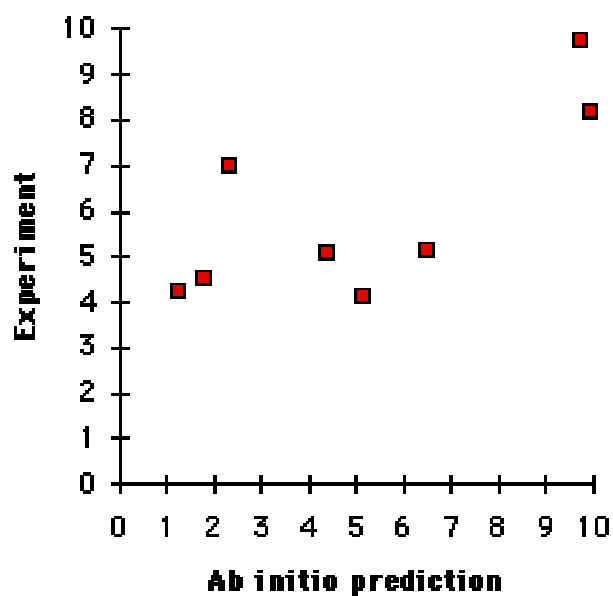


1a

Water mediated tridentate binding
of mono-oxygen substituted heterocycles

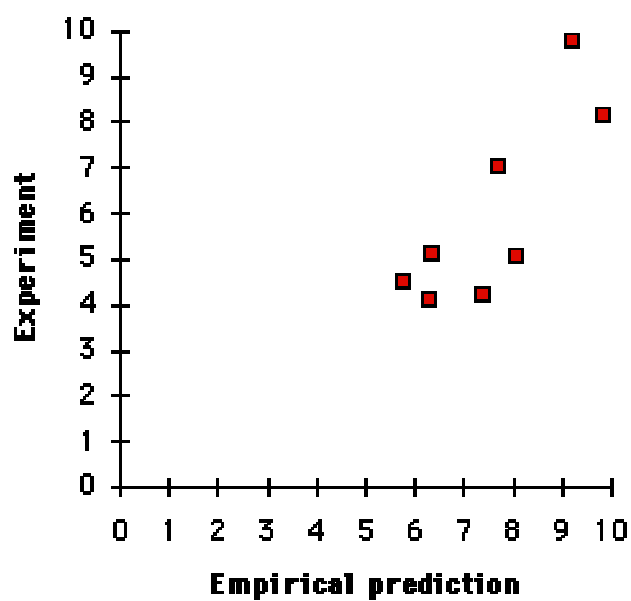
Residue tridentate binding

Graph 8.1.: Experimental pK_a s vs *ab initio* predictions ([Table 3](#))



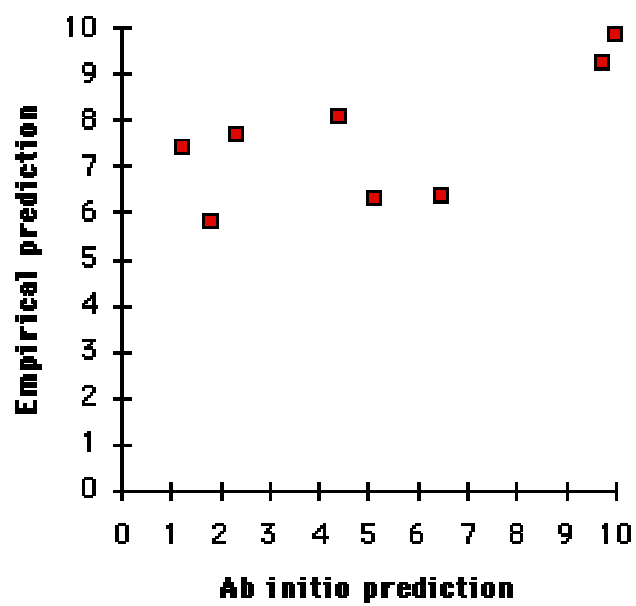
RMS deviation = 2.4

Graph 8.2.: Experimental pK_a s vs empirical predictions ([Table 3](#))



RMS deviation = 2.0

Graph 8.3: pK_a s: *ab initio* vs. empirical predictions ([Table 3](#))



RMS deviation = 3.5